Electronic Supporting Information

Friedel-Crafts acylation of antiaromatic norcorrole: electronic and steric modulation of the paratropic current

Sha Li,[a] Oskar Smaga,[b] Yahan Sun,[a] Xiaofang Li,*[,a] Miłosz Pawlicki,[b,c] Marzena Sukniewicz,[b] and Piotr J. Chmielewski*[,b]

[a.]Key Laboratory of Theoretical Chemistry and Molecular Simulation of Ministry of Education, Hunan Province College Key Laboratory of QSAR/QSPR, School of Chemistry and Chemical Engineering, Hunan University of Science and Technology, Xiangtan, Hunan 411201, China

[b.]Department of Chemistry, University of Wrocław, 14 F. Joliot-Curie Street, 50 383 Wrocław, Poland

[c.]Department of Chemistry, Jagiellonian University, Gronostajowa 2, 30 387 Kraków, Poland.

E-mail: lixiaofang@iccas.ac.cn, pjc@wchuwr.pl

Table of contents

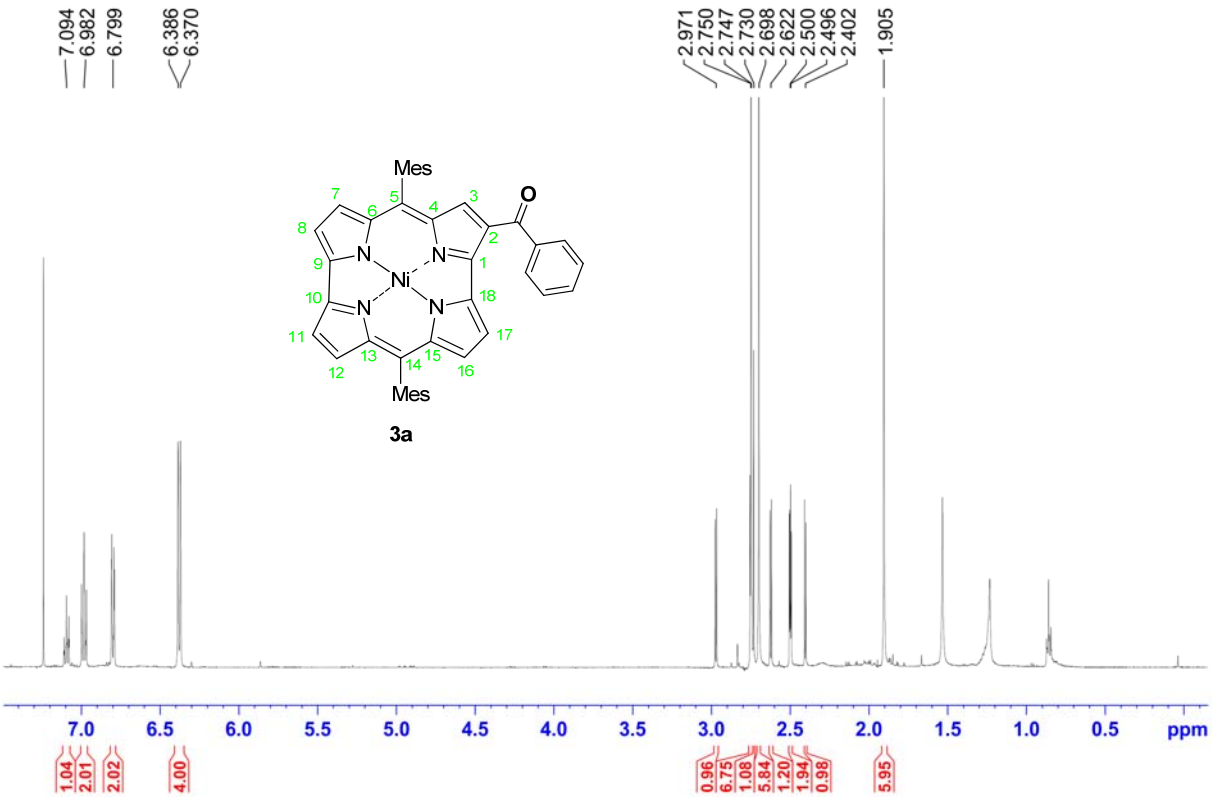

Figure S1. ^{1}H NMR spectrum of **3a** (500 MHz, 300 K, $CDCl_3$).

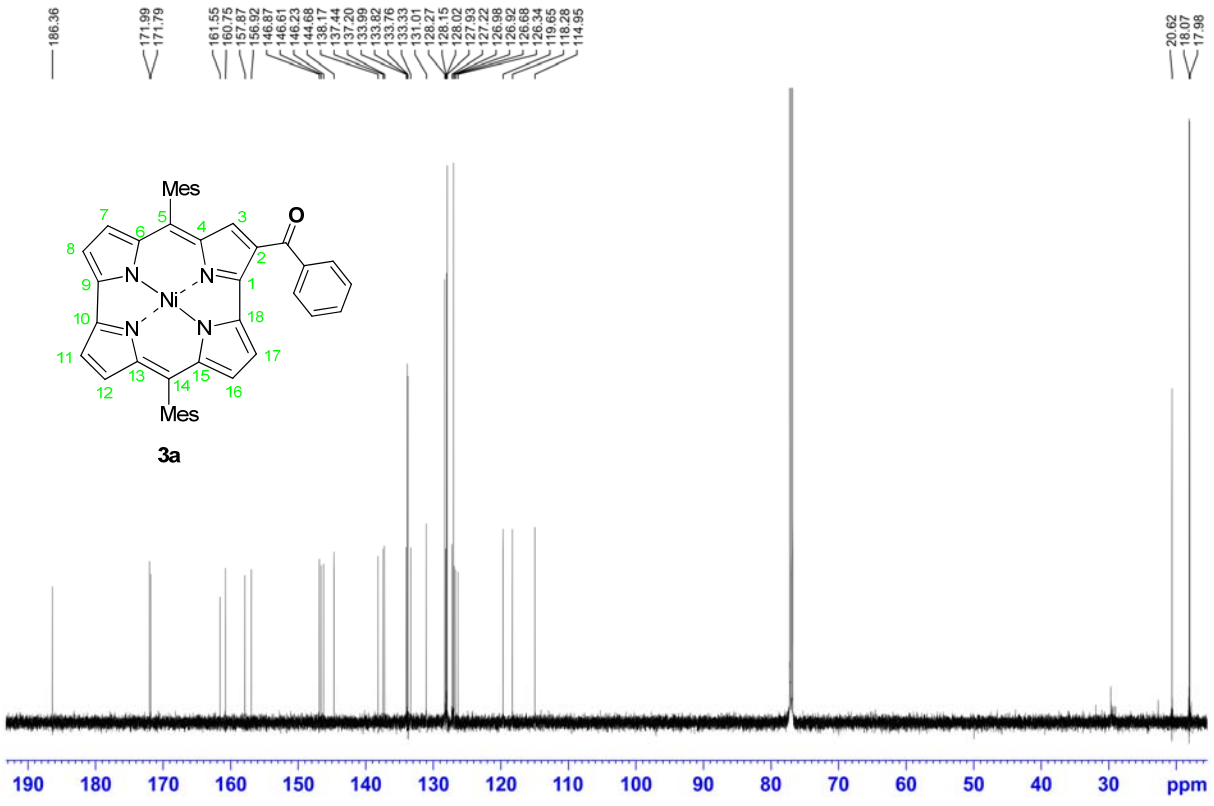

Figure S2. ^{13}C NMR spectrum of **3a** (150 MHz, 300 K, $CDCl_3$).

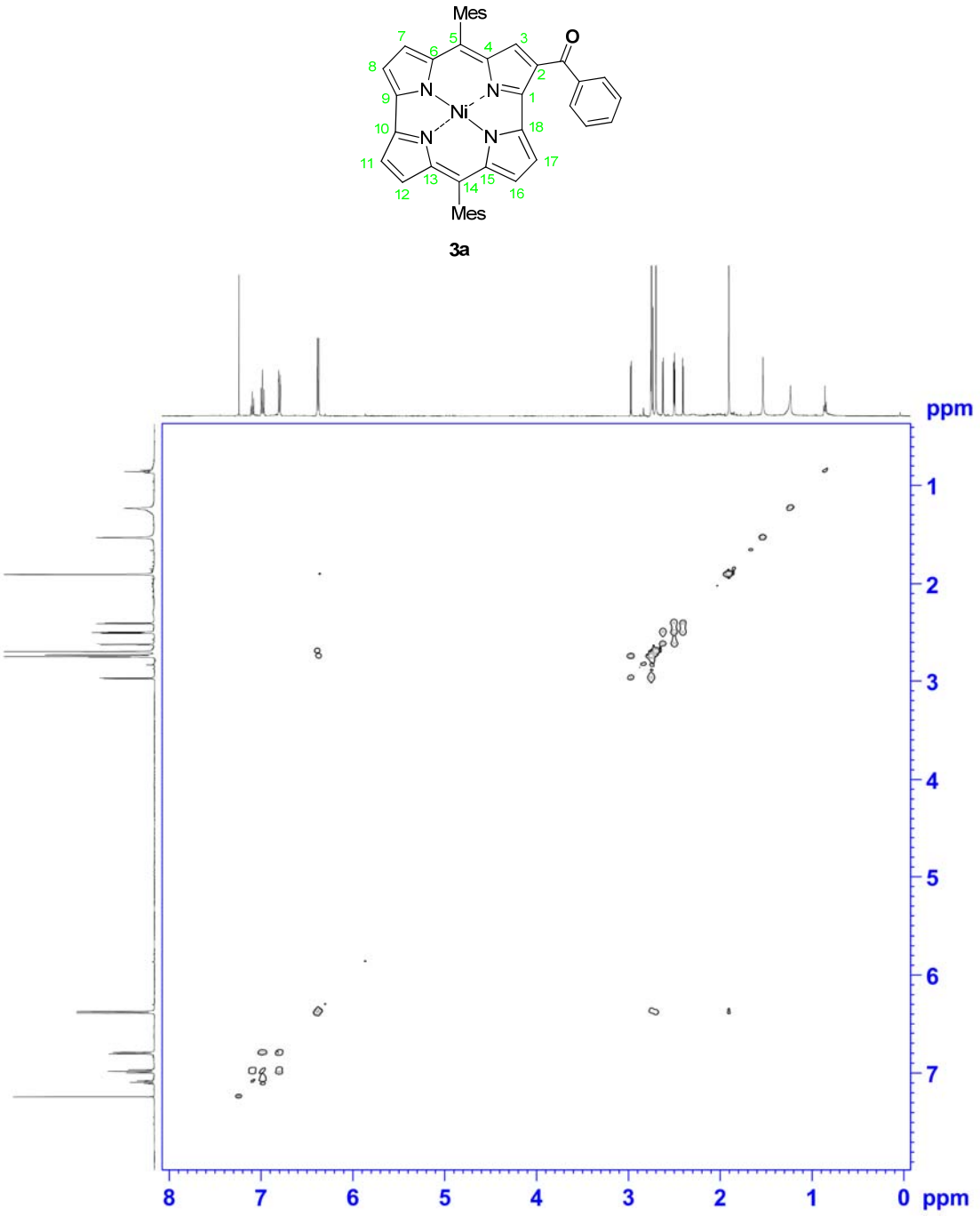

3a

Figure S3. ^{1}H, ^{1}H COSY spectrum of **3a** (500 MHz, 300 K, $CDCl_3$).

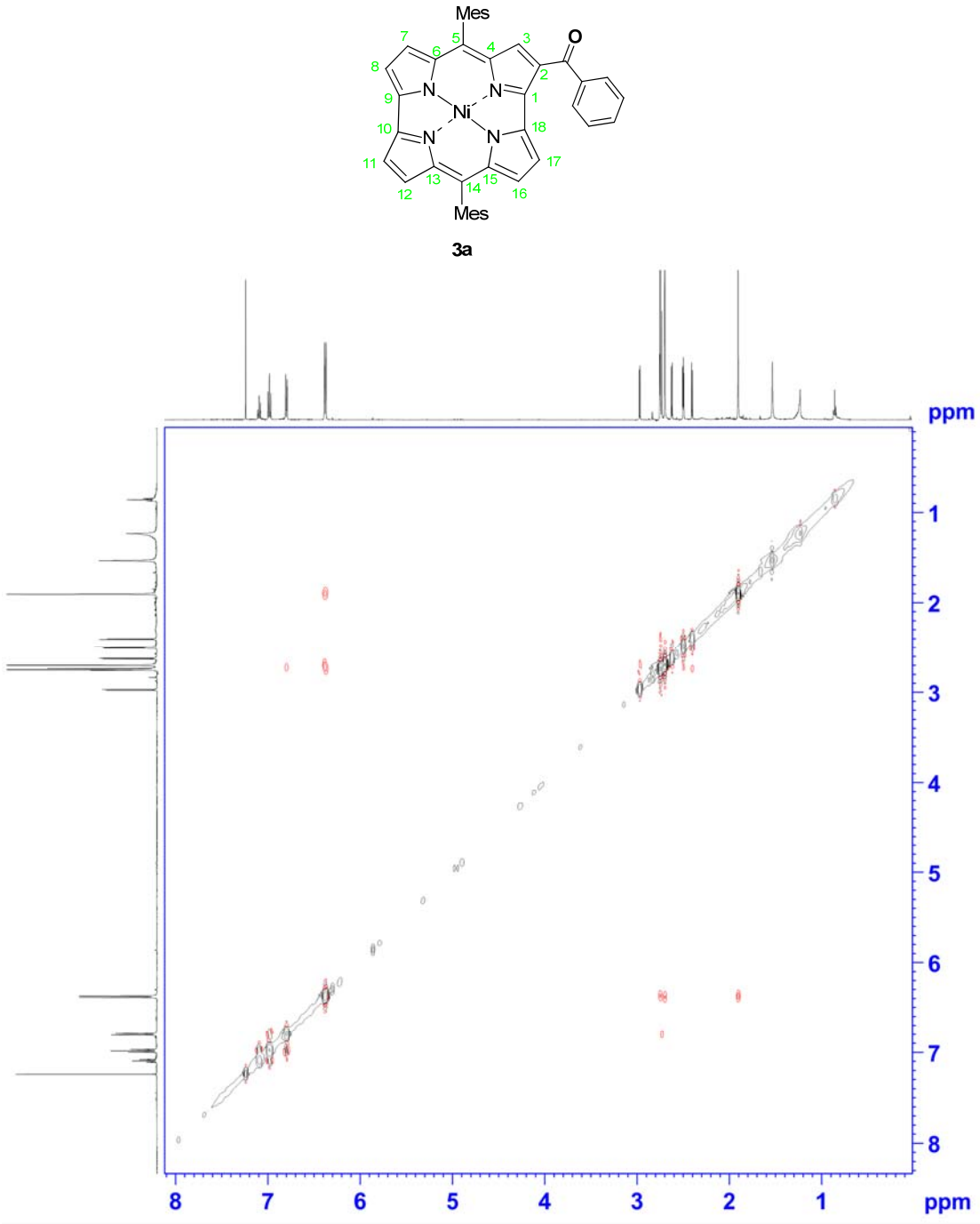

3a

Figure S4. ^{1}H, ^{1}H NOESY spectrum of **3a** (500 MHz, 300 K, $CDCl_3$).

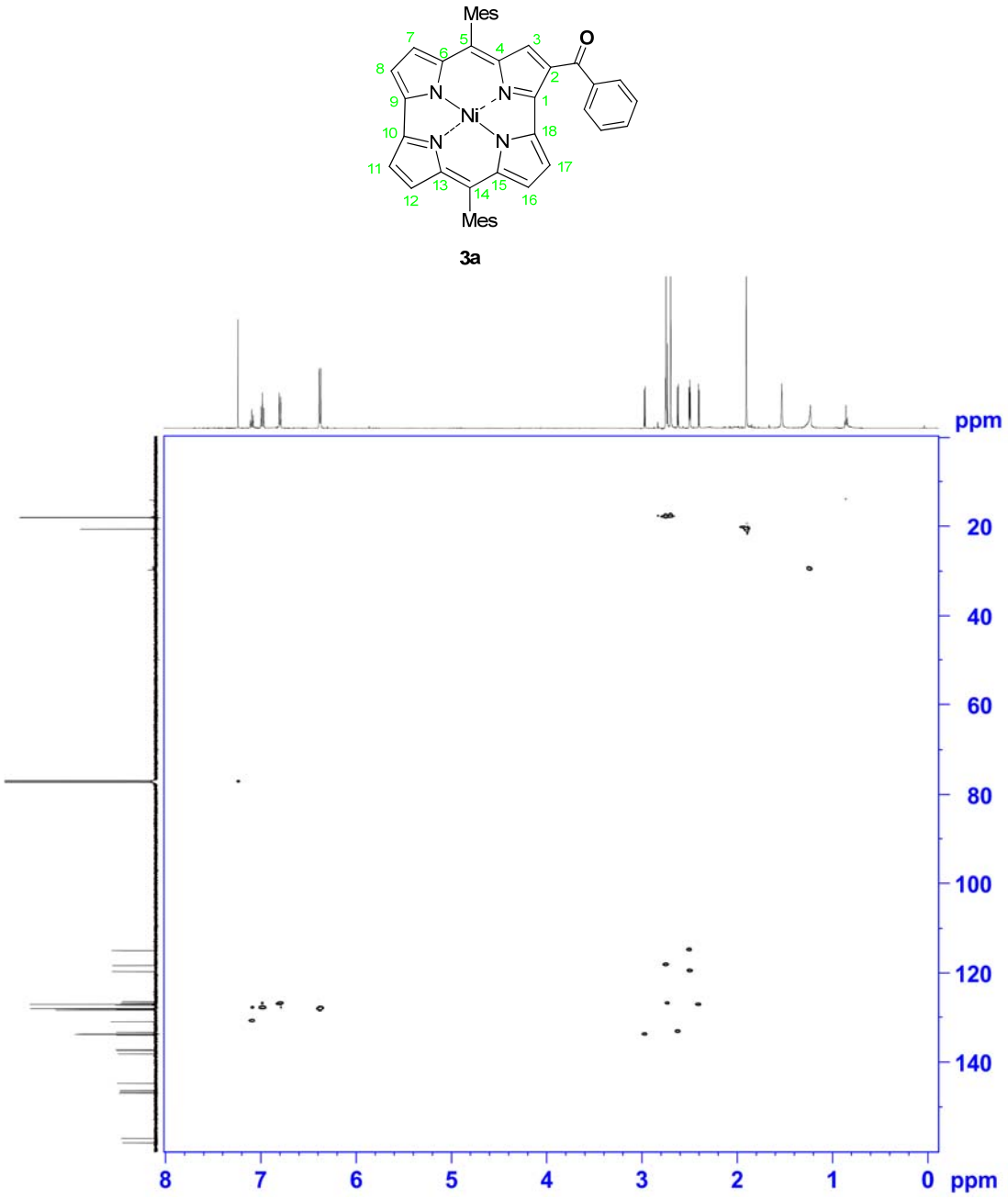

3a

Figure S5. ^{1}H, ^{13}C HSQC spectrum of **3a** (500/125 MHz, 300 K, $CDCl_3$).

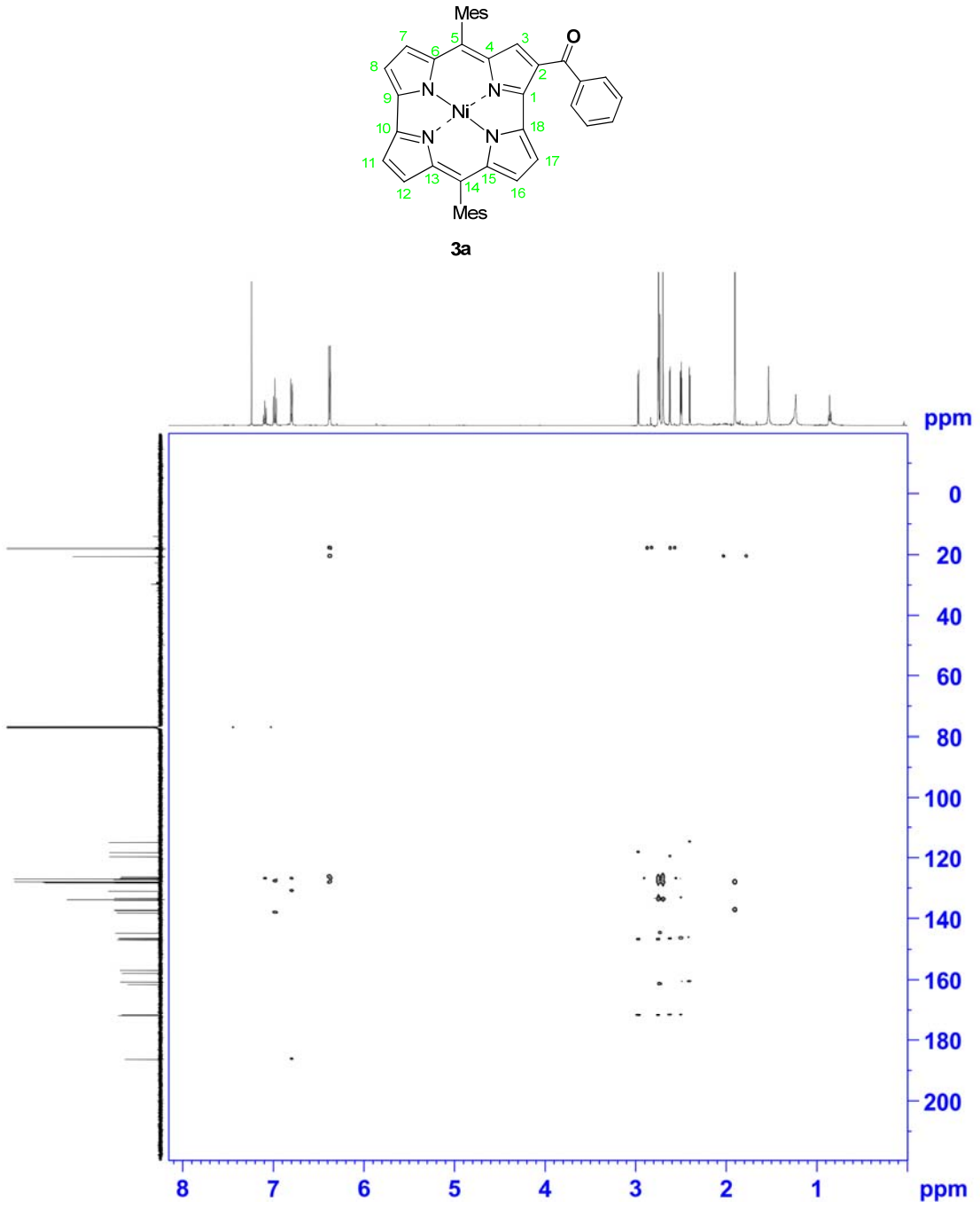

3a

Figure S6. ^{1}H, ^{13}C HMBC spectrum of **3a** (500/125 MHz, 300 K, $CDCl_3$).

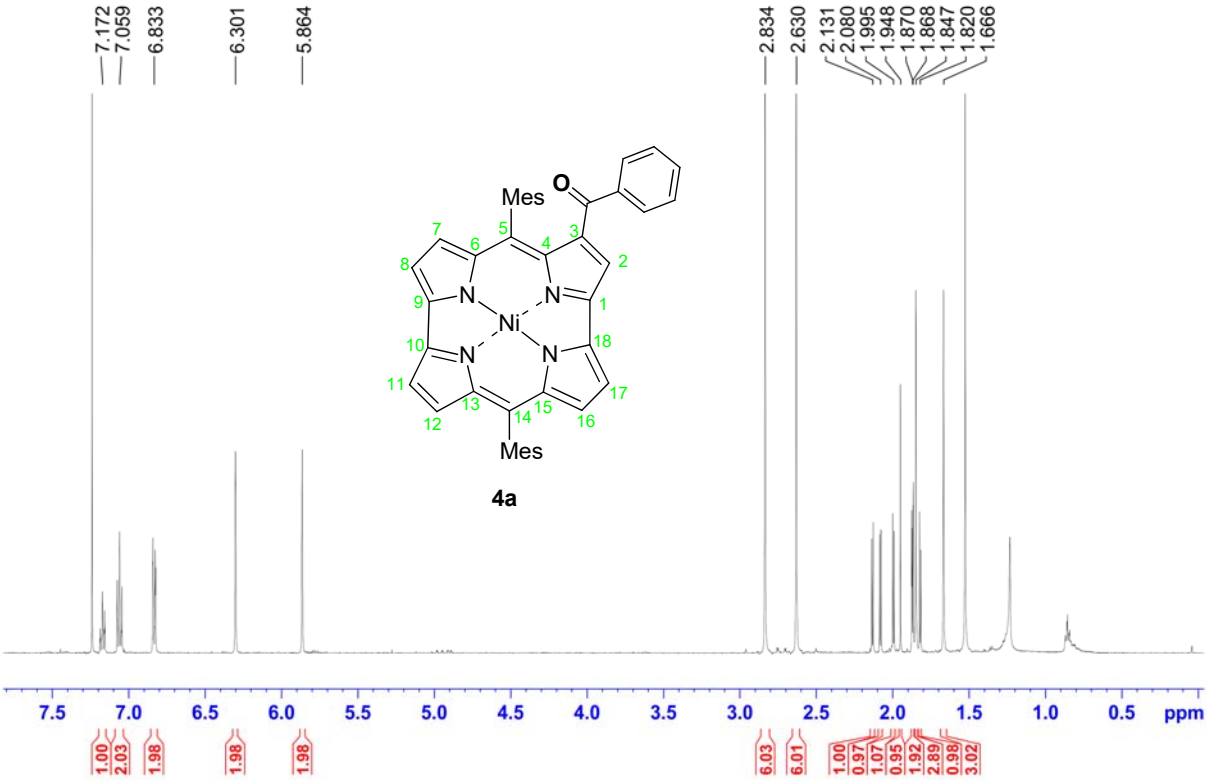

Figure S7. ^{1}H NMR spectrum of **4a** (500 MHz, 300 K, $CDCl_3$).

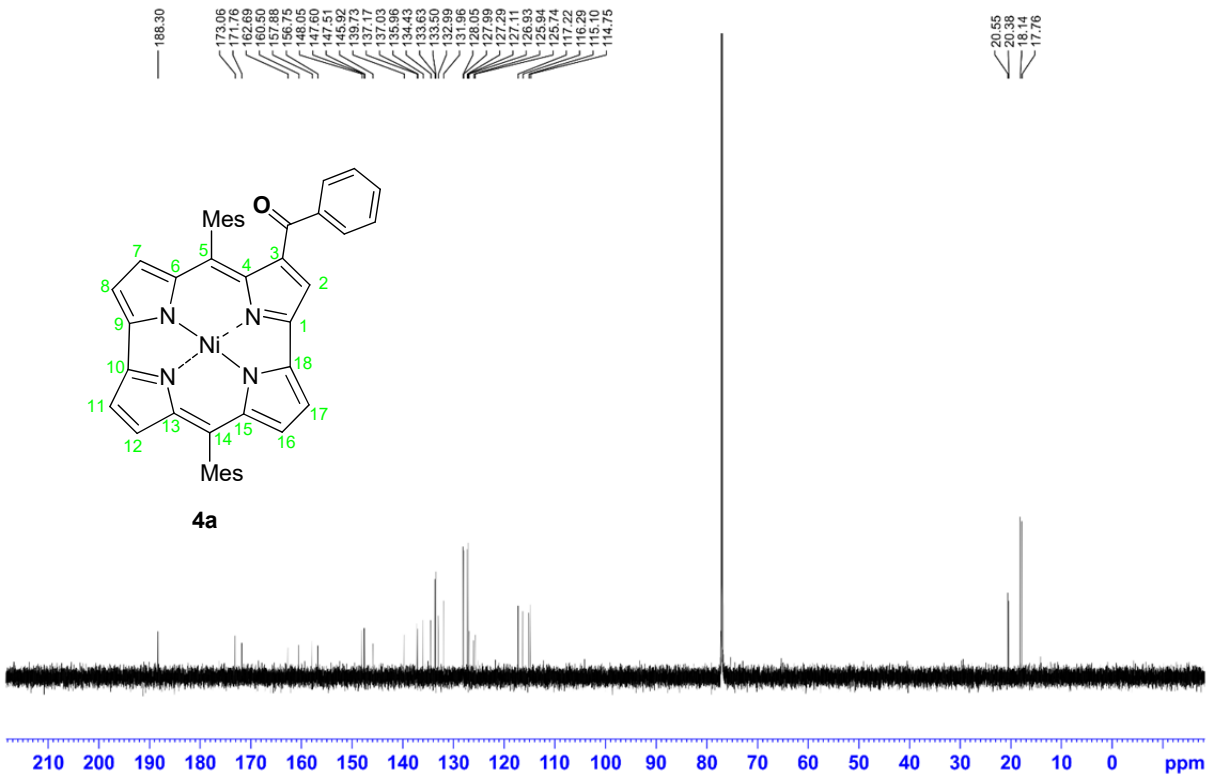

Figure S8. ^{13}C NMR spectrum of **4a** (150 MHz, 300 K, $CDCl_3$).

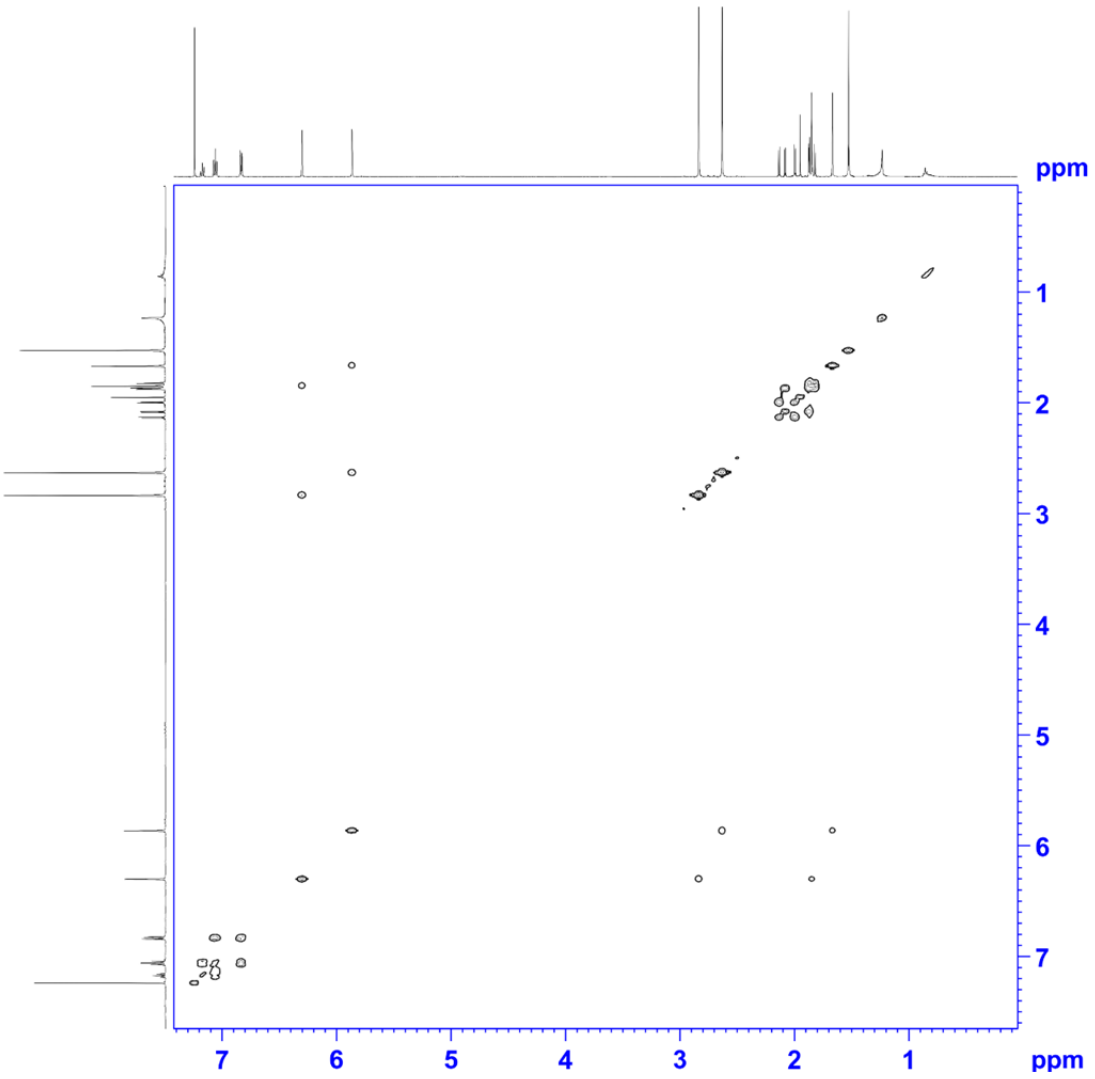

Figure S9. ^{1}H, ^{1}H COSY spectrum of **4a** (500 MHz, 300 K, $CDCl_3$).

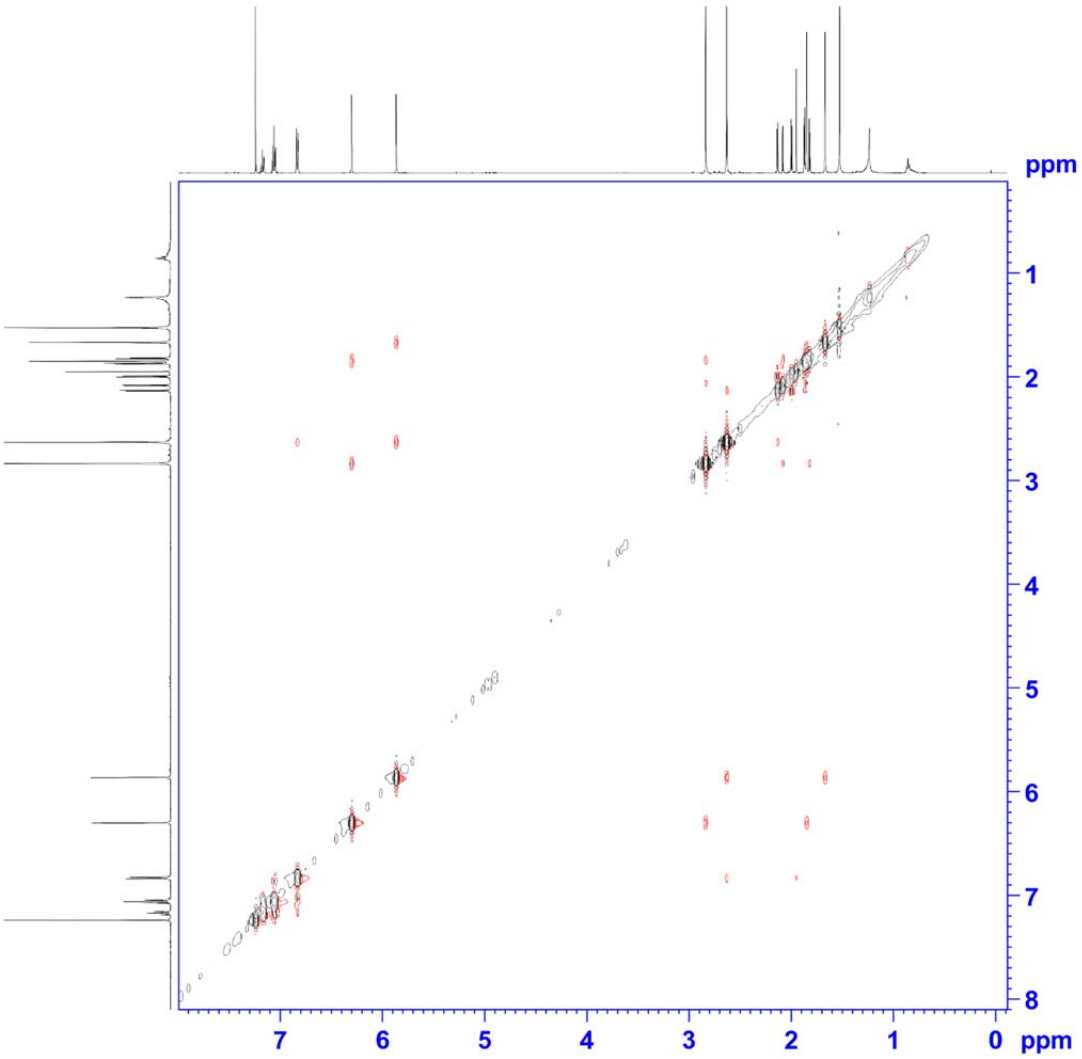

Figure S10. ^{1}H, ^{1}H NOESY spectrum of **4a** (500 MHz, 300 K, $CDCl_3$).

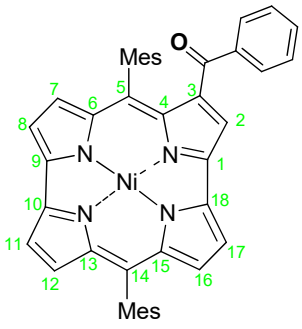

4a

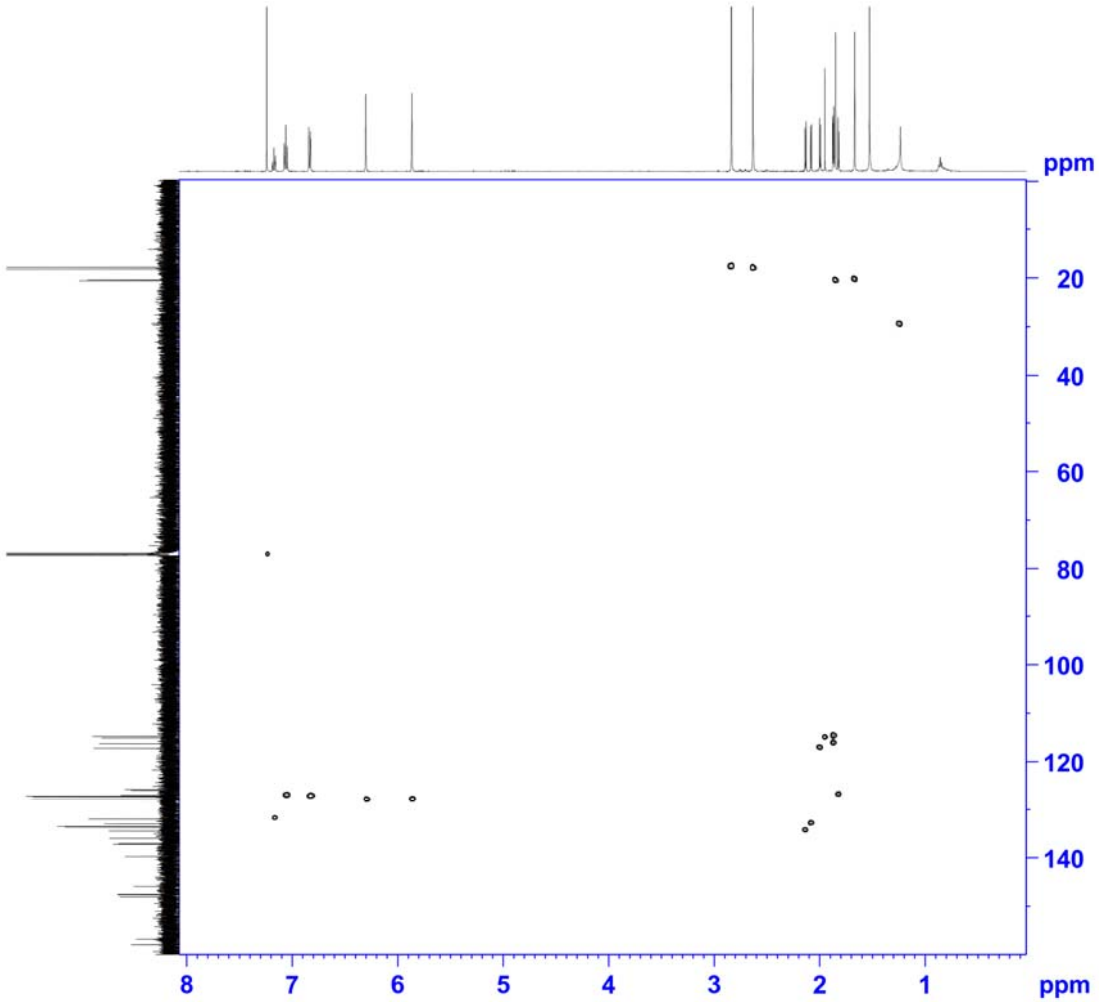

Figure S11. ^{1}H, ^{13}C HSQC spectrum of **4a** (500/125 MHz, 300 K, $CDCl_3$).

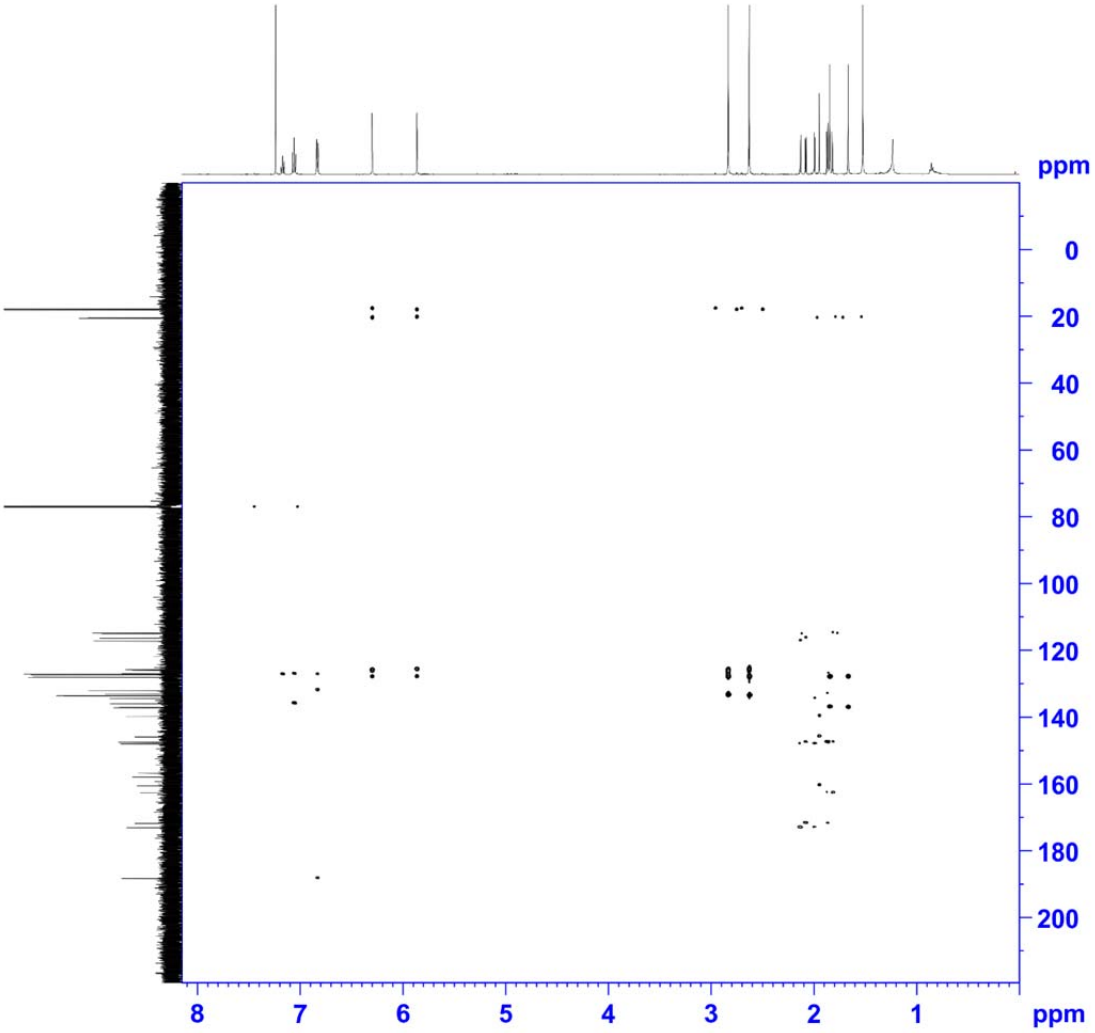

Figure S12. ^{1}H, ^{13}C HMBC spectrum of **4a** (500/125 MHz, 300 K, $CDCl_3$).

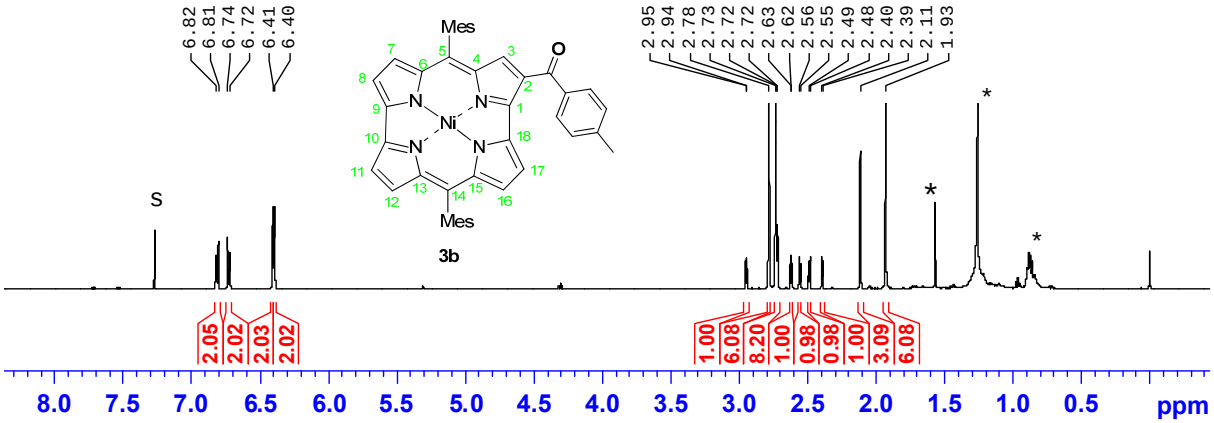

Figure S13. ^{1}H NMR spectrum of **3b** (500 MHz, 298 K, $CDCl_3$).

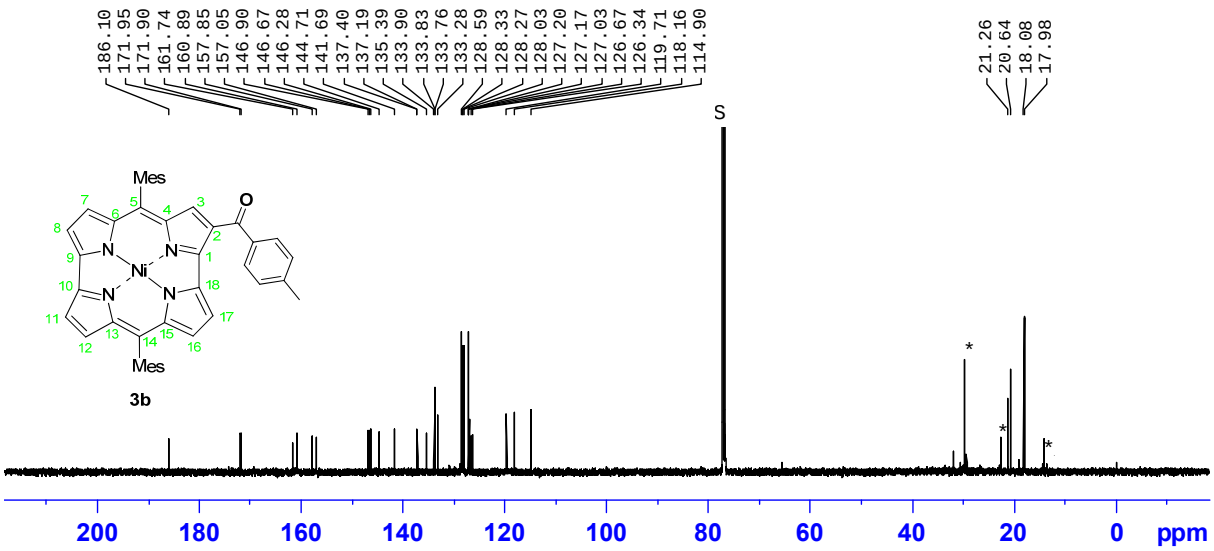

Figure S14. ^{13}C NMR spectrum of **3b** (125 MHz, 298 K, $CDCl_3$).

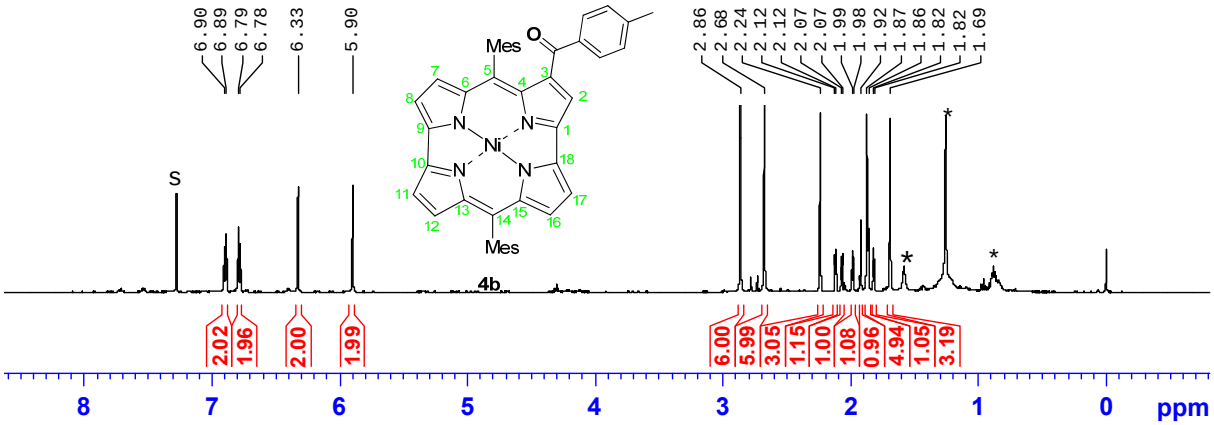

Figure S15. ^{1}H NMR spectrum of **4b** (500 MHz, 298 K, $CDCl_3$).

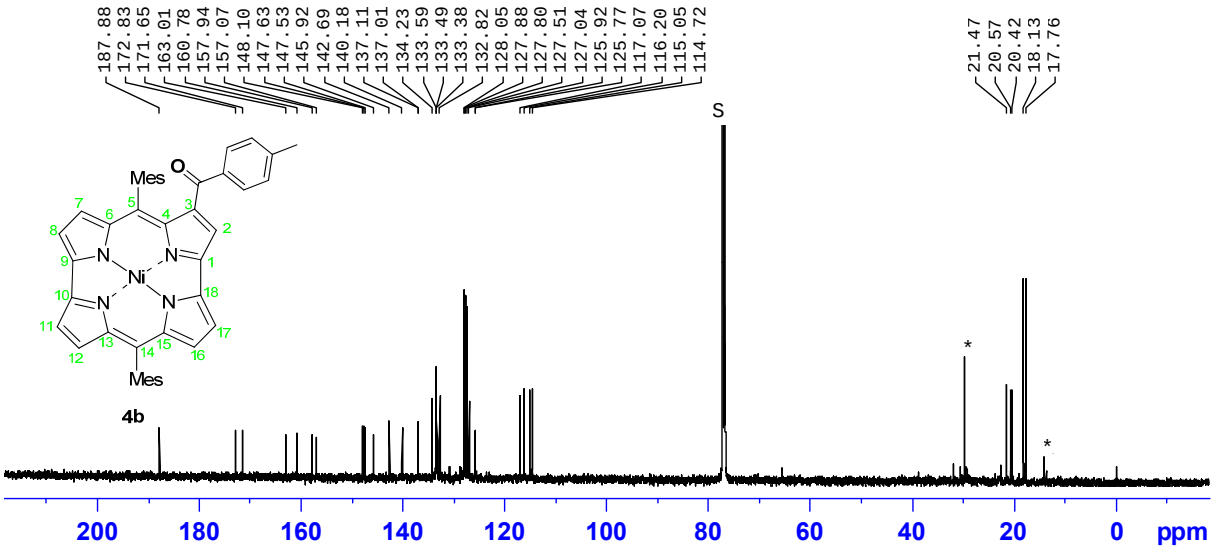

Figure S16. ^{13}C NMR spectrum of **4b** (125 MHz, 298 K, $CDCl_3$).

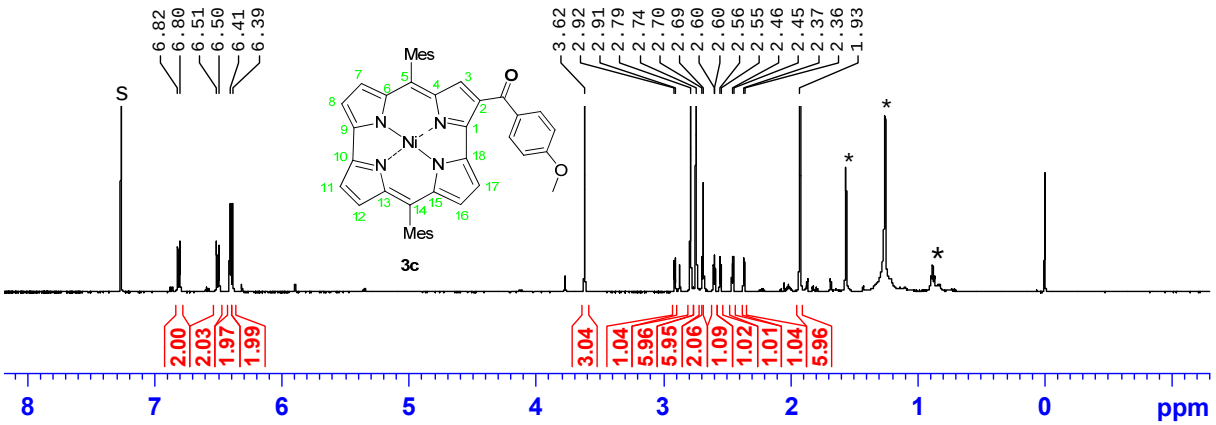

Figure S17. ^{1}H NMR spectrum of **3c** (500 Mhz, 298 K, $CDCl_3$).

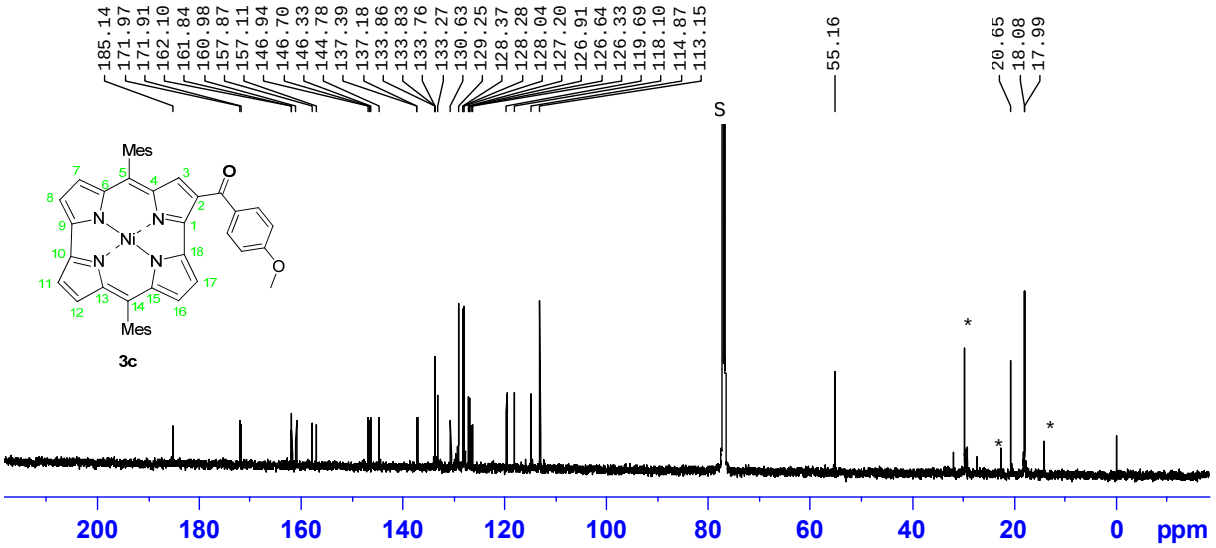

Figure S18. ^{13}C NMR spectrum of **3c** (125 Mhz, 298 K, $CDCl_3$).

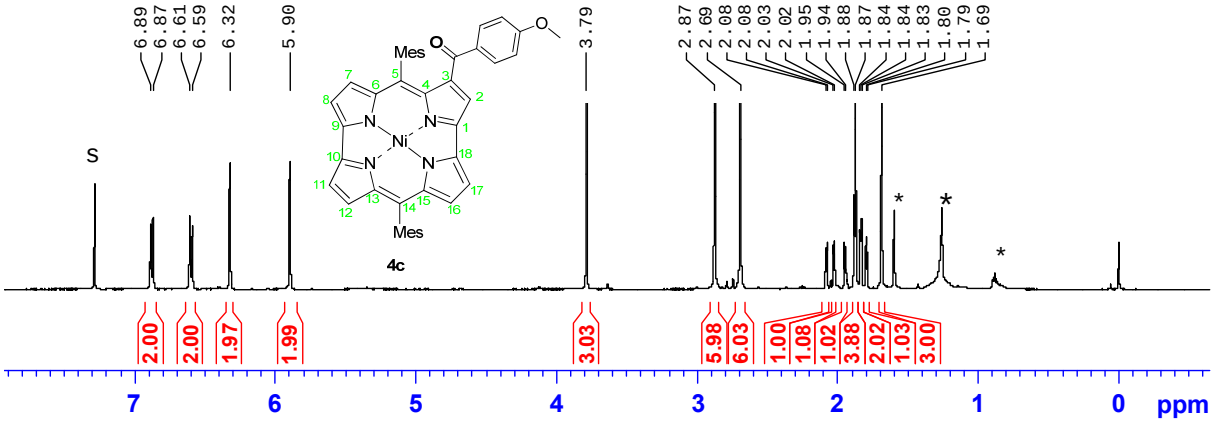

Figure S19. ^{1}H NMR spectrum of **4c** (500Mhz, 298 K, $CDCl_3$).

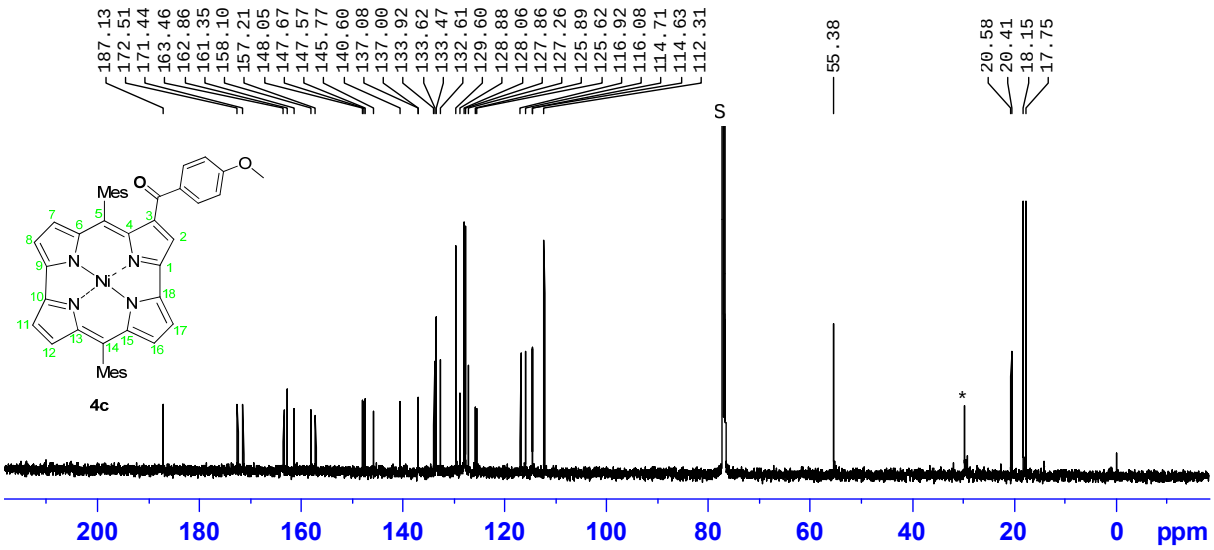

Figure S20. ^{13}C NMR spectrum of **4c** (125 Mhz, 298 K, $CDCl_3$).

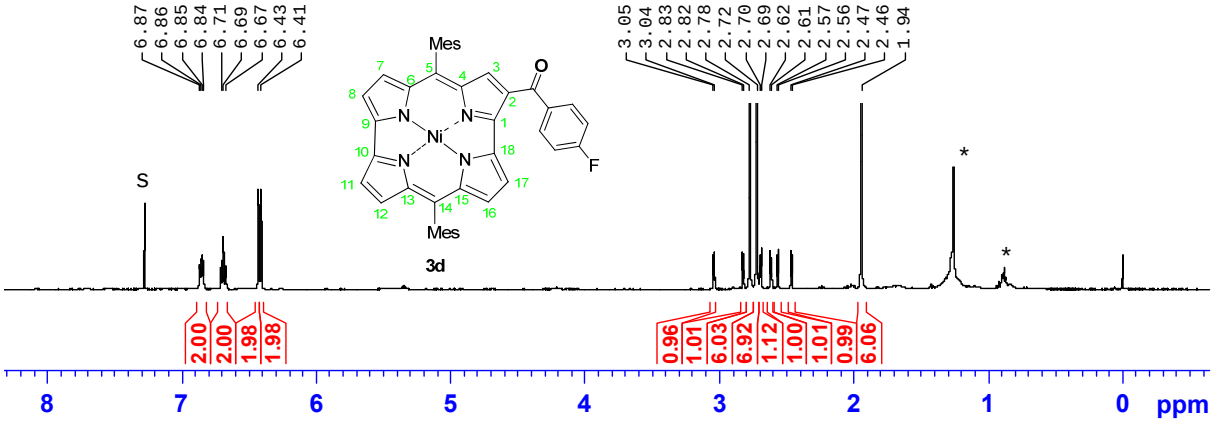

Figure S21. ^{1}H NMR spectrum of **3d** (500 Mhz, 298 K, $CDCl_3$).

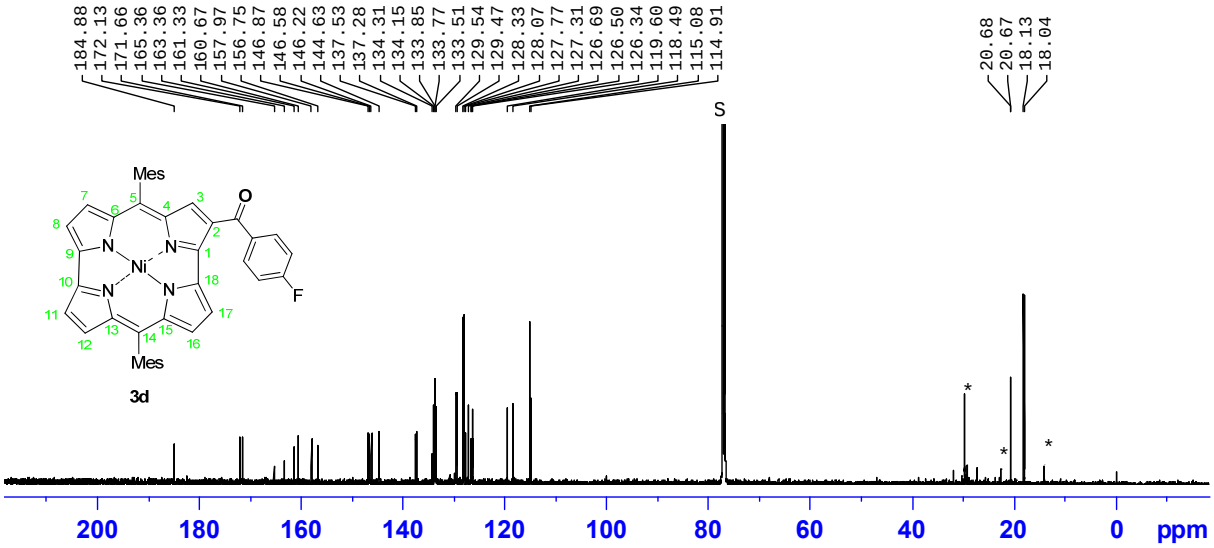

Figure S22. ^{13}C NMR spectrum of **3d** (125 Mhz, 298 K, $CDCl_3$).

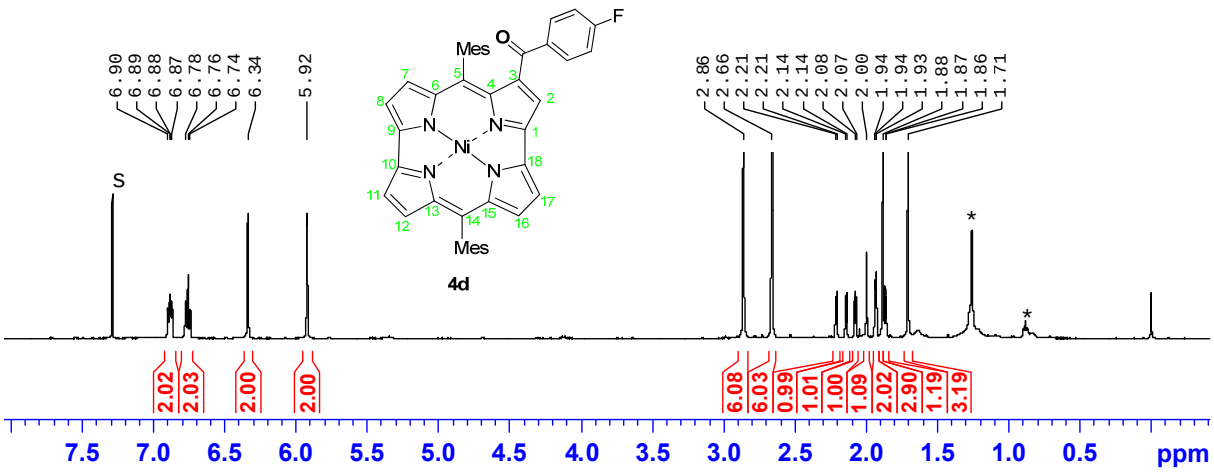

Figure S23. ^{1}H NMR spectrum of **4d** (500 Mhz, 298 K, $CDCl_3$).

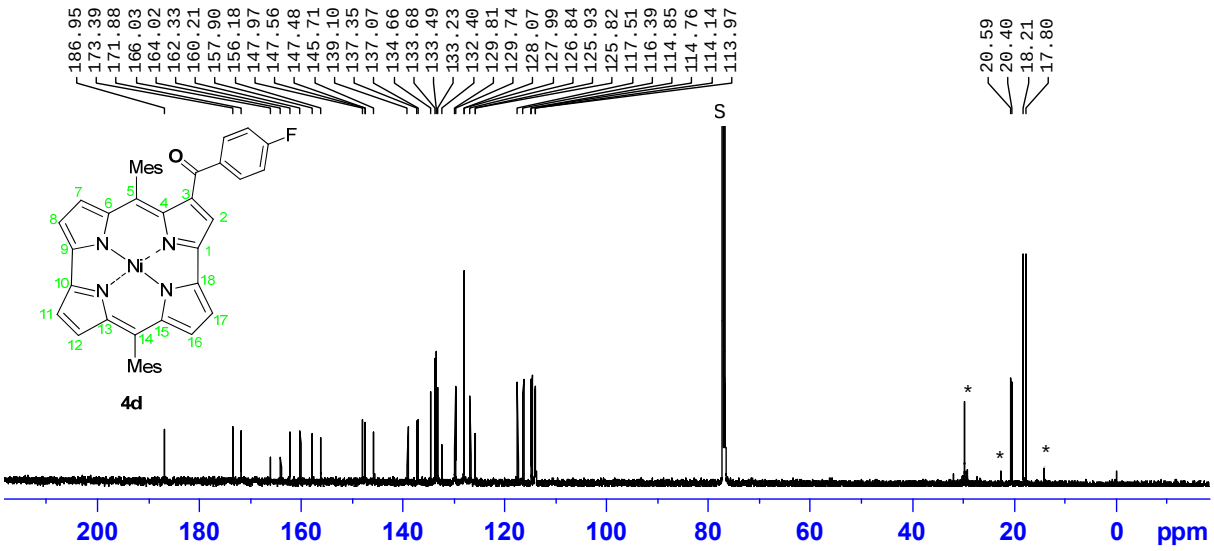

Figure S24. ^{13}C NMR spectrum of **4d** (125 Mhz, 298 K, $CDCl_3$).

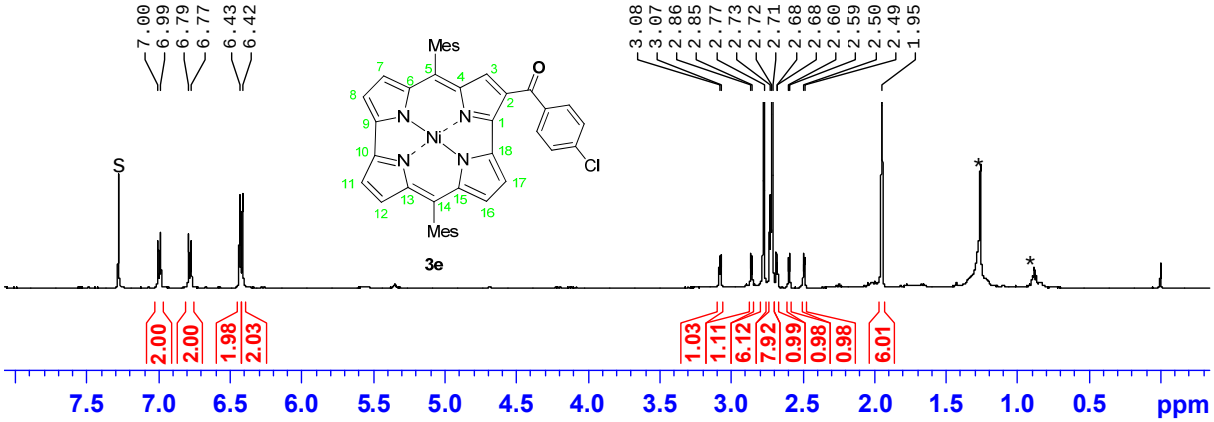

Figure S25. ^{1}H NMR spectrum of **3e** (500 Mhz, 298 K, $CDCl_3$).

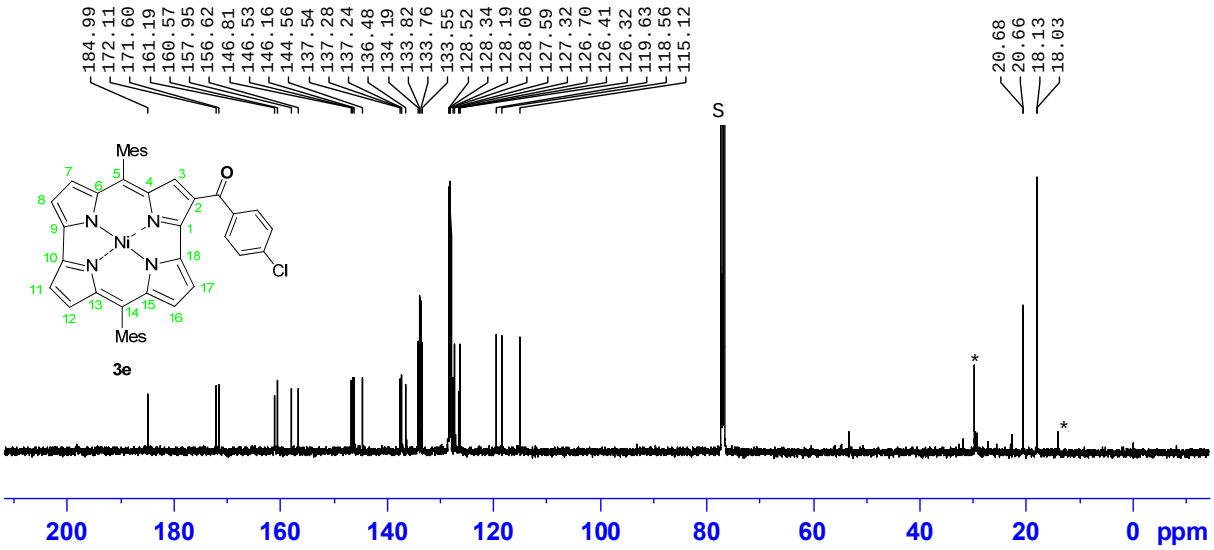

Figure S26. ^{13}C NMR spectrum of **3e** (125 Mhz, 298 K, $CDCl_3$).

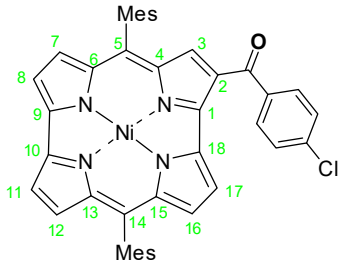

3e

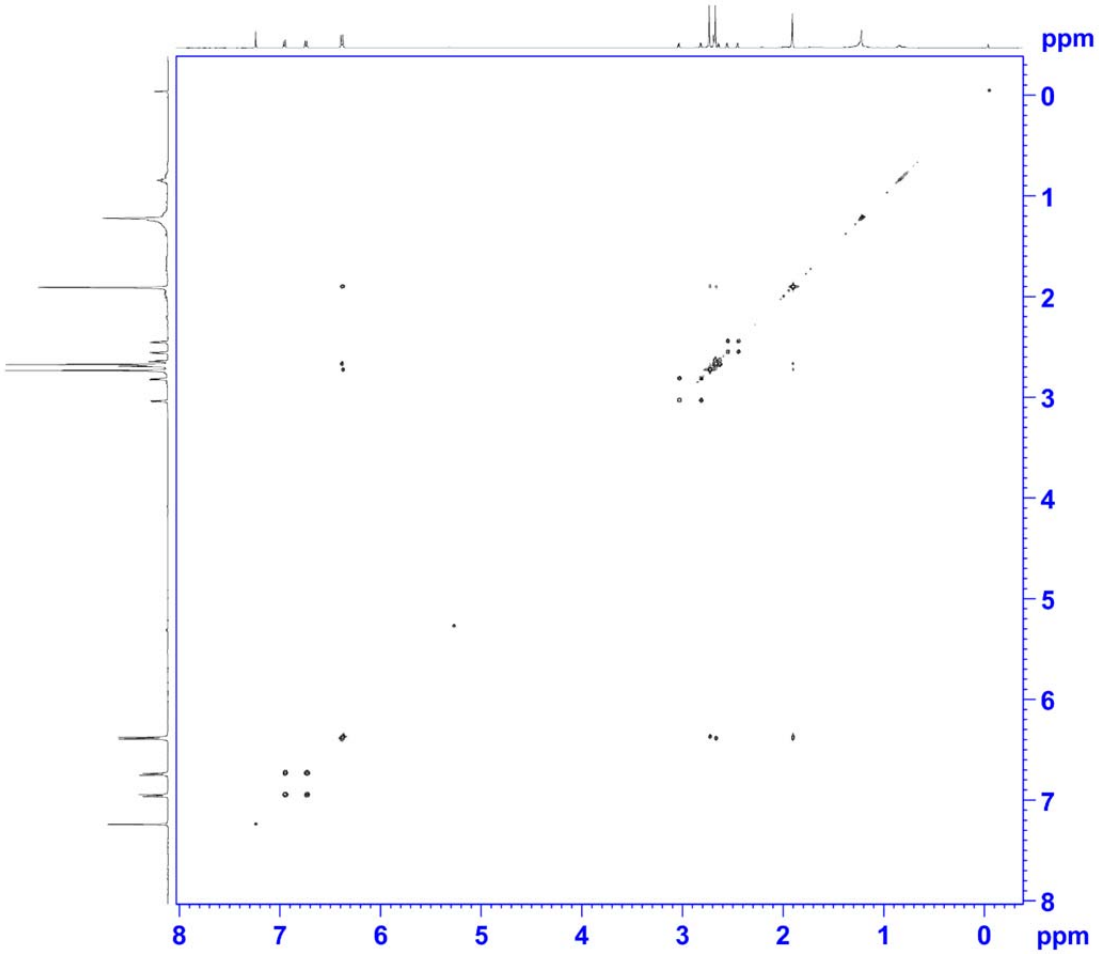

Figure S27. ^{1}H, ^{1}H COSY spectrum of **3e** (500 MHz, 298 K, $CDCl_3$).

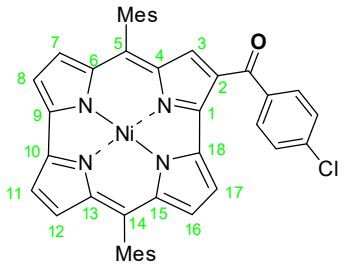

3e

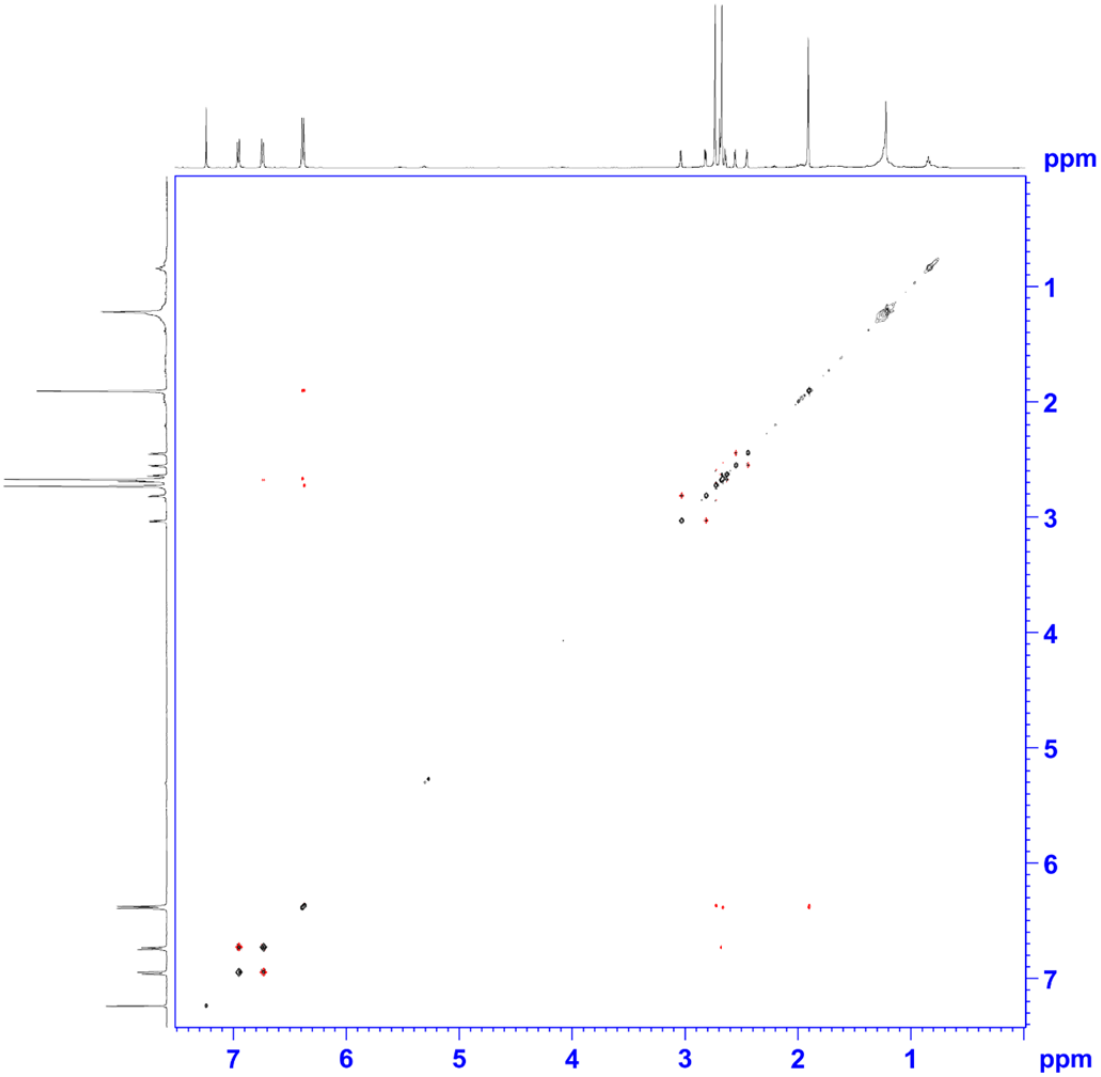

Figure S28. ^{1}H, ^{1}H NOESY spectrum of **3e** (500 MHz, 298 K, $CDCl_3$).

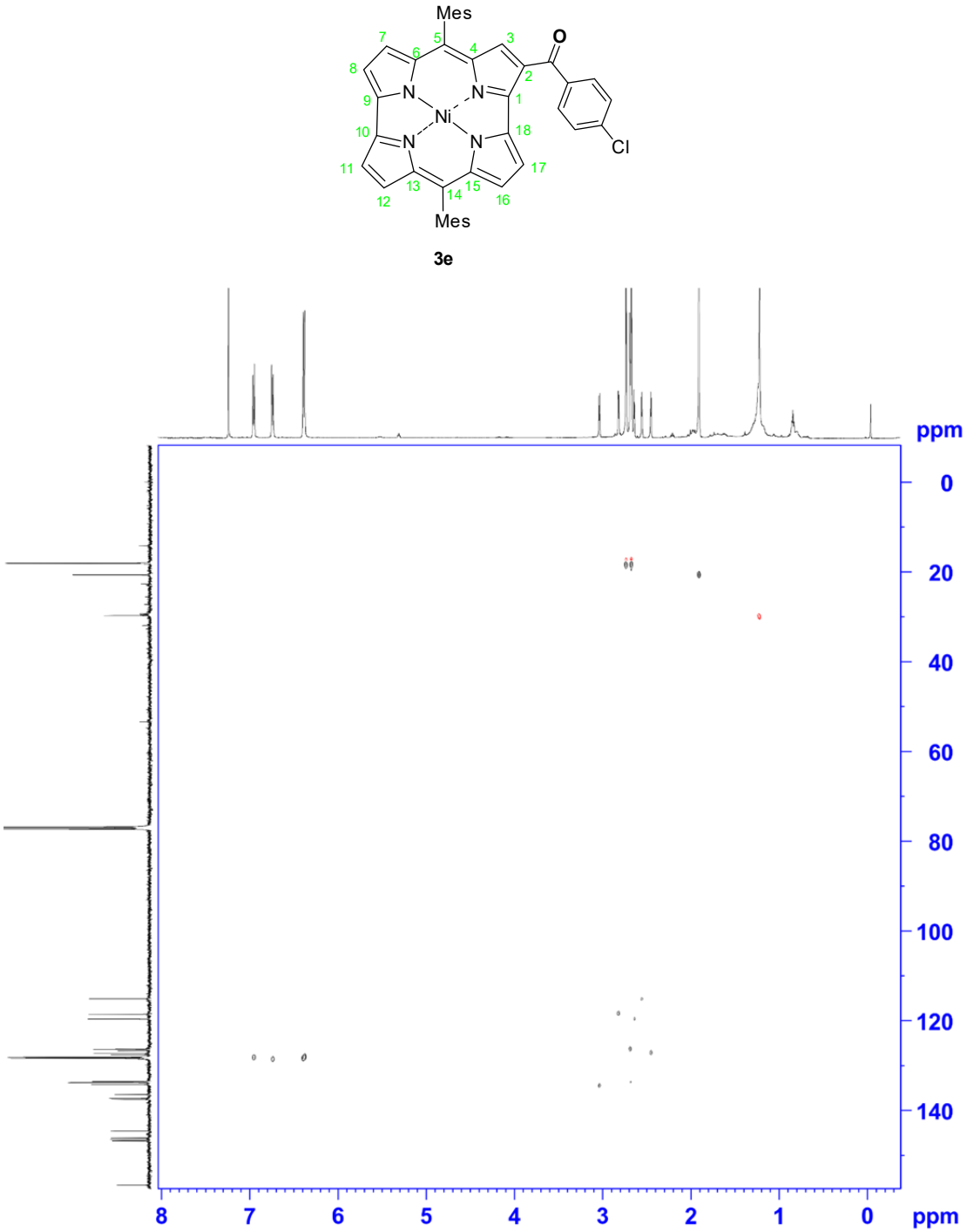

3e

Figure S29. ^{1}H, ^{13}C HSQC spectrum of **3e** (500/125 MHz, 298 K, $CDCl_3$).

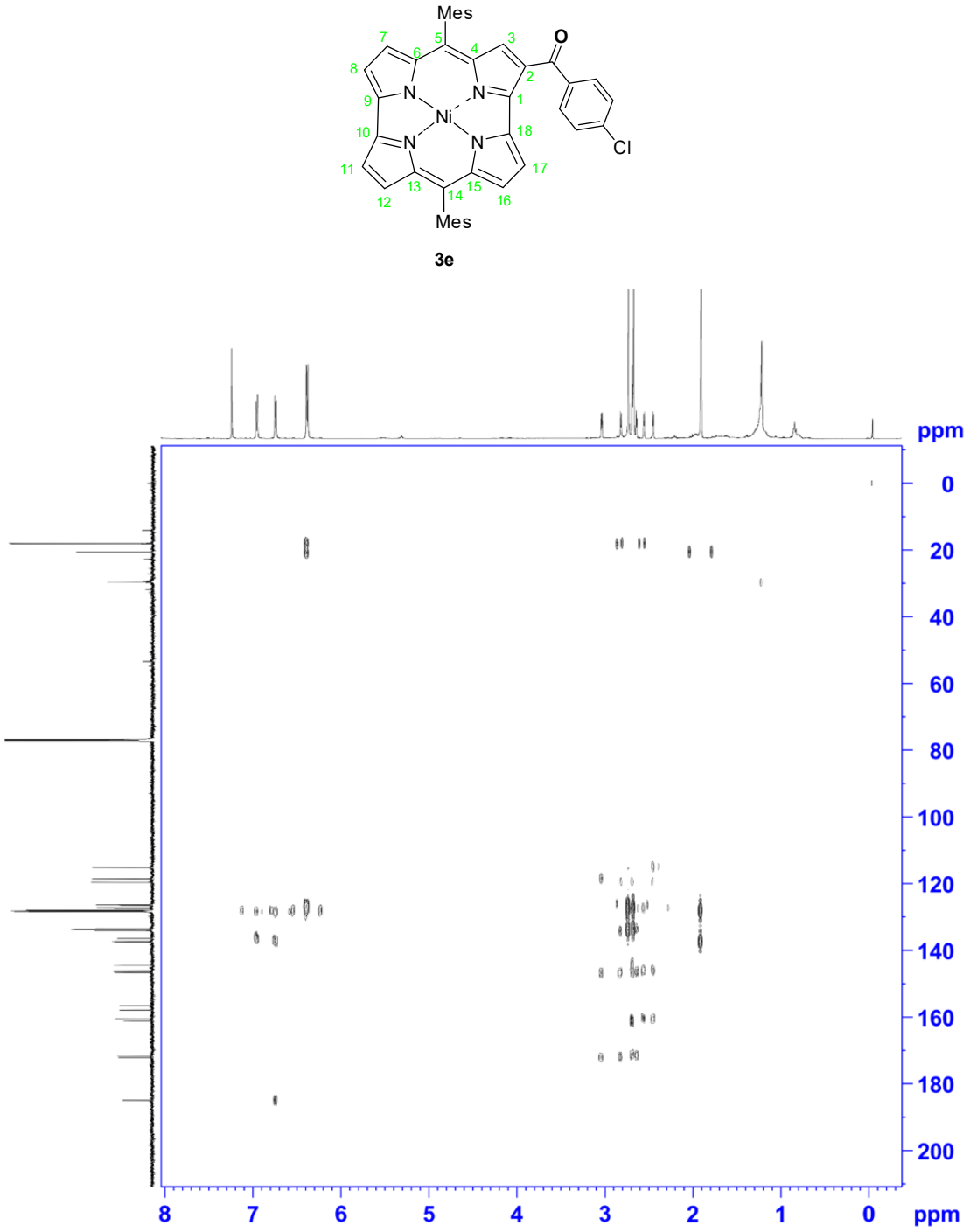

3e

Figure S30. ^{1}H, ^{13}C HMBC spectrum of **3e** (500/125 MHz, 298 K, $CDCl_3$).

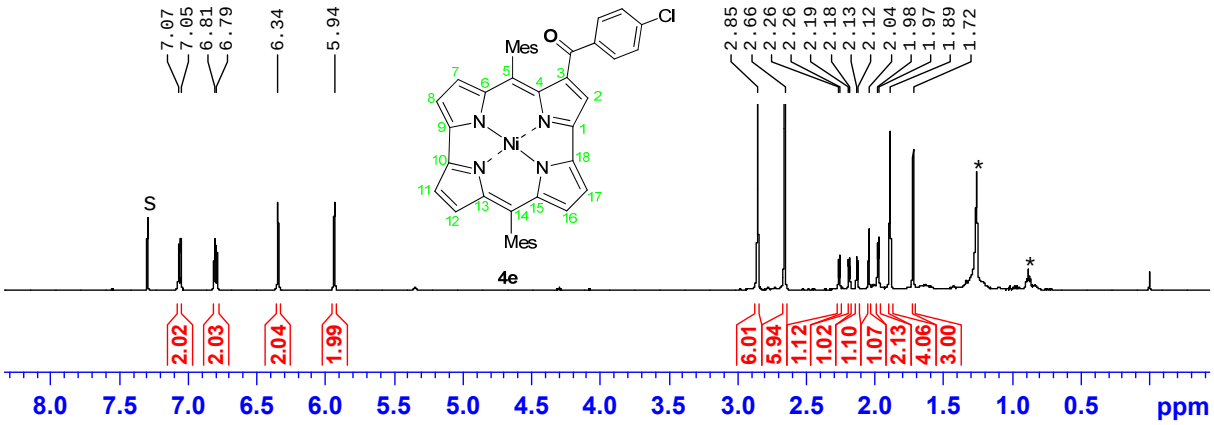

Figure S31. ^{1}H NMR spectrum of **4e** (500 MHz, 298 K, $CDCl_3$).

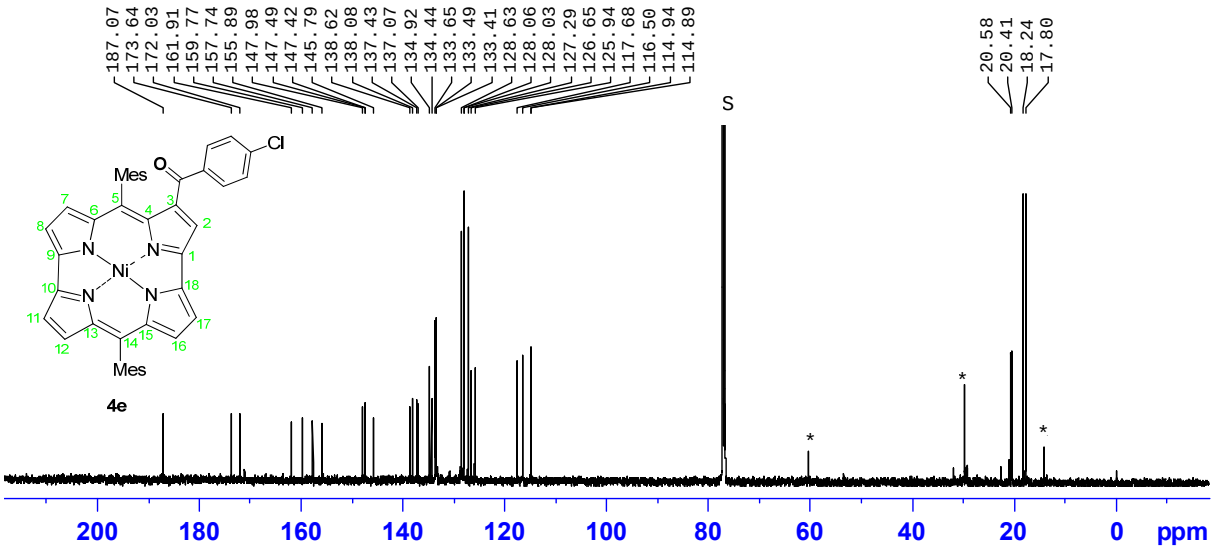

Figure S32. ^{13}C NMR spectrum of **4e** (125 MHz, 298 K, $CDCl_3$).

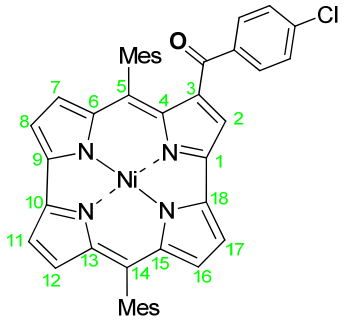

4e

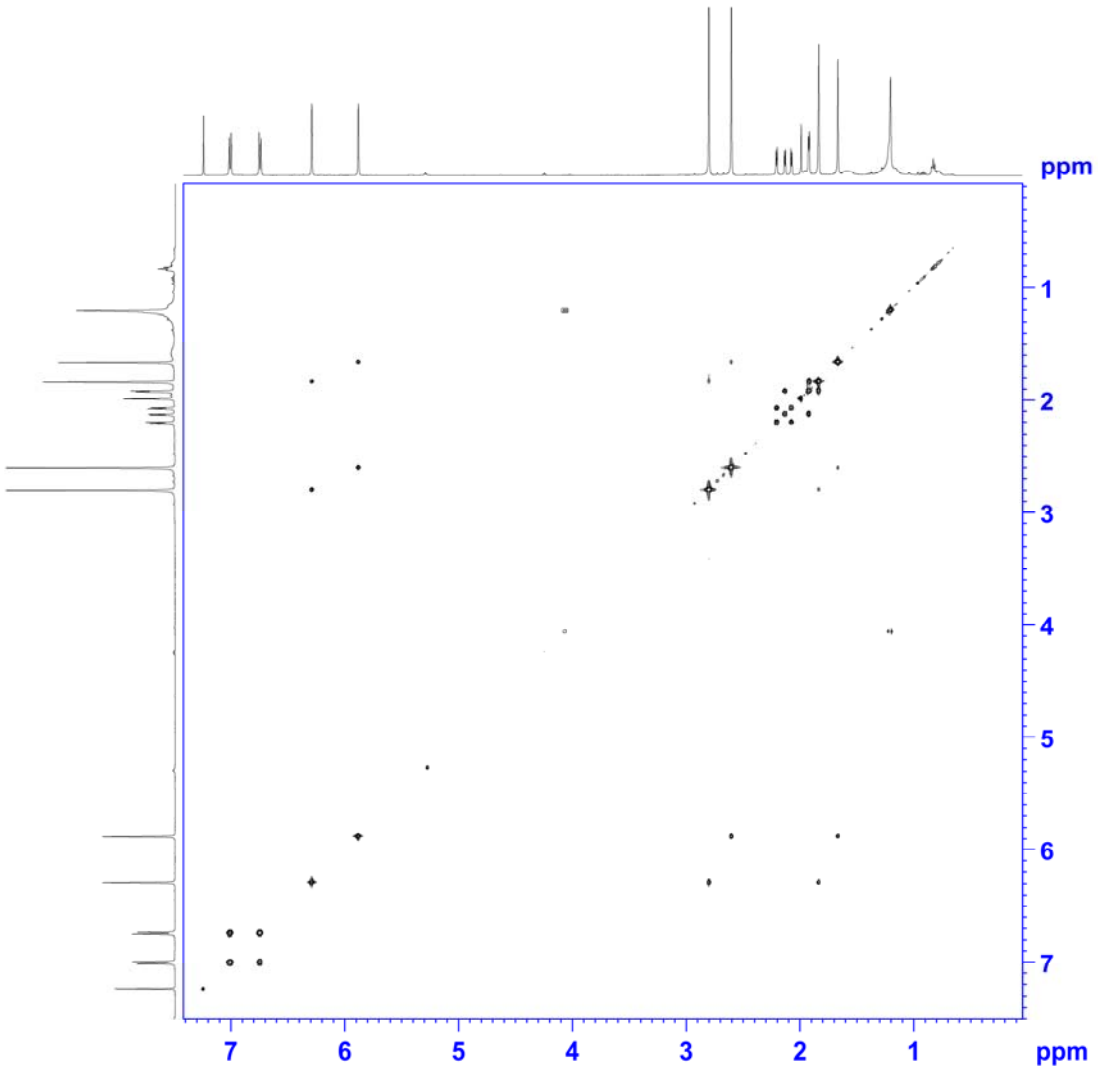

Figure S33. ^{1}H, ^{1}H COSY spectrum of **4e** (500 MHz, 298 K, $CDCl_3$).

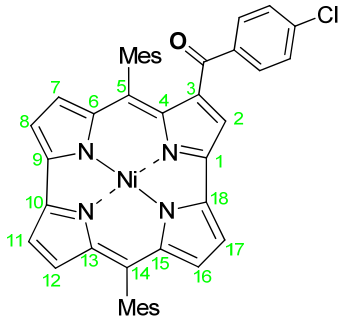

4e

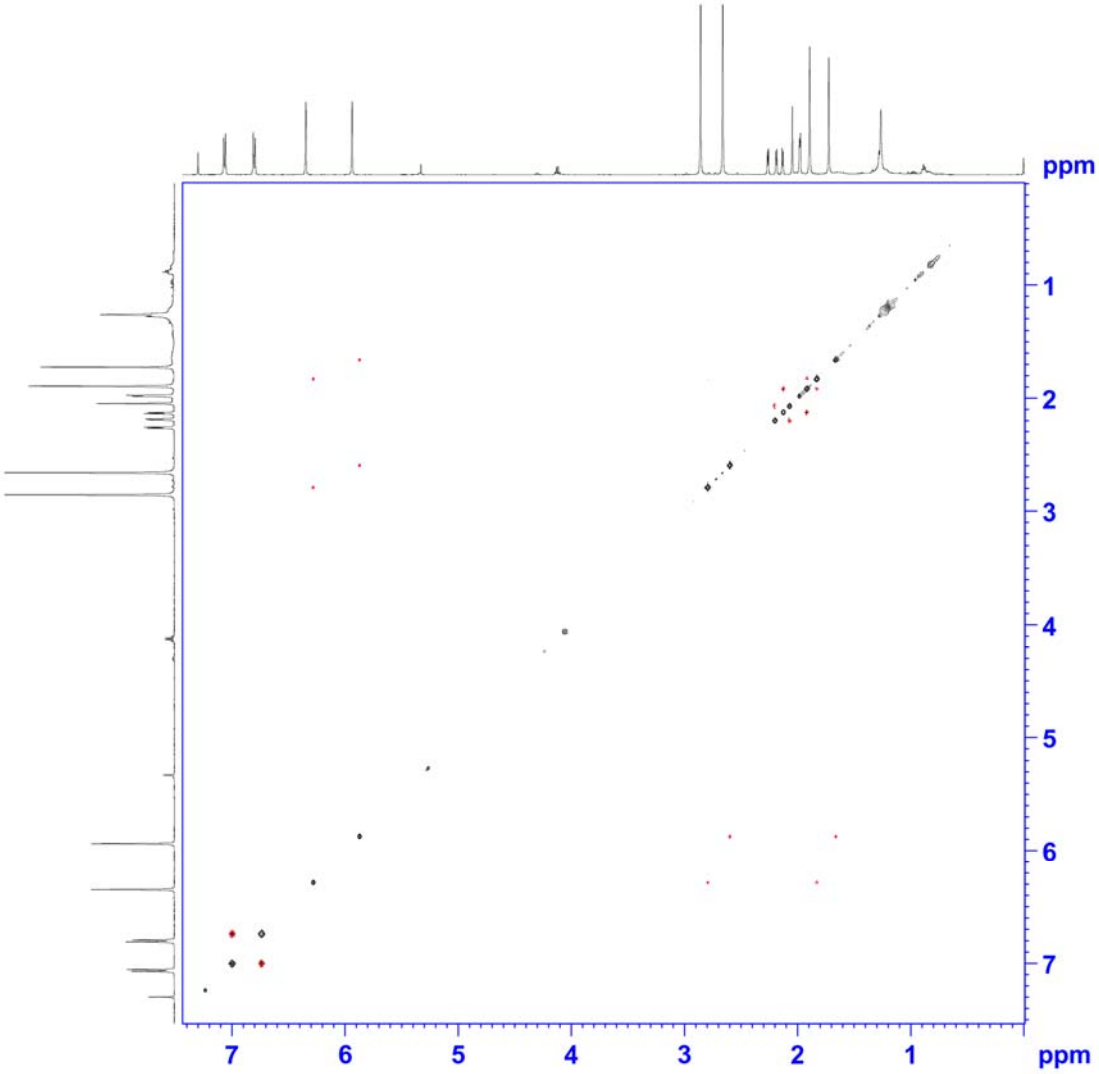

Figure S34. ^{1}H, ^{1}H NOESY spectrum of **4e** (500 MHz, 298 K, $CDCl_3$).

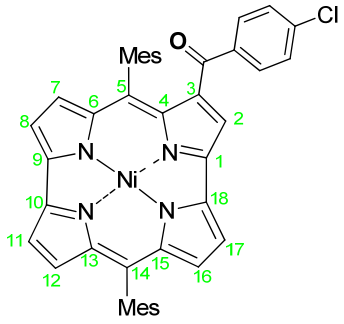

4e

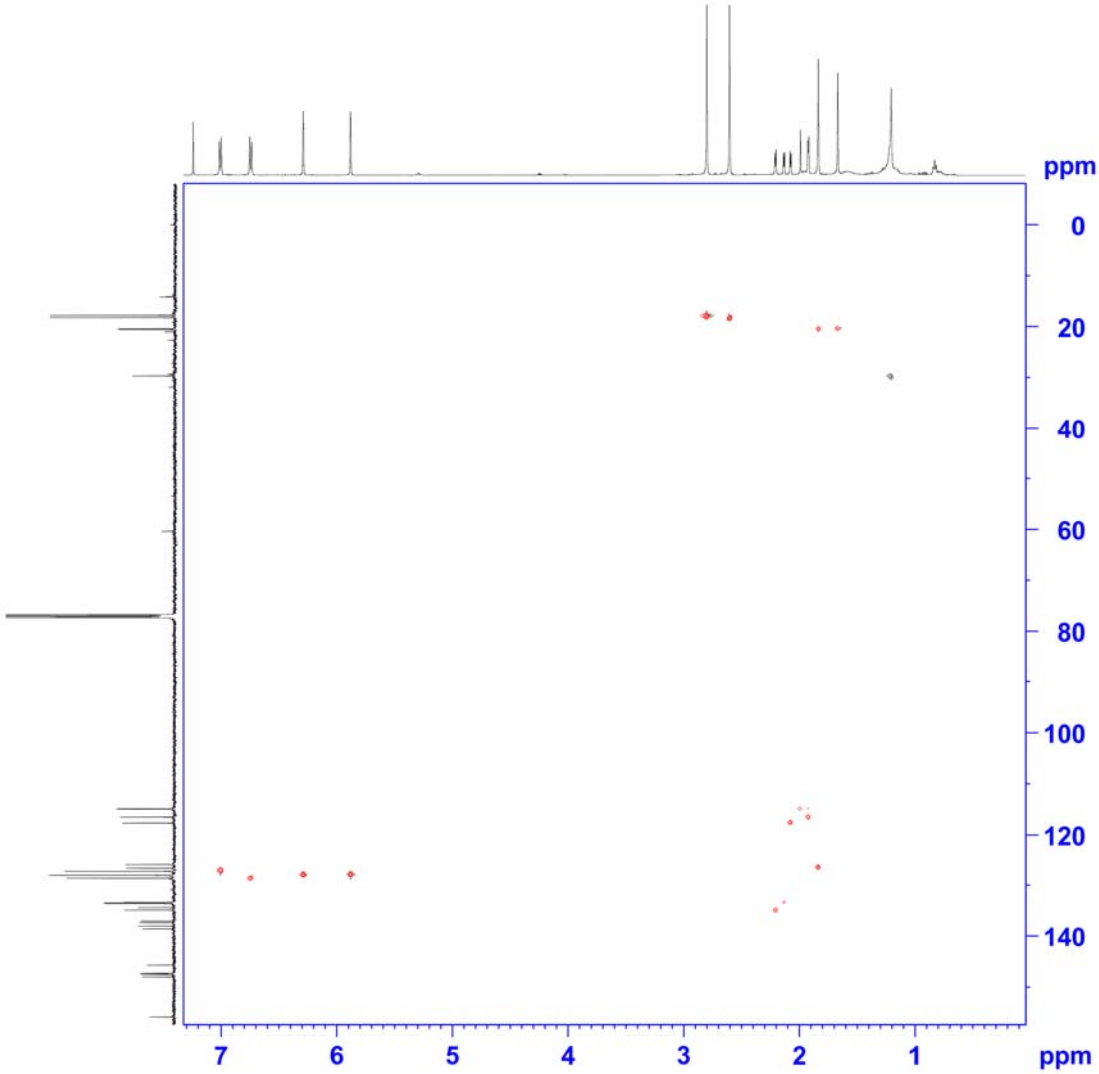

Figure S35. ^{1}H, ^{13}C HSQC spectrum of **4e** (500/125 MHz, 298 K, $CDCl_3$).

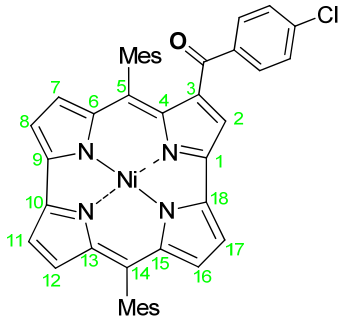

4e

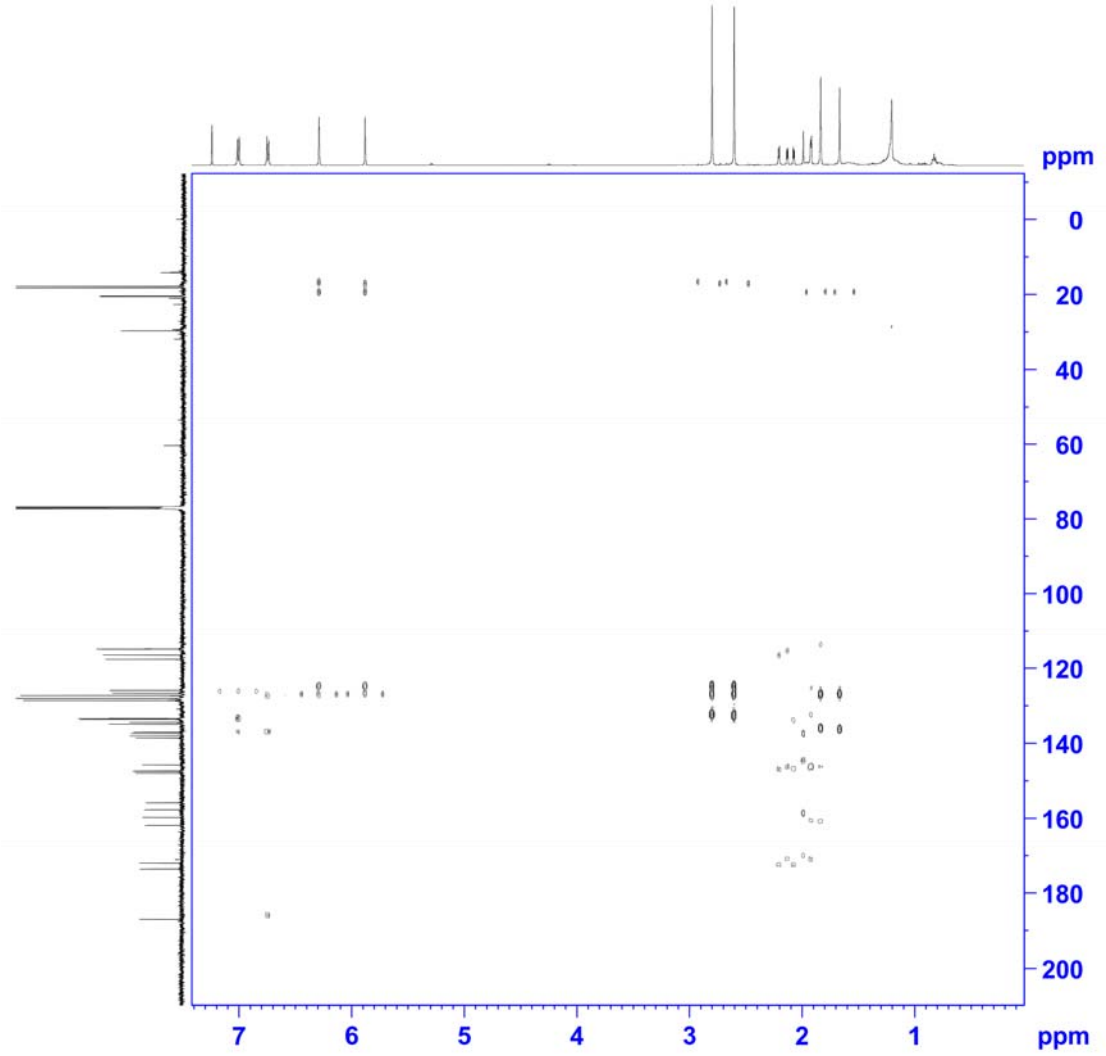

Figure S36. ^{1}H, ^{13}C HMBC spectrum of **4e** (500/125 MHz, 298 K, $CDCl_3$).

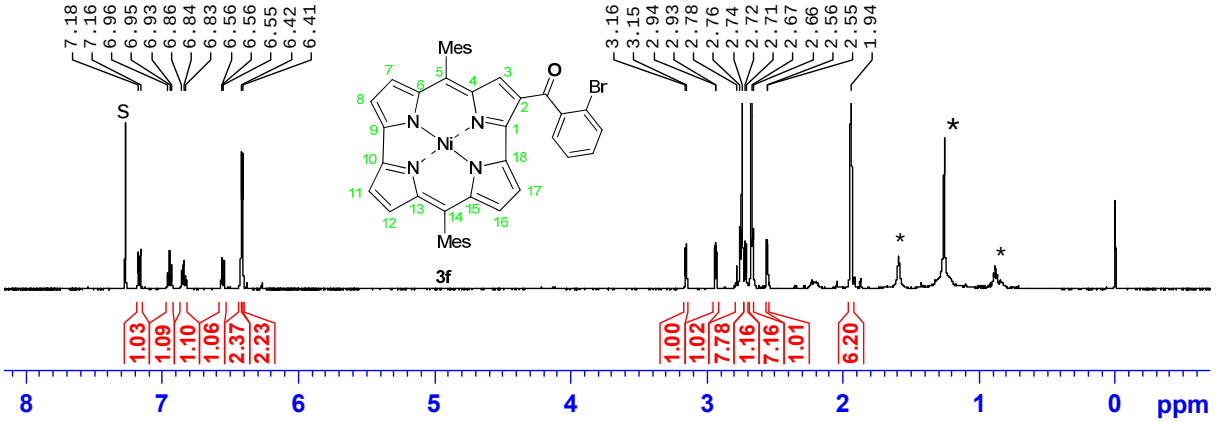

Figure S37. ^{1}H NMR spectrum of **3f** (500 MHz, 298 K, $CDCl_3$).

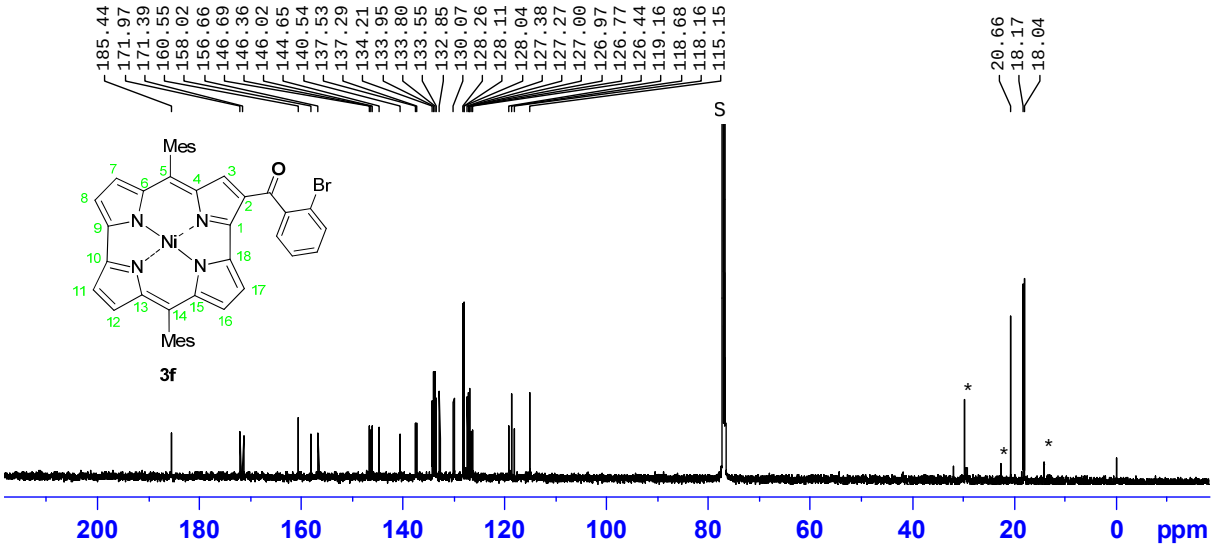

Figure S38. ^{13}C NMR spectrum of **3f** (125 MHz, 298 K, $CDCl_3$).

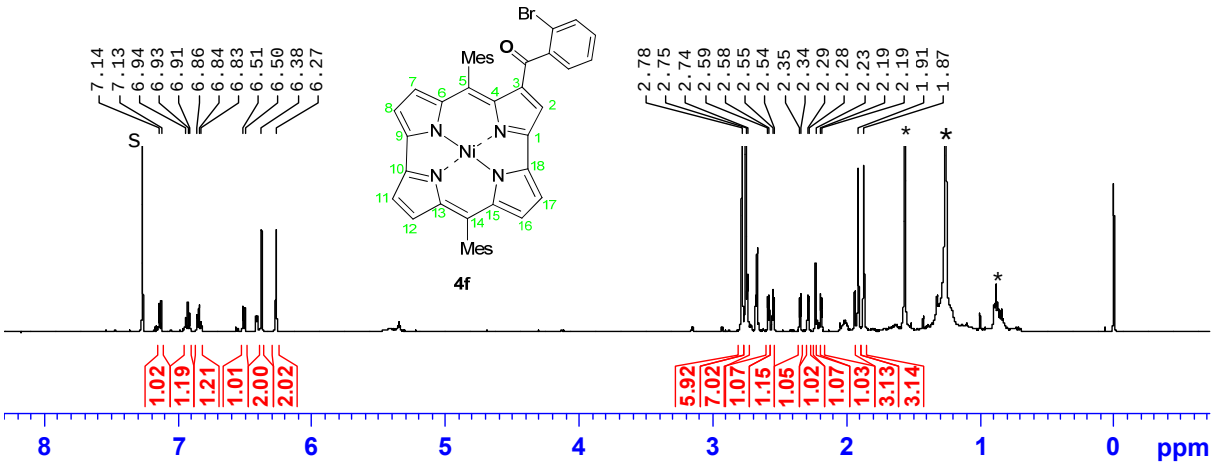

Figure S39. ^{1}H NMR spectrum of **4f** (500 MHz, 298 K, $CDCl_3$).

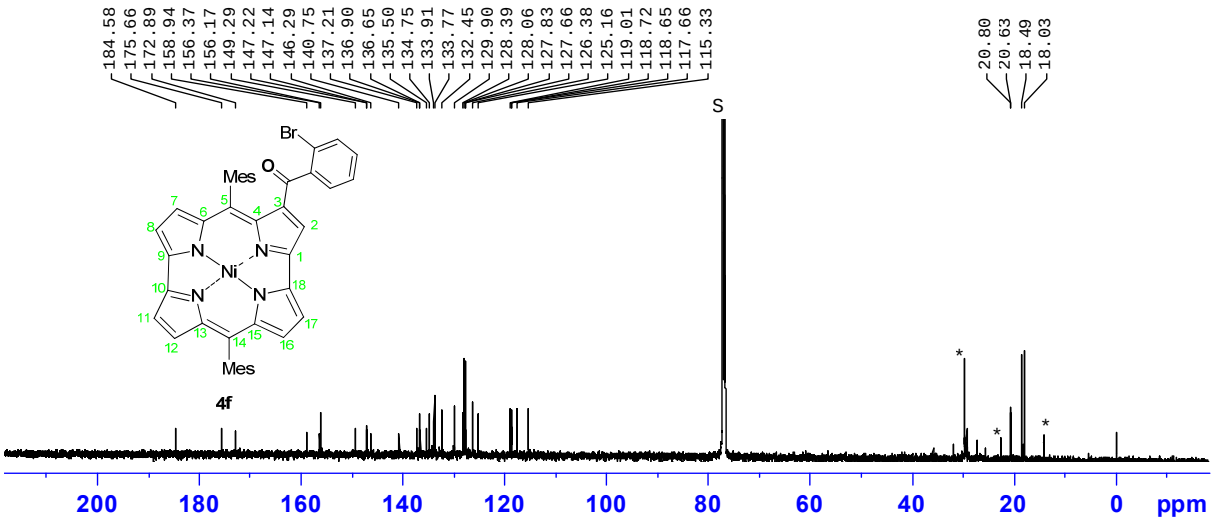

Figure S40. ^{13}C NMR spectrum of **4f** (125 MHz, 298 K, $CDCl_3$).

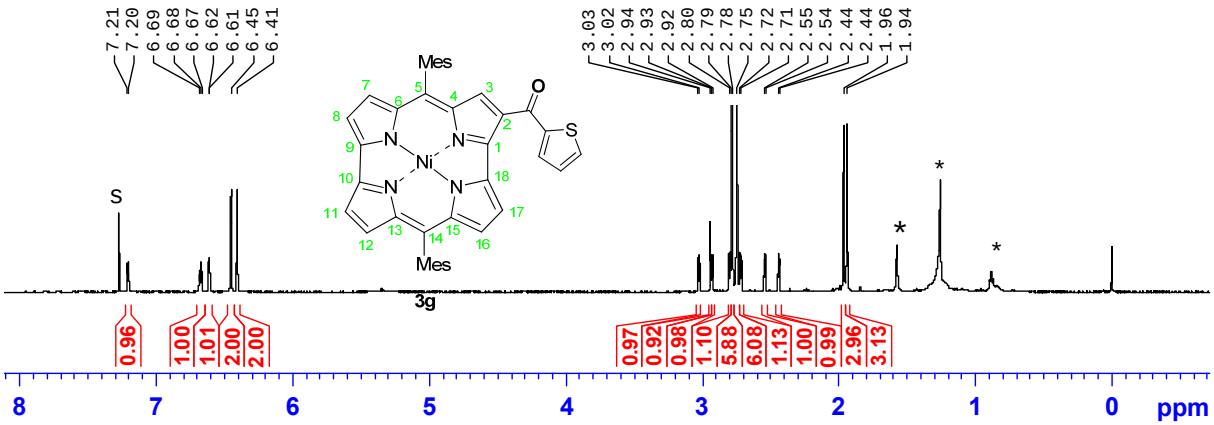

Figure S41. ^{1}H NMR spectrum of **3g** (500 MHz, 298 K, $CDCl_3$).

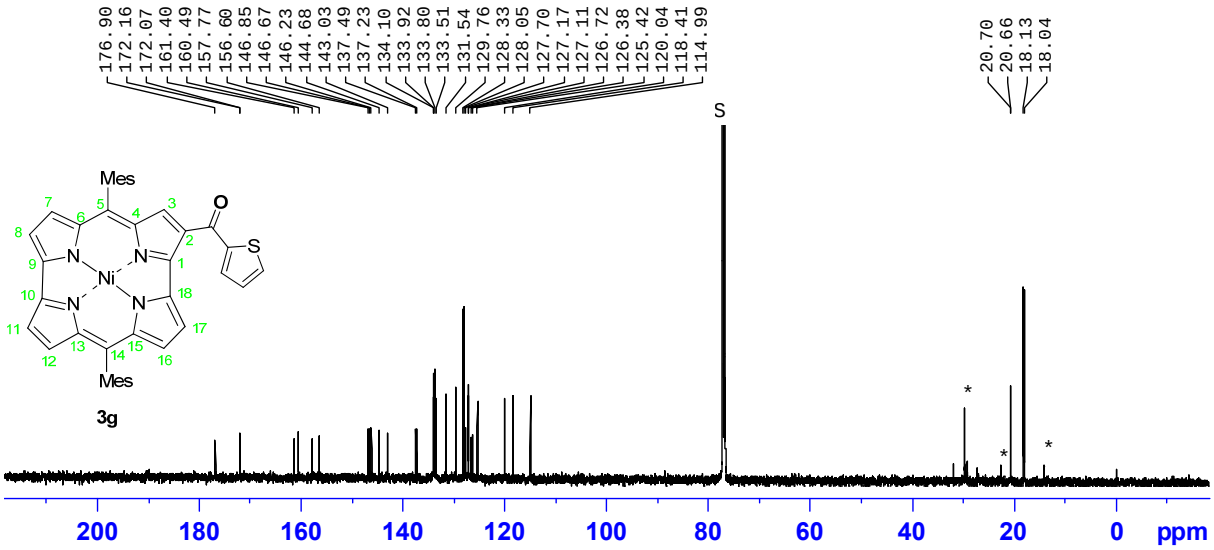

Figure S42. ^{13}C NMR spectrum of **3g** (125 MHz, 298 K, $CDCl_3$).

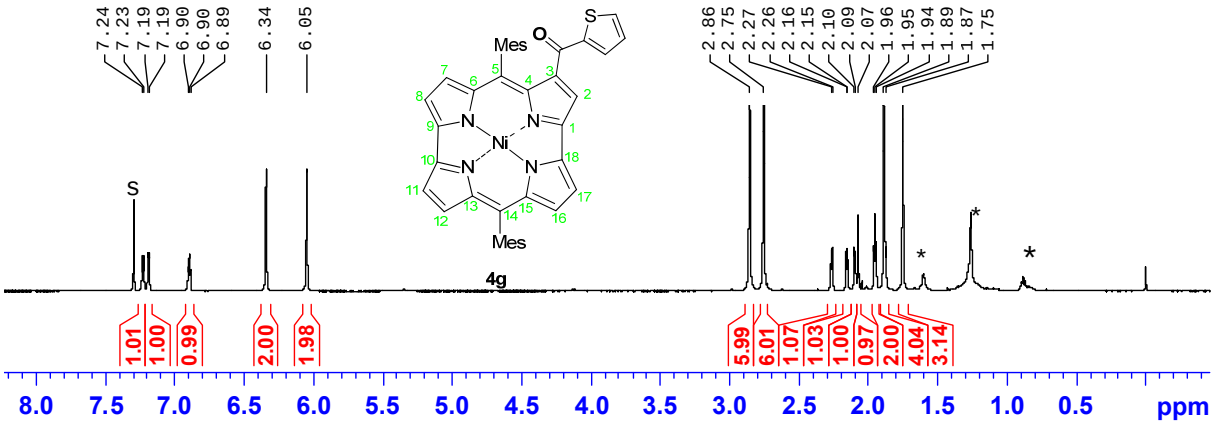

Figure S43. ^{1}H NMR spectrum of **4g** (500 MHz, 298 K, $CDCl_3$).

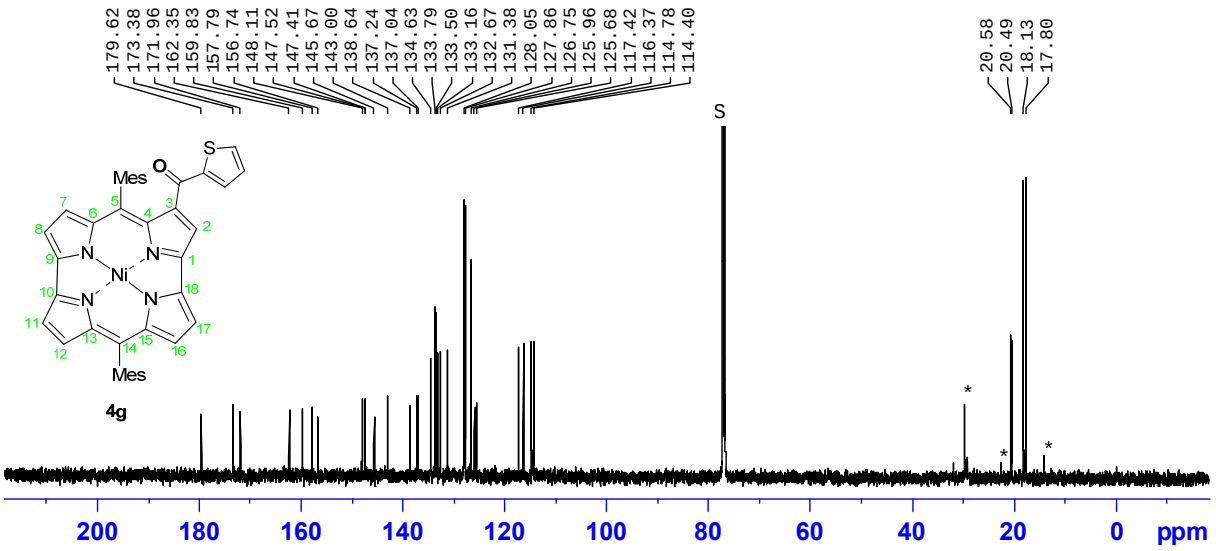

Figure S44. ^{13}C NMR spectrum of **4g** (125 MHz, 298 K, $CDCl_3$).

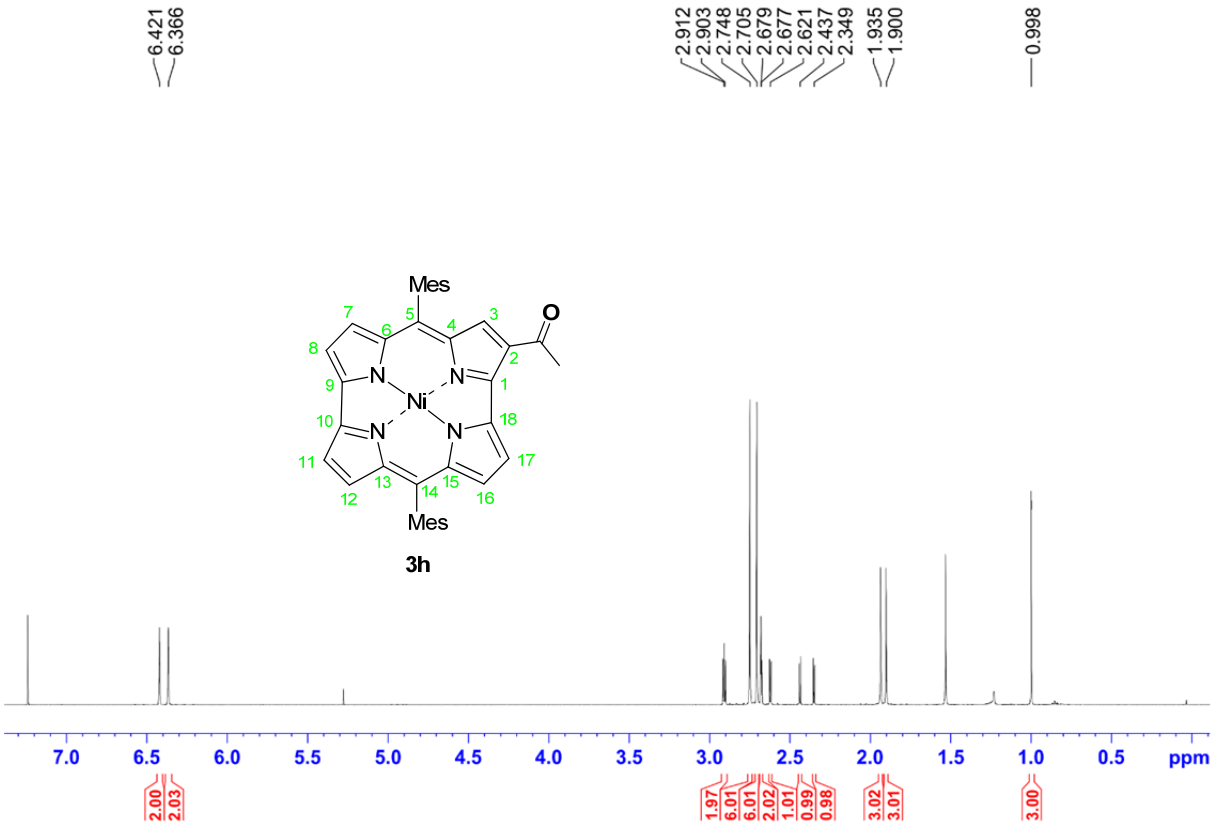

Figure S45. ^{1}H NMR spectrum of **3h** (500 MHz, 300 K, $CDCl_3$).

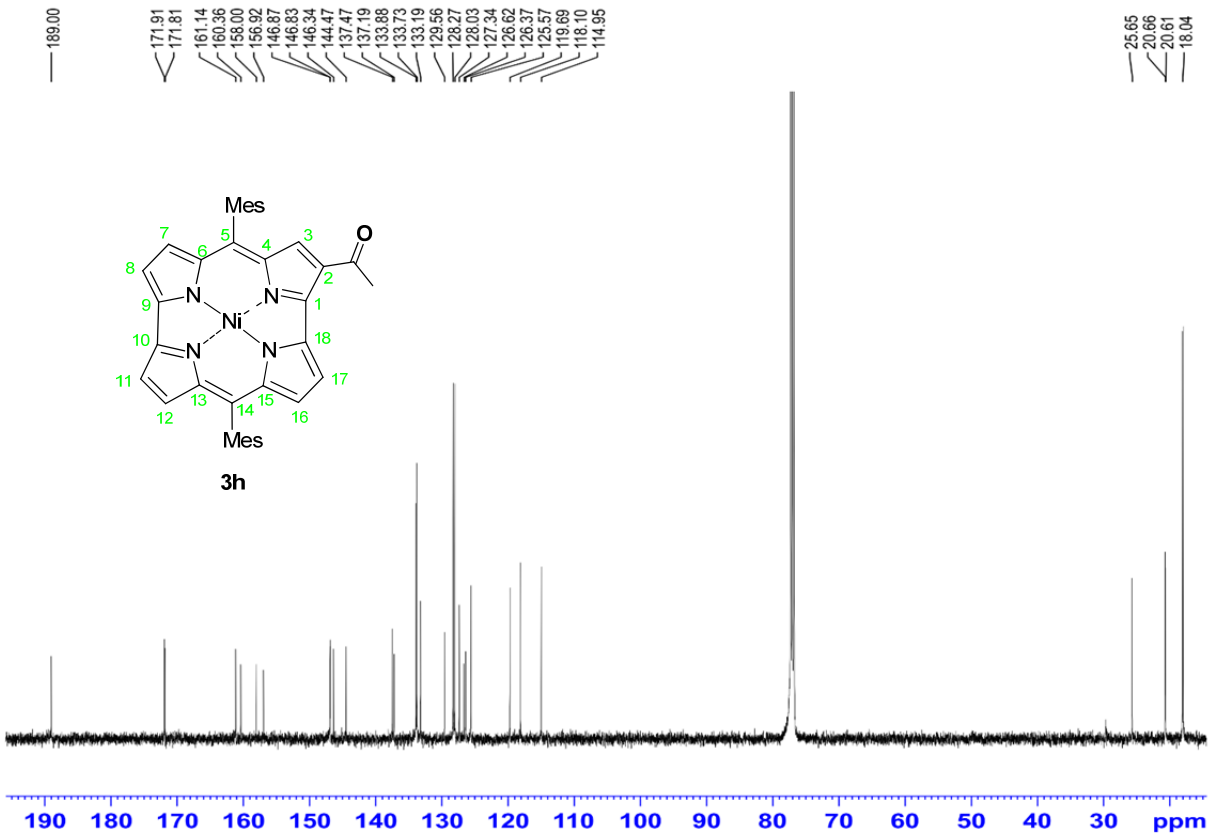

Figure S46. ^{13}C NMR spectrum of 3**h** (150 MHz, 300 K, $CDCl_3$).

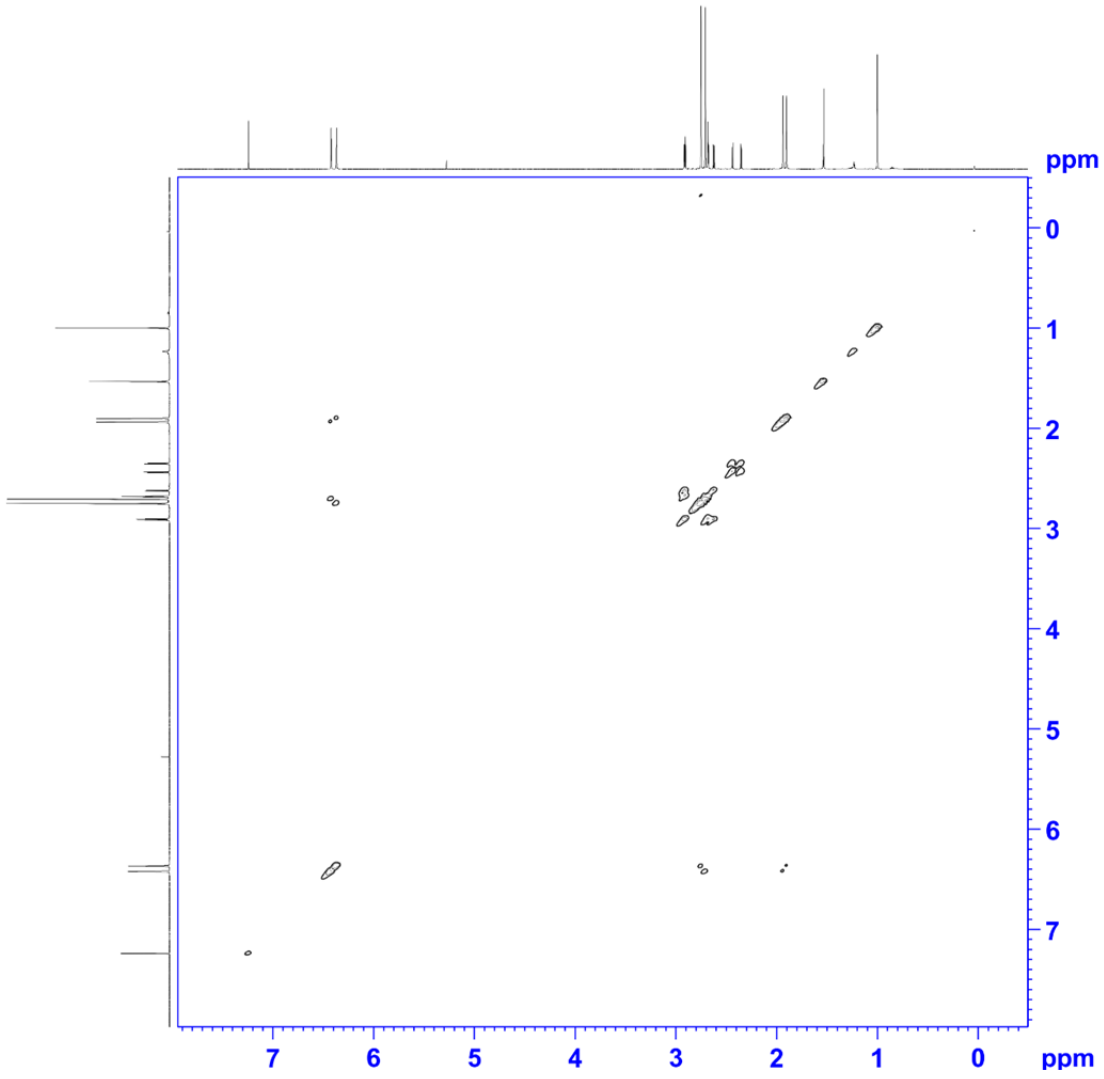

Figure S47. ^{1}H, ^{1}H COSY spectrum of **3h** (500 MHz, 300 K, $CDCl_3$).

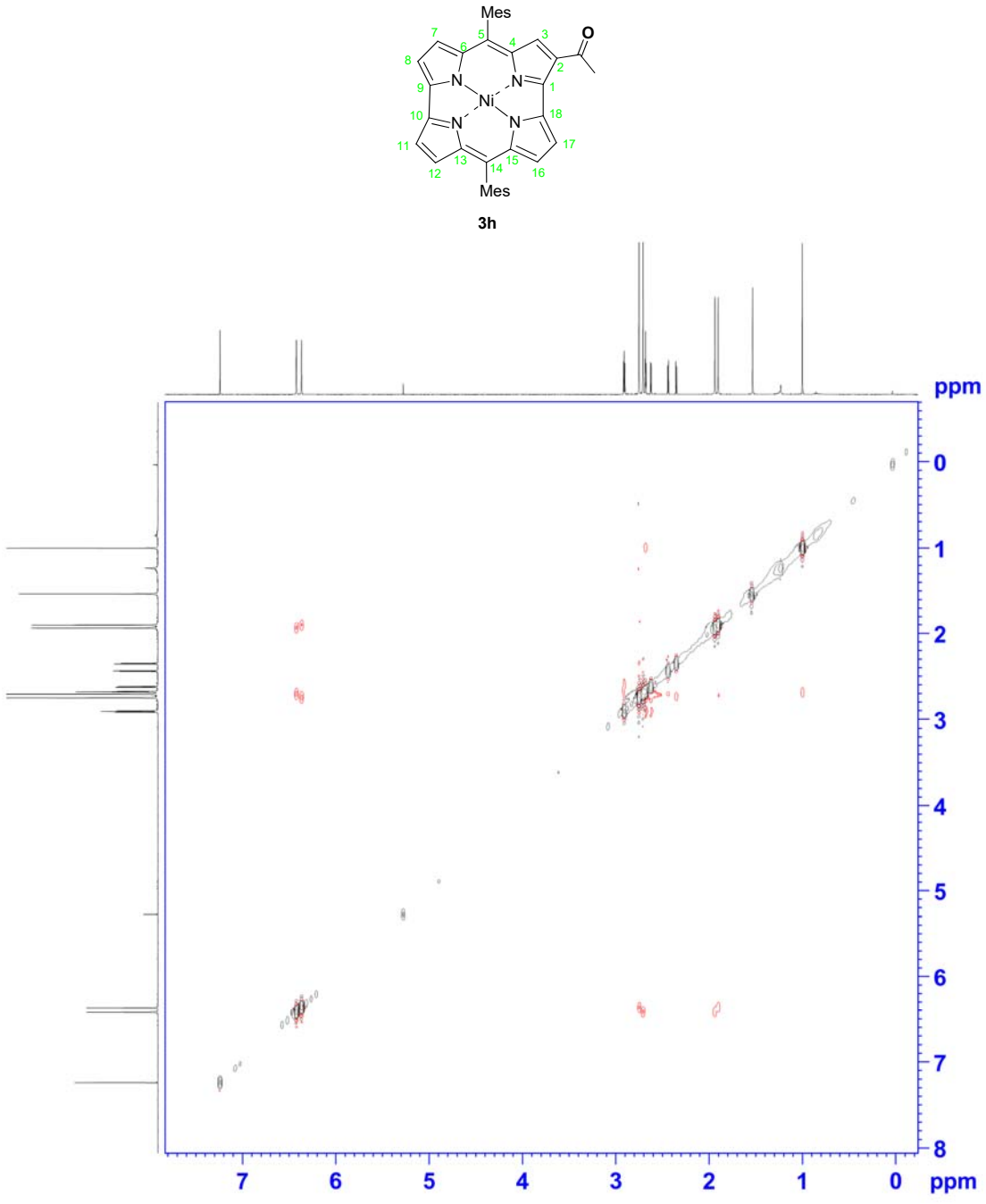

Figure S48. ^{1}H, ^{1}H NOESY spectrum of **3h** (500 MHz, 300 K, $CDCl_3$).

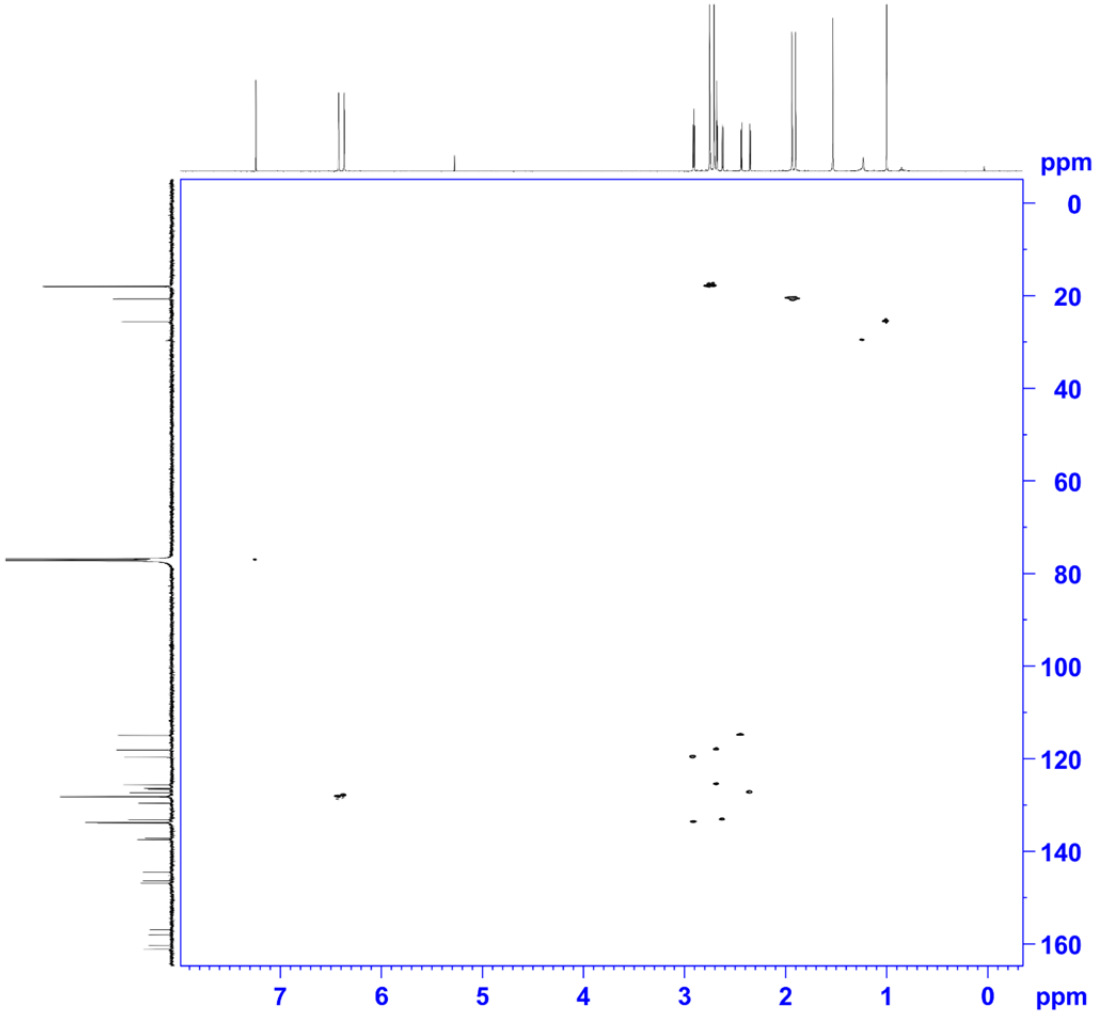

Figure S49. ^{1}H, ^{13}C HSQC spectrum of **3h** (500/125 MHz, 300 K, $CDCl_3$).

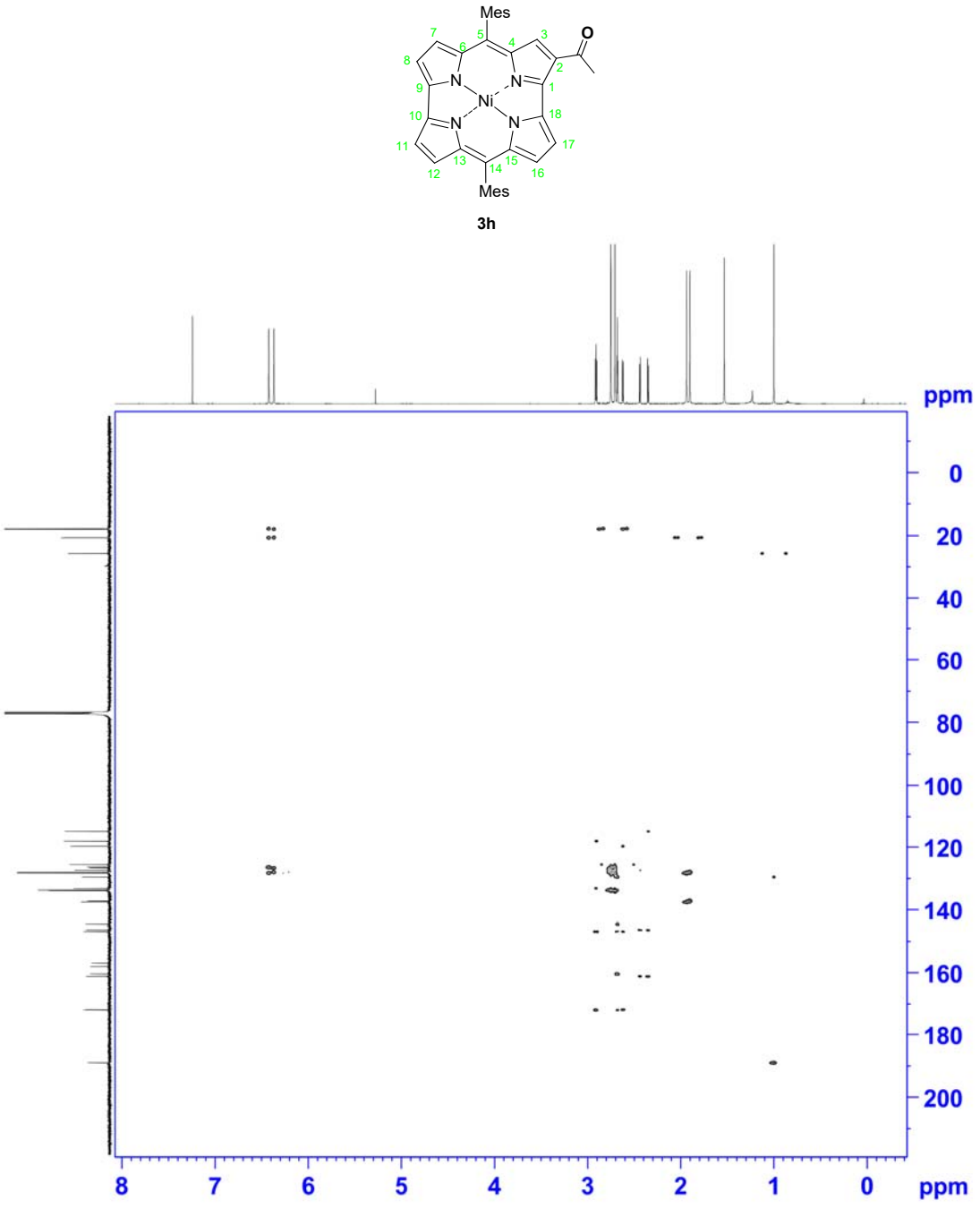

Figure S50. ^{1}H, ^{13}C HMBC spectrum of **3h** (500/125 MHz, 300 K, $CDCl_3$).

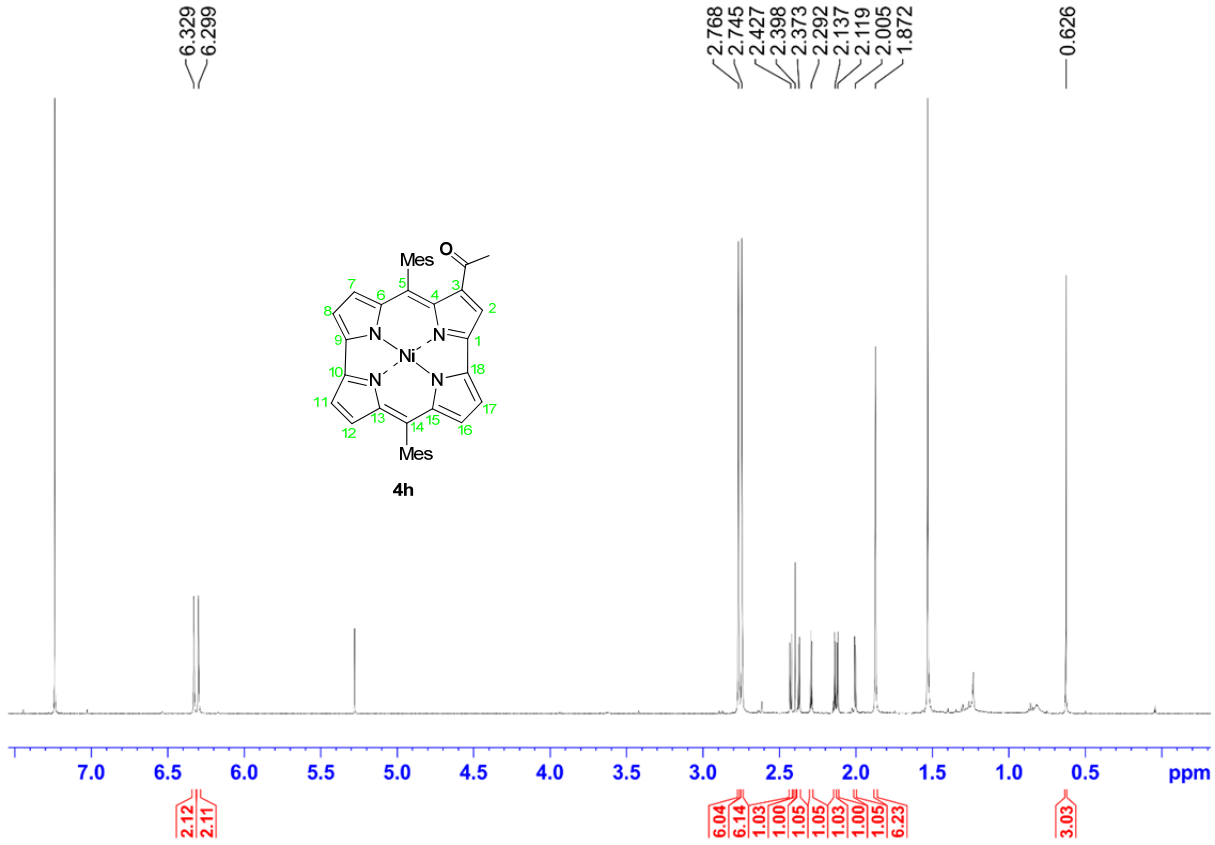

Figure S51. ^{1}H NMR spectrum of **4h** (500 MHz, 300 K, $CDCl_3$).

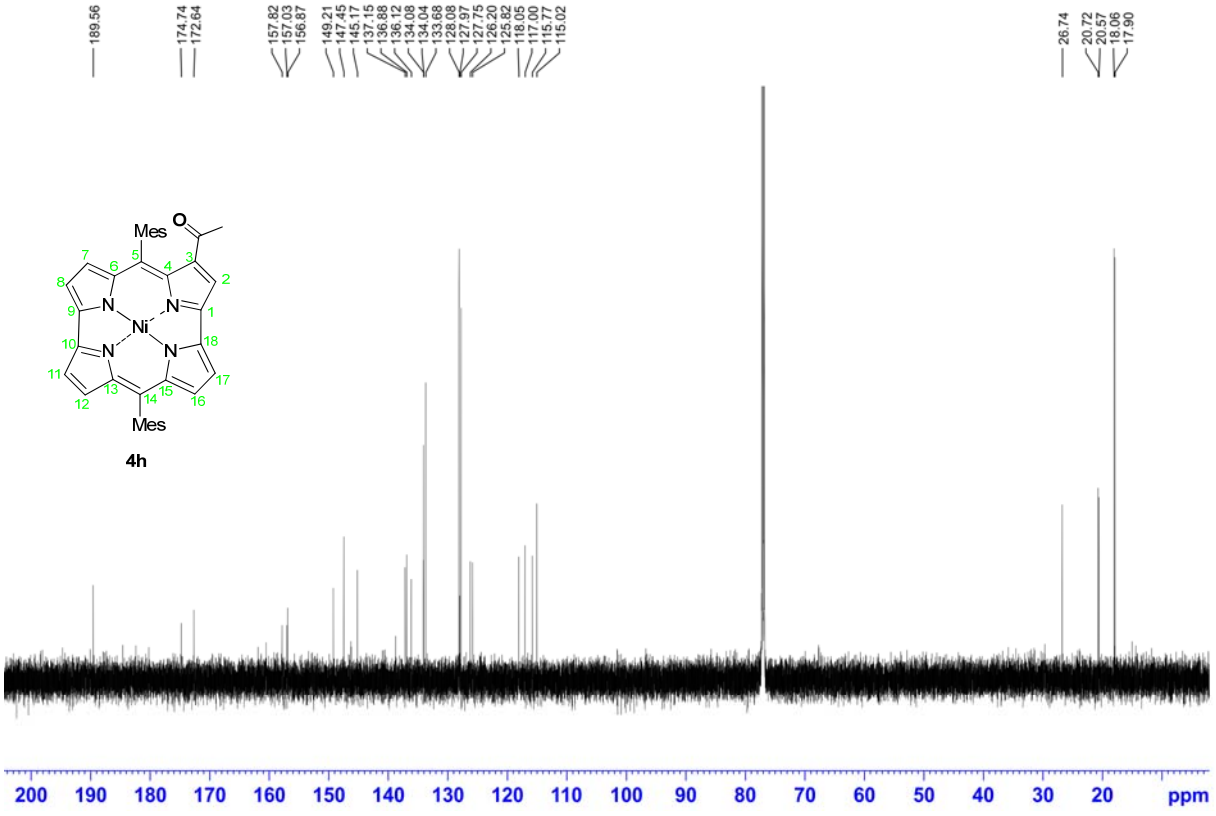

Figure S52. ^{13}C NMR spectrum of 4**h** (150 MHz, 300 K, $CDCl_3$).

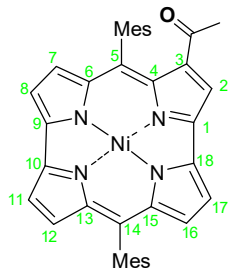

4h

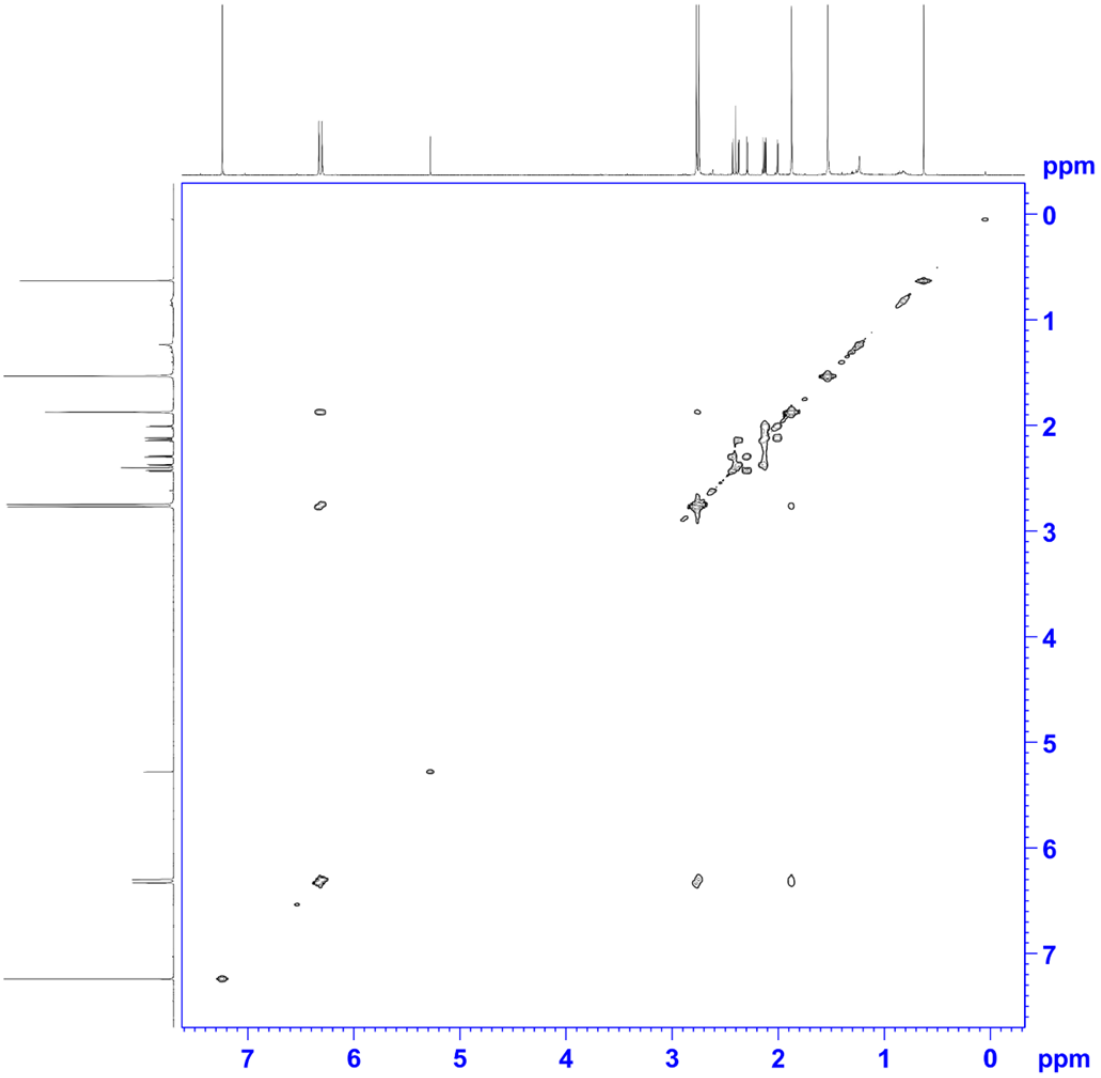

Figure S53. ^{1}H, ^{1}H COSY spectrum of **4h** (500 MHz, 300K, $CDCl_3$).

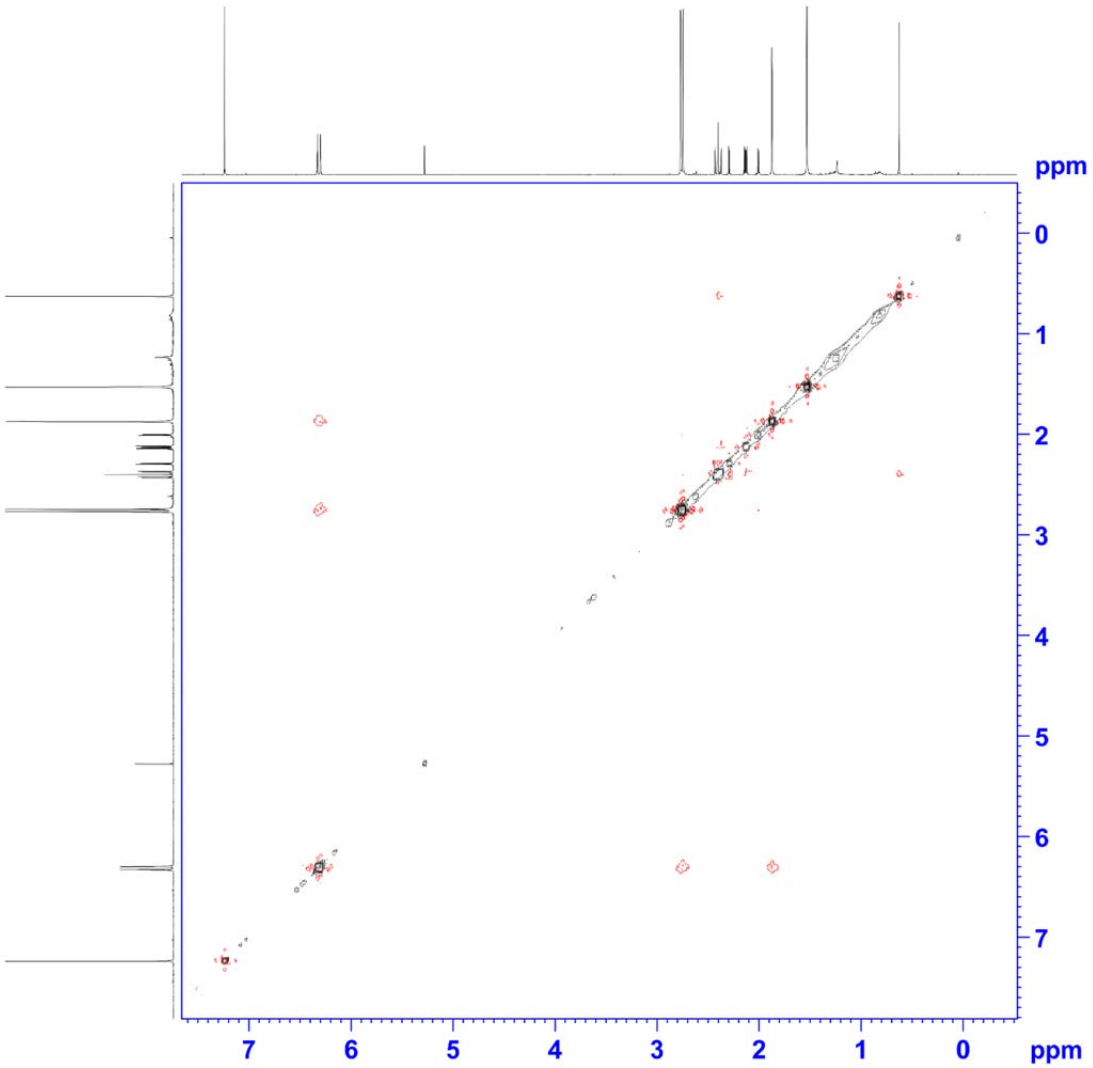

Figure S54. ^{1}H, ^{1}H NOESY spectrum of **4h** (500 MHz, 300 K, $CDCl_3$).

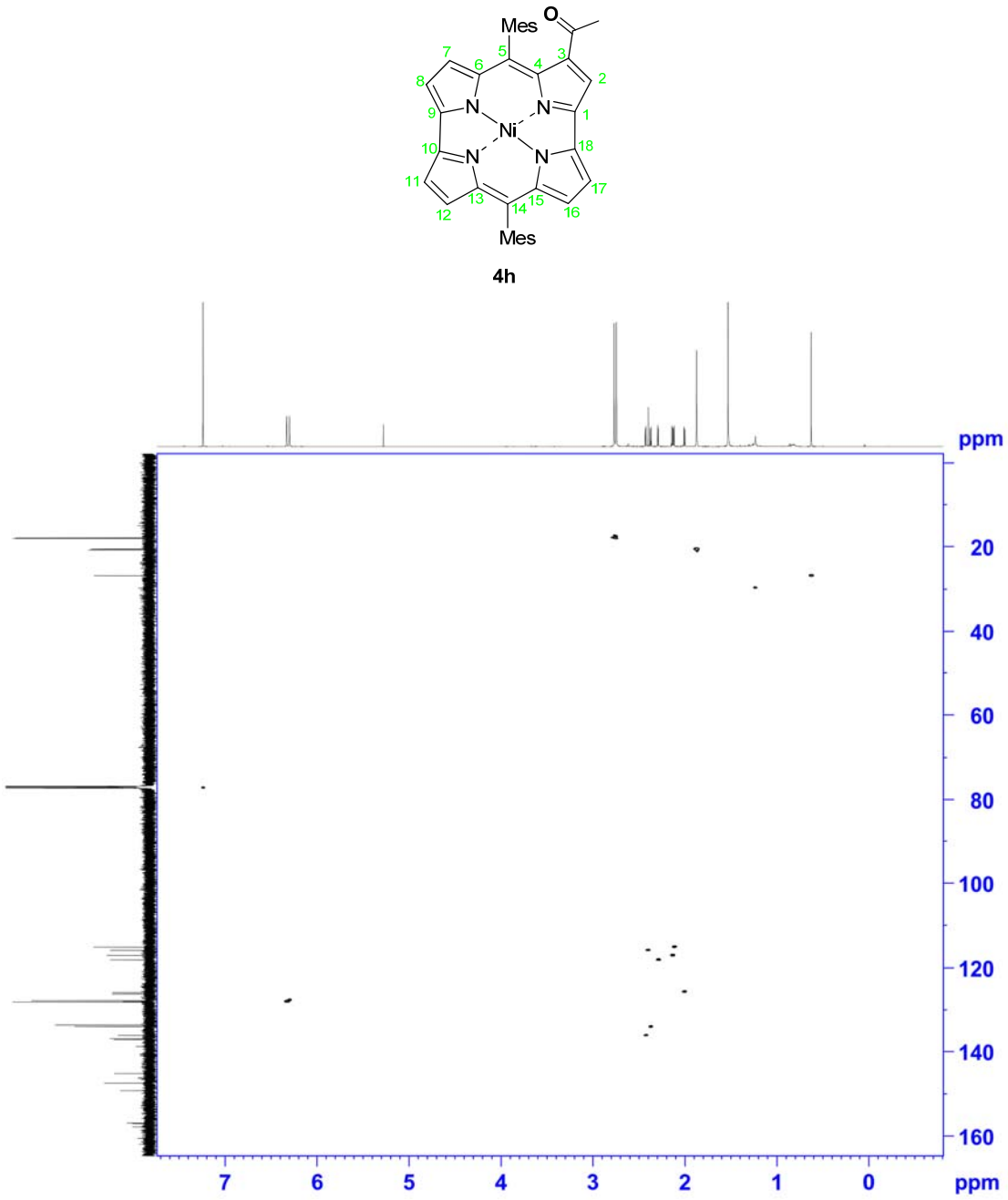

4h

Figure S55. ^{1}H, ^{13}C HSQC spectrum of **4h** (500/125 MHz, 300 K, $CDCl_3$).

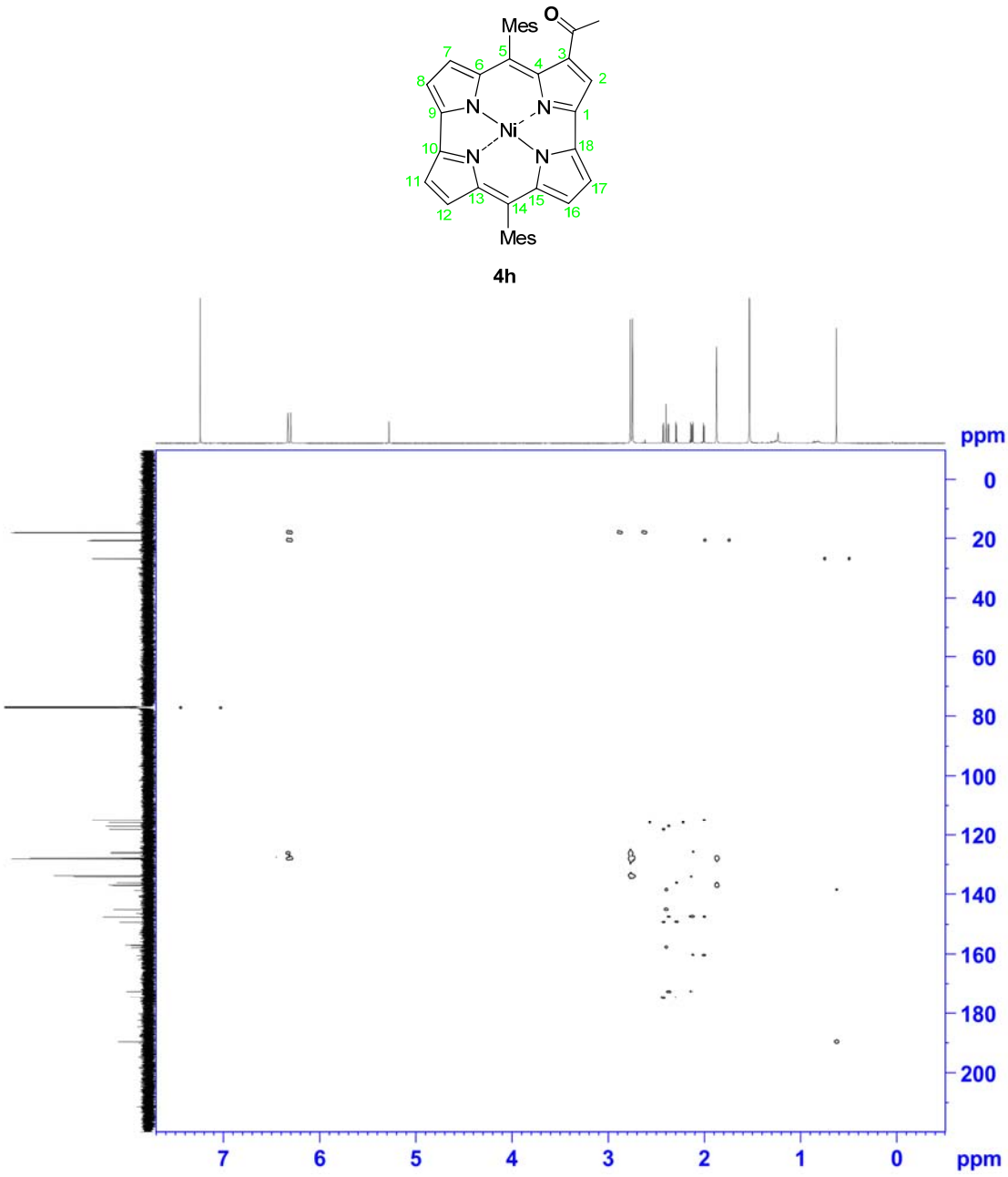

4h

Figure S56. ^{1}H, ^{13}C HMBC spectrum of **4h** (500/125 MHz, 300 K, $CDCl_3$).

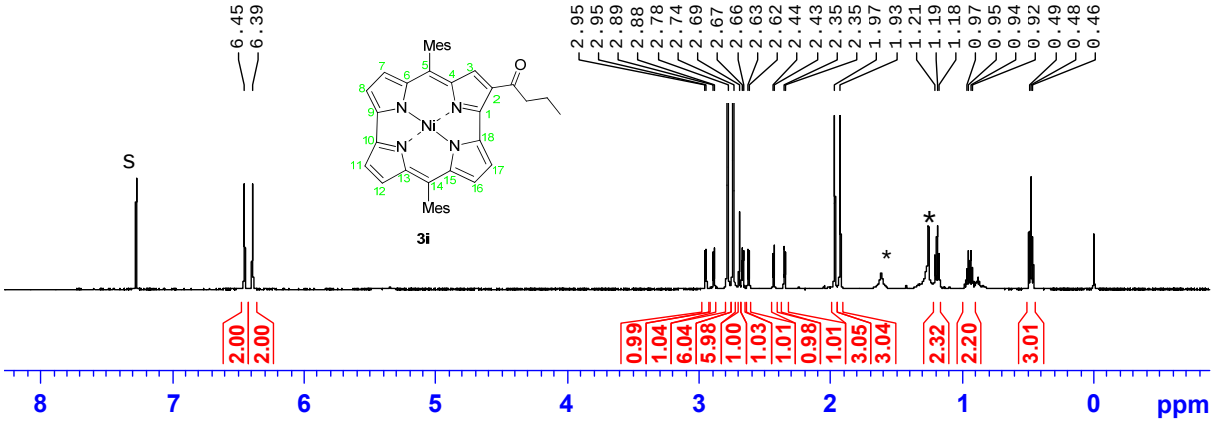

Figure S57. ^{1}H NMR spectrum of **3i** (500 MHz, 298 K, $CDCl_3$).

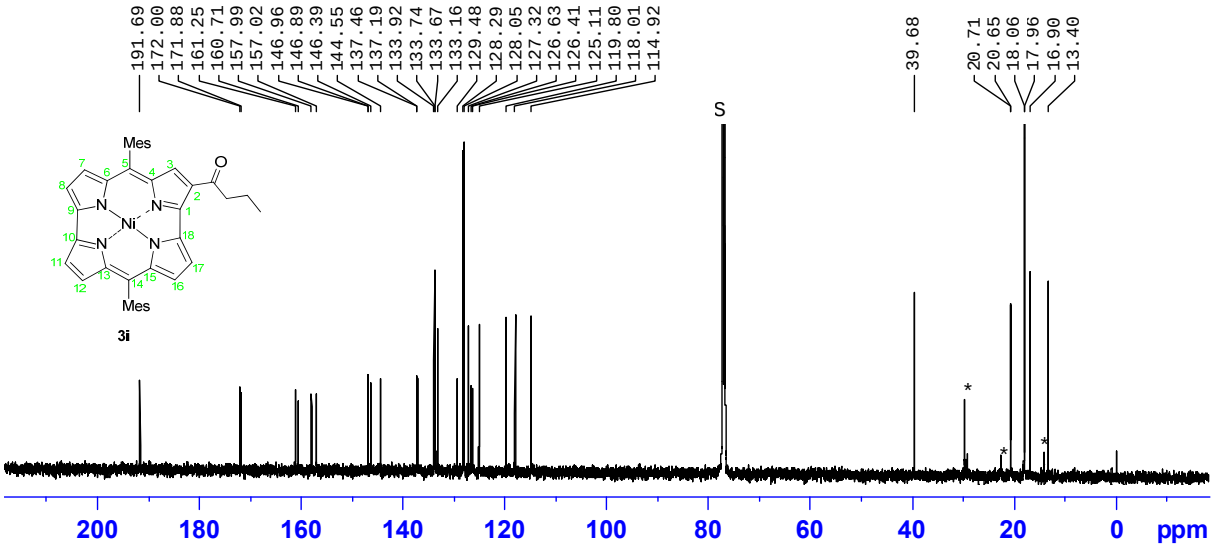

Figure S58. ^{13}C NMR spectrum of **3i** (500 MHz, 298 K, $CDCl_3$).

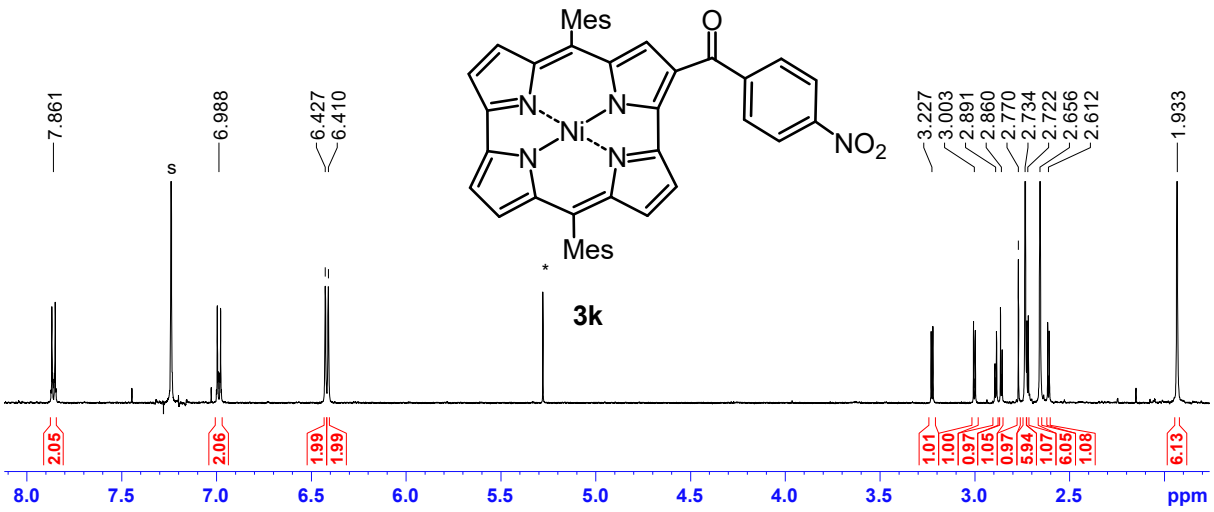

Figure S59. ^{1}H NMR spectrum of **3k** (500 MHz, 300 K, $CDCl_3$).

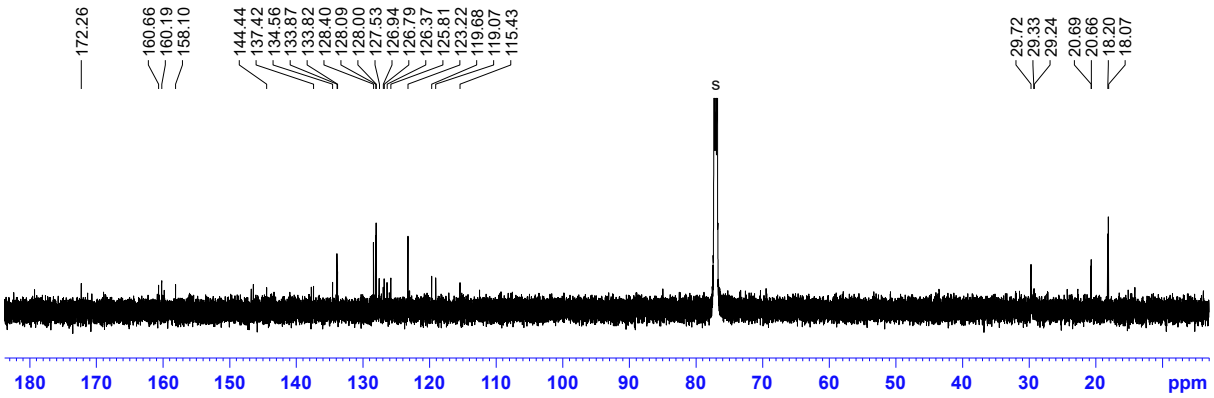

Figure S60. ^{13}C NMR spectrum of 3**k** (150 MHz, 300 K, $CDCl_3$).

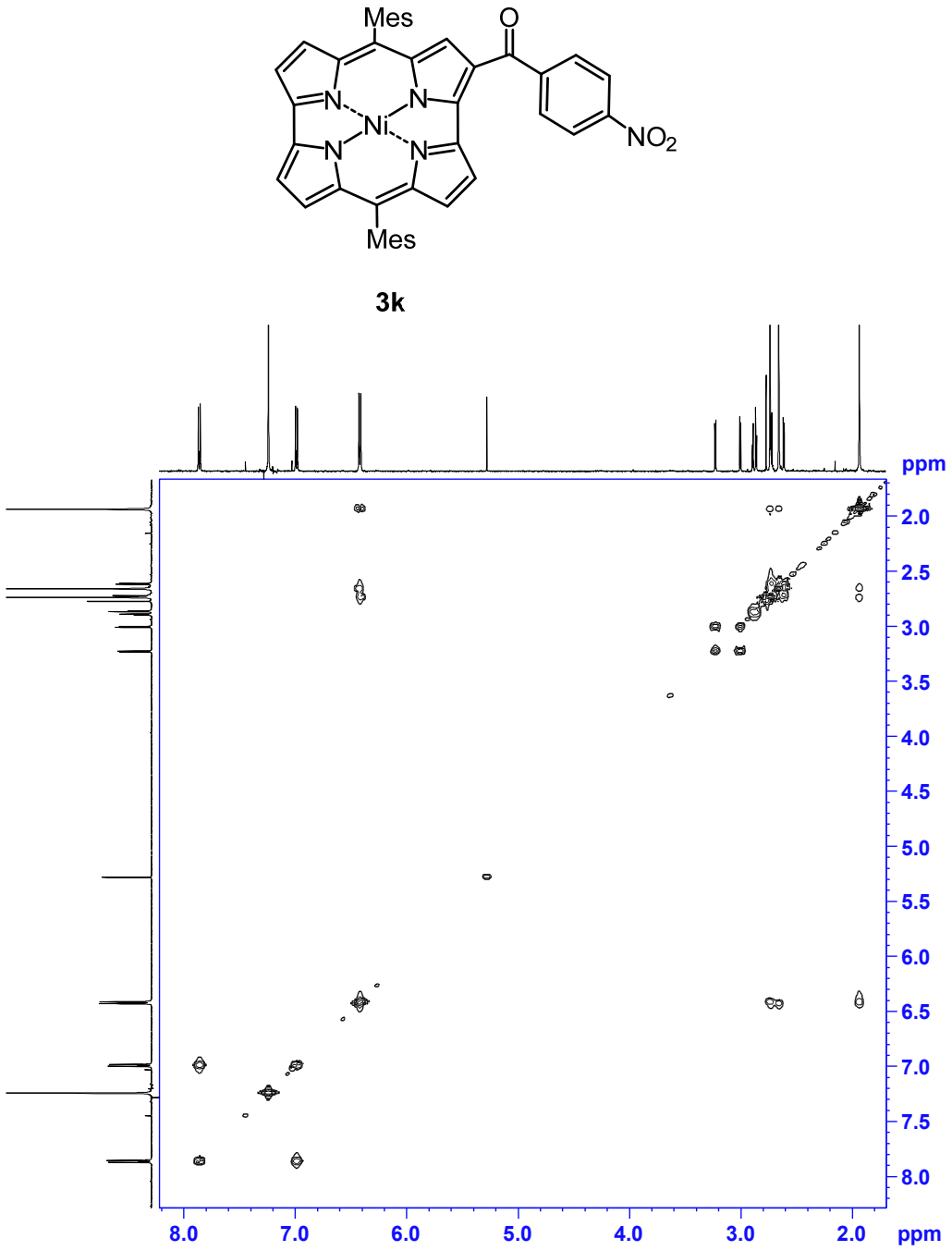

Figure S61. ^{1}H, ^{1}H COSY spectrum of **3k** (500 MHz, 300 K, $CDCl_3$).

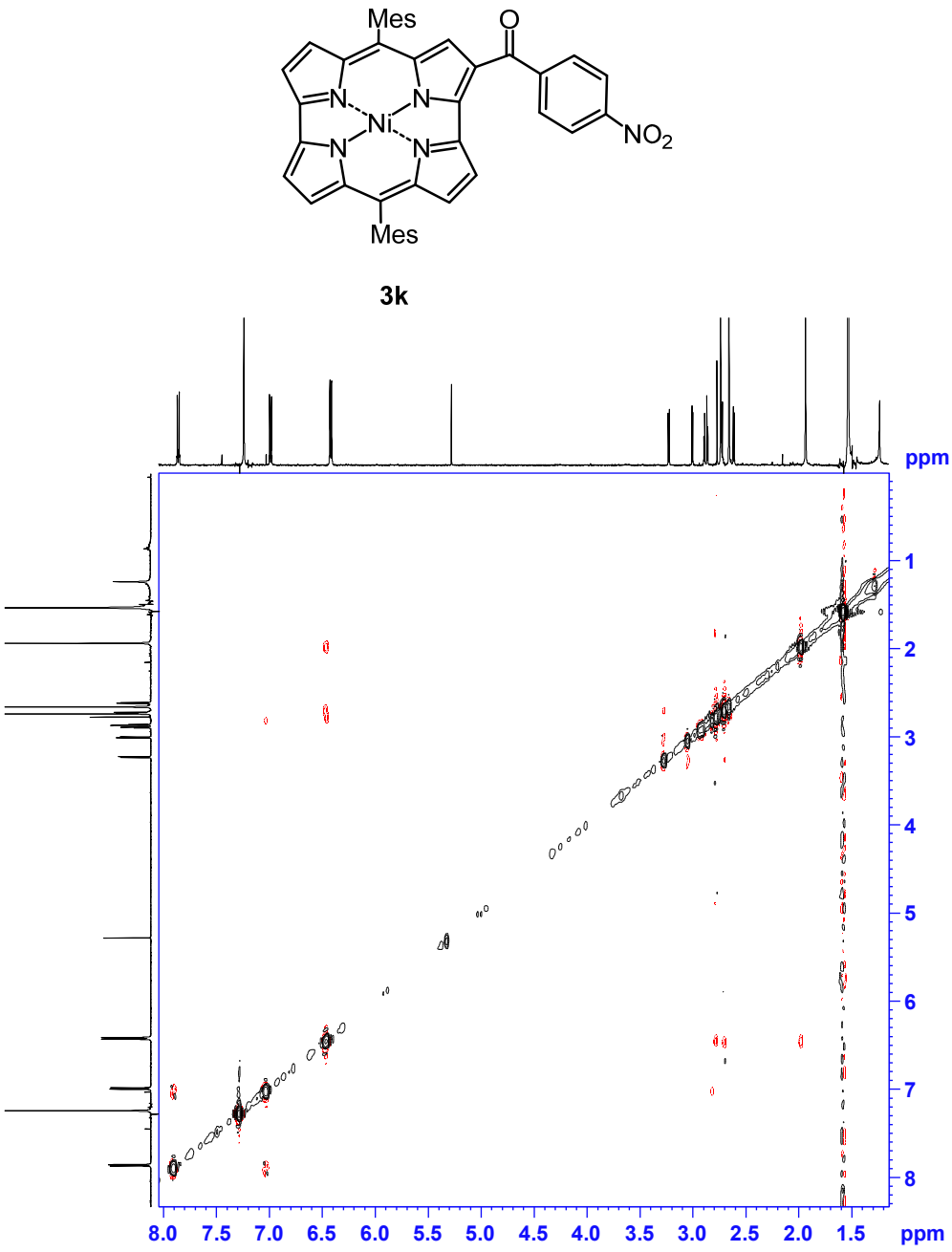

Figure S62. ^{1}H, ^{1}H NOESY spectrum of **3k** (500 MHz, 300 K, $CDCl_3$).

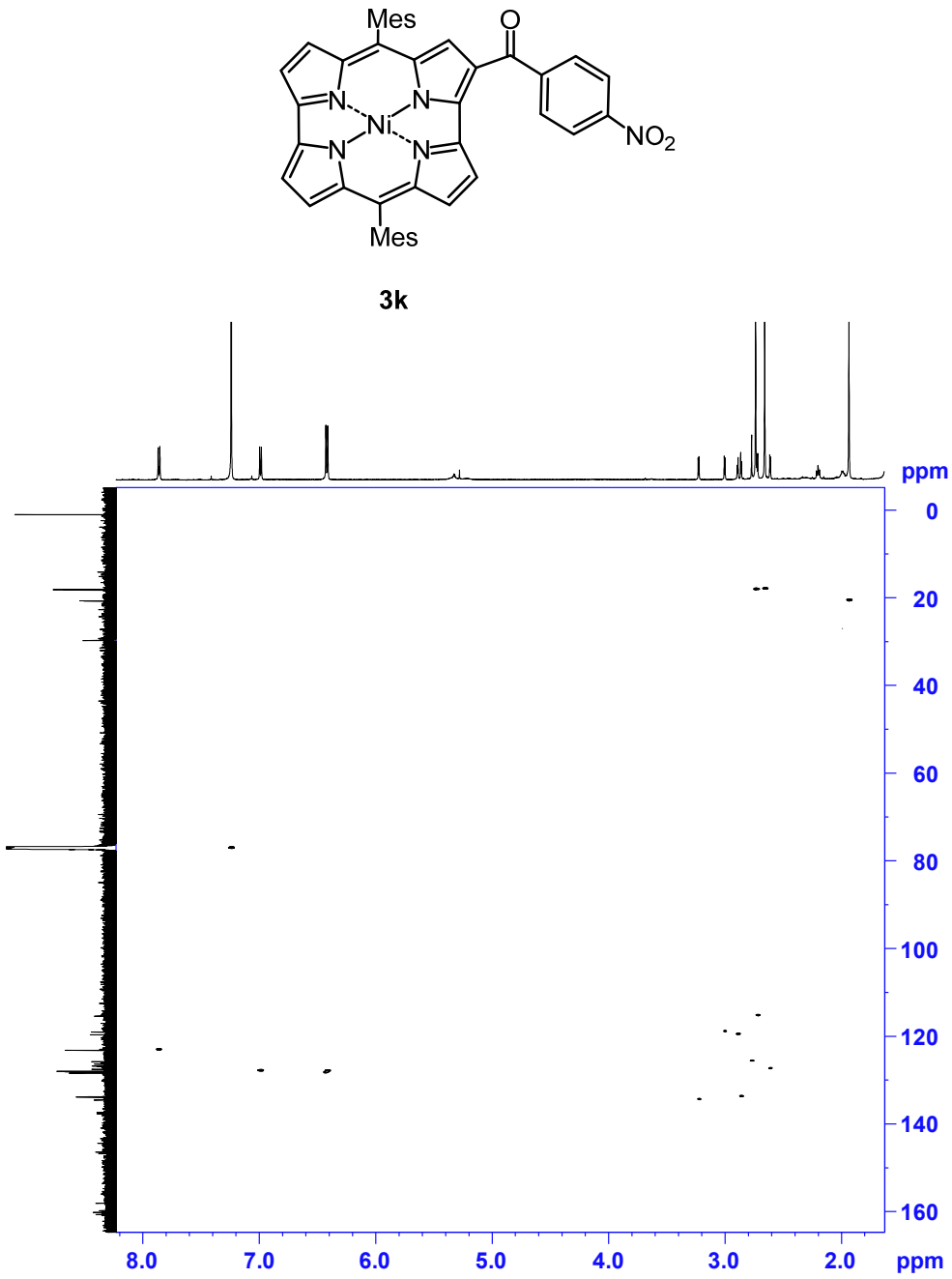

Figure S63. ^{1}H, ^{13}C HSQC spectrum of **3k** (600/150 MHz, 300 K, $CDCl_3$).

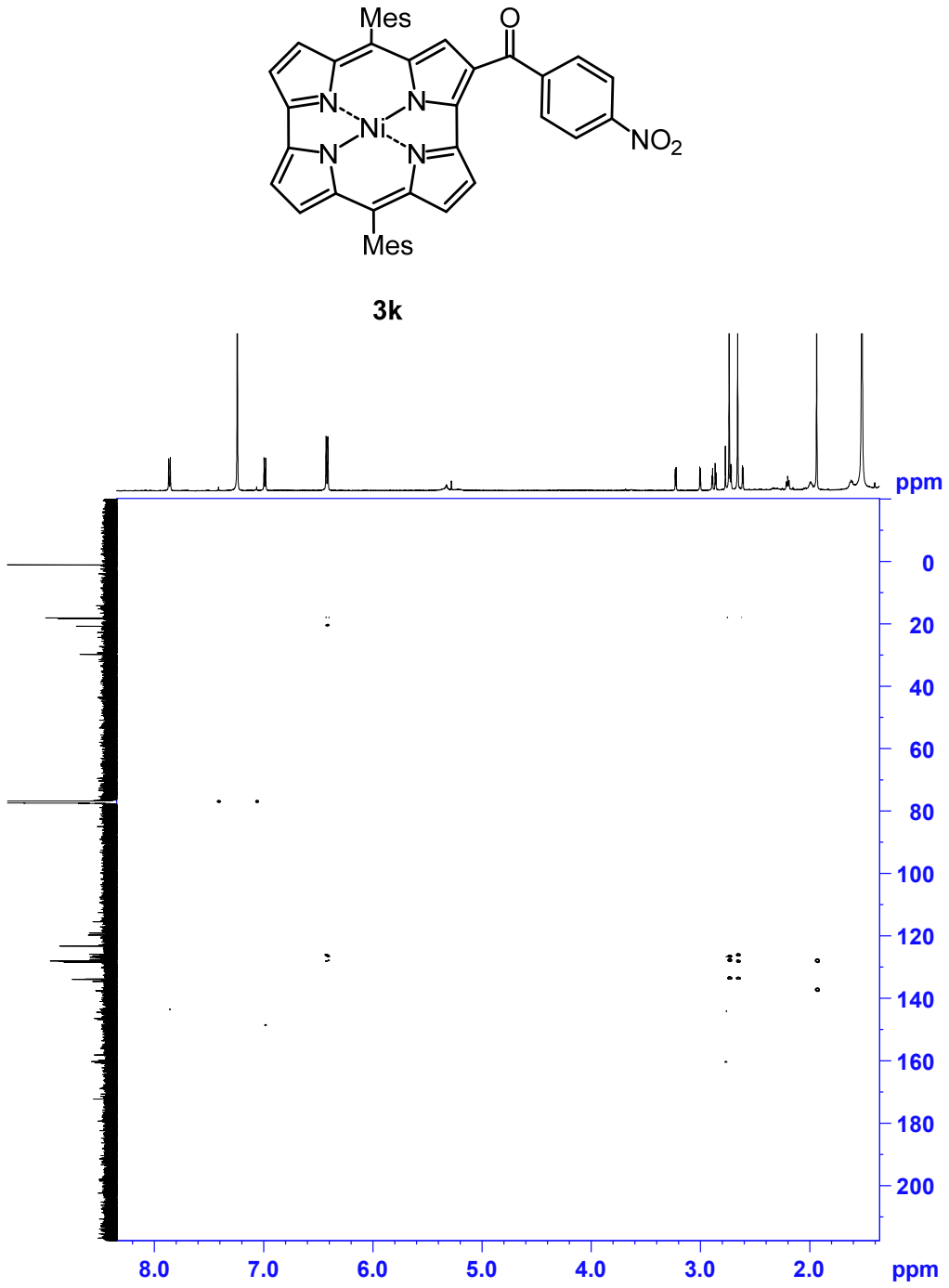

Figure S64. ^{1}H, ^{13}C HMBC spectrum of **3k** (600/150 MHz, 300 K, $CDCl_3$).

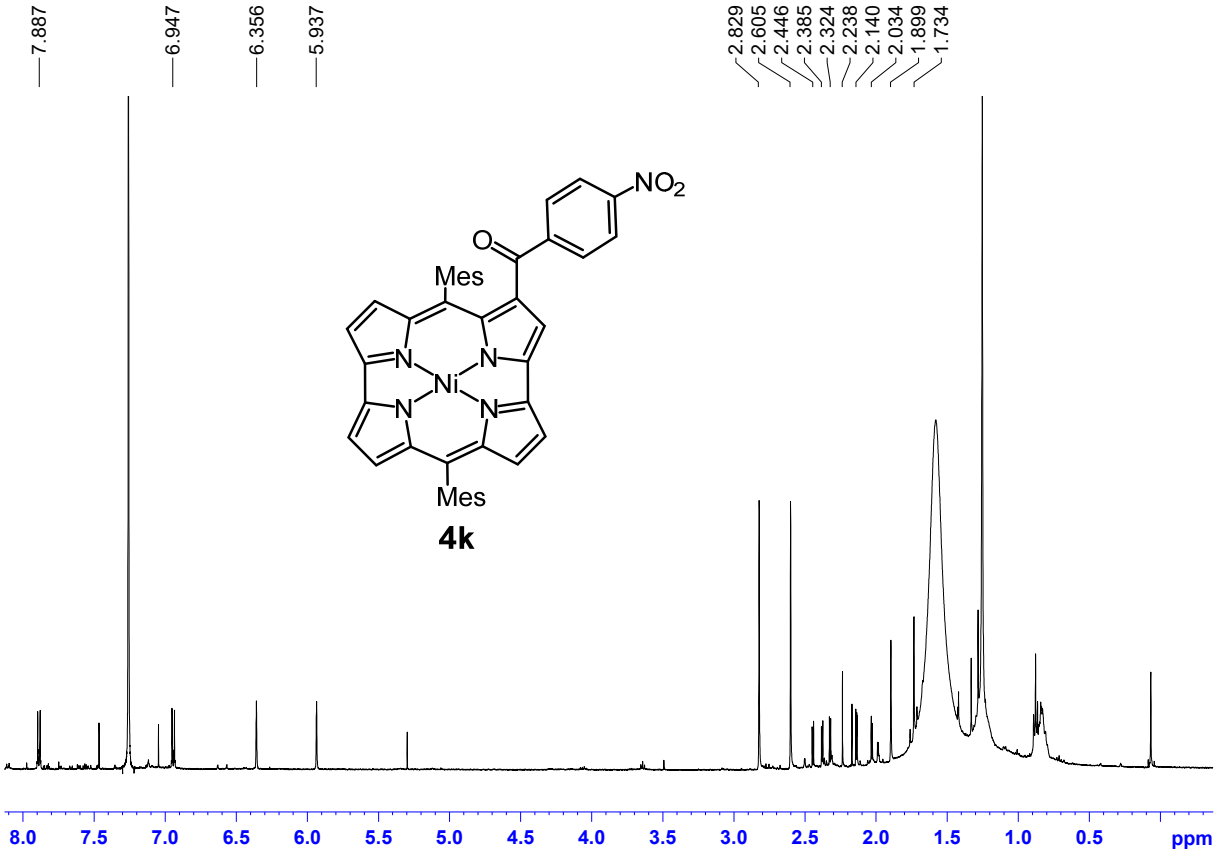

Figure S65. ^{1}H NMR spectrum of **4k** (500 MHz, 300 K, $CDCl_3$).

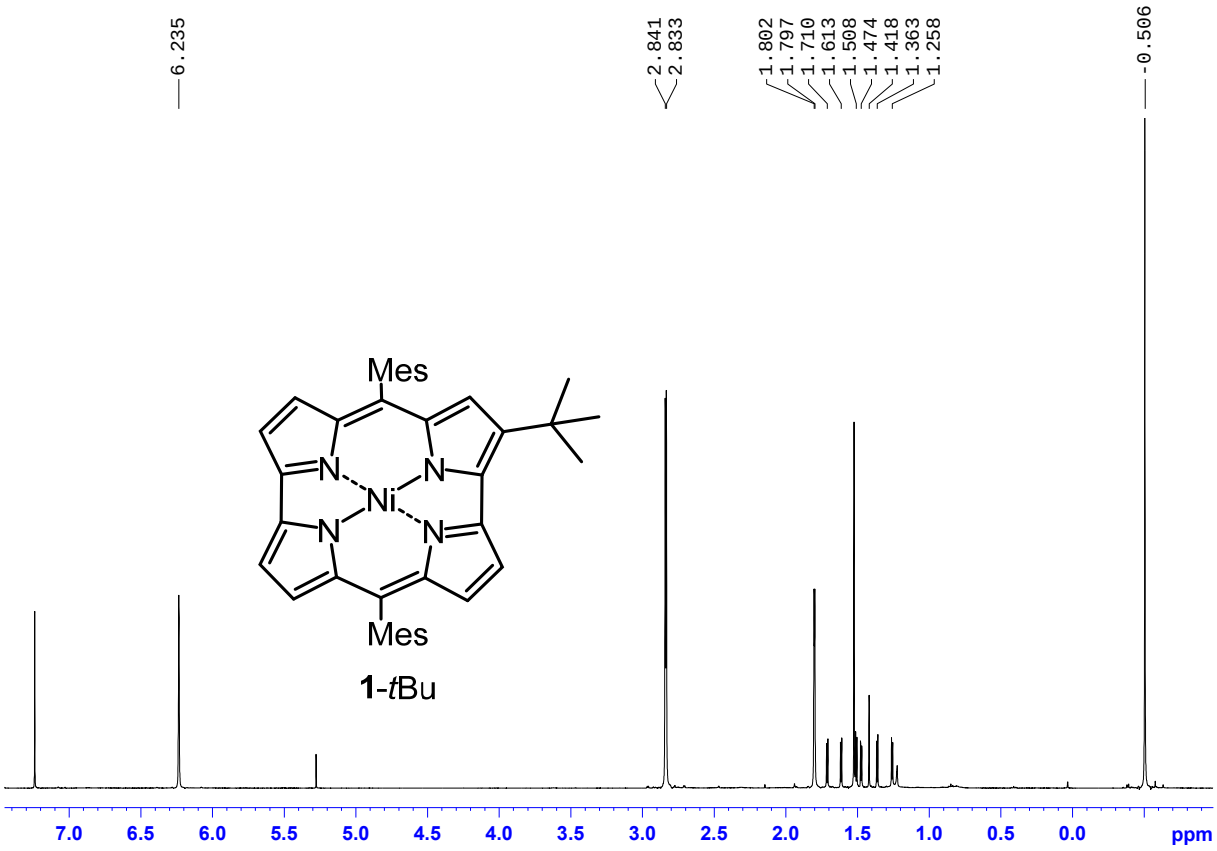

Figure S66. ^{1}H NMR spectrum of **1**-*t*Bu (500 MHz, 300 K, $CDCl_3$).

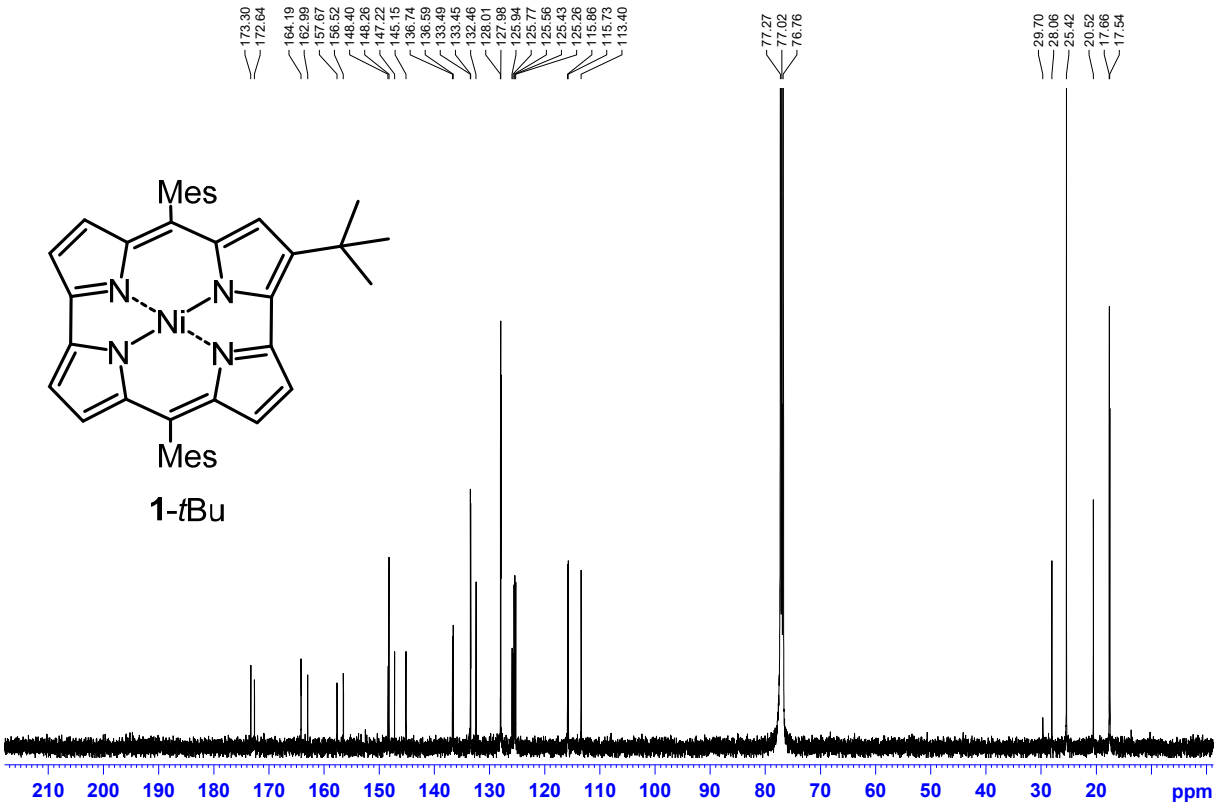

Figure S67. ^{13}C NMR spectrum of **1**-*t*Bu (125 MHz, 300 K, $CDCl_3$)

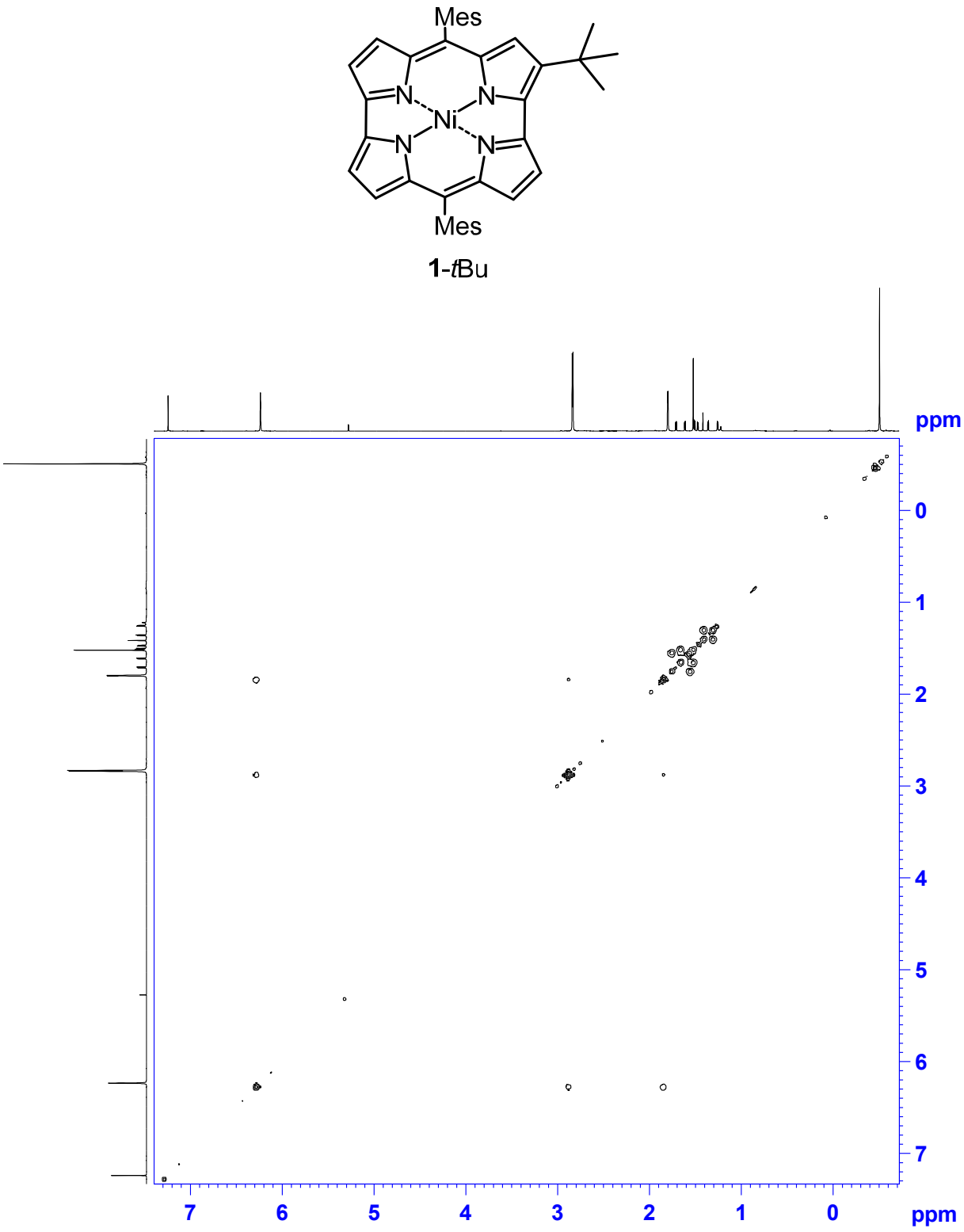

Figure S68. $^{1}H,^{1}H$ COSY spectrum of **1**-*t*Bu (500 MHz, 300 K, $CDCl_3$).

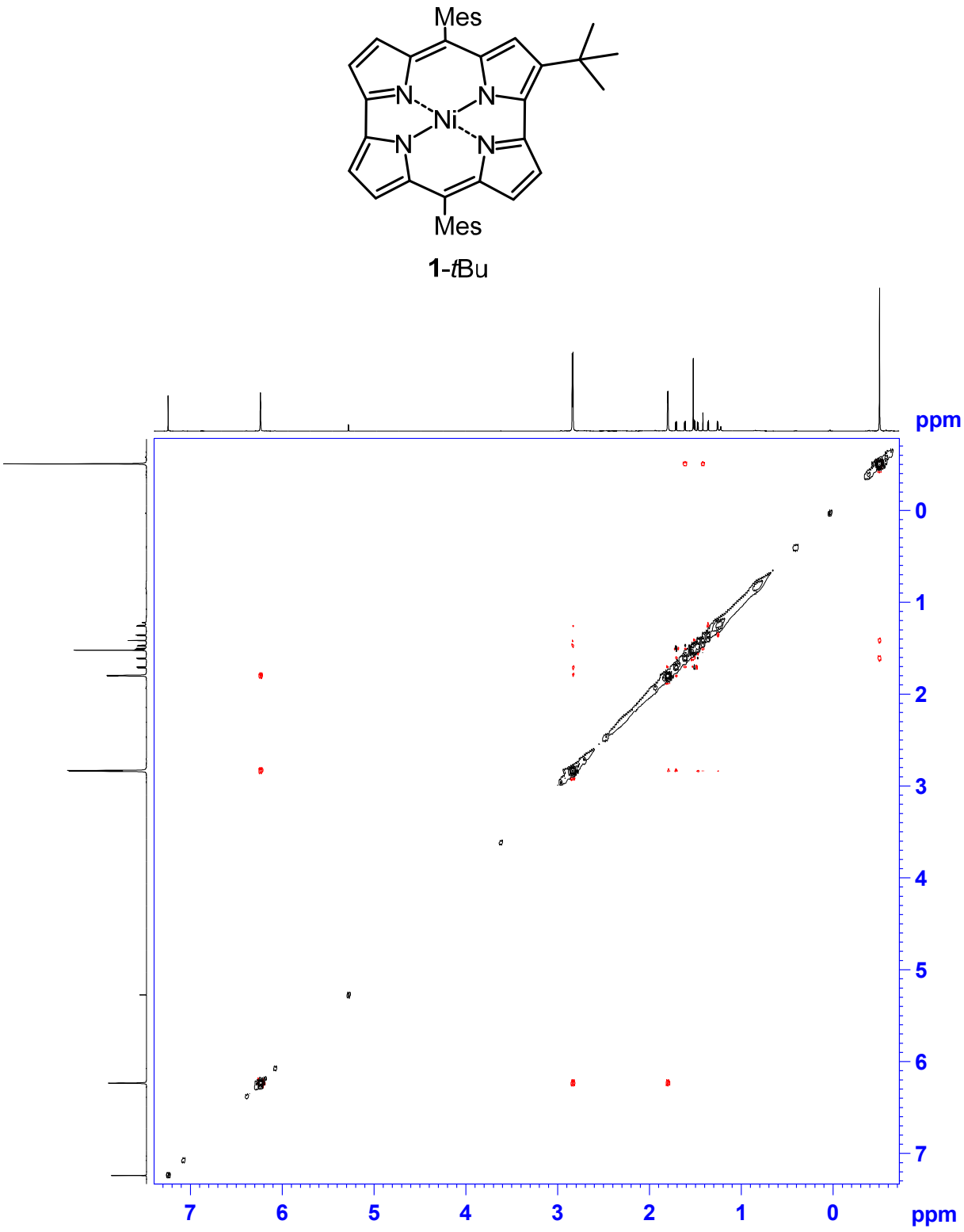

1-*t*Bu

Figure S69. ^{1}H,^{1}H NOESY spectrum of **1**-*t*Bu (500 MHz, 300 K, $CDCl_3$).

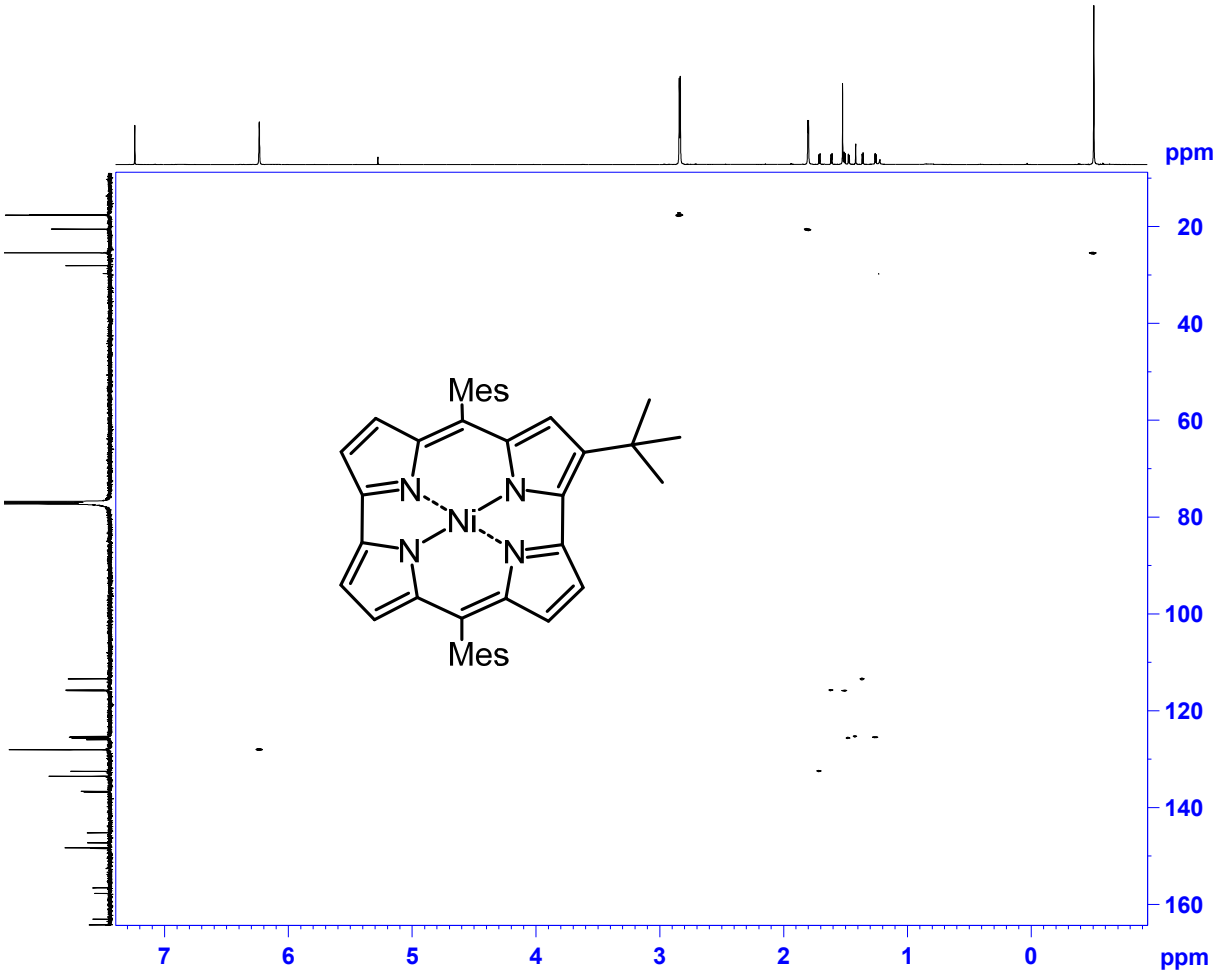

Figure S70. $^{1}H,^{13}C$ HSQC spectrum of **1**-*t*Bu (500/125 MHz, 300 K, $CDCl_3$).

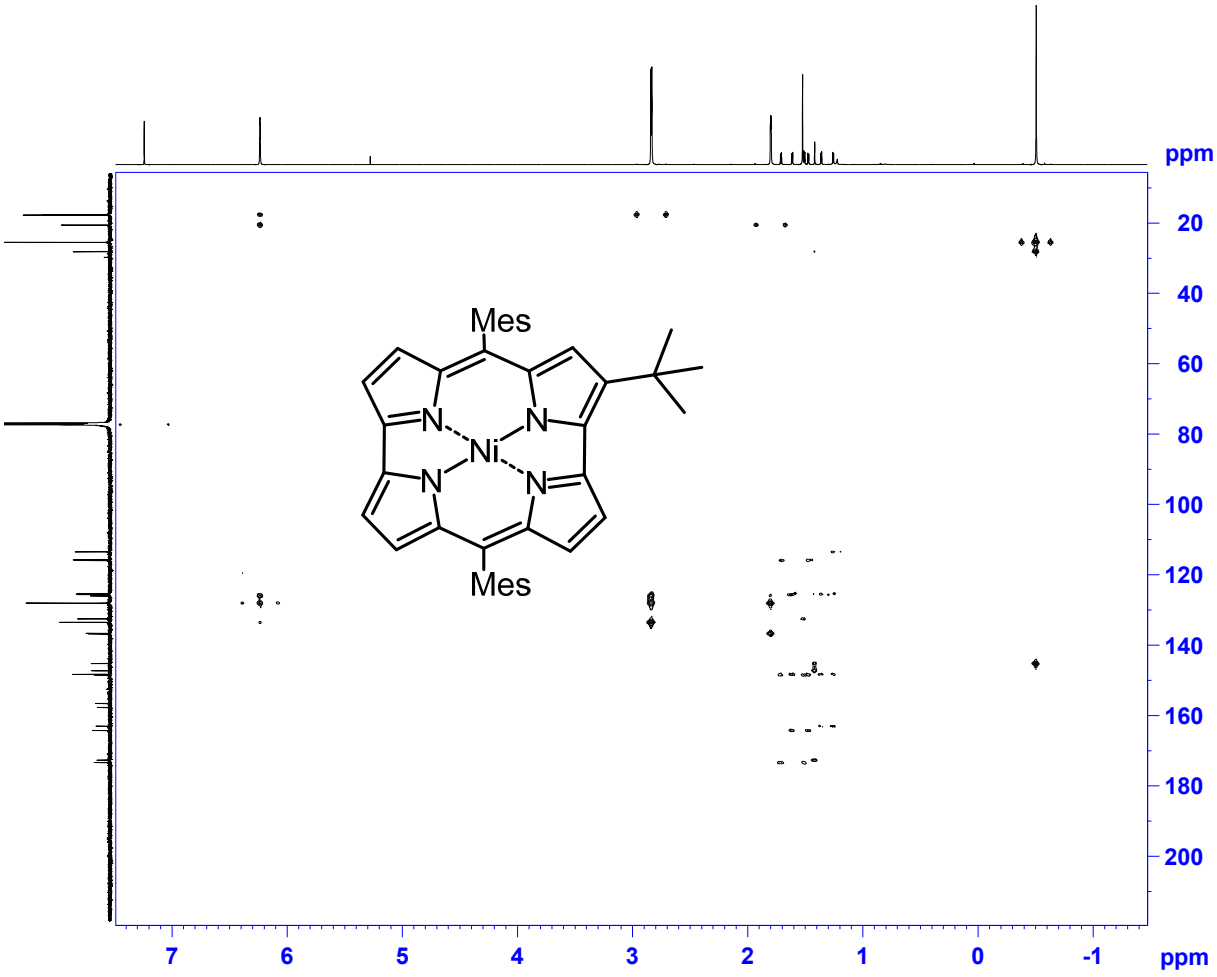

Figure S71. $^{1}H,^{13}C$ HMBC spectrum of **1**-*t*Bu (500/125 MHz, 300 K, $CDCl_3$).

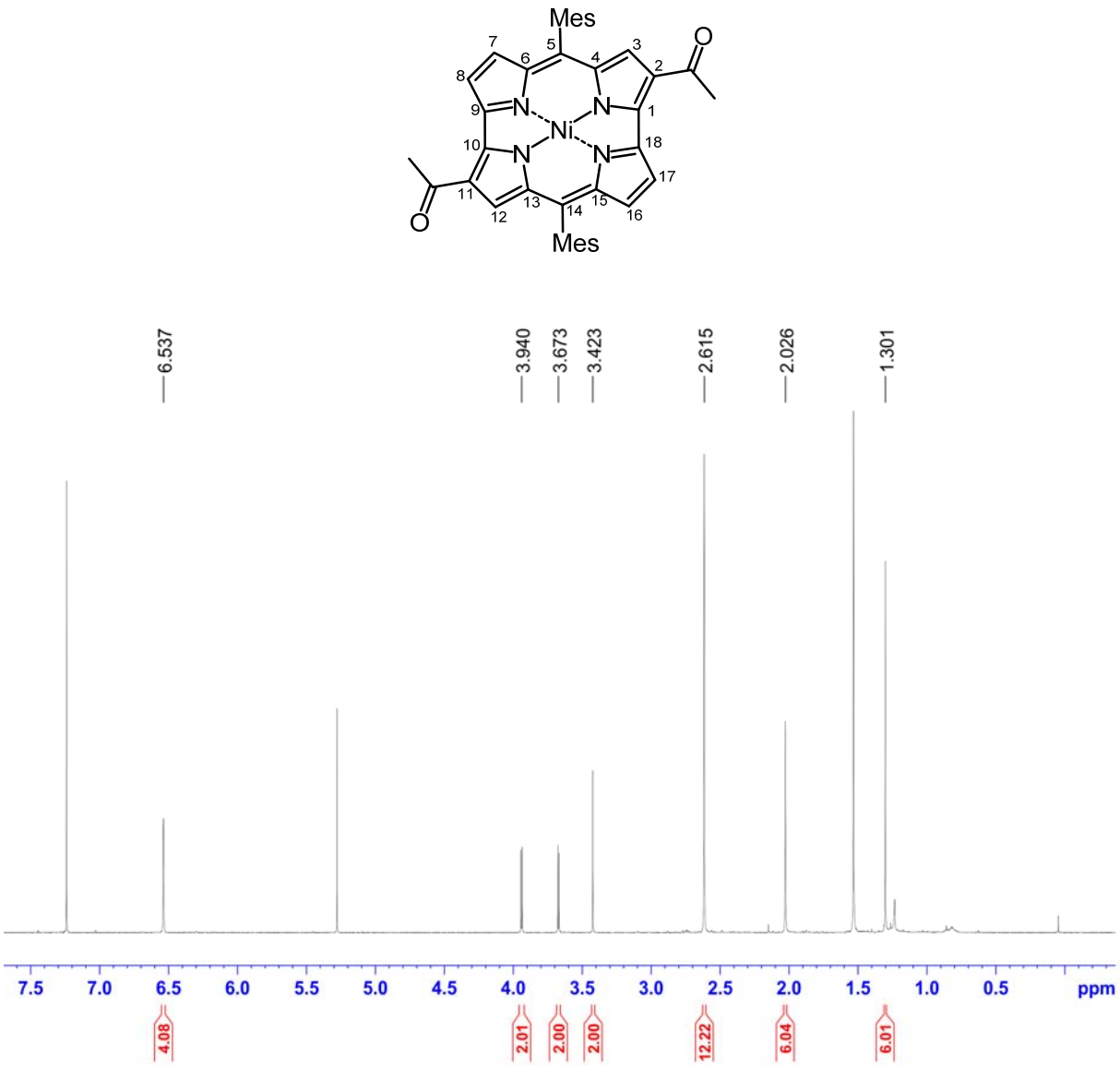

Figure S72. ^{1}H NMR spectrum of **5a** (500 MHz, 300 K, $CDCl_3$).

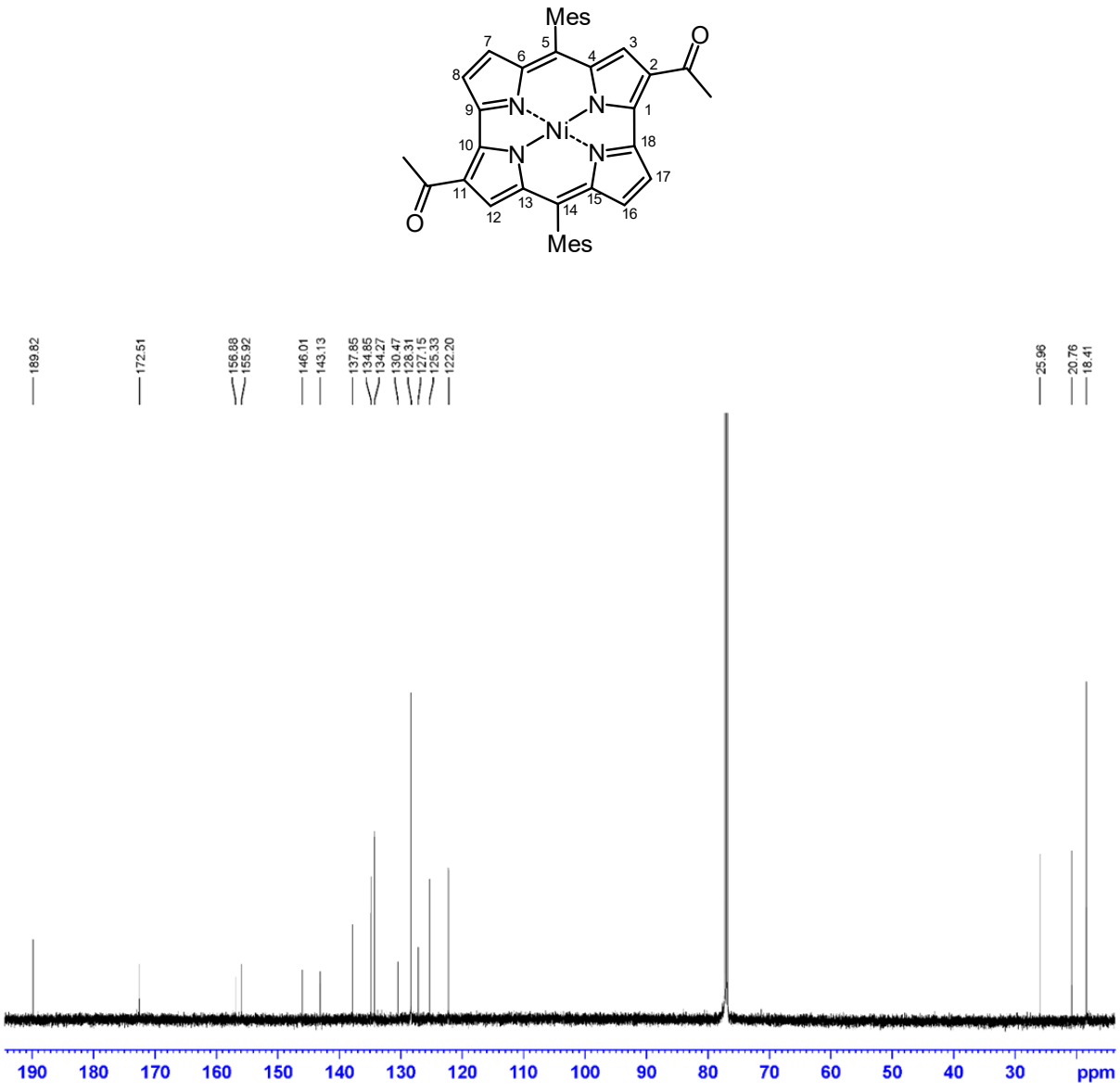

Figure S73. ^{13}C NMR spectrum of **5a** (150 MHz, 300 K, $CDCl_3$).

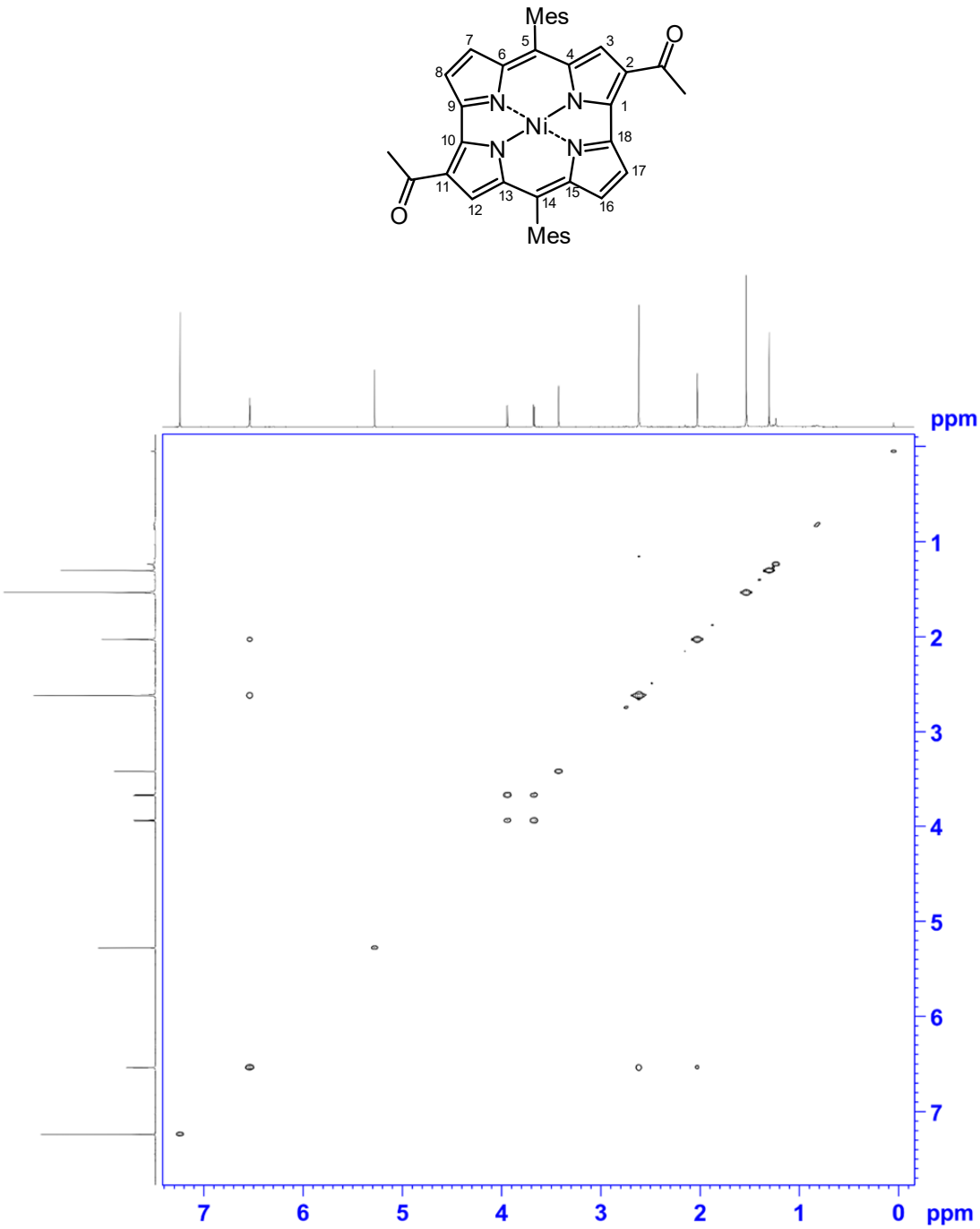

Figure S74. ^{1}H, ^{1}H COSY spectrum of **5a** (500 MHz, 300 K, $CDCl_3$).

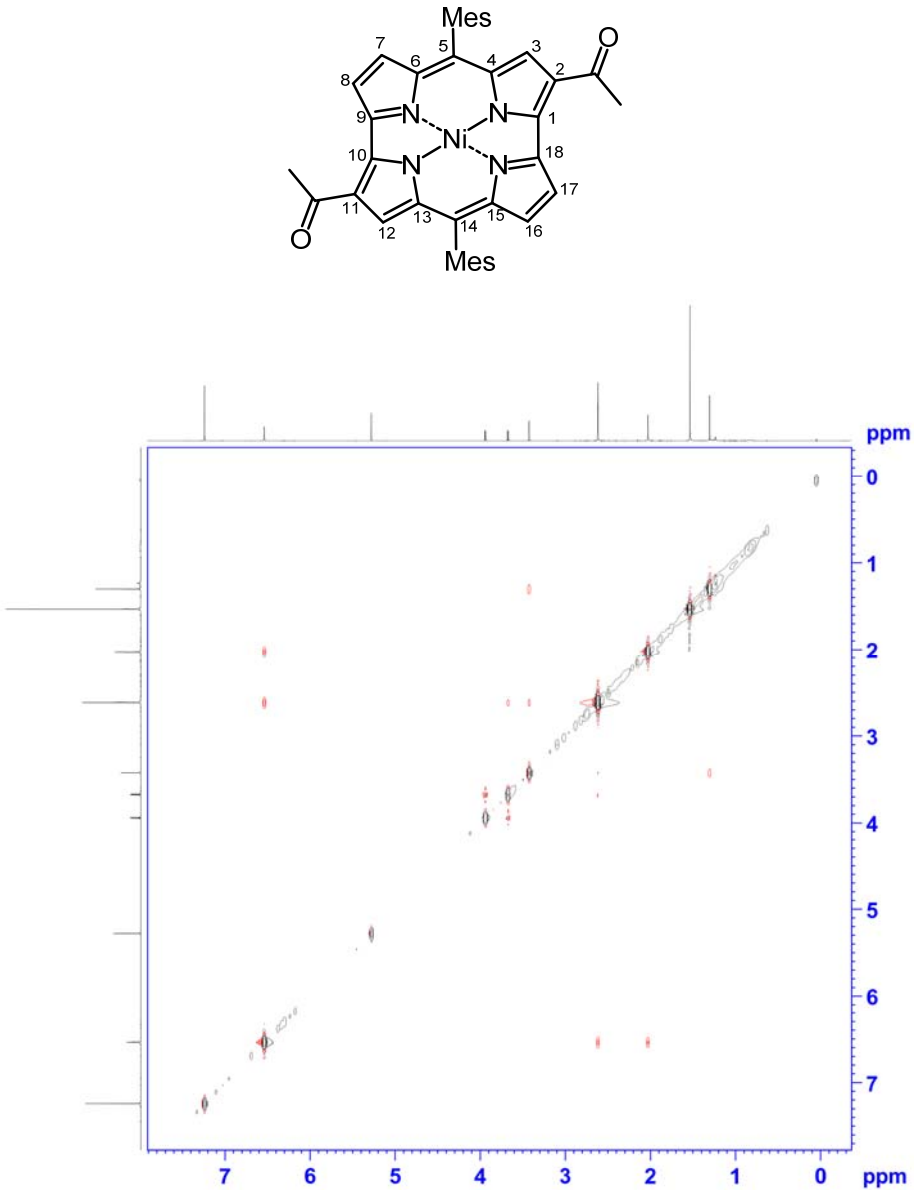

Figure S75. ^{1}H, ^{1}H NOESY spectrum of **5a** (500 MHz, 300 K, $CDCl_3$).

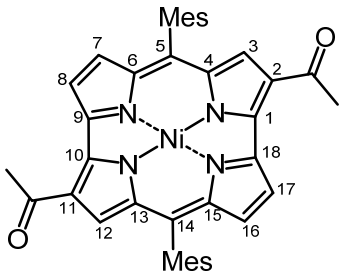

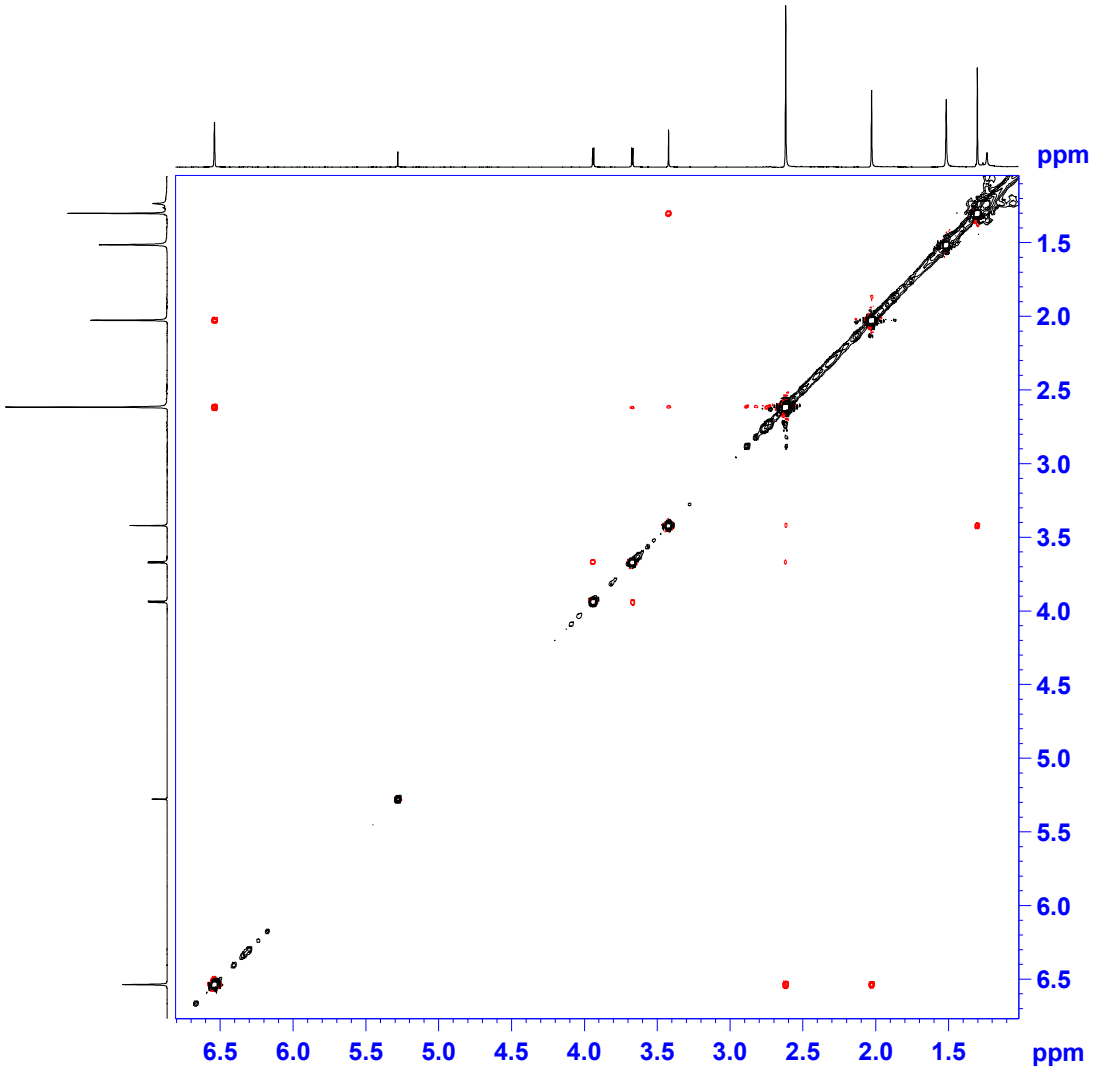

Figure S76. ^{1}H, ^{1}H ROESY spectrum of **5a** (500 MHz, 300 K, $CDCl_3$).

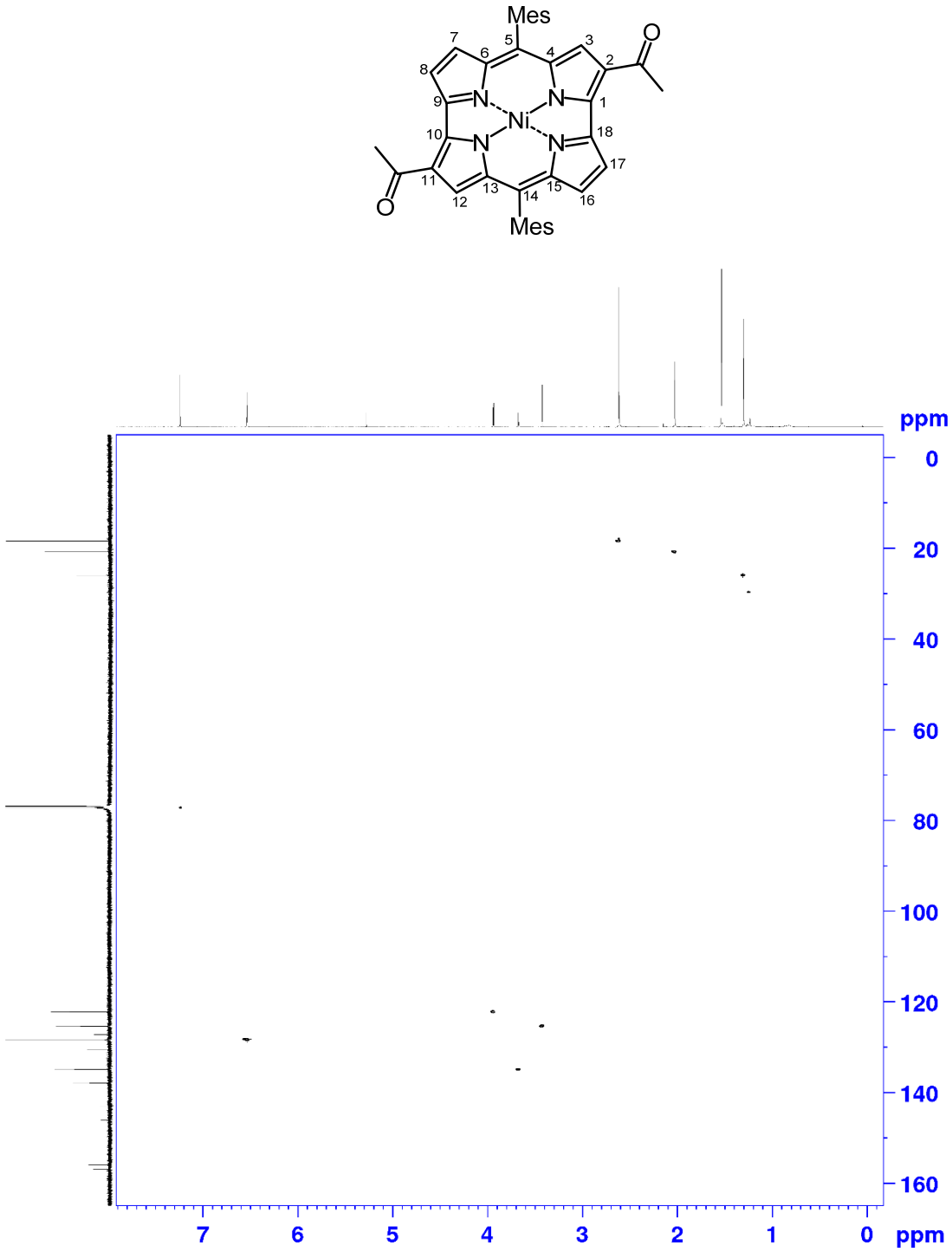

Figure S77. ^{1}H, ^{13}C HSQC spectrum of **5a** (500/125 MHz, 300 K, $CDCl_3$).

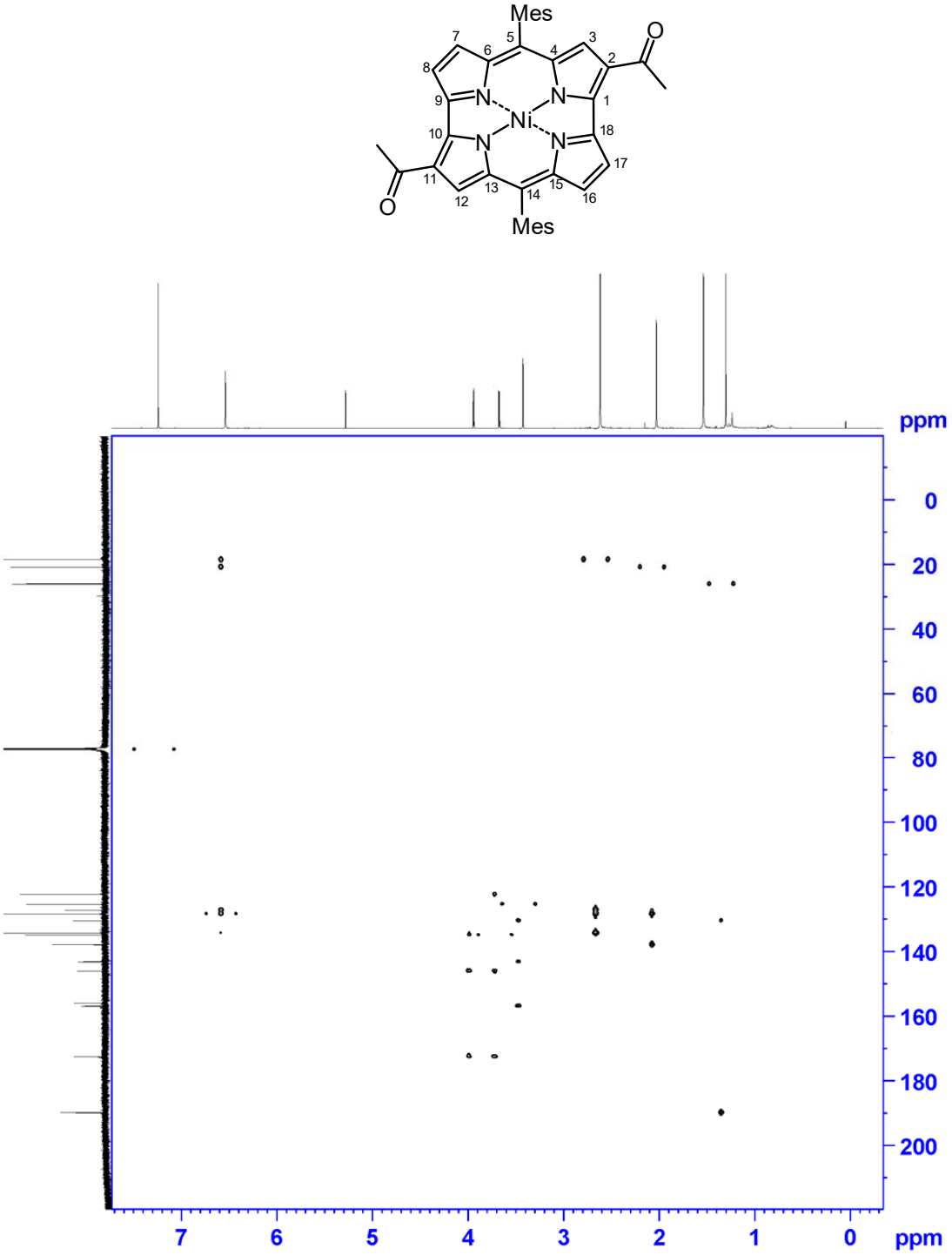

Figure S78. ^{1}H, ^{13}C HMBC spectrum of **5a** (500/125 MHz, 300 K, $CDCl_3$).

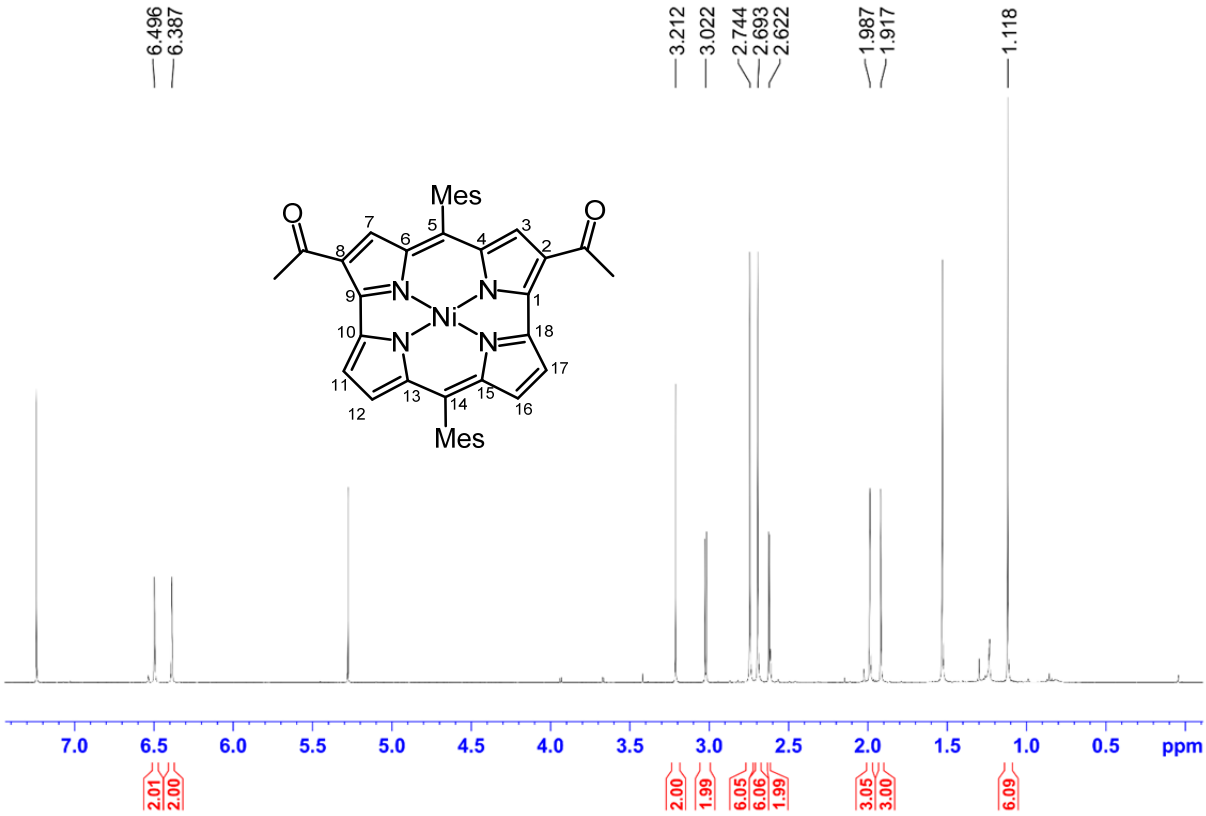

Figure S79. ^{1}H NMR spectrum of **5b** (500 MHz, 300 K, $CDCl_3$).

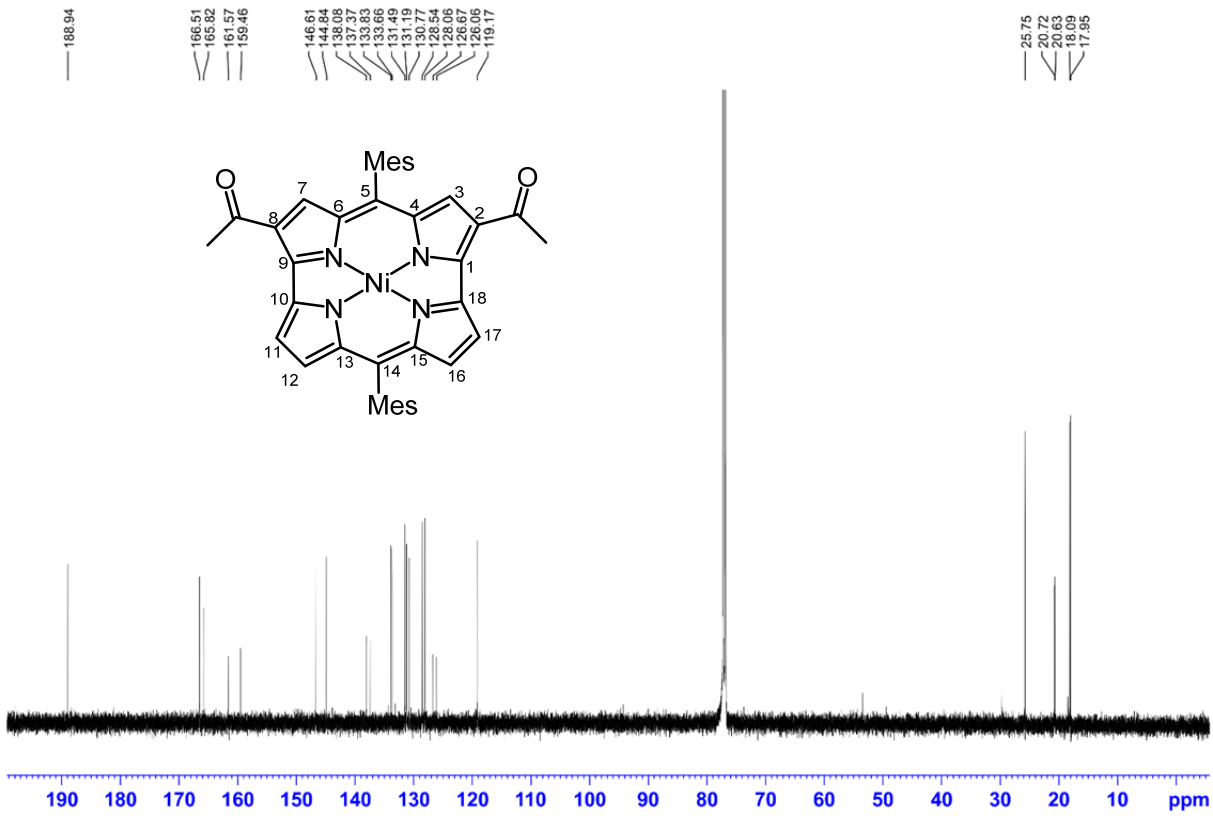

Figure S80. ^{13}C NMR spectrum of **5b** (150 MHz, 300 K, $CDCl_3$).

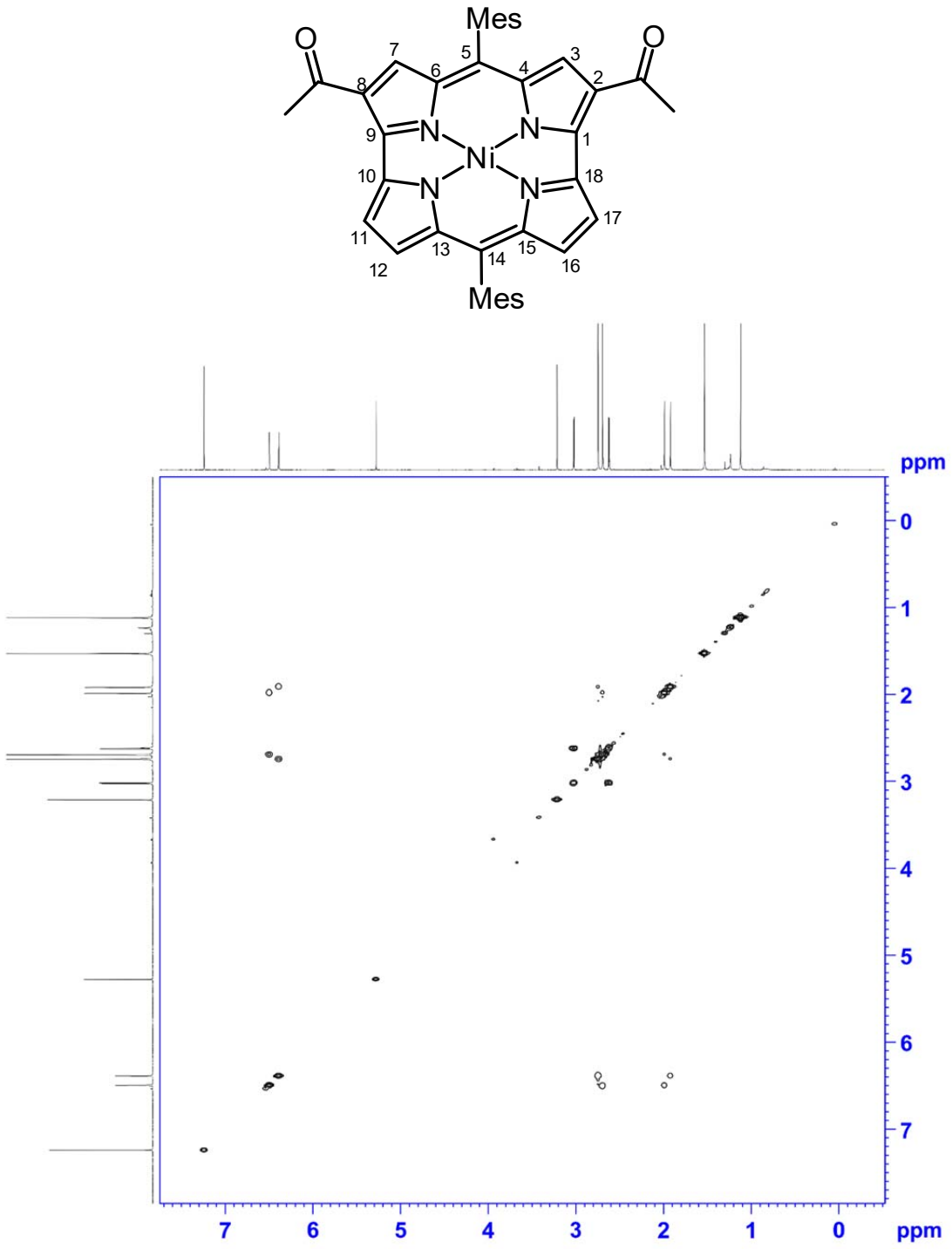

Figure S81. ^{1}H, ^{1}H COSY spectrum of **5b** (500 MHz, 300 K, $CDCl_3$).

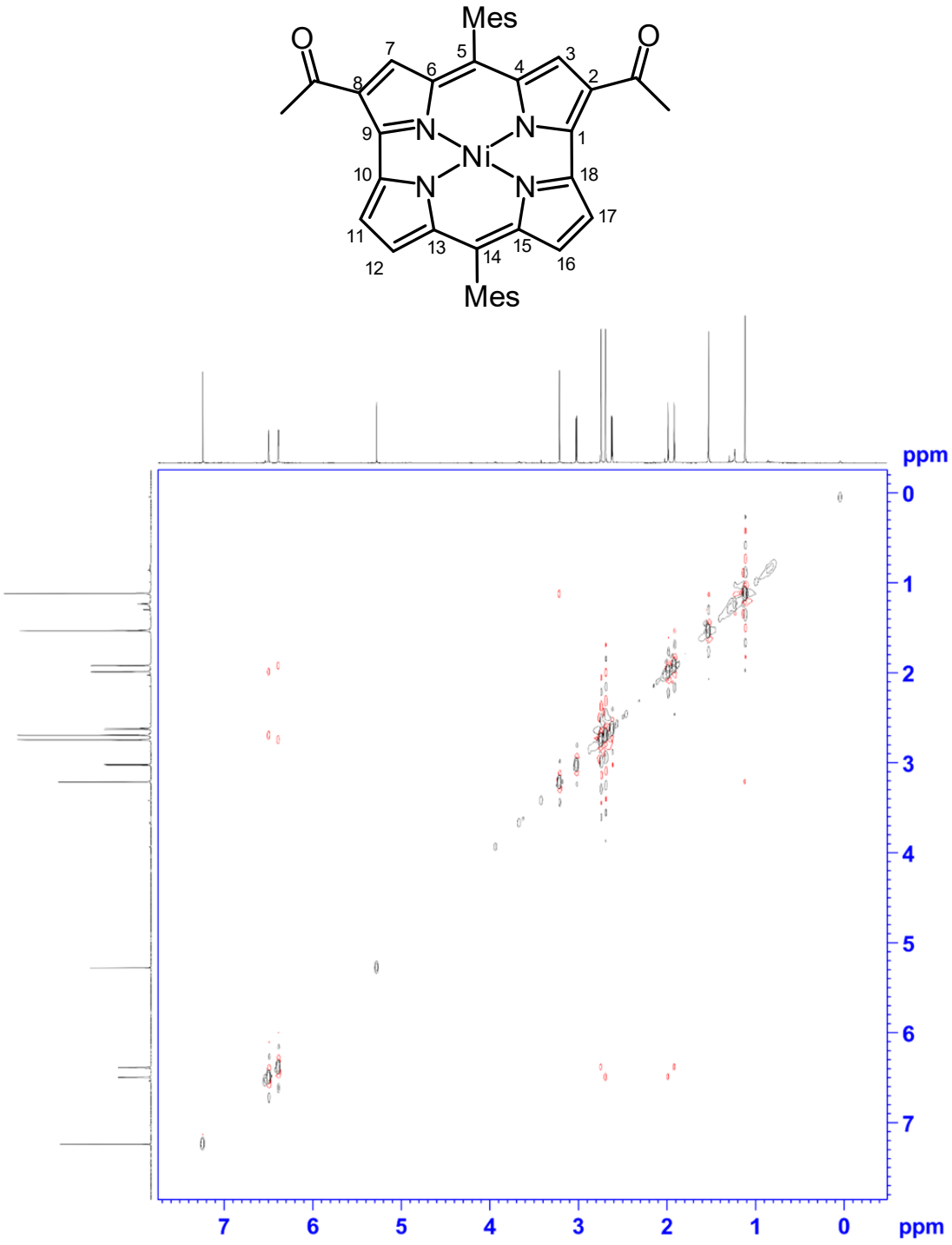

Figure S82. ^{1}H, ^{1}H NOESY spectrum of **5b** (500 MHz, 300 K, $CDCl_3$).

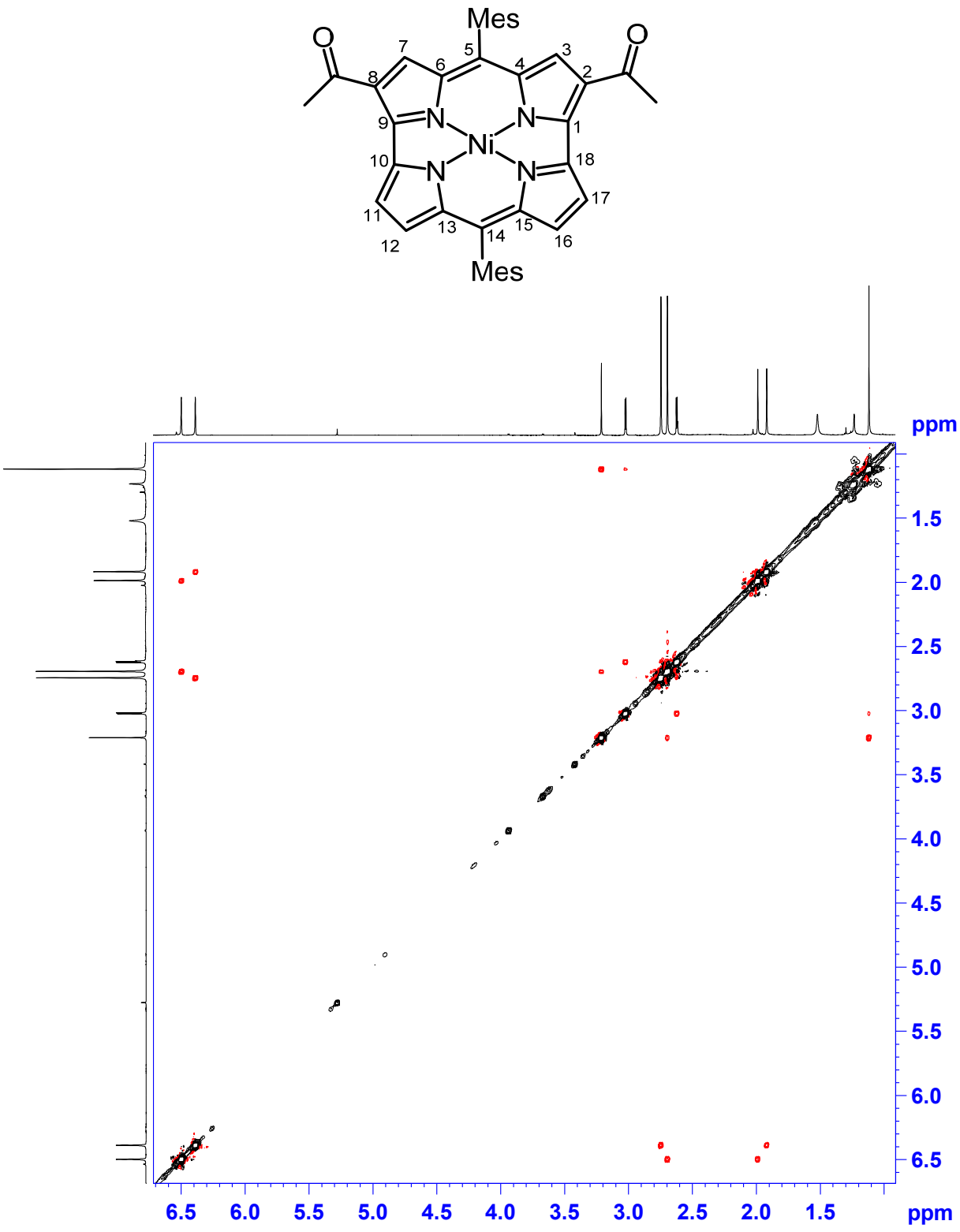

Figure S83. ^{1}H, ^{1}H ROESY spectrum of **5b** (500 MHz, 300 K, $CDCl_3$).

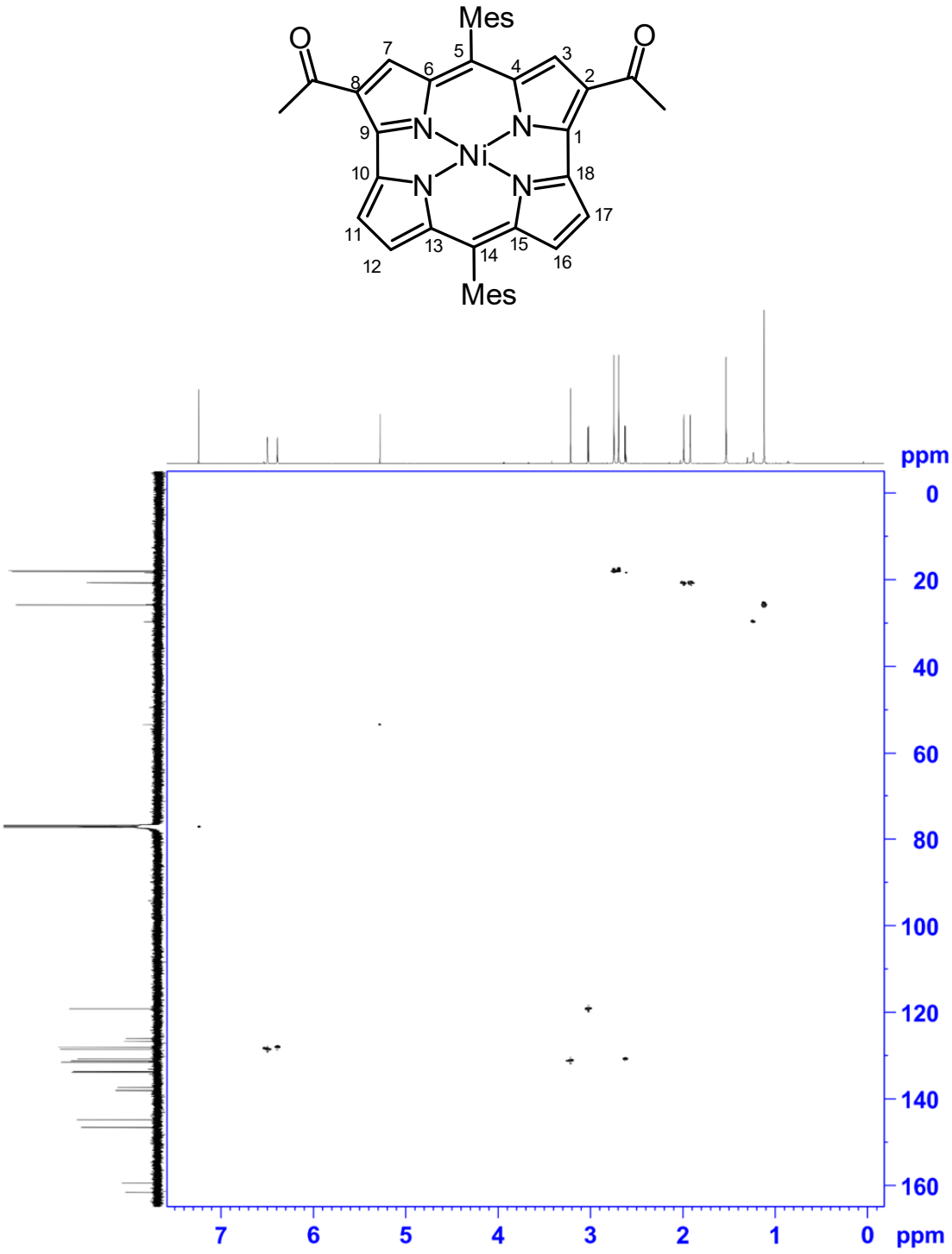

Figure S84. ^{1}H, ^{13}C HSQC spectrum of **5b** (500/125 MHz, 300 K, $CDCl_3$).

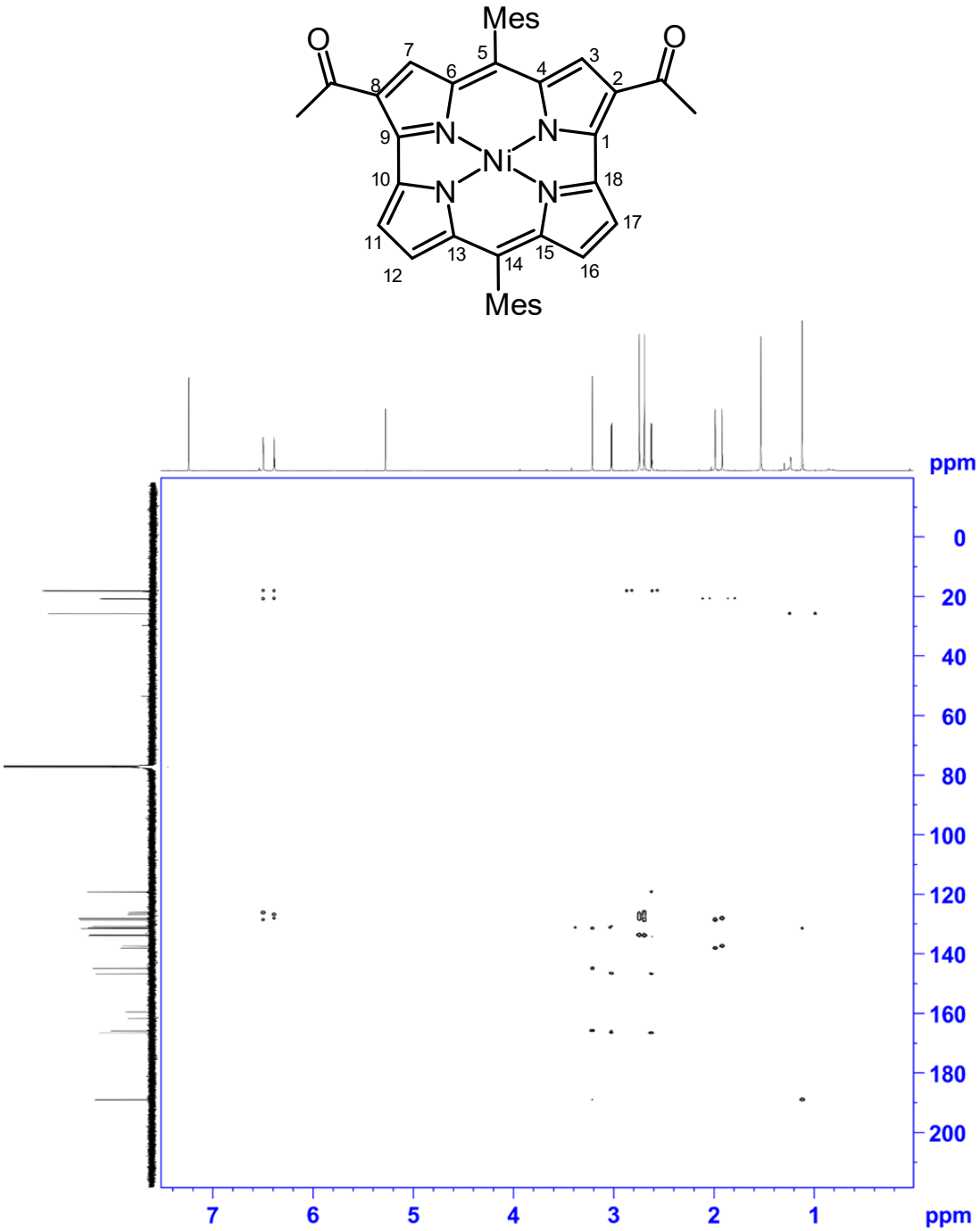

Figure S85. ^{1}H, ^{13}C HMBC spectrum of **5b** (500/125 MHz, 300 K, $CDCl_3$).

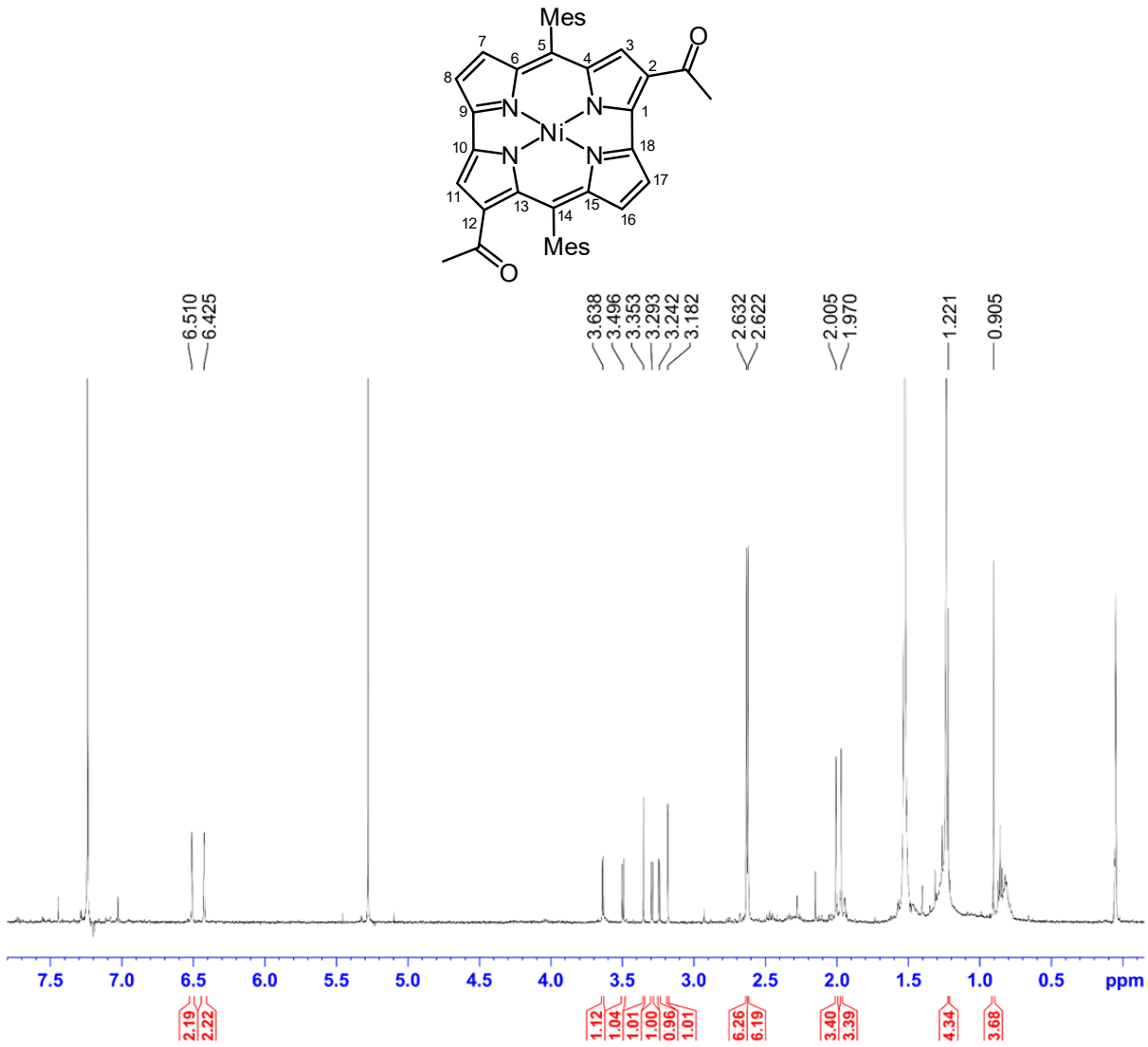

Figure S86. ^{1}H NMR spectrum of **5c** (500 MHz, 300 K, $CDCl_3$).

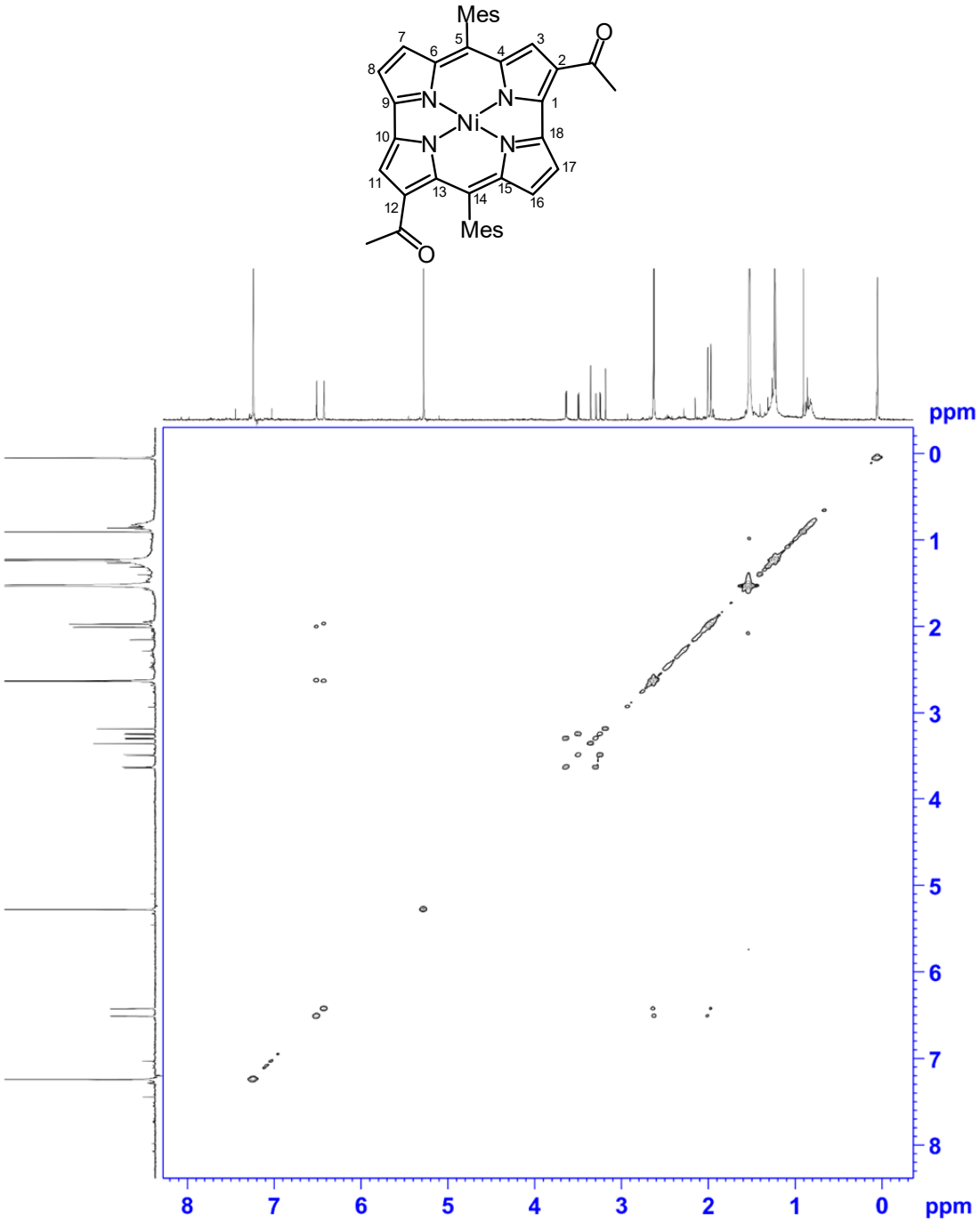

Figure S87. ^{1}H, ^{1}H COSY spectrum of **5c** (500 MHz, 300 K, $CDCl_3$).

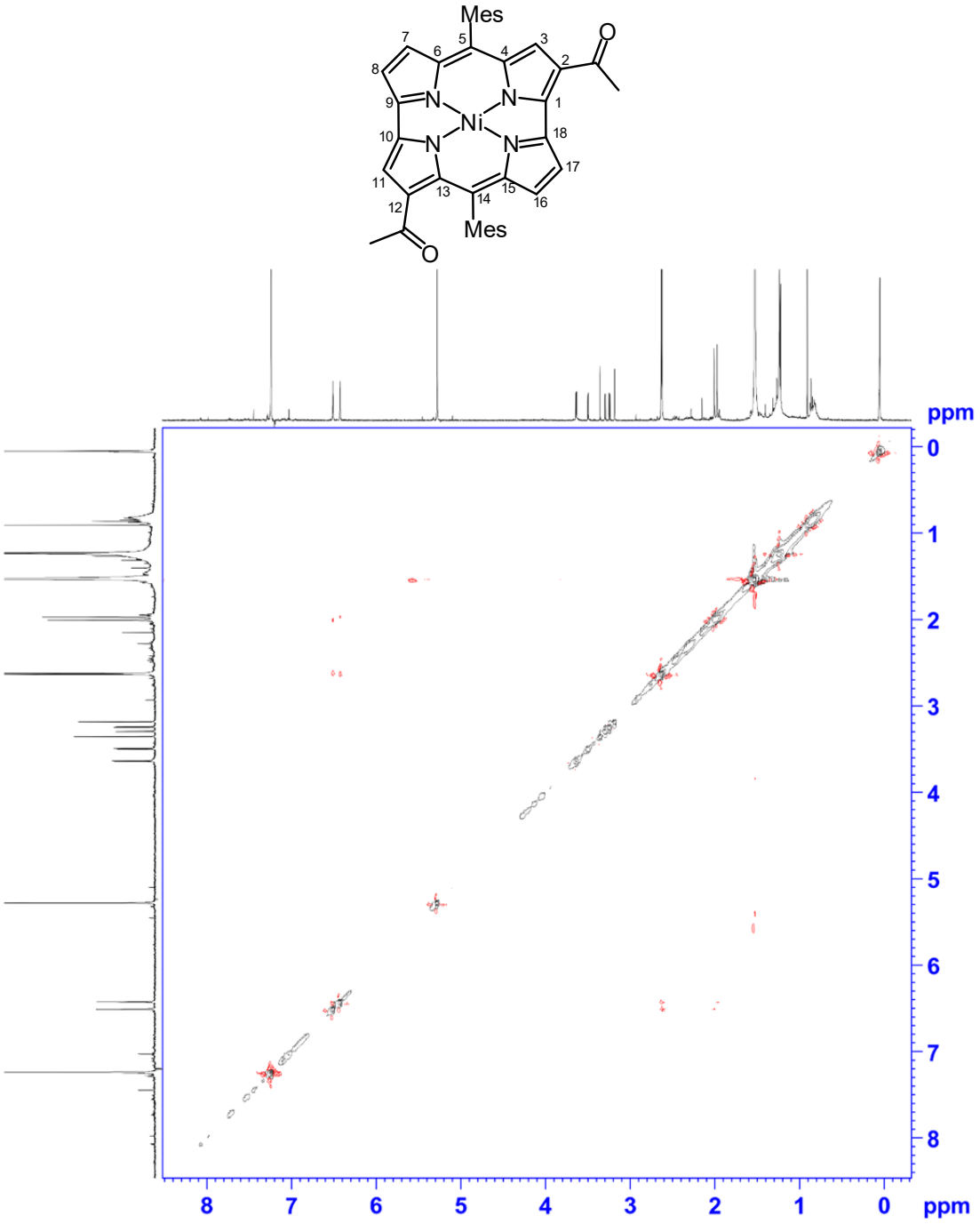

Figure S88. ^{1}H, ^{1}H NOESY spectrum of **5c** (500 MHz, 300 K, $CDCl_3$).

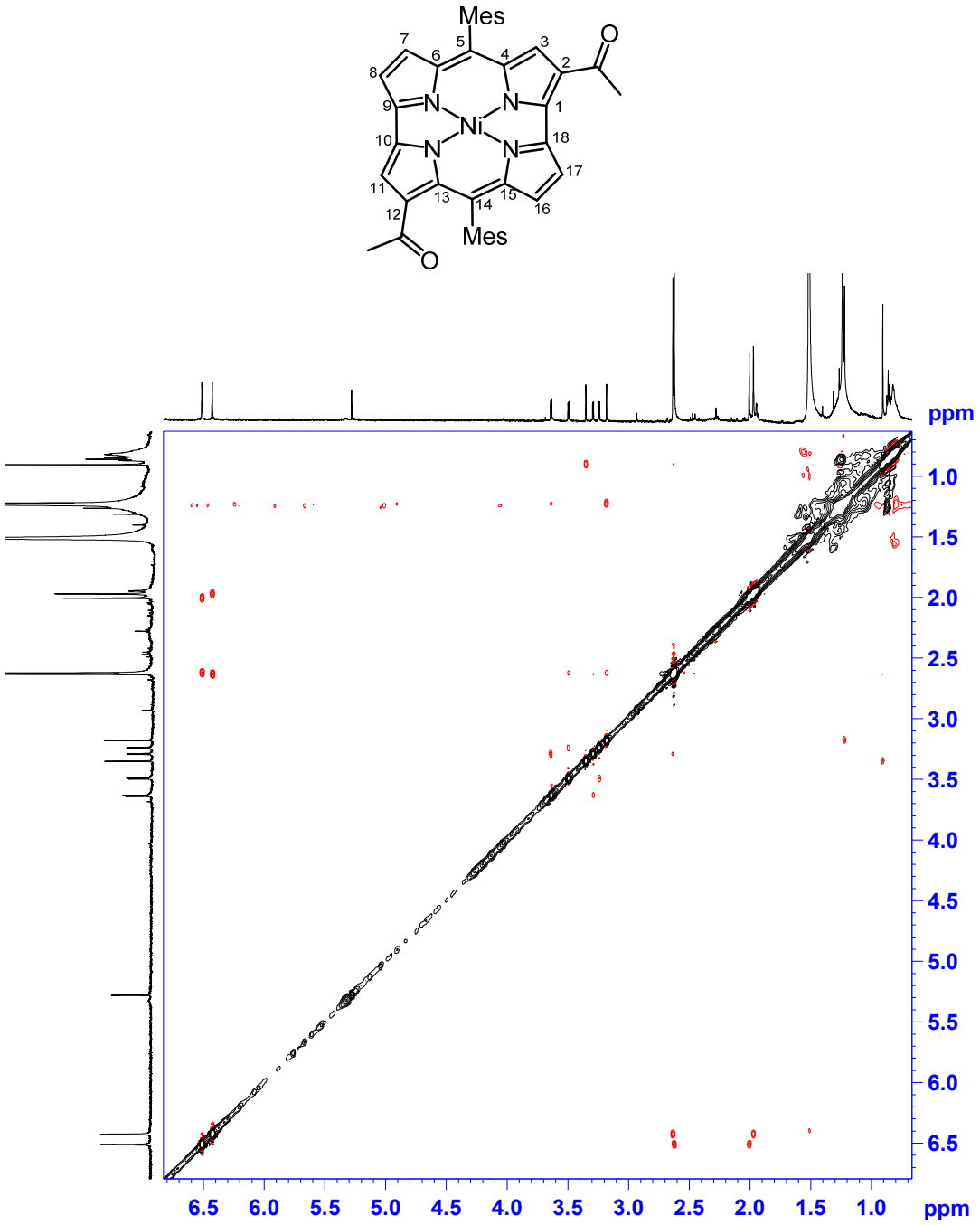

Figure S89. ^{1}H, ^{1}H ROESY spectrum of **5c** (500 MHz, 300 K, $CDCl_3$).

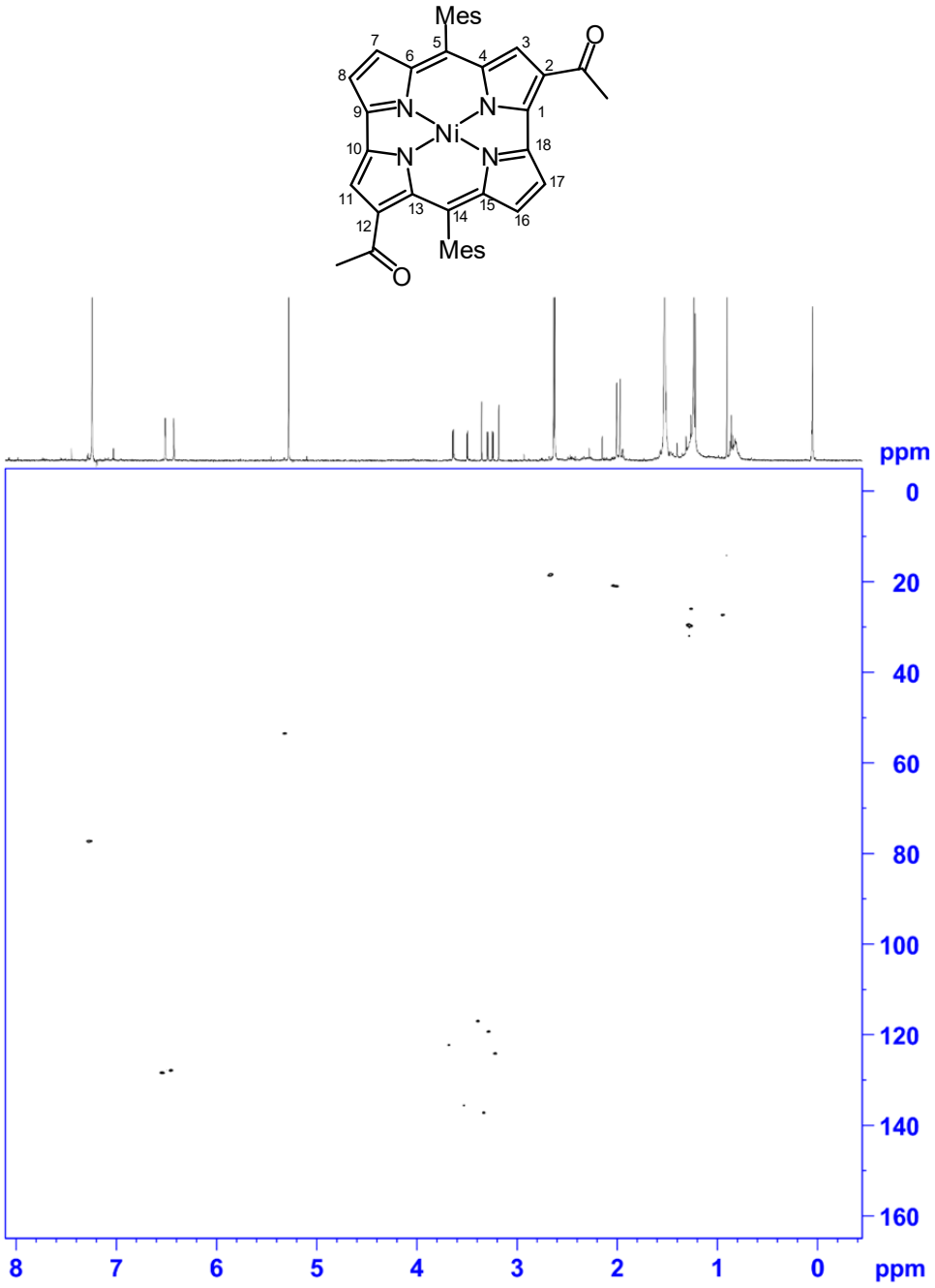

Figure S90. ^{1}H, ^{13}C HSQC spectrum of **5c** (500/125 MHz, 300 K, $CDCl_3$).

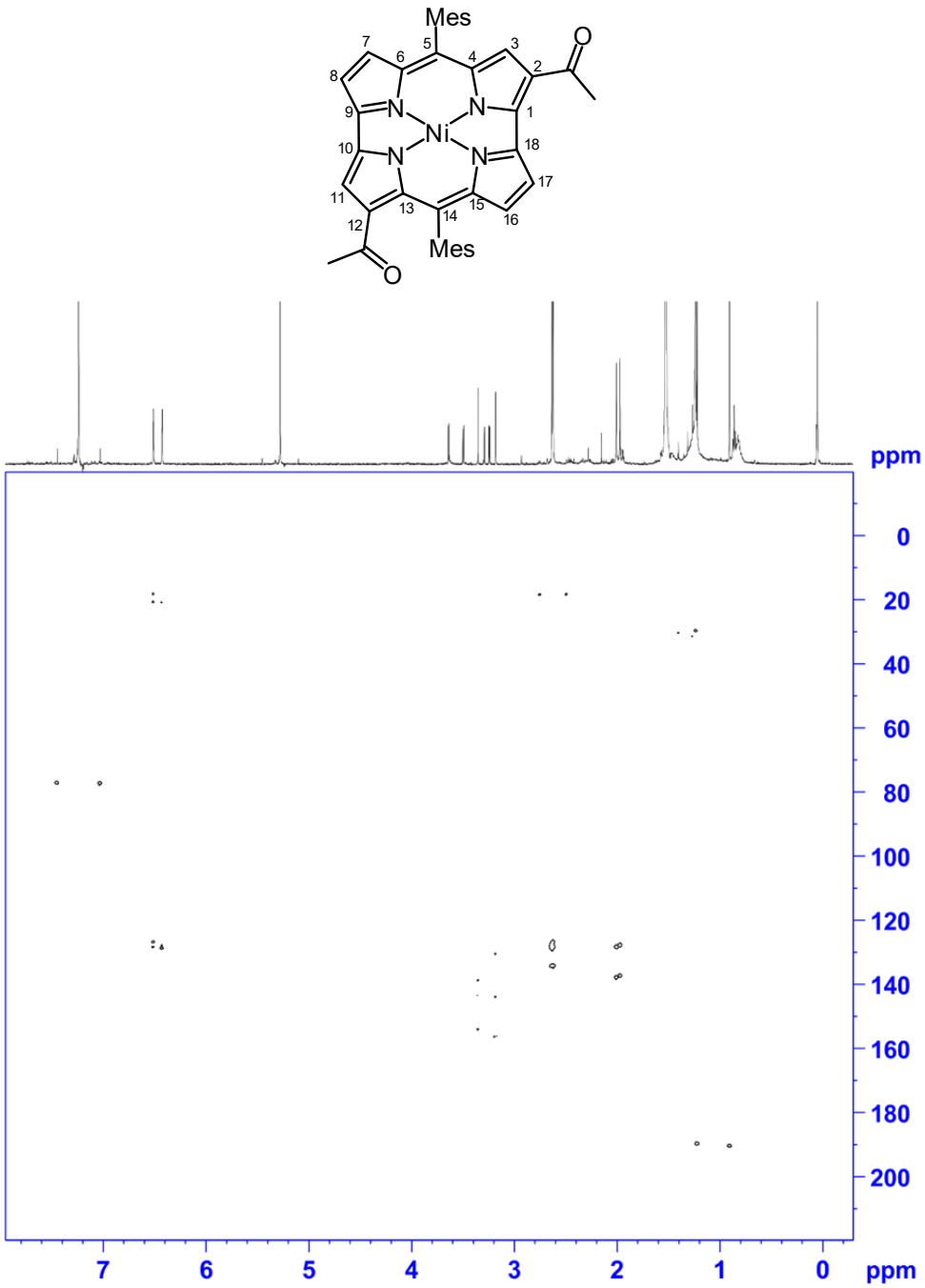

Figure S91. ^{1}H, ^{13}C HMBC spectrum of **5c** (500/125 MHz, 300 K, $CDCl_3$).

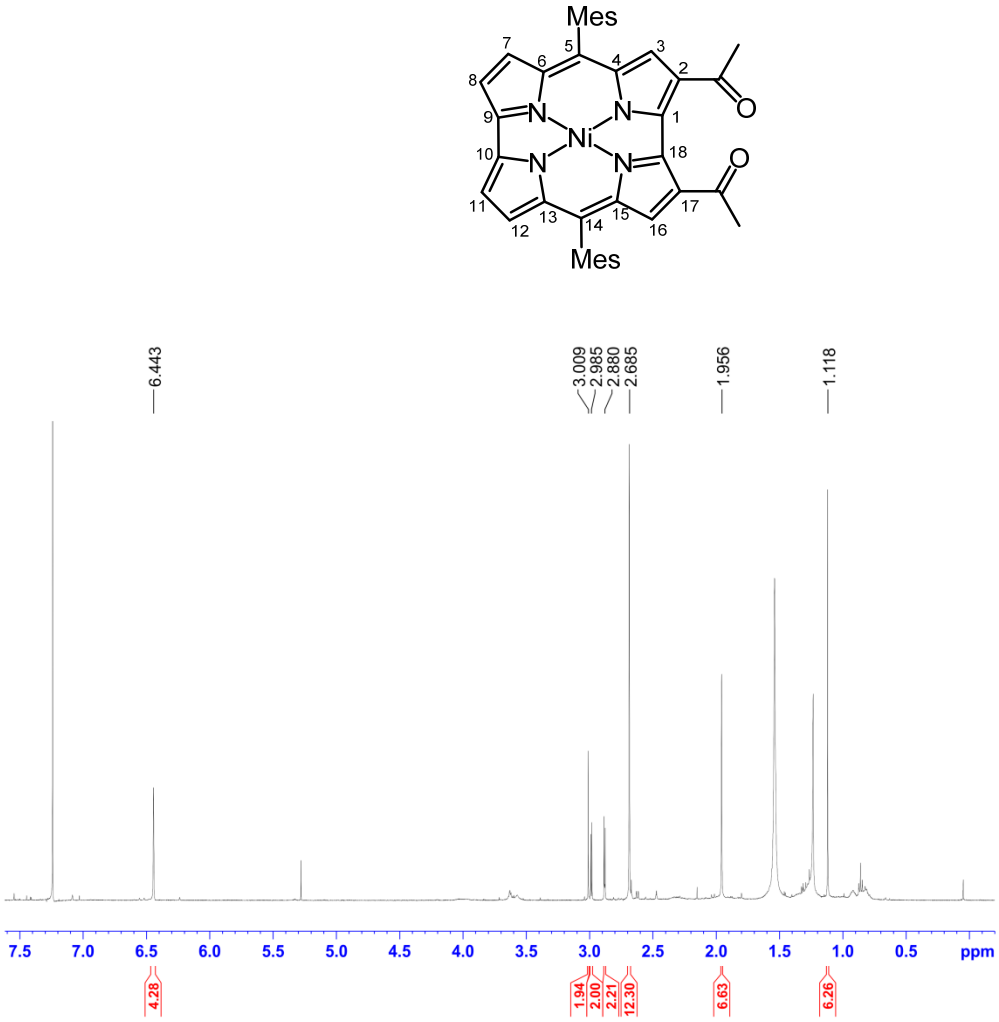

Figure S92. ^{1}H NMR spectrum of **5d** (500 MHz, 300 K, $CDCl_3$).

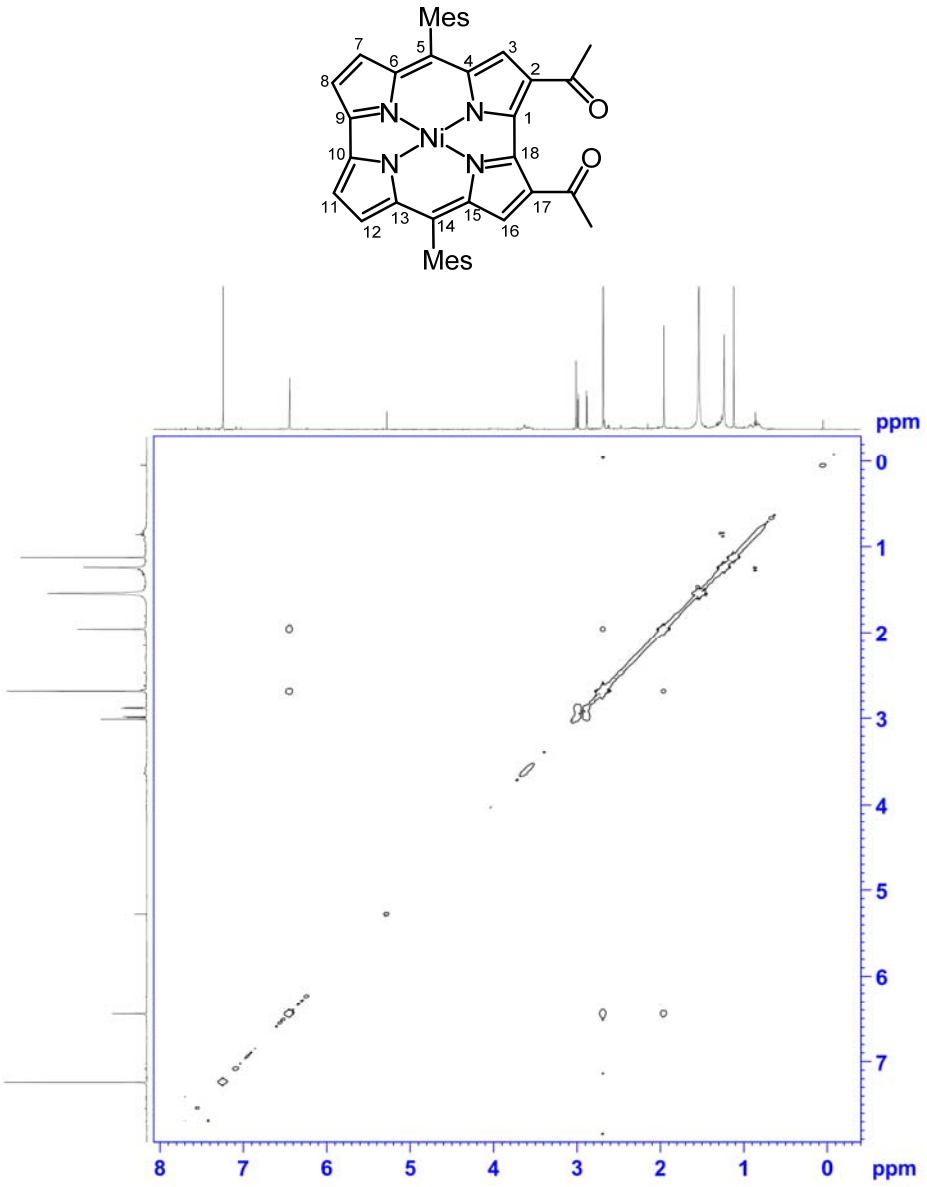

Figure S93. ^{1}H, ^{1}H COSY spectrum of **5d** (500 MHz, 300 K, $CDCl_3$).

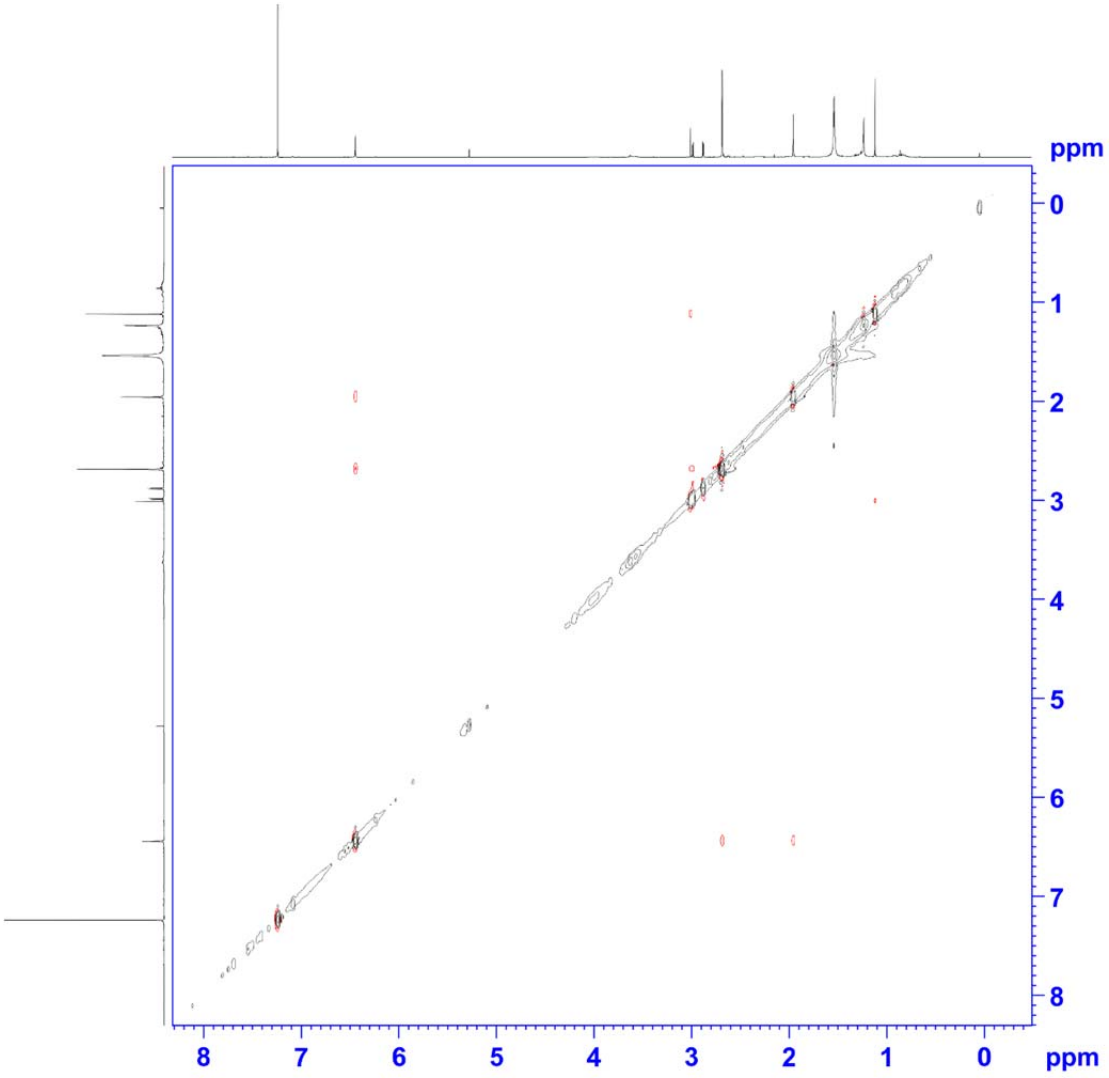

Figure S94. ^{1}H, ^{1}H NOESY spectrum of **5d** (500 MHz, 300 K, $CDCl_3$).

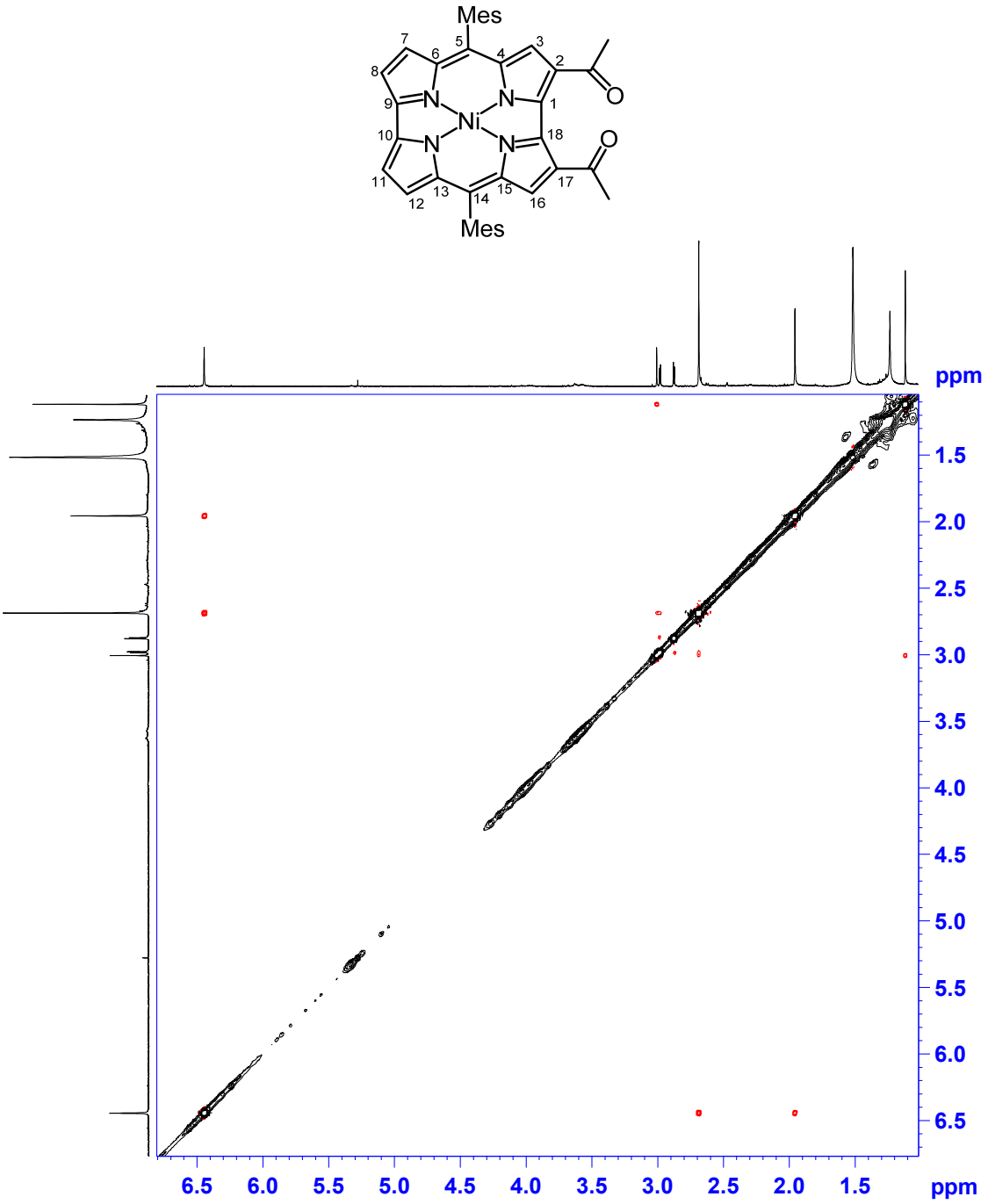

Figure S95. ^{1}H, ^{1}H ROESY spectrum of **5d** (500 MHz, 300 K, $CDCl_3$).

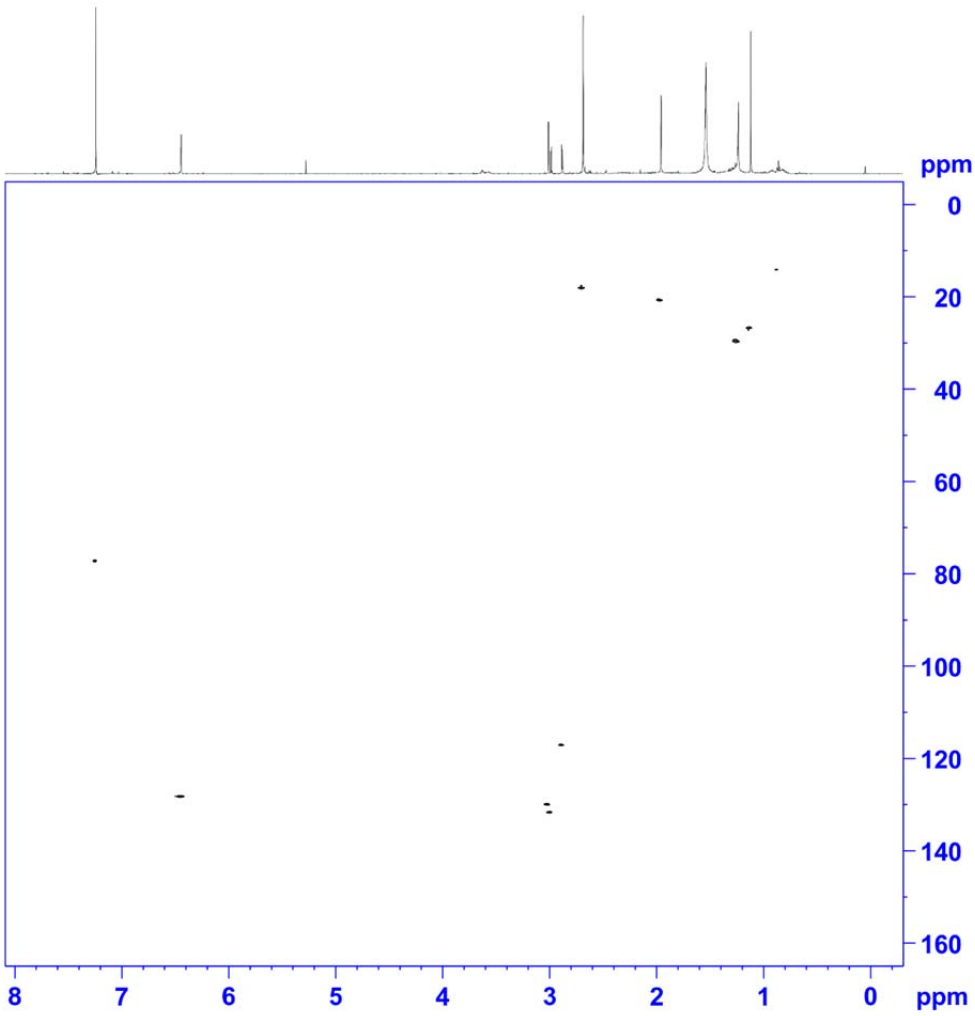

Figure S96. ^{1}H, ^{13}C HSQC spectrum of **5d** (500/125 MHz, 300 K, $CDCl_3$)

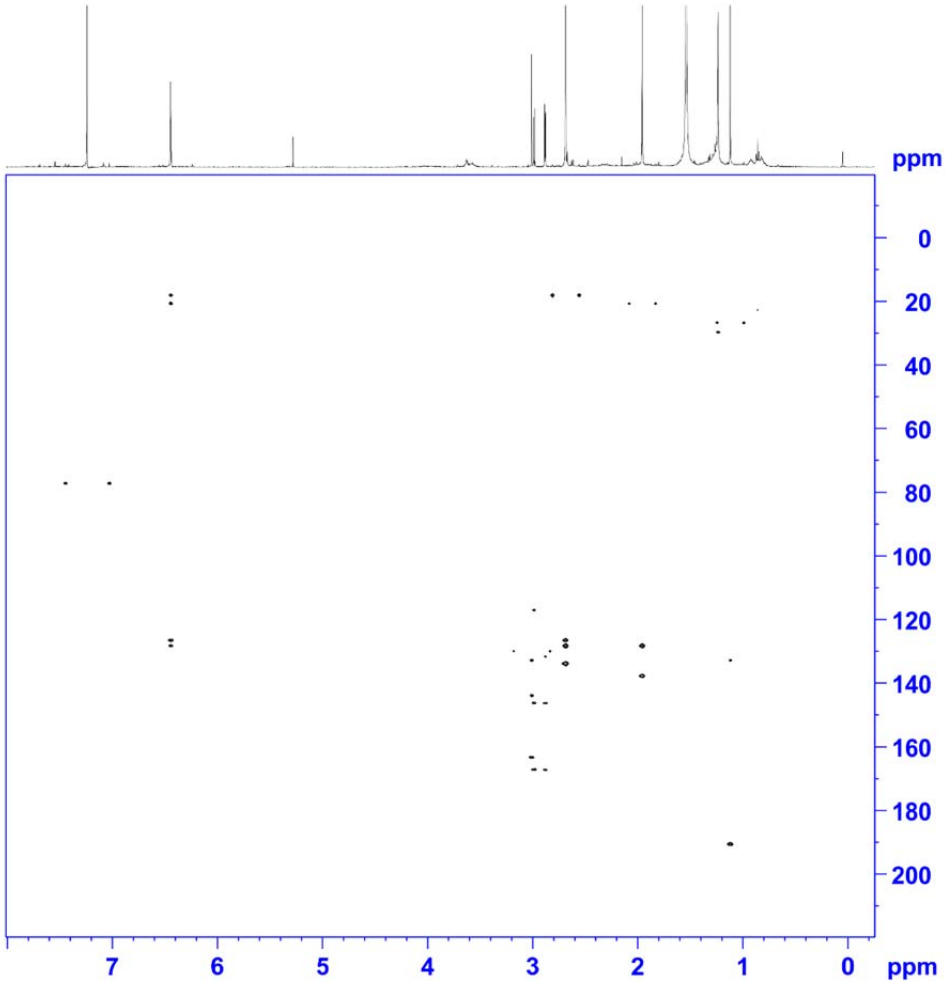

Figure S97. ^{1}H, ^{13}C HMBC spectrum of **5d** (500/125 MHz, 300 K, $CDCl_3$)

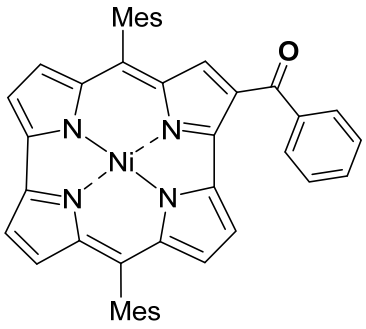

3a

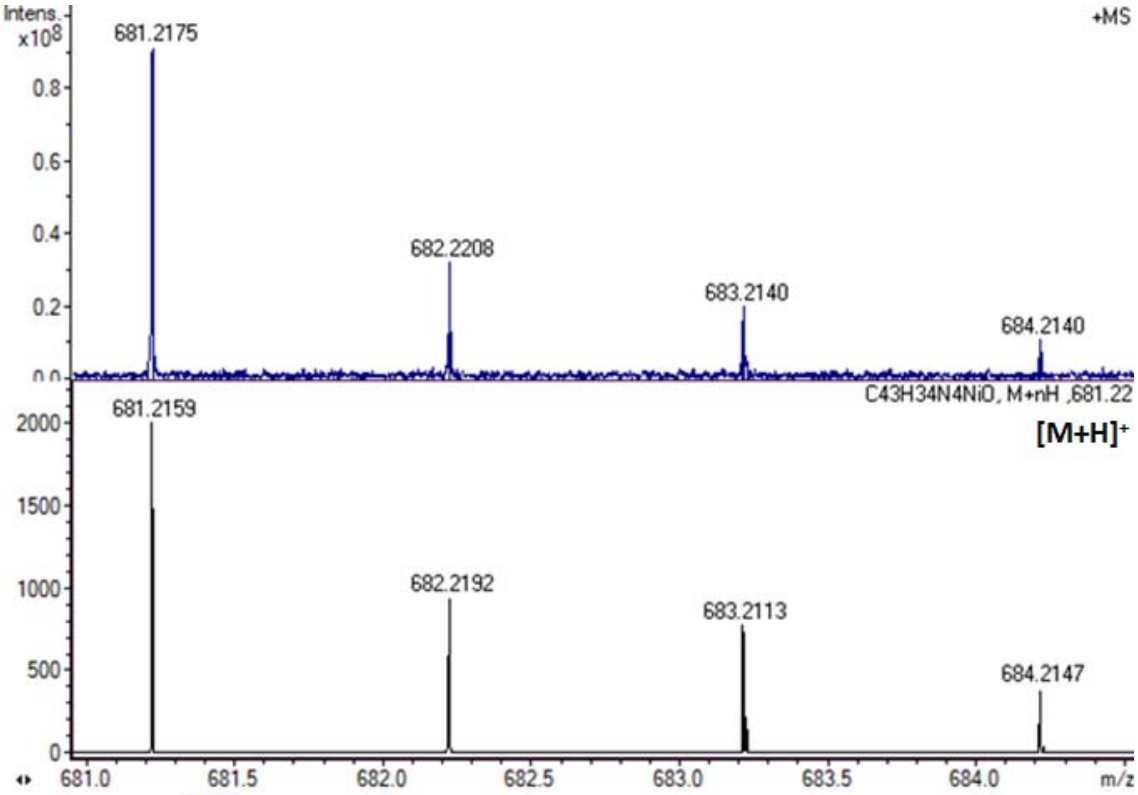

Figure S98. ESI(+) HRMS spectrum of **3a** (experimental: upper trace; simulated: black, bottom trace).

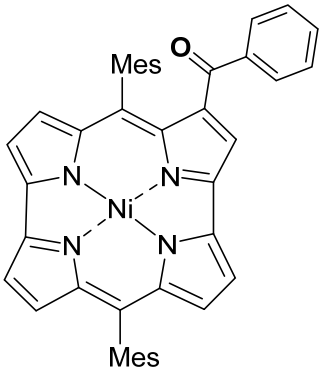

4a

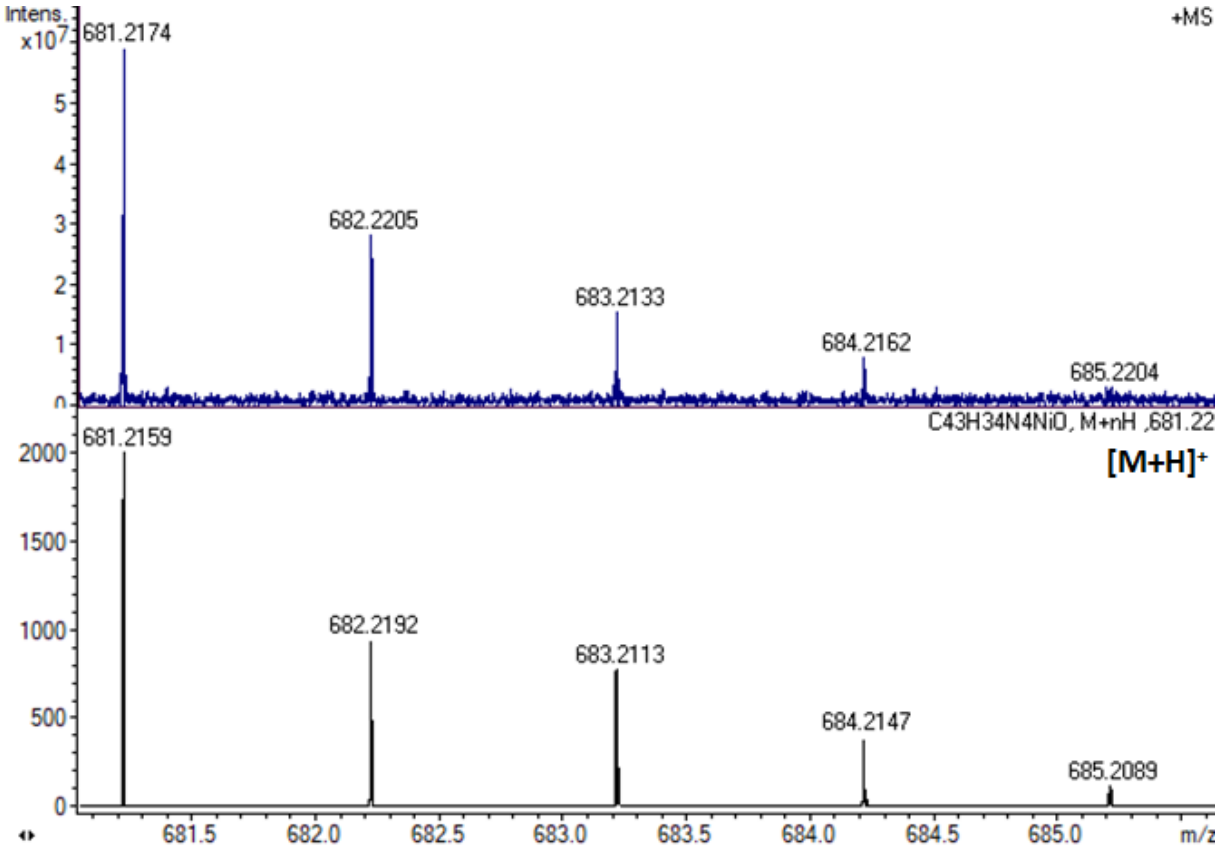

Figure S99. ESI(-) HRMS spectrum of **4a** (experimental: upper trace; simulated: black, bottom trace).

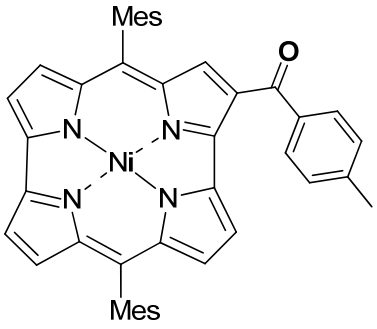

3b

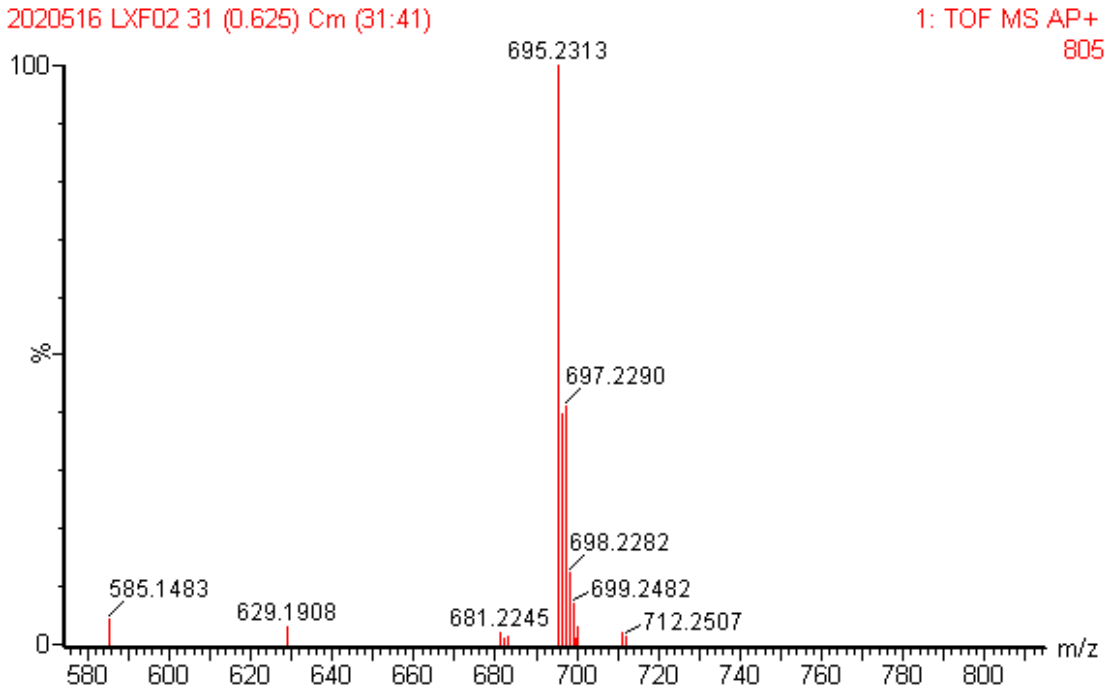

Figure S100. API(+) HRMS spectrum of **3b**.

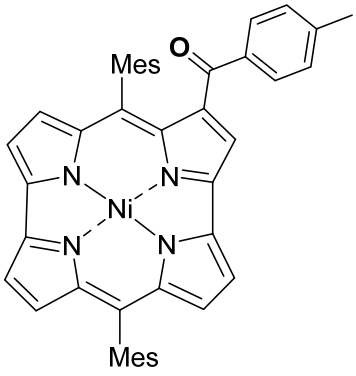

4b

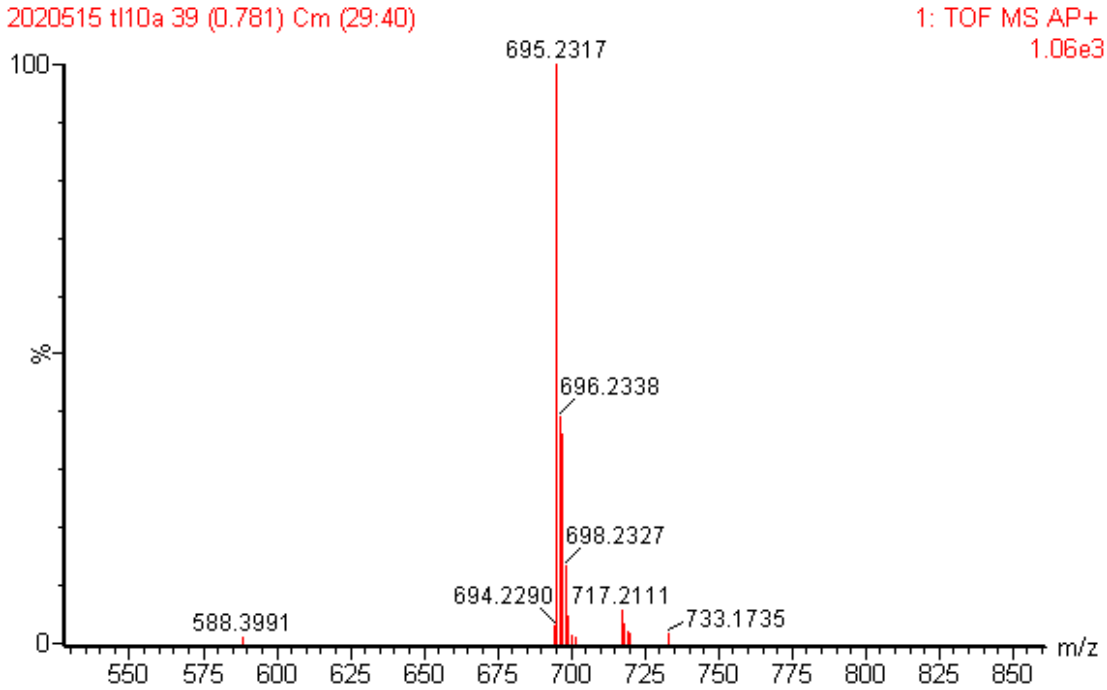

Figure S101. API(+) HRMS spectrum of **4b**.

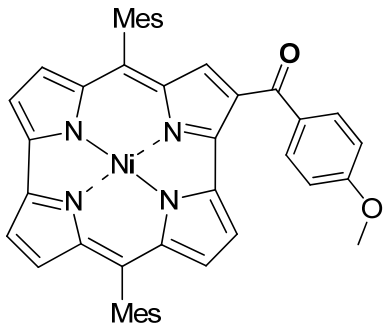

3c

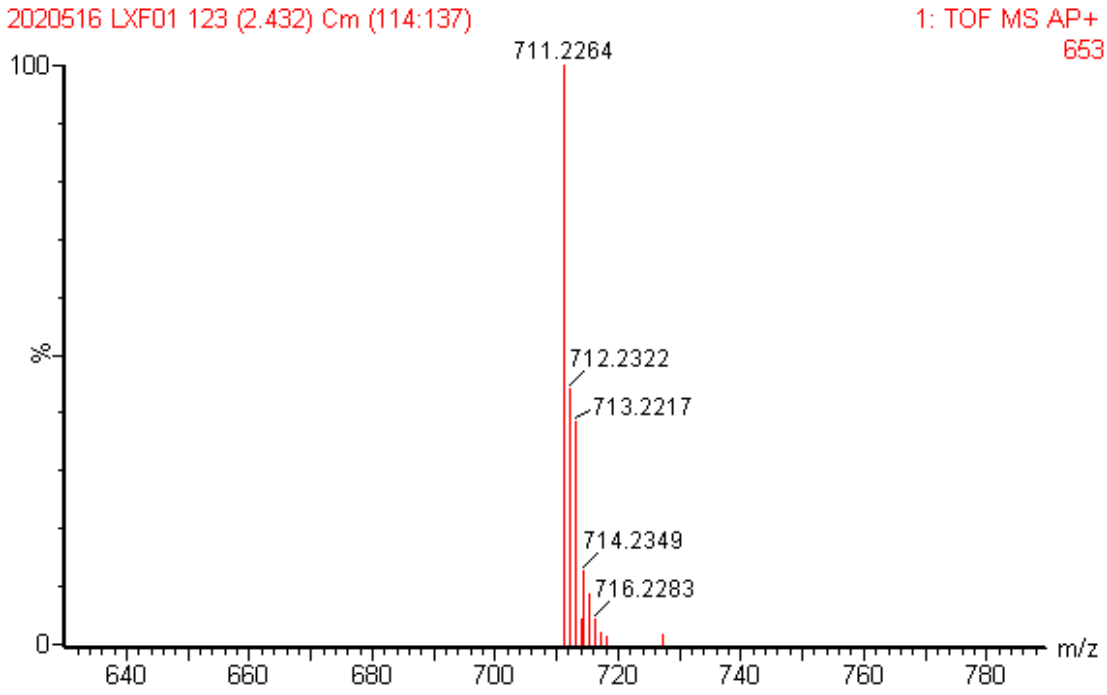

Figure S102. API(+) HRMS spectrum of **3c**.

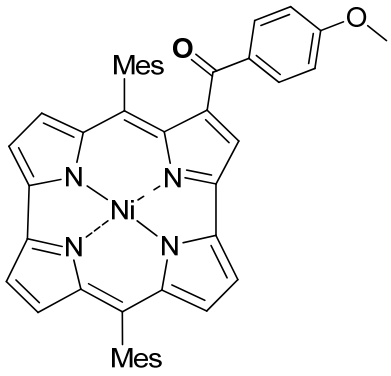

4c

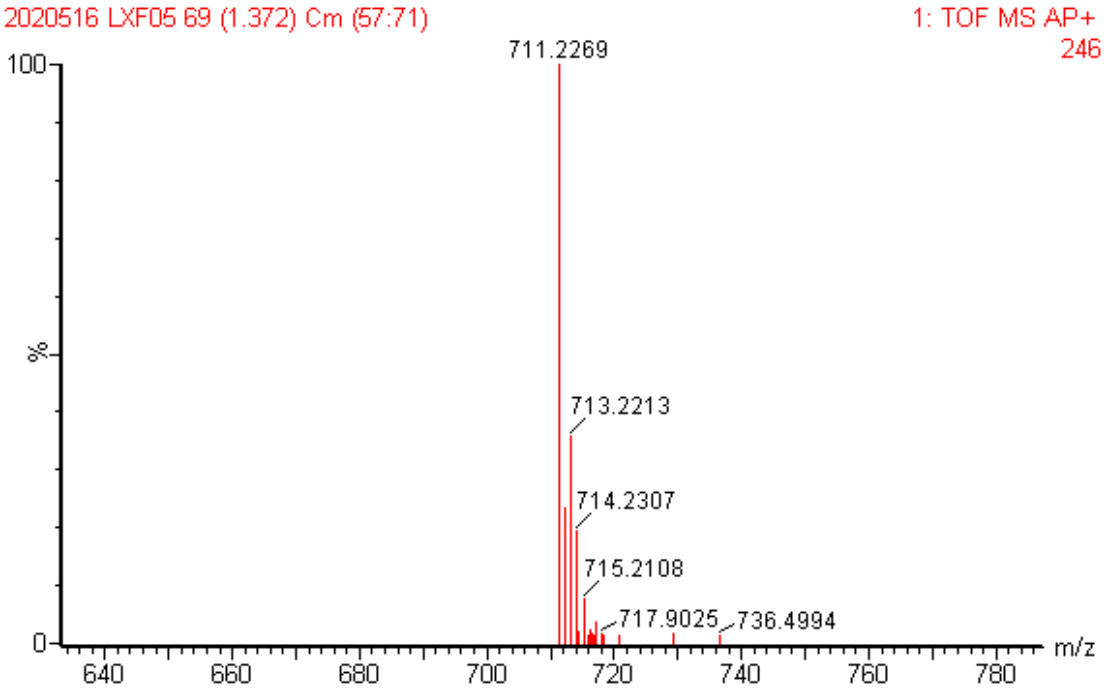

Figure S103. API(+) HRMS spectrum of **4c**.

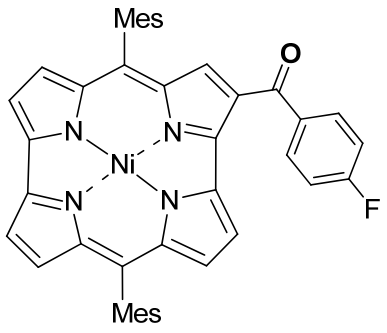

3d

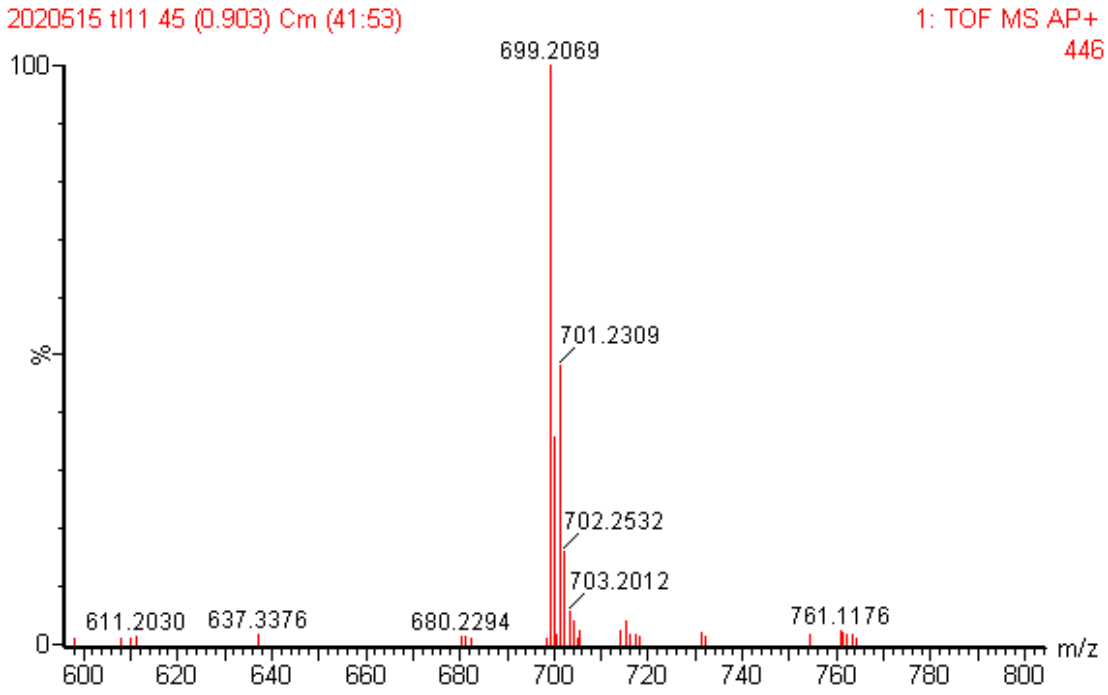

Figure S104. API(+) HRMS spectrum of **3d**.

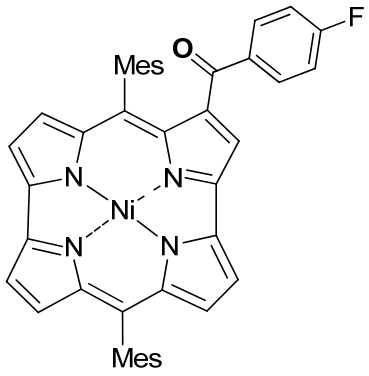

4d

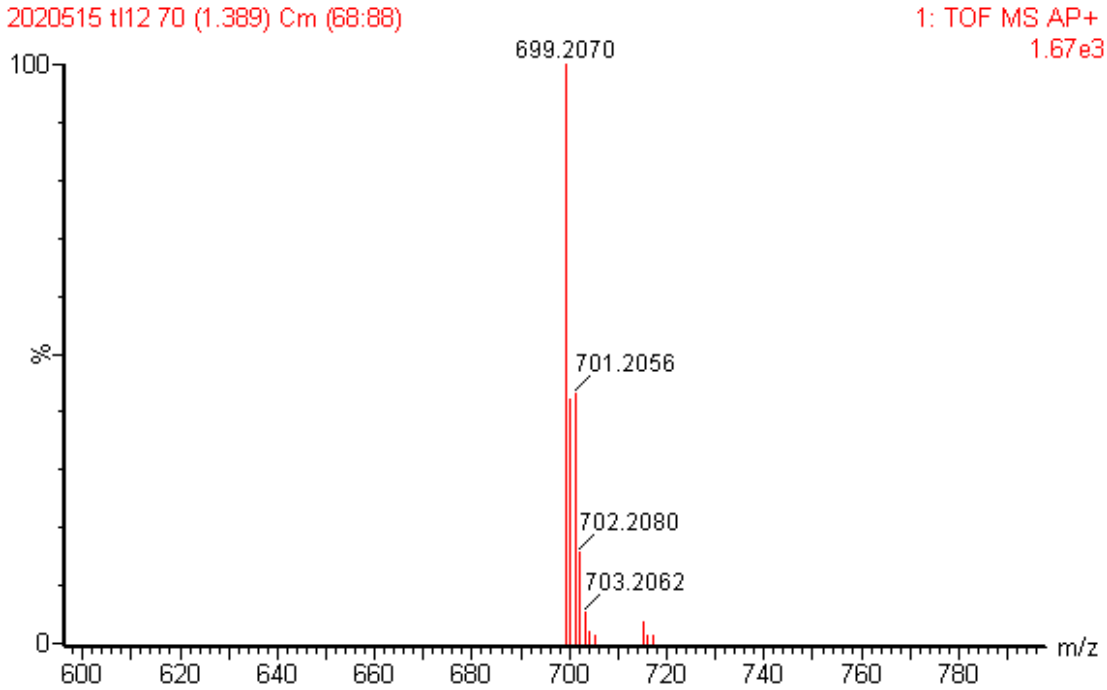

Figure S105. API(+) HRMS spectrum of **4d**.

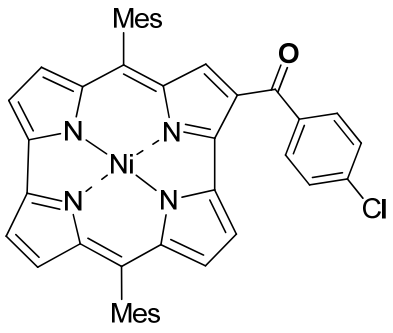

3e

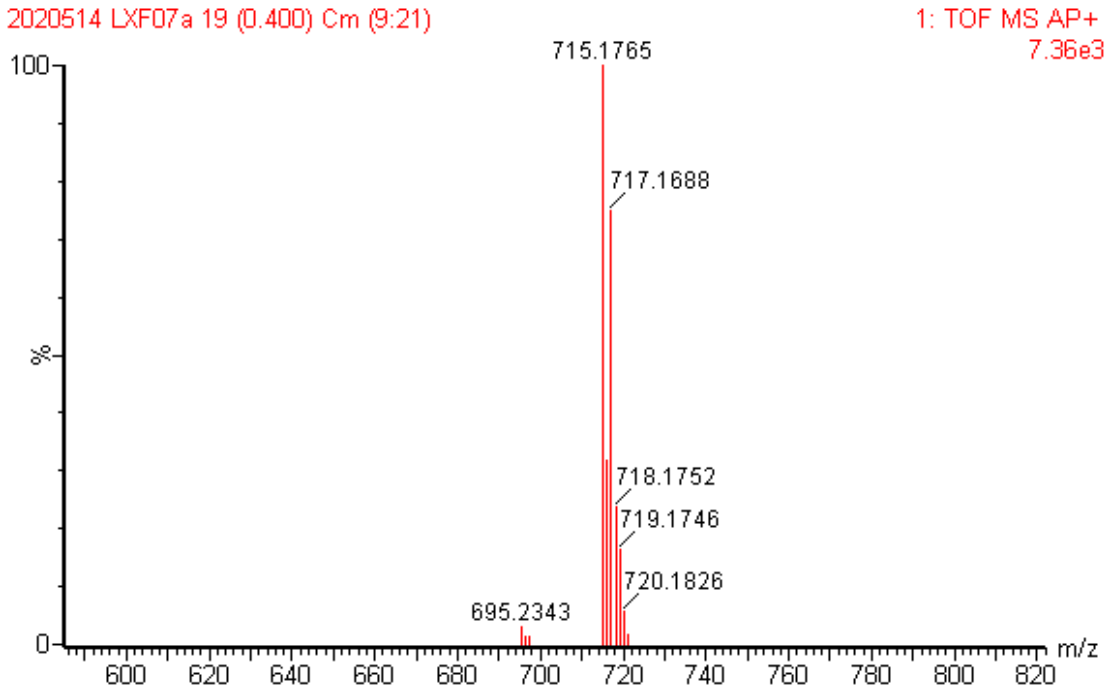

Figure S106. API(+) HRMS spectrum of **3e**.

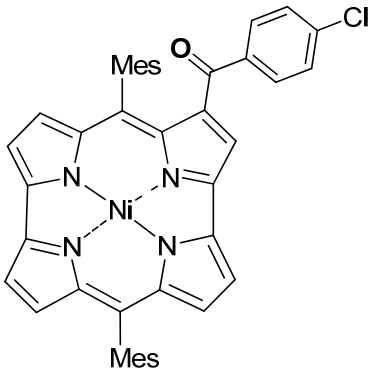

4e

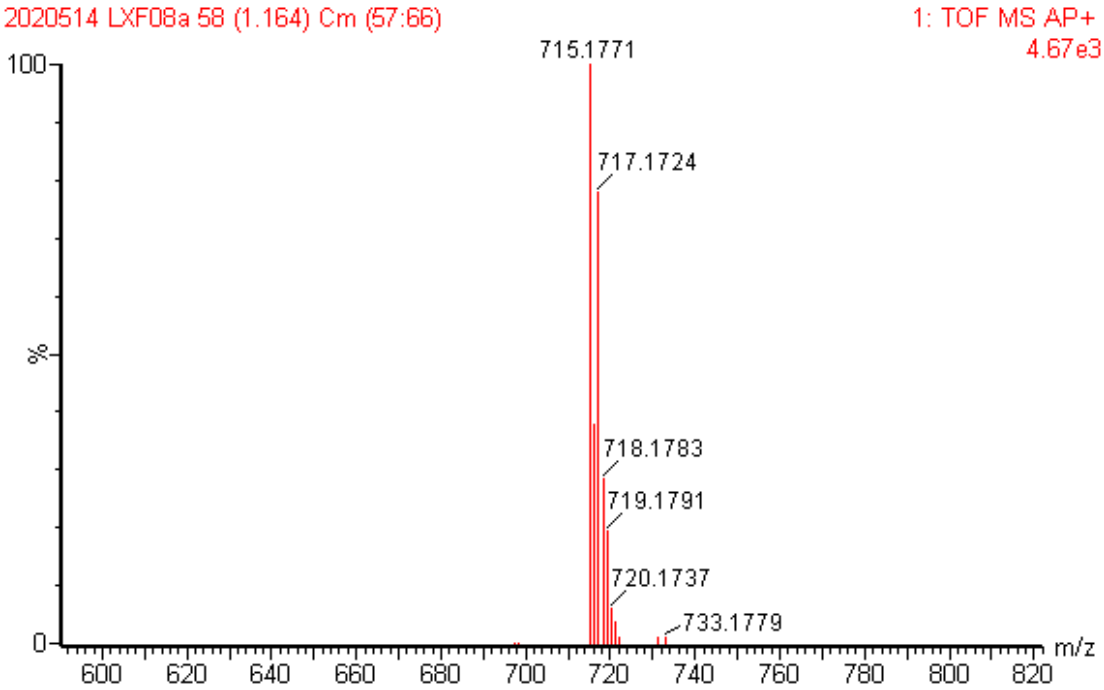

Figure S107. API(+) HRMS spectrum of **4e**.

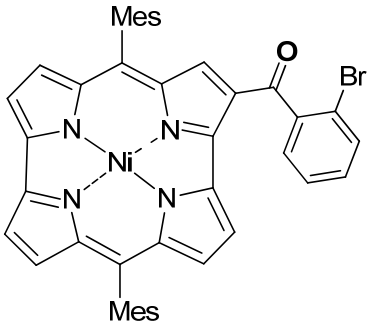

3f

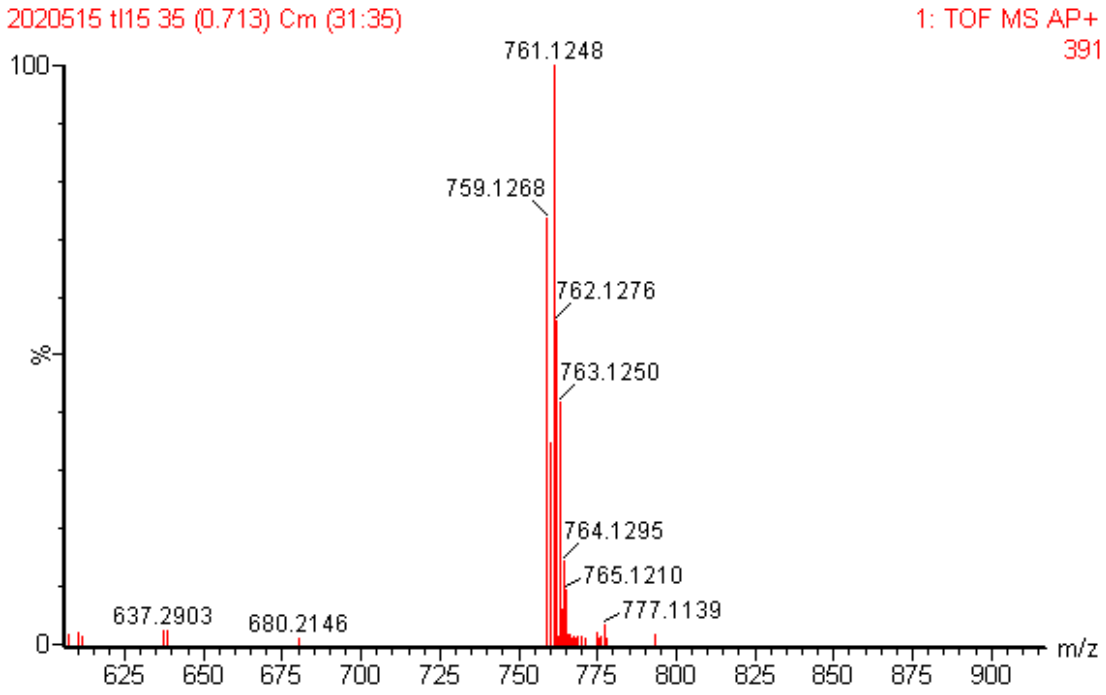

Figure S108. API(+) HRMS spectrum of **3f**.

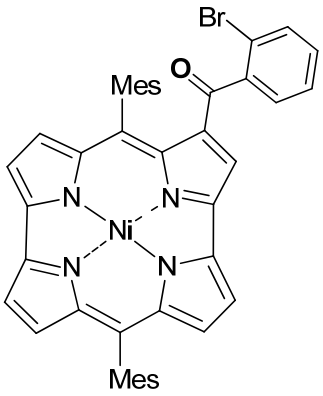

4f

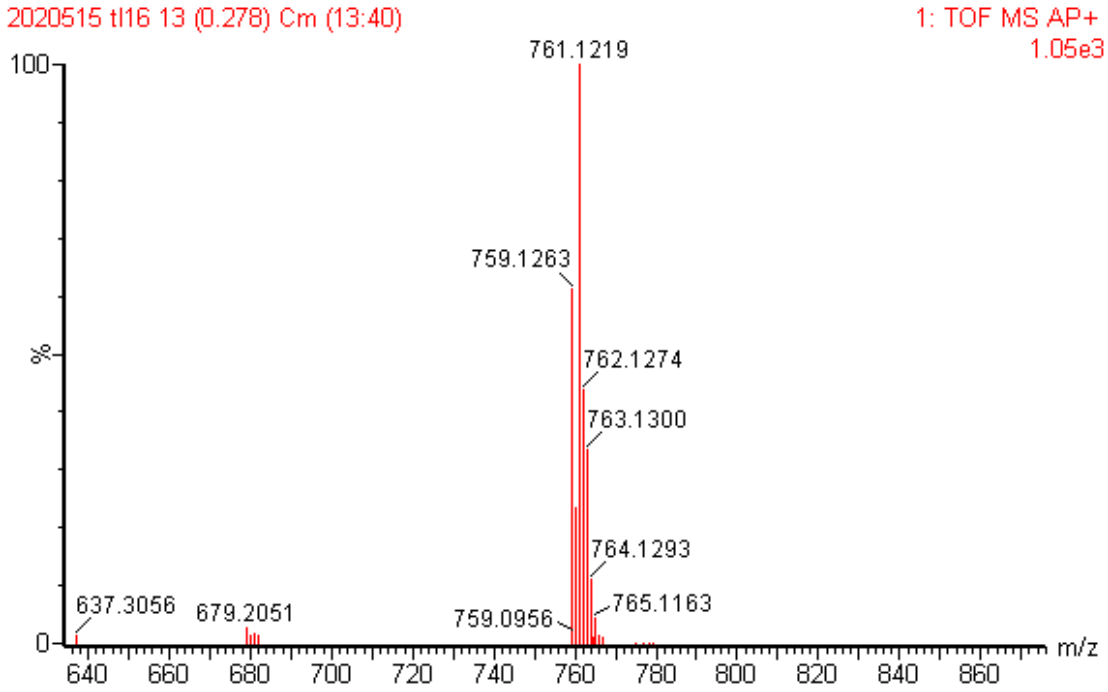

Figure S109. API(+) HRMS spectrum of **4f**.

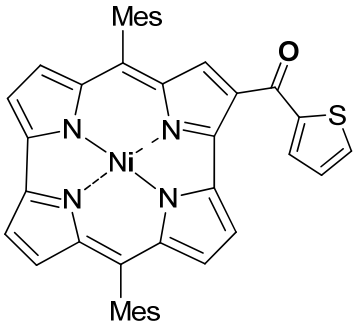

3g

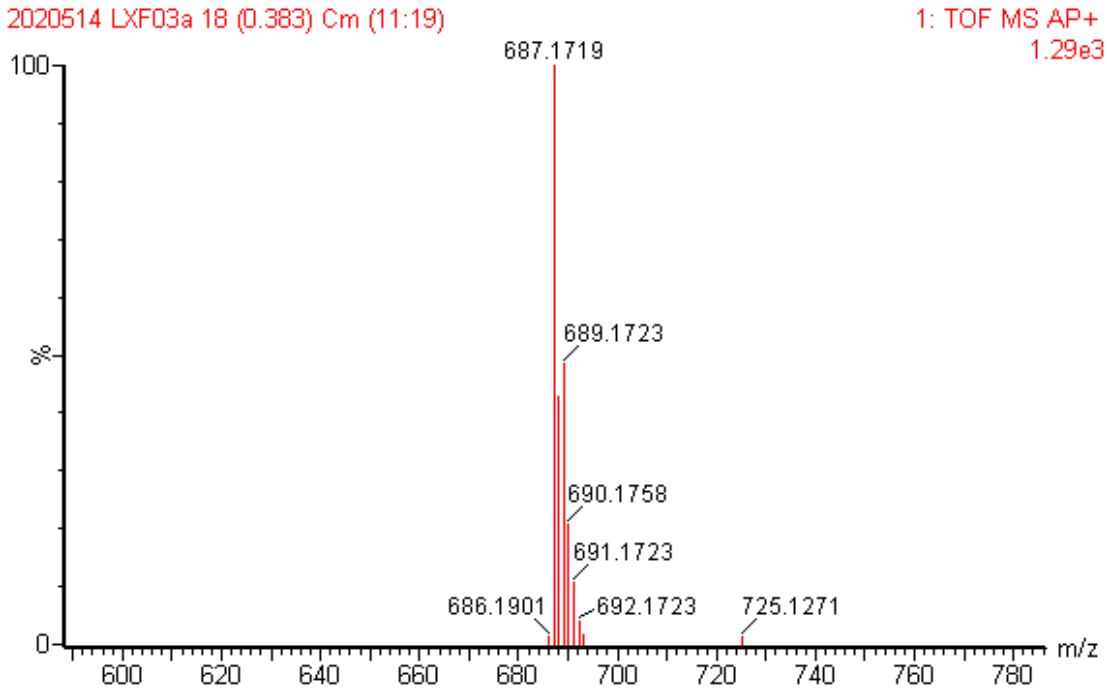

Figure S110. API(+) HRMS spectrum of **3g**.

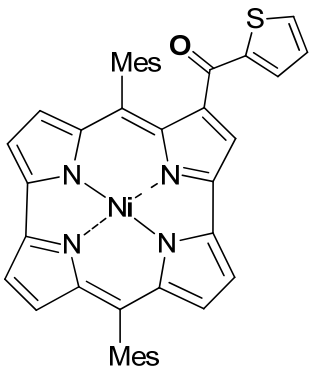

4g

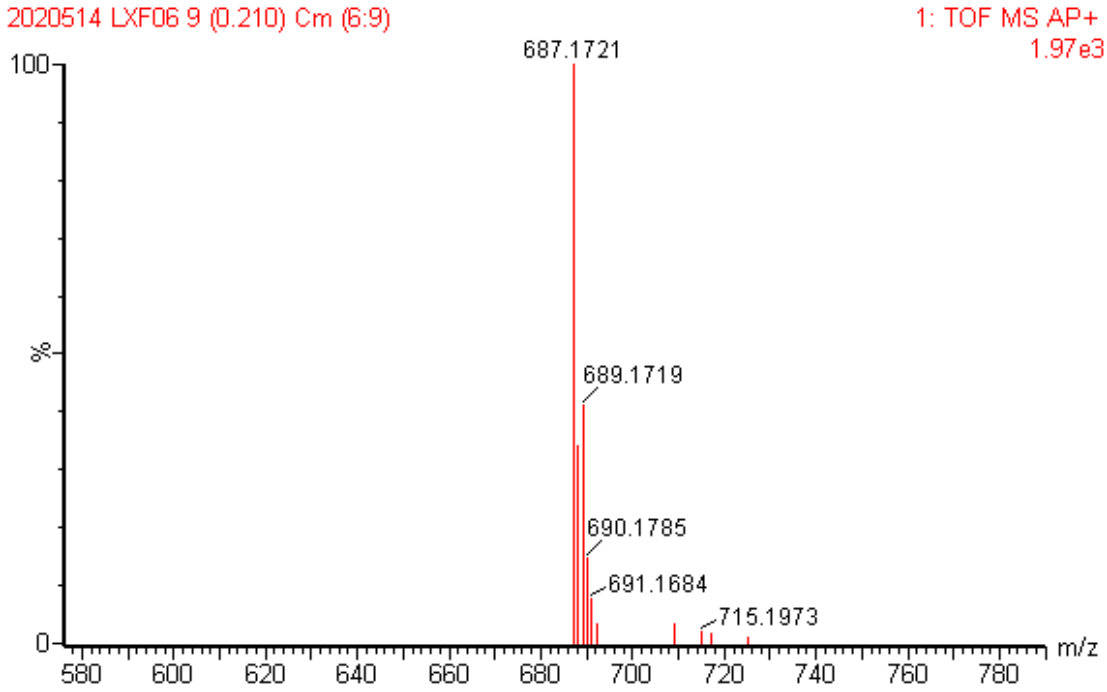

Figure S111. API(+) HRMS spectrum of **4g**.

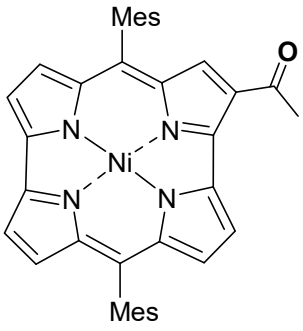

3h

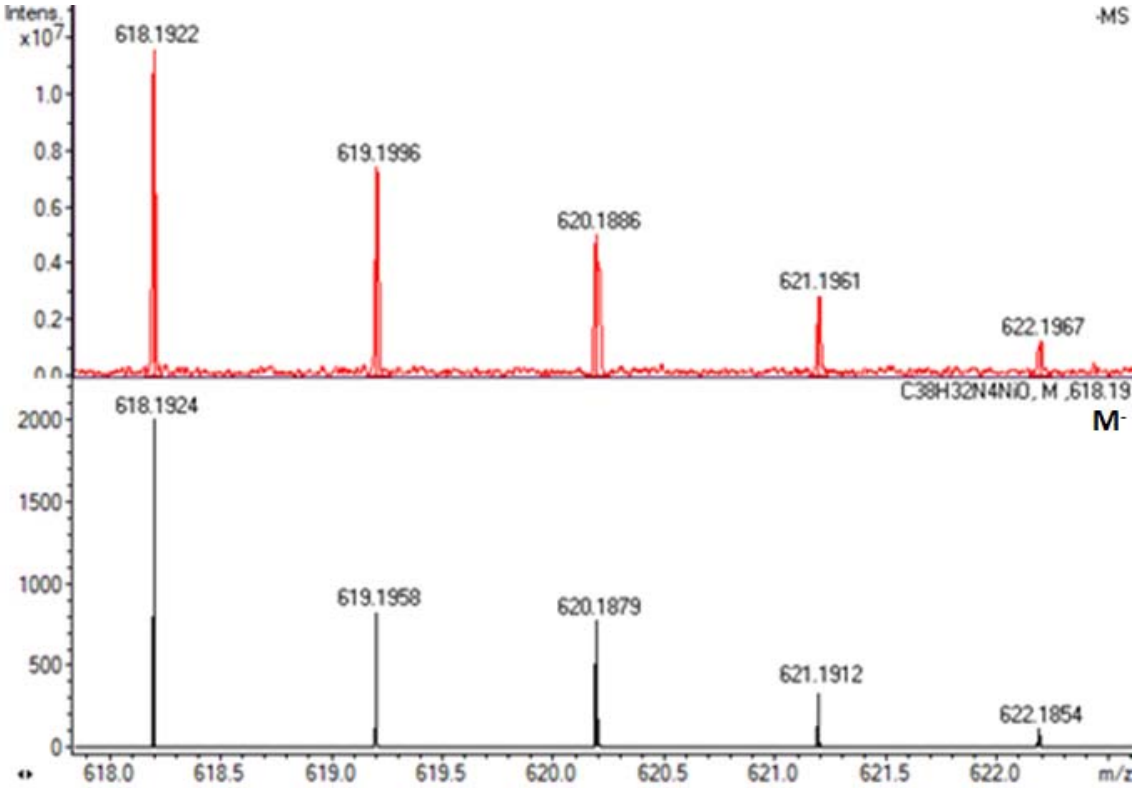

Figure S112. ESI(-) HRMS spectrum of **3h** (experimental: upper trace; simulated: black, bottom trace).

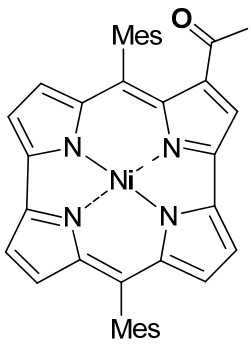

4h

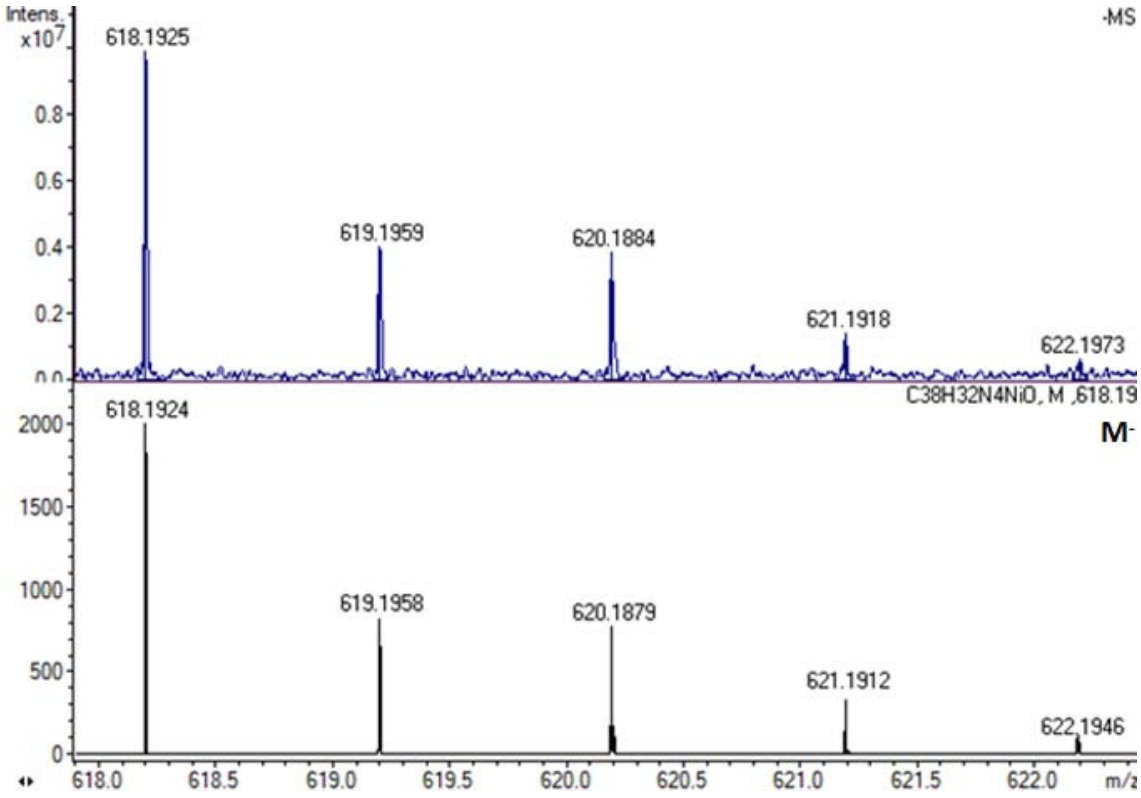

Figure S113. ESI(-) HRMS spectrum of **4h** (experimental: upper trace; simulated: black, bottom trace).

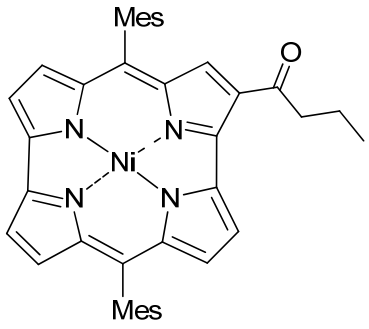

3i

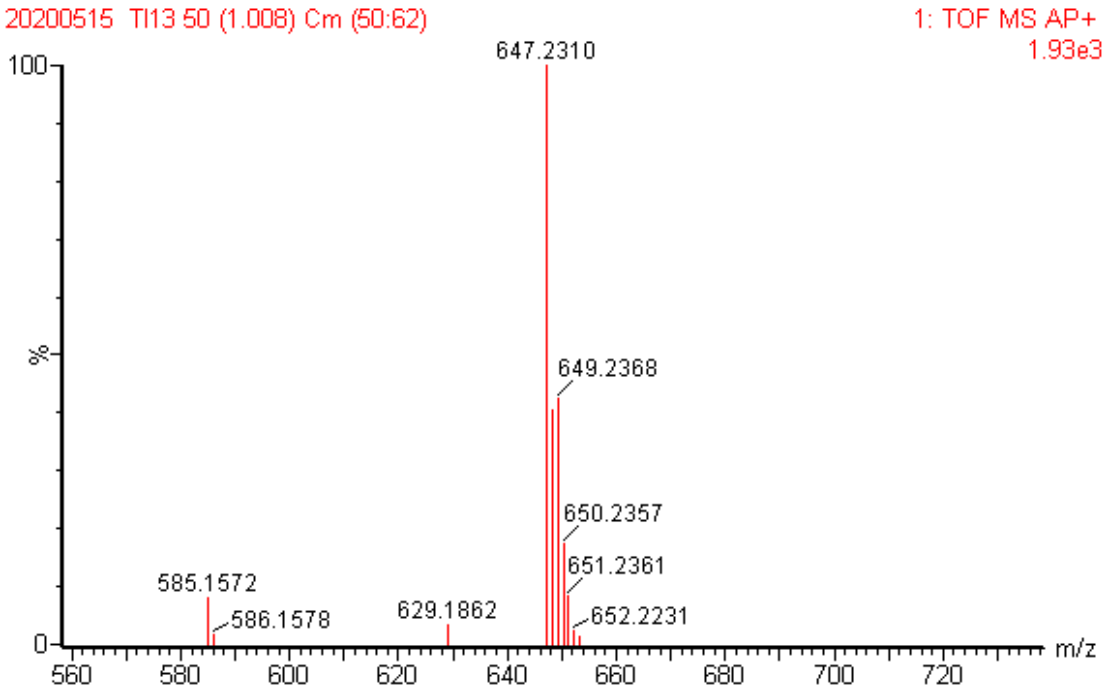

Figure S114. API(+) HRMS spectrum of **3i**.

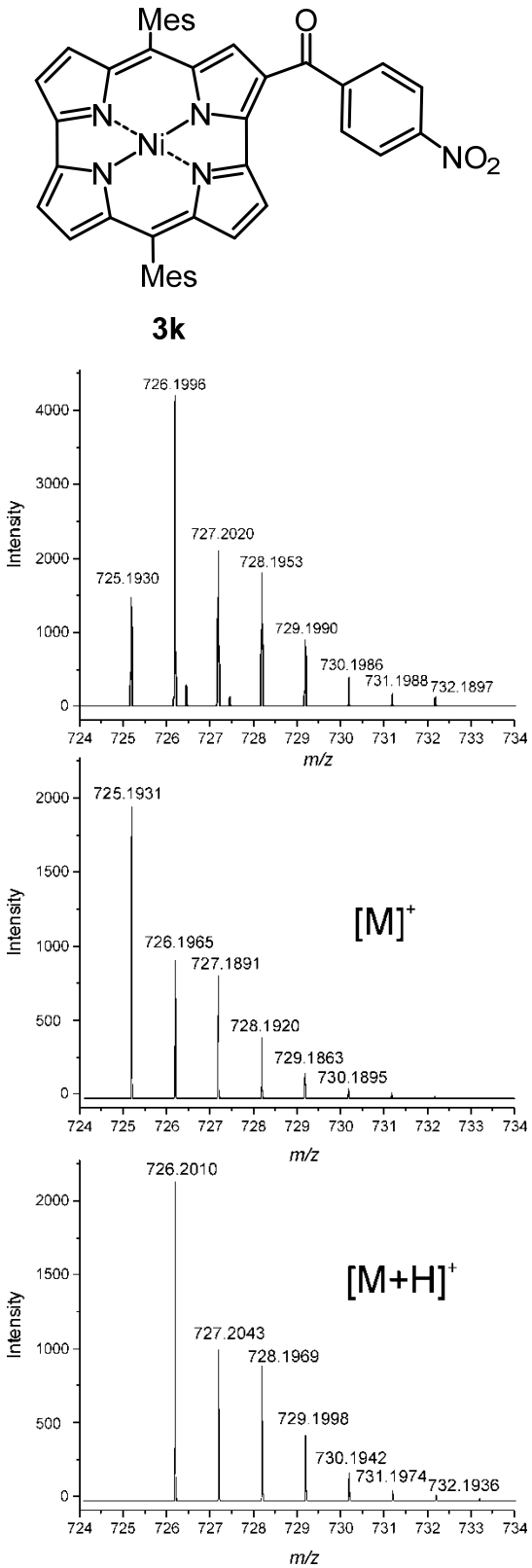

Figure S115. ESI(+) HRMS spectrum of **3k** (experimental: upper trace; simulated: bottom traces).

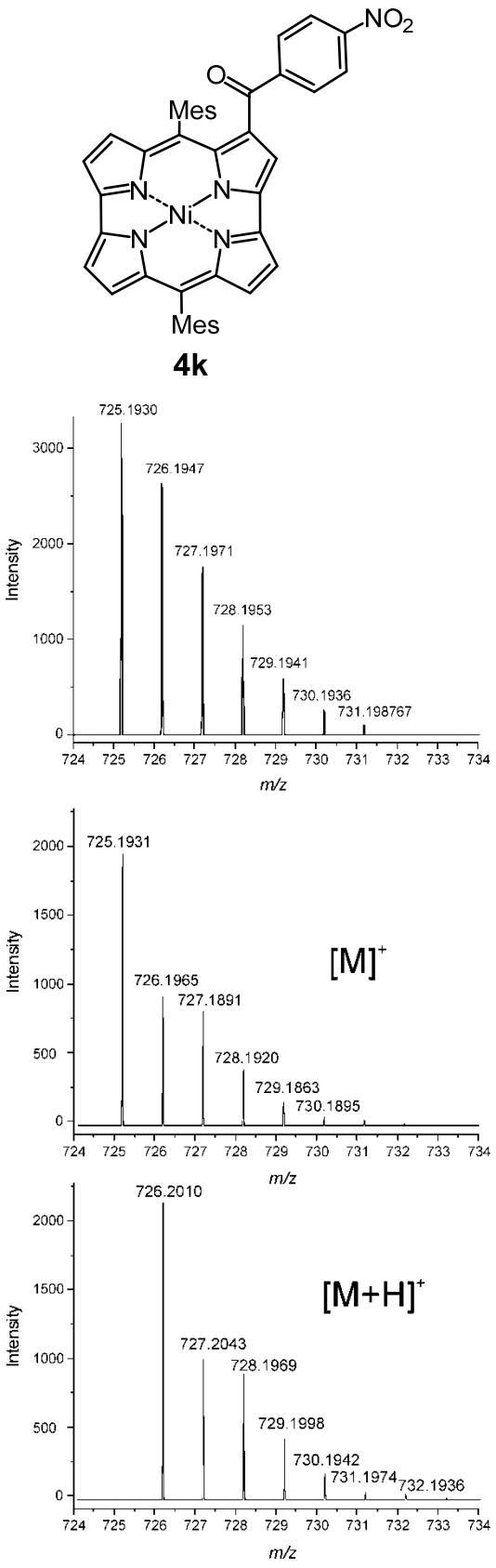

Figure S116. ESI(+) HRMS spectrum of **4k** (experimental: upper trace; simulated: bottom traces).

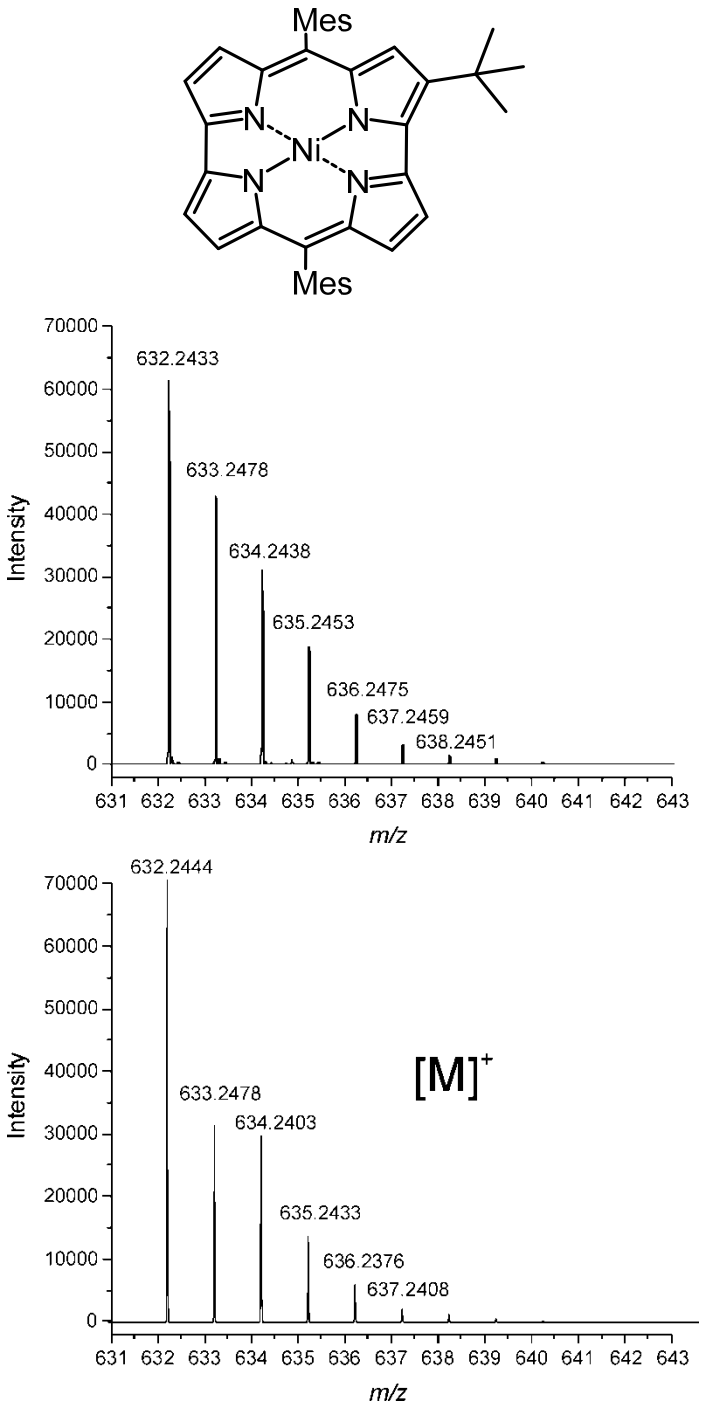

Figure S117. ESI(+) HRMS spectrum of **1-***t*Bu (experimental: upper trace; simulated: bottom trace).

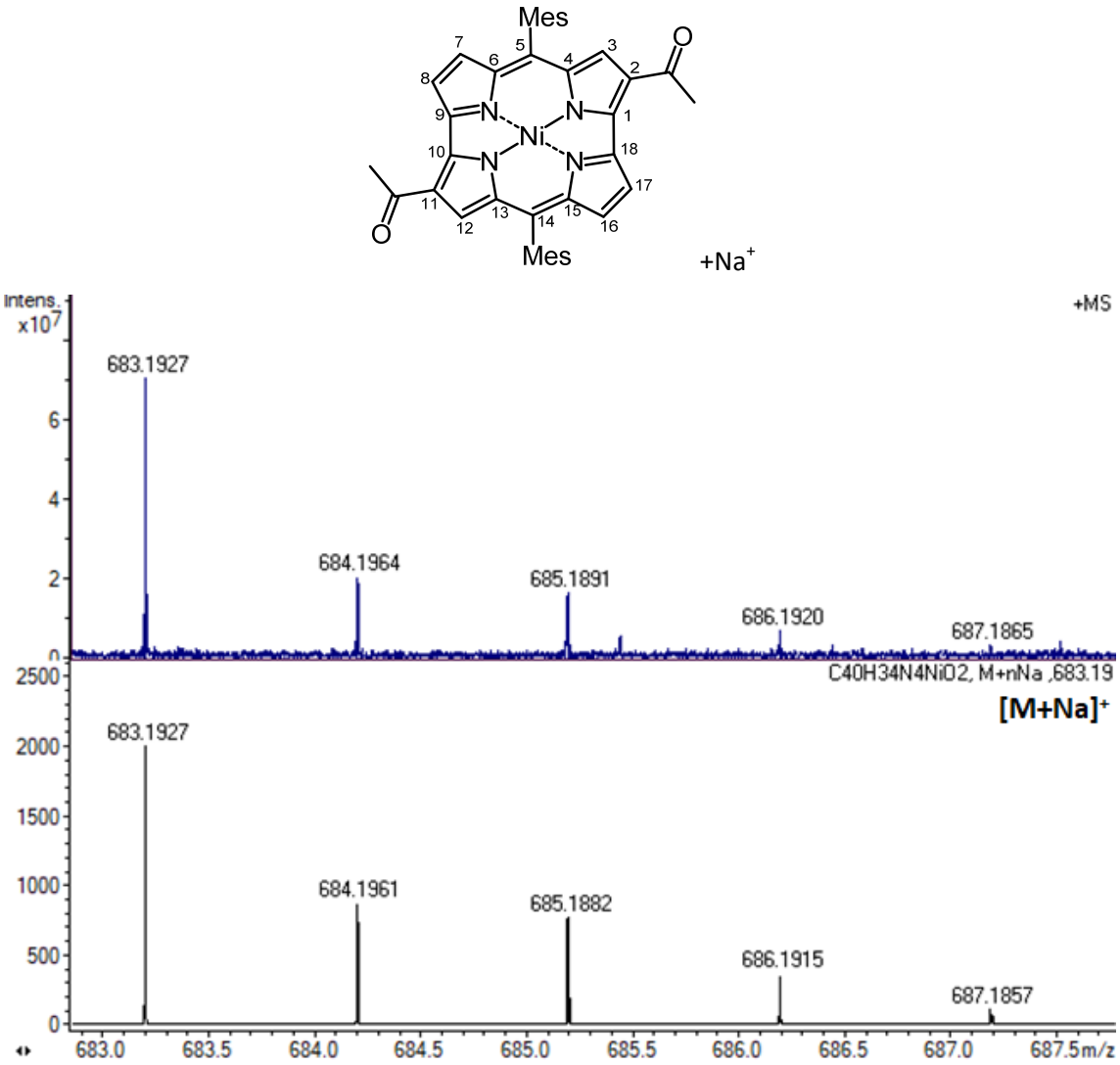

Figure S118. ESI(+) HRMS spectrum of **5a** (experimental: upper trace; simulated: black, bottom trace).

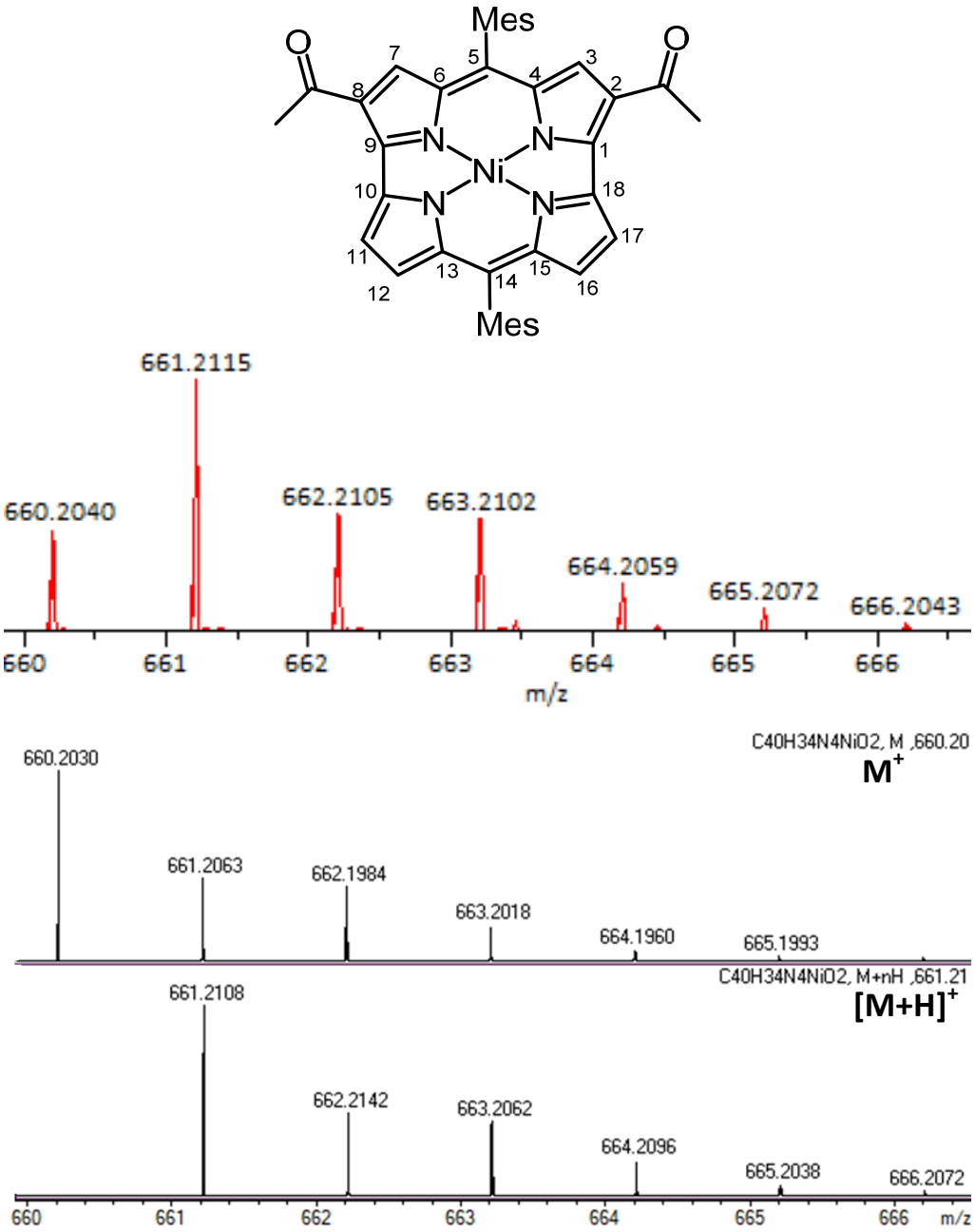

Figure S119. ESI(+) HRMS spectrum of **5b** (experimental: upper trace; simulated: black, bottom trace).

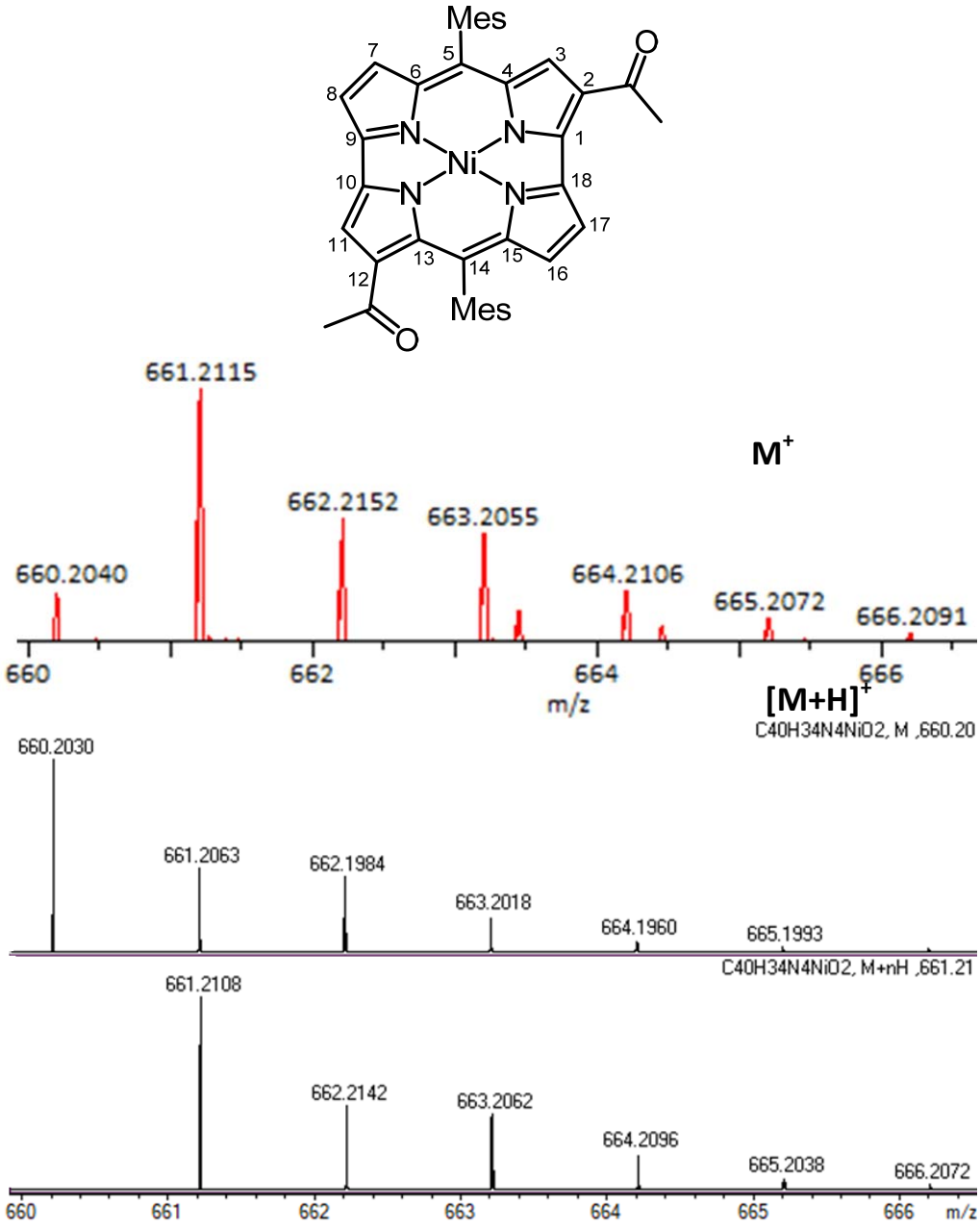

Figure S120. ESI(+) HRMS spectrum of **5c** (experimental: upper trace; simulated: black, bottom trace).

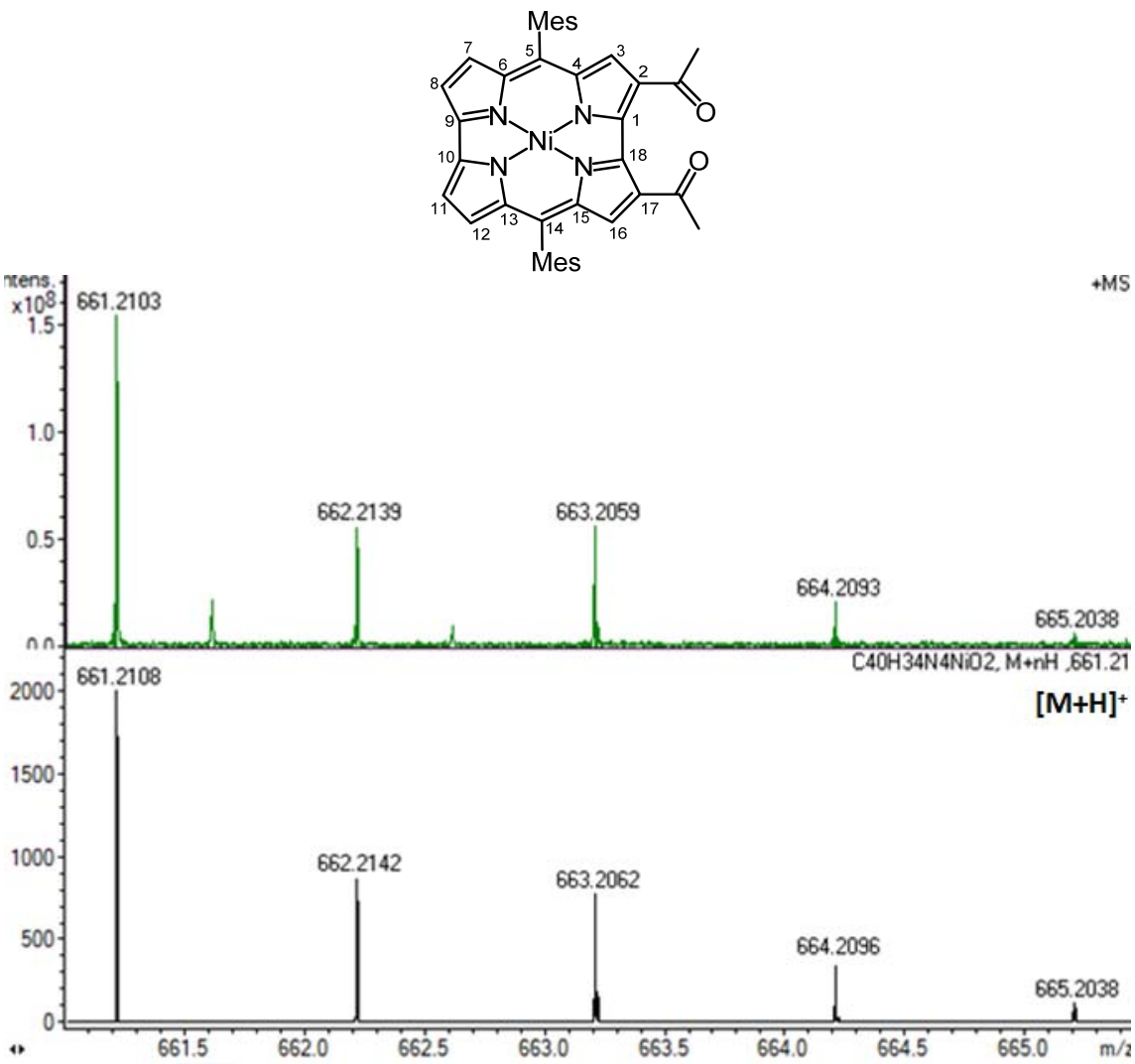

Figure S121. ESI(+) HRMS spectrum of **5d** (experimental: upper trace; simulated: black, bottom trace).

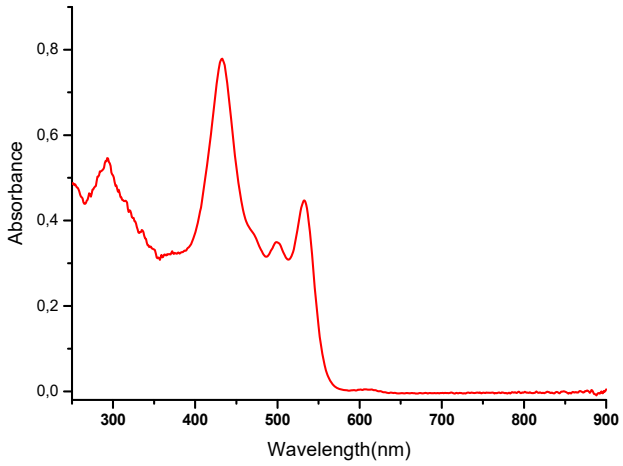

Figure S122. UV-vis spectrum of **3a** (CH_2Cl_2).

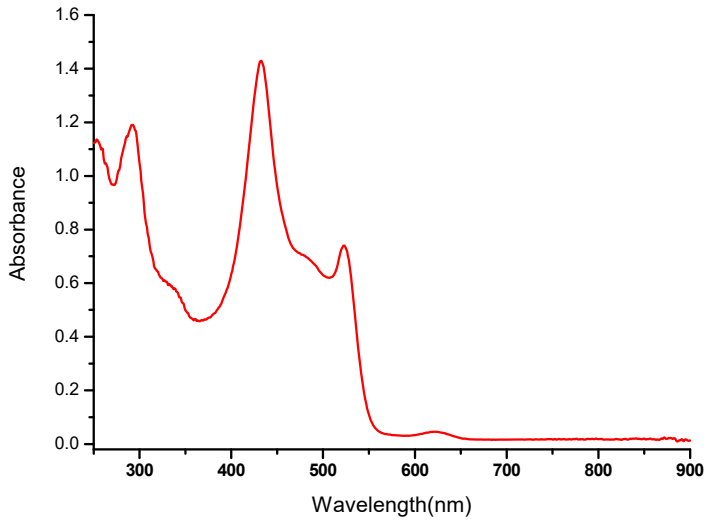

Figure S123. UV-vis spectrum of **4a** (CH_2Cl_2).

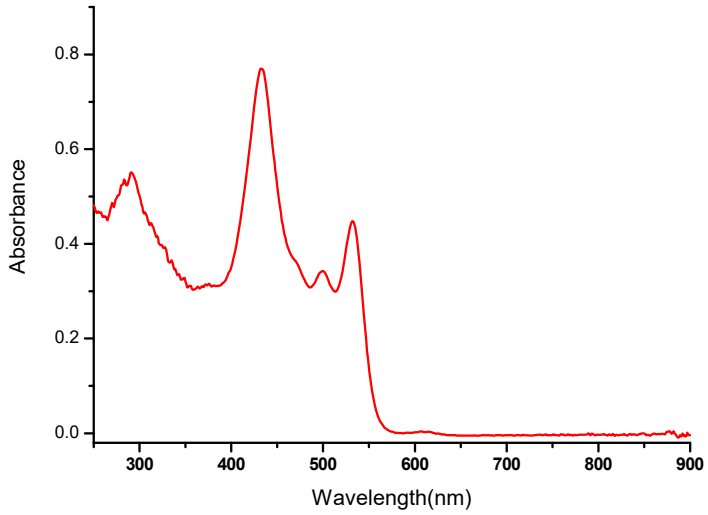

Figure S124. UV-vis spectrum of **3b** (CH_2Cl_2).

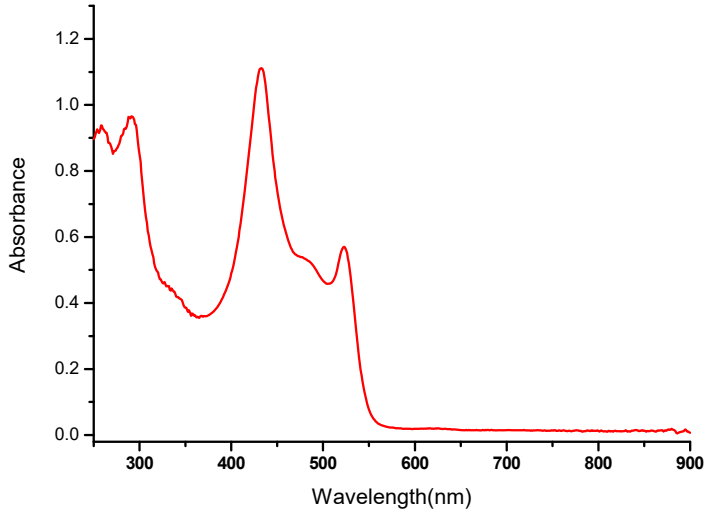

Figure S125. UV-vis spectrum of **4b** (CH_2Cl_2).

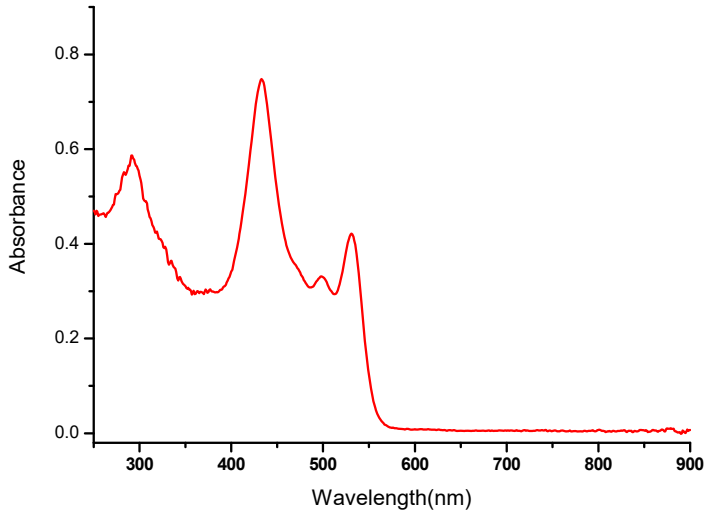

Figure S126. UV-vis spectrum of **3c** (CH_2Cl_2).

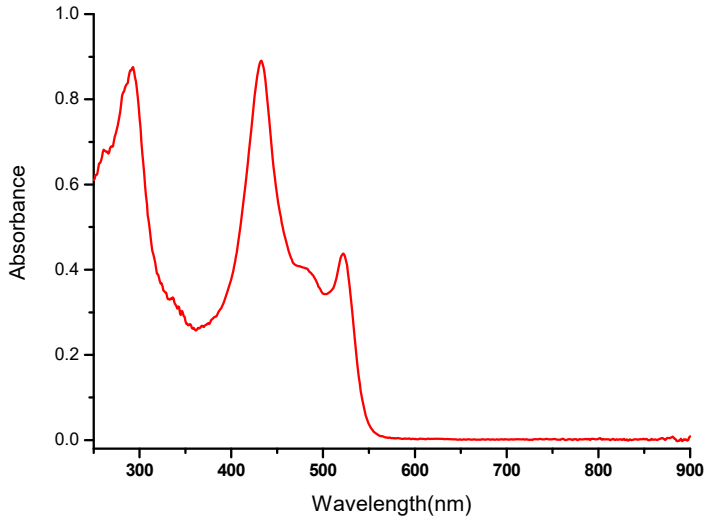

Figure S127. UV-vis spectrum of **4c** (CH_2Cl_2).

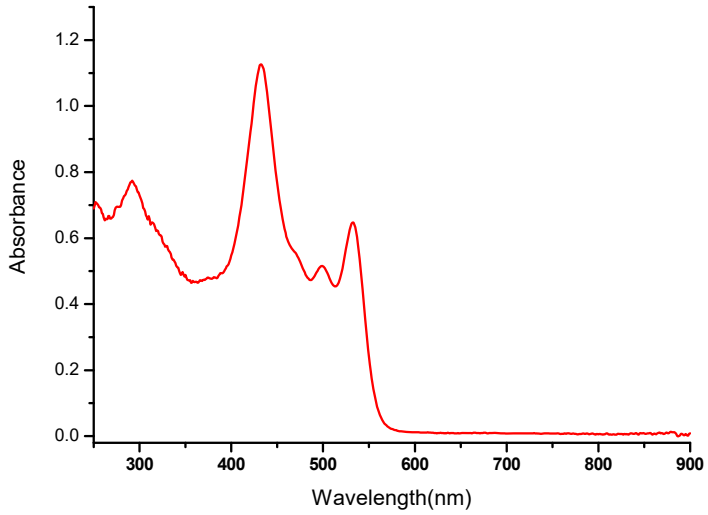

Figure S128. UV-vis spectrum of **3d** (CH_2Cl_2).

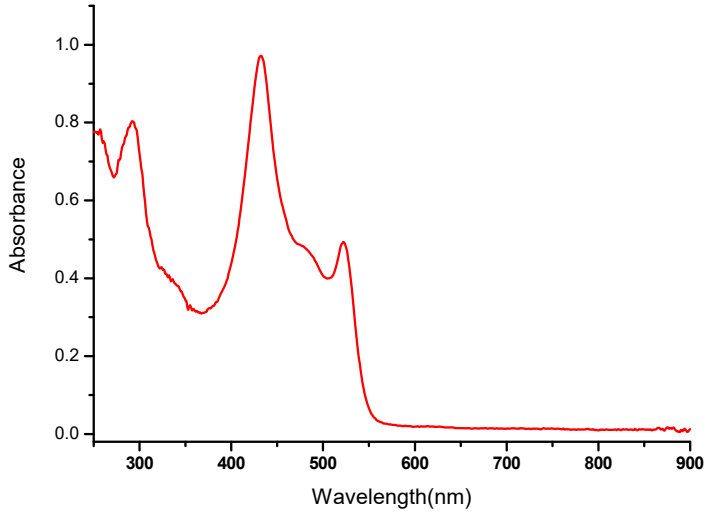

Figure S129. UV-vis spectrum of **4d** (CH_2Cl_2).

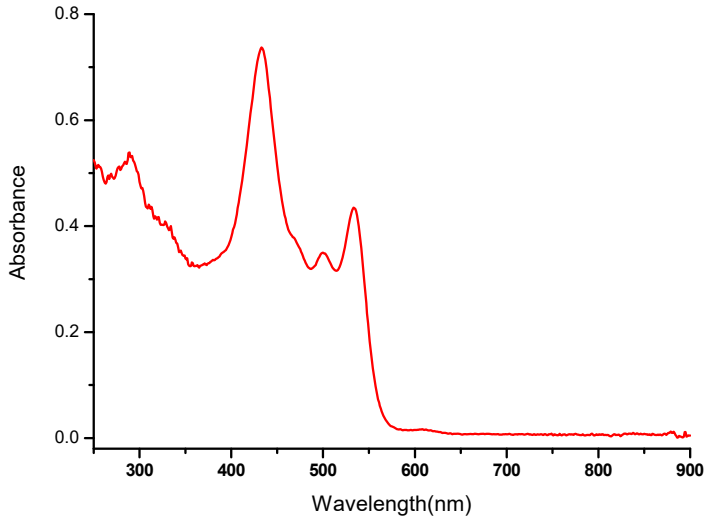

Figure S130. UV-vis spectrum of **3e** (CH_2Cl_2).

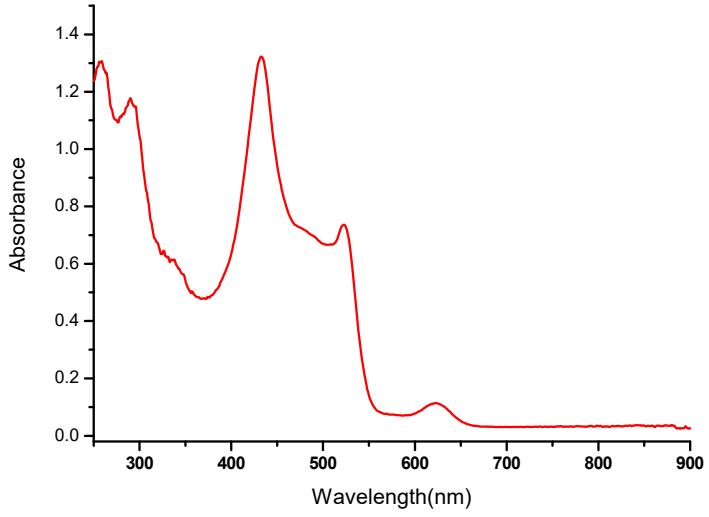

Figure S131. UV-vis spectrum of **4e** (CH_2Cl_2).

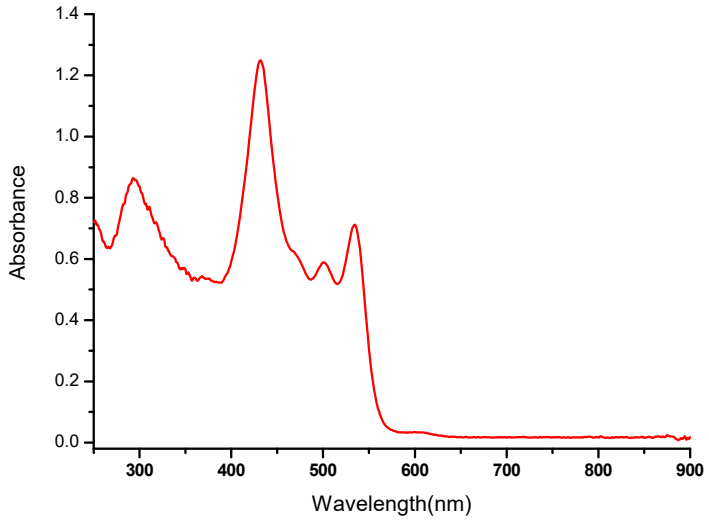

Figure S132. UV-vis spectrum of **3f** (CH_2Cl_2).

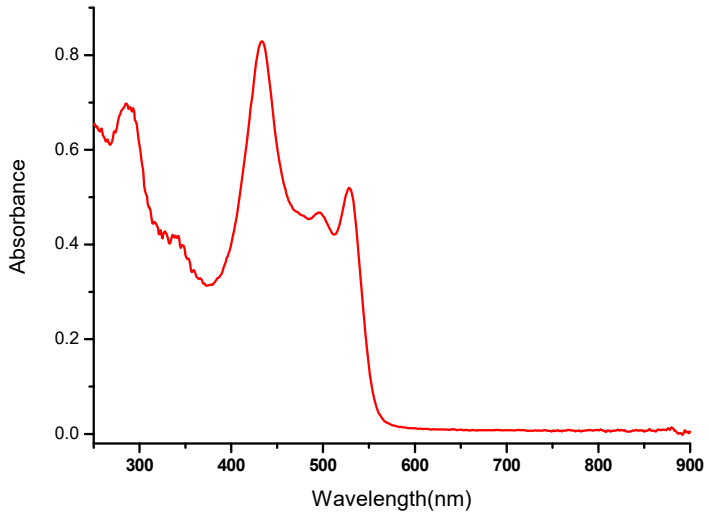

Figure S133. UV-vis spectrum of **4f** (CH_2Cl_2).

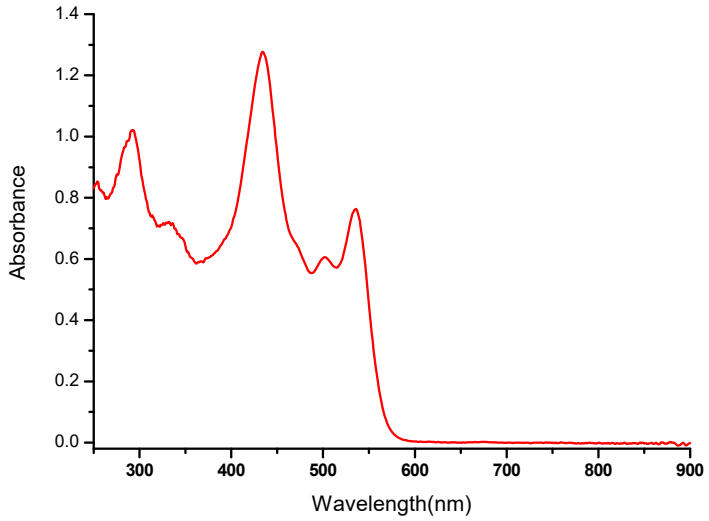

Figure S134. UV-vis spectrum of **3g** (CH_2Cl_2).

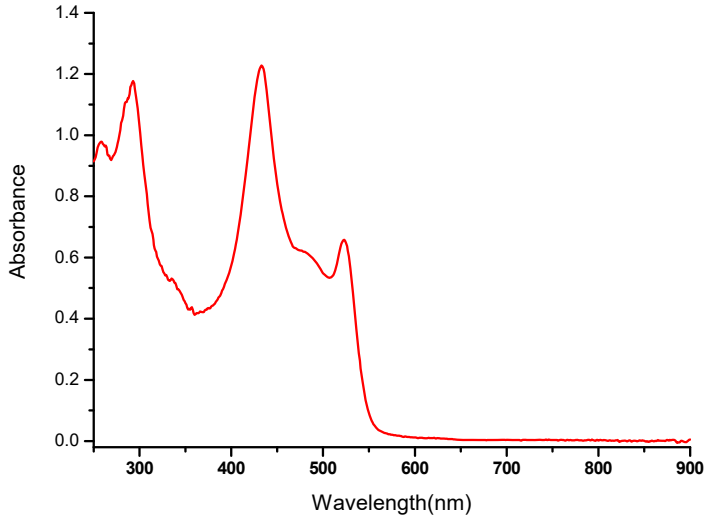

Figure S135. UV-vis spectrum of **4g** (CH_2Cl_2).

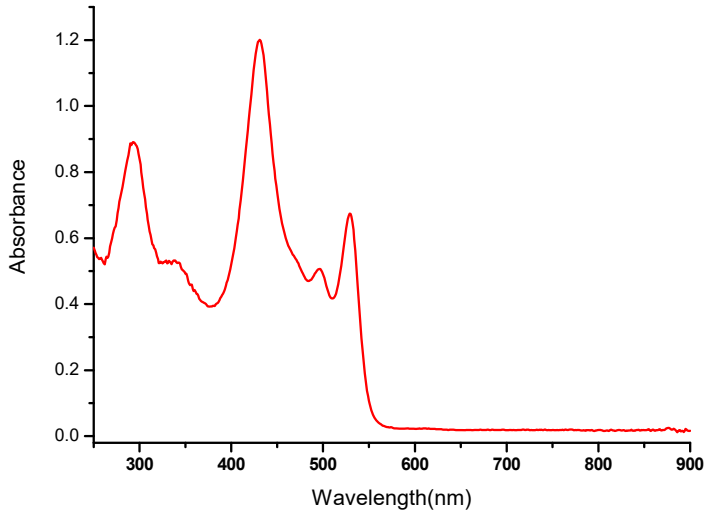

Figure S136. UV-vis spectrum of **3h** (CH_2Cl_2).

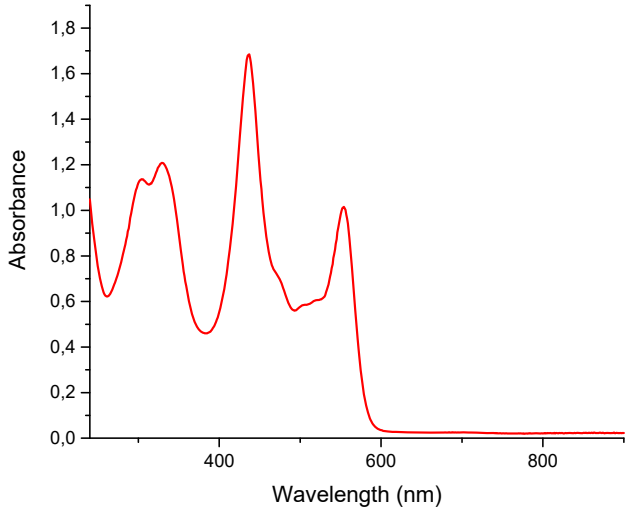

Figure S137. UV-vis spectrum of **4h** (CH_2Cl_2).

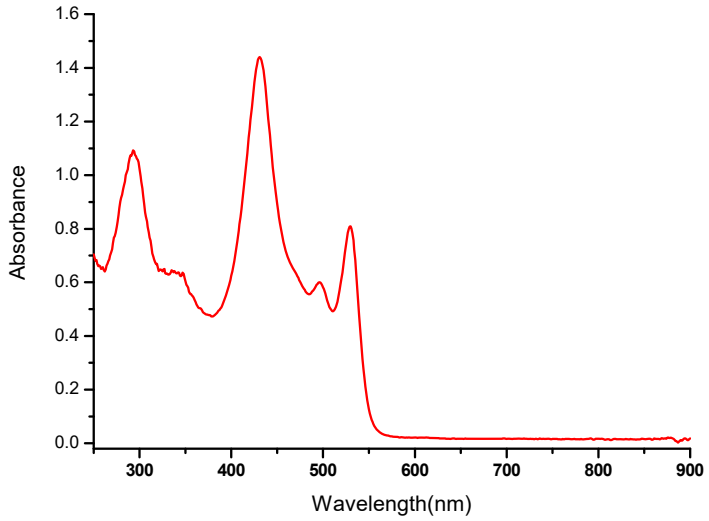

Figure S138. UV-vis spectrum of **3i** (CH_2Cl_2).

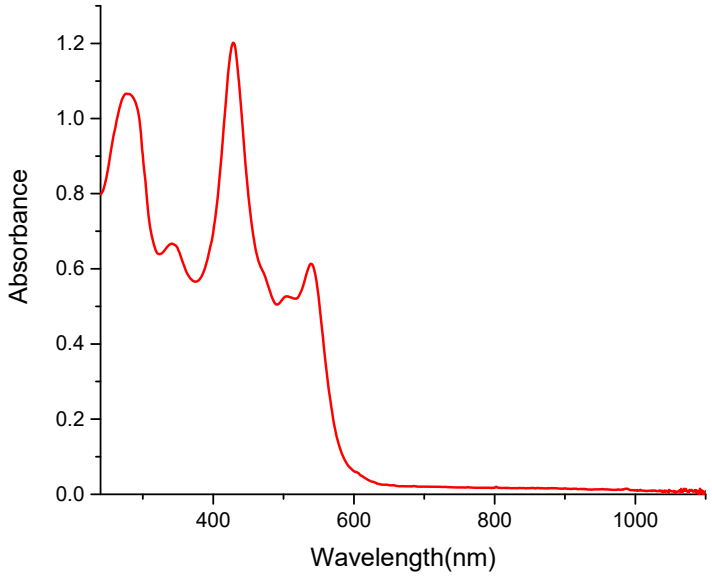

Figure S139. UV-vis spectrum of **3k** (CH_2Cl_2).

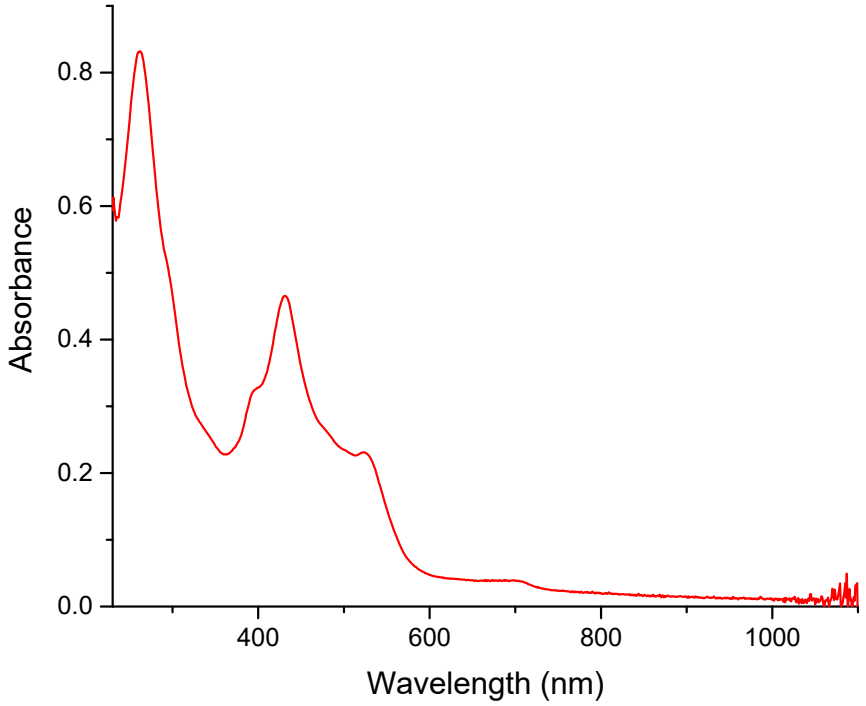

Figure S140. UV-vis spectrum of **4k** (CH_2Cl_2).

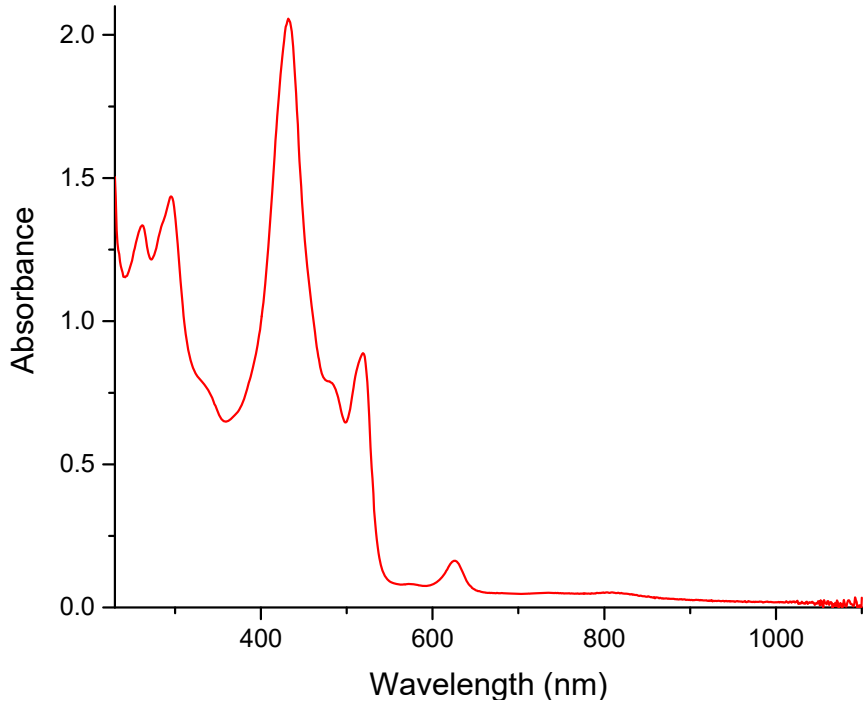

Figure S141. UV-vis spectrum of **1**-*t*Bu (CH_2Cl_2).

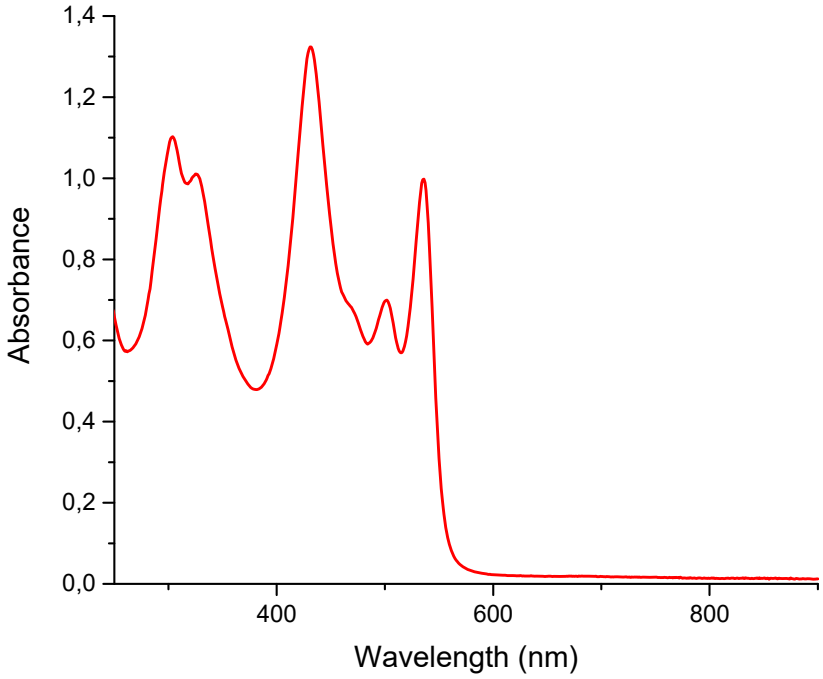

Figure S142. UV-vis spectrum of **5a** (CH_2Cl_2).

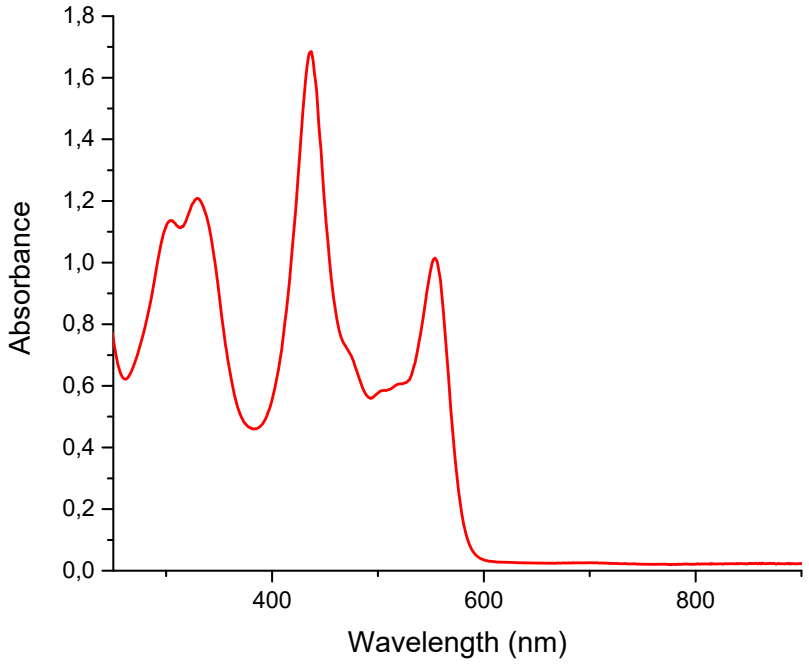

Figure S143. UV-vis spectrum of **5b** (CH_2Cl_2).

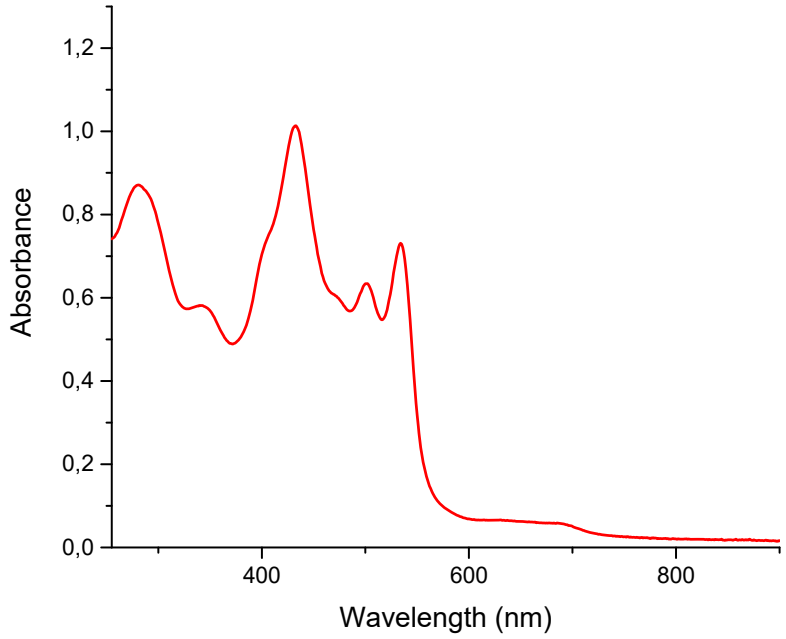

Figure S144. UV-vis spectrum of **5c** (CH_2Cl_2).

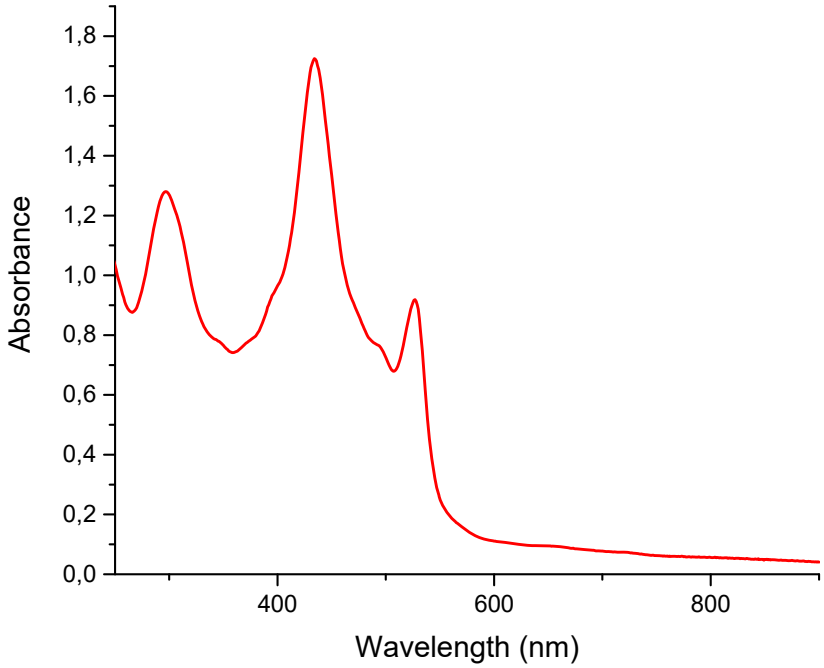

Figure S145. UV-vis spectrum of **5d** (CH_2Cl_2).

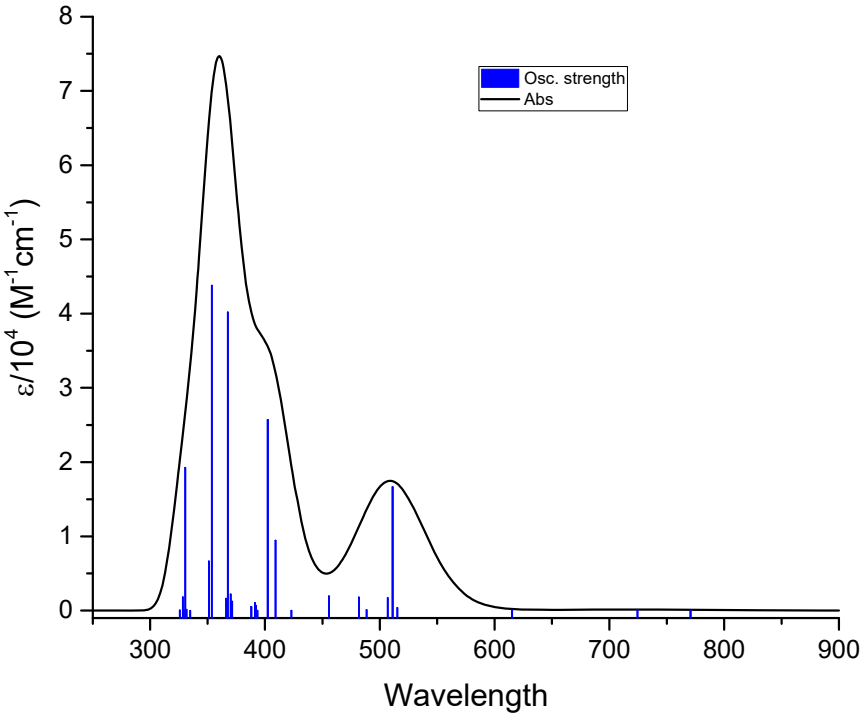

Figure S146. TD DFT-calculated electronic transitions (blue sticks) and UV-vis spectrum (black line) of **3a** (CH_2Cl_2).

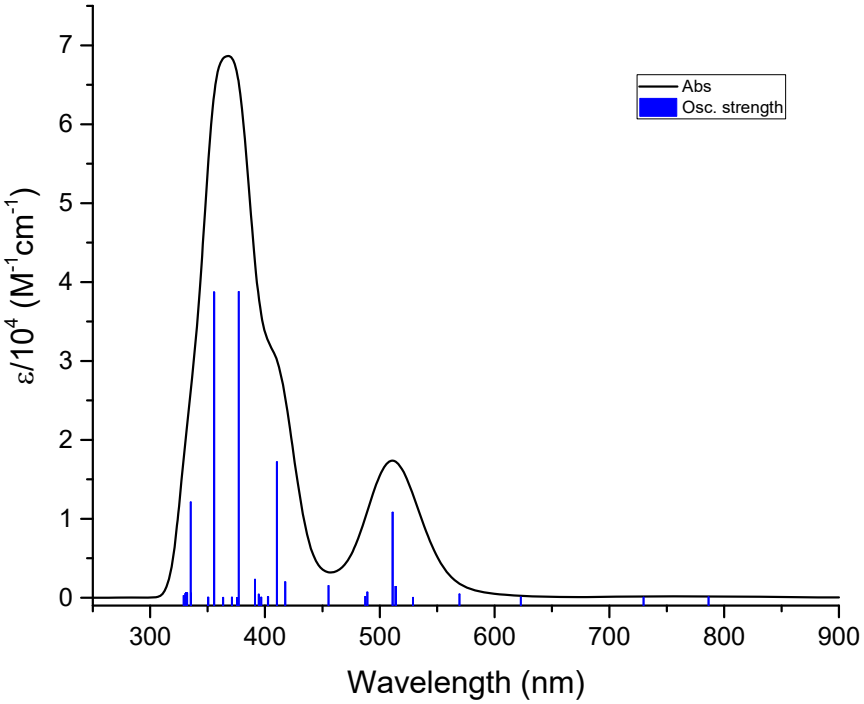

Figure S147. TD DFT-calculated electronic transitions (blue sticks) and UV-vis spectrum (black line) of **4a** (CH_2Cl_2).

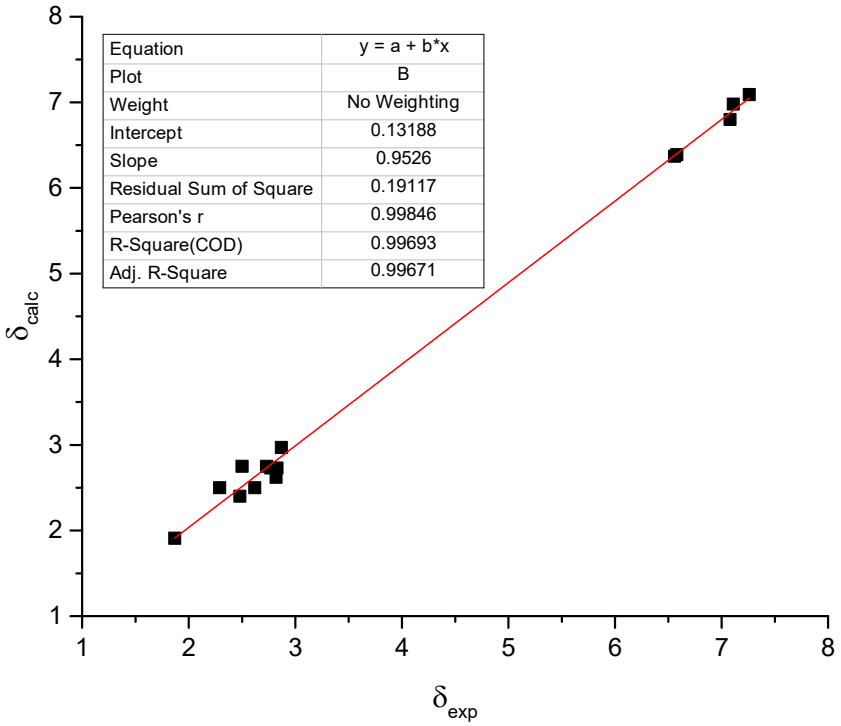

Figure S148. Correlation of experimental (500 MHz, $CDCl_3$, 300 K) and GIAO-calculated ^{1}H NMR chemical shifts of **3a**.

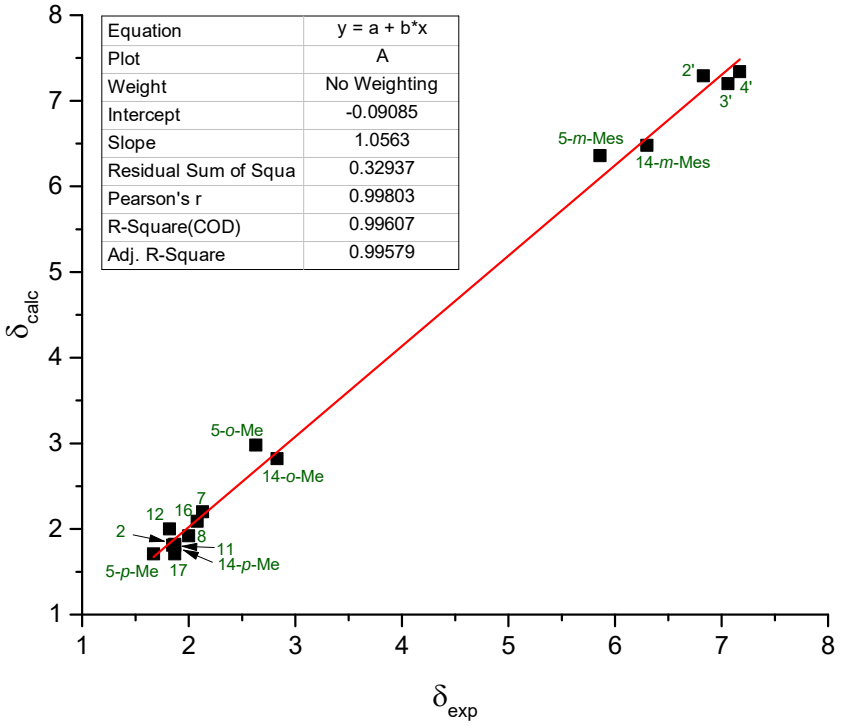

Figure S149. Correlation of experimental (500 MHz, $CDCl_3$, 300 K) and GIAO-calculated ^{1}H NMR chemical shifts of **4a**.

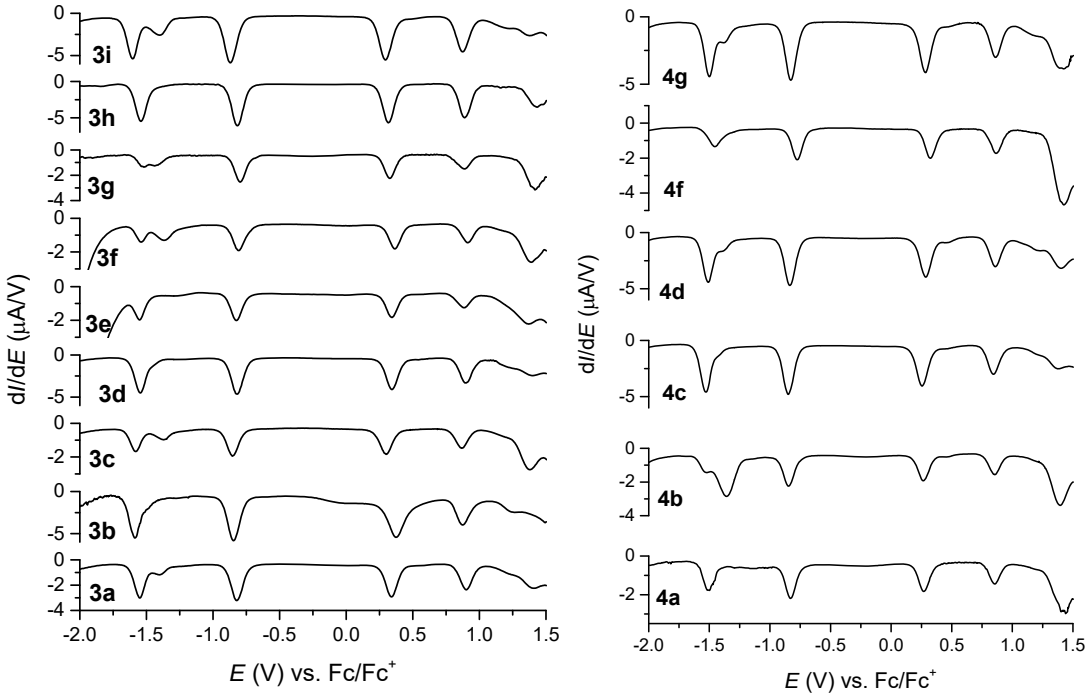

Figure S150. Differential pulse voltammograms of selected acylated norcorroles recorded for DCM solutions with Bu_4NPF_6 (0.1 M) as supporting electrolyte, glassy carbon working electrode, platinum rod auxiliary electrode, and saturated calomel reference electrode.

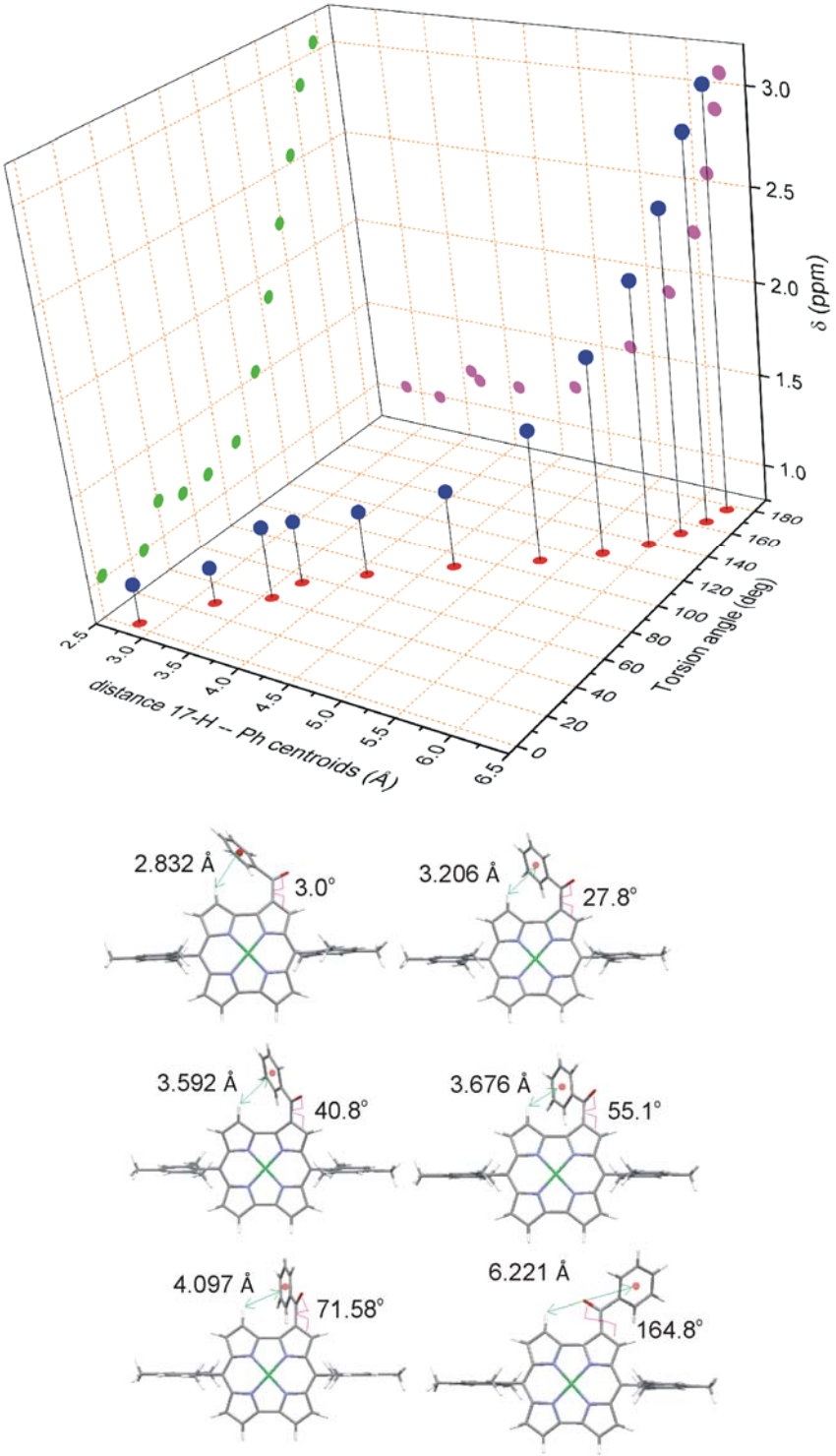

Figure S151. Dependence of the calculated chemical shift of 17-H on O-C1'-C2-C3 torsion angle and the 17-H–phenyl centroid distance for **3a** (top) and selected structures calculated upon the relaxed DFT potential energy surface scan (bottom).

Computational methods

Density functional theory (DFT) calculations were performed by using the Gaussian 09.E01 program[1]. DFT geometry optimizations were carried out in the unconstrained C_1 symmetry by using molecular mechanics or semiempirical models as starting geometries. DFT geometries were refined with the polarizable continuum model of solvation (PCM, standard dichloromethane parametrization) to meet standard convergence criteria, and the existence of a local minimum was verified by a normal mode frequency calculation. DFT calculations were performed by using the hybrid B3LYP functiona[2-4] functional combined with the 6-31G(d,p) basis set for organic part of analyzed molecules and LANL2DZ pseudopotential for nickel(II) center. The structure optimization results are collected in the Table S1. The GIAO calculations of chemical shifts and NICS were performed on the same level of theory. The relaxed DFT potential energy surface scan with torsion angle for **3a** was performed by restraining the respected angle with ModRedundant option and optimization of geometry. The electronic spectra were simulated by means of time-dependent density functional theory (TD DFT) using the Tamm-Dancoff approximation for 30 states. The electronic transitions and UV/Vis/NIR were analyzed by means of the GaussSum program.[5] The transitions were convoluted by Gaussian curves with 2000 cm^{-1} half line width. The population analysis was performed with NBO5.0 package implemented in Gaussian.

Table S1. Computational details for **3a** and **4a**. Optimizations were performed at the PCM(CH_2Cl_2)/B3LYP/6-31G(d,p) level of theory and LANL2DZ pseudopotential applied for nickel canter.

Structure	Code[a]	SCF *E*[b]	ZPV[c]	I. freq.[d]	*G*[e]	HOMO	LUMO	HLG
		a.u.	a.u.	cm^{-1}	a.u.	eV	eV	eV
3a	PJC_3_002	-2122.705927	-2122.049433	11.89	-2122.129385	–5.03	–3.45	1.58
4a	PJC_3_001	-2122.696930	-2122.040874	12.52	-2122.120469	–4.99	–3.47	1.52

[a] Optimized geometry available as <code>.pdb file. [b] Electronic energy. [c] Zero-point vibrational energy. [d] Lowest vibrational frequency. [e] Gibbs free energy.

Table S2. TD DFT-calculated electronic transitions for **3a**

No.	Energy (cm^{-1})	Wavelength (nm)	Oscillator Strength	Major contributions
1	7140.42635994	1400.47659564	0.0005	HOMO->LUMO (100%)
2	12975.8476538	770.662562234	0.0002	H-1->LUMO (99%)
3	13804.1790523	724.418305651	0.0016	H-2->LUMO (98%)
4	16252.8782988	615.275634024	0.0009	H-3->LUMO (99%)
5	19403.2798985	515.376784355	0.004	H-4->LUMO (93%)
6	19559.7514577	511.253940094	0.1667	H-10->LUMO (11%), HOMO->L+1 (70%)
7	19729.9344422	506.844056137	0.0173	H-6->LUMO (88%)
8	20471.1579624	488.492151658	0.0012	H-5->LUMO (96%)
9	20754.258567	481.82882408	0.0183	H-9->LUMO (38%), H-8->LUMO (41%), H-7->LUMO (12%)
10	20755.8716759	481.791377214	0.0004	H-7->LUMO (86%)
11	21943.1197954	455.723711726	0.0199	H-9->LUMO (53%), H-8->LUMO (39%)
12	23641.7234228	422.98100782	0.0002	H-1->L+1 (96%)
13	24432.9533177	409.283309716	0.0948	H-10->LUMO (22%), H-2->L+1 (50%), HOMO->L+2 (17%)
14	24847.5222942	402.454614251	0.2572	H-10->LUMO (22%), H-2->L+1 (41%), HOMO->L+2 (22%)
15	25422.5956021	393.350866156	0.0003	H-12->LUMO (15%), H-11->LUMO (80%)
16	25494.3789463	392.243326307	0.007	H-13->LUMO (35%), H-12->LUMO (28%), H-11->LUMO (12%), H-1->L+3 (13%)
17	25560.5164094	391.228402424	0.0108	H-12->LUMO (15%), H-1->L+3 (39%)
18	25770.220561	388.044796758	0.0055	H-13->LUMO (49%), H-12->LUMO (39%)
19	26924.3999489	371.41031997	0.0128	H-3->L+1 (28%), H-3->L+3 (21%), H-2->L+3 (20%)
20	27016.3471538	370.146265262	0.0224	H-3->L+3 (41%), H-2->L+3 (13%)
21	27199.4350092	367.654695645	0.4022	H-10->LUMO (29%), HOMO->L+2 (51%)
22	27310.7395204	366.156324421	0.0165	H-3->L+1 (58%), H-2->L+3 (18%)
23	28269.7327364	353.735215441	0.4382	H-15->LUMO (12%), H-14->LUMO (73%)
24	28472.9844526	351.210109943	0.0667	H-9->L+1 (18%), H-8->L+1 (37%), H-8->L+2 (10%)
25	29860.2580704	334.893287808	0.0001	H-4->L+1 (95%)
26	30161.9094269	331.543996717	0.0018	H-6->L+1 (92%)
27	30253.8566318	330.536371667	0.1929	H-15->LUMO (76%), H-14->LUMO (10%)
28	30395.0036569	329.001440924	0.0002	H-17->LUMO (79%), H-16->LUMO (14%)
29	30441.7838137	328.495861517	0.0184	H-17->LUMO (16%), H-16->LUMO (66%)
30	30694.23535	325.794074554	0.0007	H-5->L+1 (96%)

Table S3. TD DFT-calculated electronic transitions for **4a**

No.	Energy (cm^{-1})	Wavelength (nm)	Oscillator Strength	Major contributions
1	6615.35942666	1511.63366267	0.0015	HOMO->LUMO (100%)
2	12716.1371276	786.402340557	0.0012	H-1->LUMO (98%)
3	13702.5531943	729.791000131	0.0008	H-2->LUMO (98%)
4	16056.8855725	622.785779647	0.0009	H-5->LUMO (99%)
5	17561.1095826	569.44010018	0.0058	H-3->LUMO (97%)
6	18904.0227069	528.987938443	0.0003	H-4->LUMO (97%)
7	19462.9649262	513.796332569	0.0175	H-6->LUMO (81%), HOMO->L+1 (13%)
8	19562.9776754	511.169626931	0.1354	H-6->LUMO (16%), HOMO->L+1 (64%)
9	20442.9285574	489.166704854	0.0088	H-8->LUMO (86%)
10	20519.5512282	487.340092812	0.0018	H-7->LUMO (97%)
11	21961.6705472	455.338767535	0.019	H-10->LUMO (18%), H-9->LUMO (63%)
12	23944.1813337	417.637999839	0.0251	H-1->L+1 (93%)
13	24367.6224089	410.380620324	0.2152	H-10->LUMO (35%), HOMO->L+2 (46%)
14	24834.6174233	402.663742692	0.0018	H-2->L+1 (84%)
15	25206.4390151	396.724027301	0.0007	H-12->LUMO (59%), H-11->LUMO (26%)
16	25329.8418427	394.791253024	0.004	H-15->L+3 (13%), H-1->L+3 (67%)
17	25346.7794858	394.527439102	0.0054	H-13->LUMO (19%), H-12->LUMO (25%), H-11->LUMO (51%)
18	25559.709855	391.240747909	0.0292	H-13->LUMO (68%), H-11->LUMO (20%)
19	26521.1227344	377.057943593	0.4848	H-10->LUMO (24%), HOMO->L+1 (10%), HOMO->L+2 (40%)
20	26622.7485924	375.618616736	0.0001	H-5->L+1 (17%), H-5->L+3 (36%), H-2->L+3 (27%)
21	26937.3048197	371.232388204	0.0007	H-5->L+3 (36%), H-2->L+3 (36%)
22	27508.3453555	363.526045306	0.0005	H-5->L+1 (81%)
23	28117.2939494	355.653001957	0.4842	H-15->LUMO (16%), H-14->LUMO (76%)
24	28535.0891436	350.4457249	0.0006	H-3->L+1 (86%)
25	29801.3795971	335.554935214	0.0073	H-4->L+1 (95%)
26	29827.1893388	335.264576437	0.1515	H-15->LUMO (70%), H-14->LUMO (12%)
27	30108.6768346	332.130171477	0.0079	H-17->LUMO (14%), H-8->L+1 (11%), H-6->L+1 (37%)
28	30189.3322775	331.242834657	0.0083	H-17->LUMO (54%), H-16->LUMO (17%), H-6->L+1 (21%)
29	30256.2762951	330.509937921	0.0062	H-8->L+1 (12%), H-6->L+1 (36%)
30	30376.452905	329.202360502	0.0034	H-17->LUMO (23%), H-16->LUMO (65%)

Table S4. NICS(*z*) indices (*z* = –1, 0, 1) for DFT-optimized structures of **3a** and **4a**

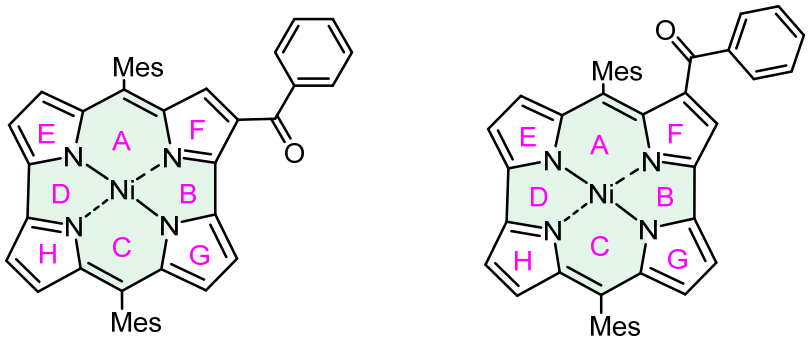

Bq	3a			4a		
	NICS(–1)	NICS(0)	NICS(1)	NICS(–1)	NICS(0)	NICS(1)
A	29.2	32.6	25.2	35.1	38.7	29.6
B	32.0	34.1	27.6	34.8	37.3	30.8
C	32.1	35.6	27.5	35.2	38.6	29.6
D	32.8	33.7	26.1	38.7	39.4	28.8
E	2.2	2.8	–1.2	3.4	4.7	–1.7
F	2.8	1.3	–1.6	3.7	1.9	–0.1
G	4.7	4.4	1.3	6.0	5.4	2.1
H	3.4	3.7	–0.2	3.4	4.2	–1.2

Due to a bowl-shaped distortion of the norcorrole ring, the paratropic ring current, and thus, the NICS values calculated on the convex (NICS(1)) and the concave (NICS(–1)) face differ. Nevertheless, for each set of NICS(*z*), the values calculated for **3a** are considerably lower than for **4**a.

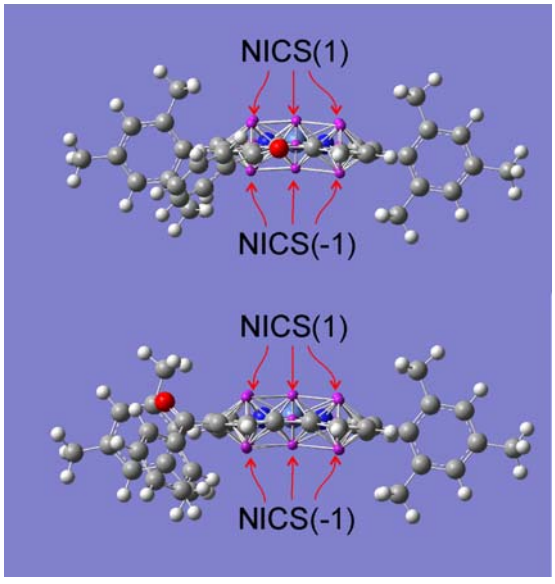

Situations of the dummy atoms Bq in **3a** (top) and **4a** (bottom).

Table S5. Natural Population Analysis Results for **1b**

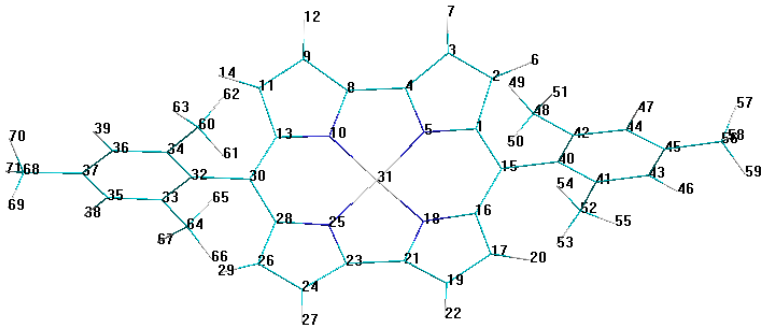

Atom		Charge	Core	Valence	Rydberg	Total
C	1	0.09809	1.99889	3.88200	0.02102	5.90191
C	2	-0.23744	1.99893	4.22676	0.01175	6.23744
C	3	-0.30335	1.99892	4.29191	0.01253	6.30335
C	4	0.19331	1.99893	3.78685	0.02091	5.80669
N	5	-0.45966	1.99906	5.44657	0.01403	7.45966
H	6	0.25533	0.00000	0.74338	0.00129	0.74467
H	7	0.25442	0.00000	0.74441	0.00118	0.74558
C	8	0.19330	1.99893	3.78686	0.02091	5.80670
C	9	-0.30332	1.99892	4.29188	0.01253	6.30332
N	10	-0.45965	1.99906	5.44657	0.01403	7.45965
C	11	-0.23751	1.99893	4.22683	0.01176	6.23751
H	12	0.25443	0.00000	0.74440	0.00118	0.74557
C	13	0.09806	1.99889	3.88203	0.02102	5.90194
H	14	0.25539	0.00000	0.74332	0.00129	0.74461
C	15	0.09704	1.99886	3.88744	0.01666	5.90296
C	16	0.09806	1.99889	3.88203	0.02102	5.90194
C	17	-0.23751	1.99893	4.22683	0.01176	6.23751
N	18	-0.45965	1.99906	5.44657	0.01403	7.45965
C	19	-0.30332	1.99892	4.29188	0.01253	6.30332
H	20	0.25539	0.00000	0.74332	0.00129	0.74461
C	21	0.19330	1.99893	3.78686	0.02091	5.80670
H	22	0.25443	0.00000	0.74440	0.00118	0.74557
C	23	0.19331	1.99893	3.78685	0.02091	5.80669
C	24	-0.30335	1.99892	4.29191	0.01253	6.30335
N	25	-0.45966	1.99906	5.44657	0.01403	7.45966
C	26	-0.23744	1.99893	4.22676	0.01175	6.23744
H	27	0.25442	0.00000	0.74441	0.00118	0.74558
C	28	0.09809	1.99889	3.88200	0.02102	5.90191
H	29	0.25533	0.00000	0.74338	0.00129	0.74467
C	30	0.09704	1.99886	3.88744	0.01666	5.90296
Ni	31	0.52442	17.99125	9.46774	0.01659	27.47558
C	32	-0.07739	1.99876	4.06378	0.01485	6.07739
C	33	0.00285	1.99882	3.98433	0.01400	5.99715
C	34	0.00189	1.99882	3.98532	0.01397	5.99811
C	35	-0.23903	1.99882	4.22826	0.01195	6.23903
C	36	-0.23943	1.99882	4.22865	0.01195	6.23943
C	37	-0.01551	1.99887	4.00237	0.01426	6.01551

H	38	0.23881	0.00000	0.75930	0.00190	0.76119
H	39	0.23867	0.00000	0.75944	0.00189	0.76133
C	40	-0.07739	1.99876	4.06378	0.01485	6.07739
C	41	0.00285	1.99882	3.98433	0.01400	5.99715
C	42	0.00189	1.99882	3.98532	0.01397	5.99811
C	43	-0.23903	1.99882	4.22826	0.01195	6.23903
C	44	-0.23943	1.99882	4.22865	0.01195	6.23943
C	45	-0.01551	1.99887	4.00237	0.01426	6.01551
H	46	0.23881	0.00000	0.75930	0.00190	0.76119
H	47	0.23867	0.00000	0.75944	0.00189	0.76133
C	48	-0.70430	1.99923	4.69793	0.00714	6.70430
H	49	0.25201	0.00000	0.74617	0.00182	0.74799
H	50	0.25198	0.00000	0.74619	0.00183	0.74802
H	51	0.24427	0.00000	0.75429	0.00144	0.75573
C	52	-0.70476	1.99923	4.69842	0.00711	6.70476
H	53	0.25220	0.00000	0.74600	0.00180	0.74780
H	54	0.25222	0.00000	0.74599	0.00180	0.74778
H	55	0.24483	0.00000	0.75372	0.00144	0.75517
C	56	-0.69946	1.99923	4.69300	0.00722	6.69946
H	57	0.25012	0.00000	0.74820	0.00168	0.74988
H	58	0.24442	0.00000	0.75403	0.00155	0.75558
H	59	0.24498	0.00000	0.75346	0.00157	0.75502
C	60	-0.70430	1.99923	4.69793	0.00714	6.70430
H	61	0.25201	0.00000	0.74617	0.00182	0.74799
H	62	0.25198	0.00000	0.74619	0.00183	0.74802
H	63	0.24427	0.00000	0.75429	0.00144	0.75573
C	64	-0.70476	1.99923	4.69842	0.00711	6.70476
H	65	0.25220	0.00000	0.74600	0.00180	0.74780
H	66	0.25222	0.00000	0.74599	0.00180	0.74778
H	67	0.24483	0.00000	0.75372	0.00144	0.75517
C	68	-0.69946	1.99923	4.69300	0.00722	6.69946
H	69	0.25012	0.00000	0.74820	0.00168	0.74988
H	70	0.24442	0.00000	0.75403	0.00155	0.75558
H	71	0.24498	0.00000	0.75346	0.00157	0.75502

==========

* Total *	-0.00000	97.94909	203.42781	0.62310	302.00000

Table S6. Natural Population Analysis Results for **3a**

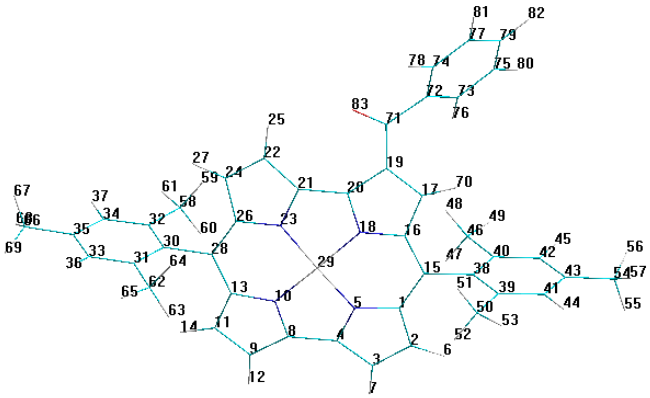

Atom		Charge	Core	Valence	Rydberg	Total
C	1	0.10661	1.99888	3.87365	0.02086	5.89339
C	2	-0.22490	1.99893	4.21423	0.01174	6.22490
C	3	-0.29396	1.99892	4.28247	0.01258	6.29396
C	4	0.21707	1.99894	3.76286	0.02113	5.78293
N	5	-0.45965	1.99905	5.44647	0.01413	7.45965
H	6	0.25905	0.00000	0.73968	0.00127	0.74095
H	7	0.25833	0.00000	0.74051	0.00116	0.74167
C	8	0.17763	1.99893	3.80263	0.02081	5.82237
C	9	-0.29910	1.99892	4.28771	0.01247	6.29910
N	10	-0.45738	1.99905	5.44428	0.01405	7.45738
C	11	-0.24125	1.99893	4.23055	0.01177	6.24125
H	12	0.25505	0.00000	0.74378	0.00117	0.74495
C	13	0.10124	1.99890	3.87865	0.02121	5.89876
H	14	0.25604	0.00000	0.74267	0.00129	0.74396
C	15	0.09978	1.99886	3.88473	0.01663	5.90022
C	16	0.10068	1.99889	3.87902	0.02140	5.89932
C	17	-0.20909	1.99889	4.19964	0.01055	6.20909
N	18	-0.44721	1.99906	5.43395	0.01420	7.44721
C	19	-0.20425	1.99884	4.18992	0.01549	6.20425
C	20	0.23614	1.99890	3.74195	0.02301	5.76386
C	21	0.20682	1.99893	3.77195	0.02229	5.79318
C	22	-0.28877	1.99891	4.27631	0.01355	6.28877
N	23	-0.45889	1.99905	5.44580	0.01404	7.45889
C	24	-0.23275	1.99893	4.22224	0.01158	6.23275
H	25	0.26576	0.00000	0.73263	0.00161	0.73424
C	26	0.10222	1.99889	3.87791	0.02097	5.89778
H	27	0.25676	0.00000	0.74197	0.00127	0.74324
C	28	0.09899	1.99886	3.88552	0.01663	5.90101
Ni	29	0.52904	17.99125	9.46310	0.01661	27.47096
C	30	-0.07883	1.99876	4.06527	0.01480	6.07883
C	31	0.00331	1.99882	3.98389	0.01399	5.99669
C	32	0.00222	1.99882	3.98499	0.01397	5.99778
C	33	-0.23867	1.99882	4.22790	0.01195	6.23867
C	34	-0.23903	1.99882	4.22826	0.01195	6.23903
C	35	-0.01486	1.99887	4.00173	0.01425	6.01486

H	36	0.23917	0.00000	0.75894	0.00189	0.76083
H	37	0.23900	0.00000	0.75911	0.00189	0.76100
C	38	-0.08145	1.99876	4.06791	0.01477	6.08145
C	39	0.00387	1.99882	3.98333	0.01399	5.99613
C	40	0.00176	1.99882	3.98546	0.01396	5.99824
C	41	-0.23793	1.99882	4.22715	0.01196	6.23793
C	42	-0.23882	1.99882	4.22803	0.01196	6.23882
C	43	-0.01367	1.99887	4.00054	0.01425	6.01367
H	44	0.23993	0.00000	0.75819	0.00188	0.76007
H	45	0.23943	0.00000	0.75868	0.00189	0.76057
C	46	-0.70439	1.99923	4.69799	0.00717	6.70439
H	47	0.25241	0.00000	0.74580	0.00179	0.74759
H	48	0.25052	0.00000	0.74763	0.00185	0.74948
H	49	0.24567	0.00000	0.75289	0.00144	0.75433
C	50	-0.70530	1.99923	4.69892	0.00715	6.70530
H	51	0.25275	0.00000	0.74546	0.00179	0.74725
H	52	0.25207	0.00000	0.74617	0.00175	0.74793
H	53	0.24620	0.00000	0.75237	0.00143	0.75380
C	54	-0.69977	1.99923	4.69329	0.00724	6.69977
H	55	0.25072	0.00000	0.74762	0.00167	0.74928
H	56	0.24492	0.00000	0.75353	0.00155	0.75508
H	57	0.24554	0.00000	0.75291	0.00155	0.75446
C	58	-0.70446	1.99923	4.69808	0.00715	6.70446
H	59	0.25245	0.00000	0.74575	0.00180	0.74755
H	60	0.25133	0.00000	0.74685	0.00182	0.74867
H	61	0.24484	0.00000	0.75372	0.00144	0.75516
C	62	-0.70497	1.99923	4.69861	0.00713	6.70497
H	63	0.25174	0.00000	0.74646	0.00180	0.74826
H	64	0.25274	0.00000	0.74548	0.00177	0.74726
H	65	0.24532	0.00000	0.75324	0.00144	0.75468
C	66	-0.69956	1.99923	4.69310	0.00723	6.69956
H	67	0.25056	0.00000	0.74777	0.00167	0.74944
H	68	0.24454	0.00000	0.75391	0.00155	0.75546
H	69	0.24496	0.00000	0.75348	0.00156	0.75504
H	70	0.26219	0.00000	0.73629	0.00152	0.73781
C	71	0.54956	1.99898	3.41615	0.03531	5.45044
C	72	-0.13188	1.99883	4.11767	0.01538	6.13188
C	73	-0.21979	1.99892	4.20806	0.01282	6.21979
C	74	-0.19859	1.99892	4.18560	0.01408	6.19859
C	75	-0.24022	1.99895	4.22719	0.01408	6.24022
H	76	0.24940	0.00000	0.74857	0.00204	0.75060
C	77	-0.24041	1.99895	4.22766	0.01379	6.24041
H	78	0.25525	0.00000	0.74218	0.00257	0.74475
C	79	-0.22340	1.99895	4.21081	0.01363	6.22340
H	80	0.24806	0.00000	0.75031	0.00163	0.75194
H	81	0.24828	0.00000	0.75009	0.00163	0.75172
H	82	0.24723	0.00000	0.75116	0.00161	0.75277
O	83	-0.60197	1.99975	6.58610	0.01612	8.60197

==========

* Total *	-0.00000	113.94117	241.28506	0.77378	356.00000

Table S7. Natural Population Analysis Results for **4a**

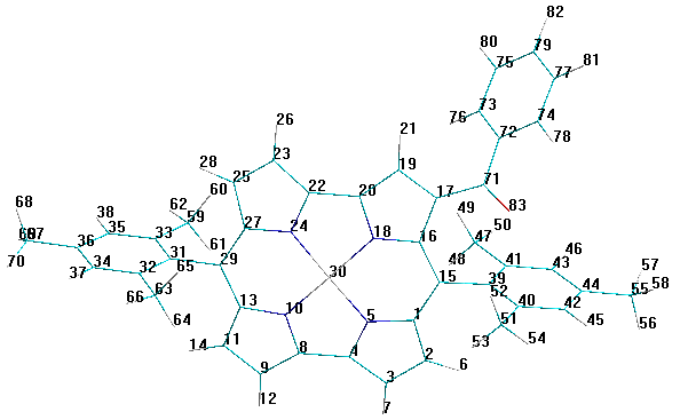

Atom		Charge	Core	Valence	Rydberg	Total
C	1	0.10463	1.99888	3.87566	0.02083	5.89537
C	2	-0.21978	1.99893	4.20907	0.01177	6.21978
C	3	-0.29780	1.99891	4.28627	0.01262	6.29780
C	4	0.21854	1.99893	3.76141	0.02112	5.78146
N	5	-0.46075	1.99905	5.44749	0.01421	7.46075
H	6	0.25964	0.00000	0.73903	0.00133	0.74036
H	7	0.25797	0.00000	0.74087	0.00116	0.74203
C	8	0.17609	1.99892	3.80415	0.02084	5.82391
C	9	-0.29852	1.99891	4.28713	0.01248	6.29852
N	10	-0.45792	1.99906	5.44482	0.01404	7.45792
C	11	-0.24270	1.99893	4.23199	0.01178	6.24270
H	12	0.25494	0.00000	0.74388	0.00118	0.74506
C	13	0.10123	1.99890	3.87870	0.02118	5.89877
H	14	0.25579	0.00000	0.74292	0.00129	0.74421
C	15	0.10687	1.99886	3.87746	0.01682	5.89313
C	16	0.13978	1.99887	3.83886	0.02248	5.86022
C	17	-0.14956	1.99884	4.13559	0.01513	6.14956
N	18	-0.44292	1.99907	5.42980	0.01404	7.44292
C	19	-0.26752	1.99885	4.25716	0.01151	6.26752
C	20	0.16926	1.99892	3.81090	0.02092	5.83074
H	21	0.26128	0.00000	0.73739	0.00133	0.73872
C	22	0.20884	1.99894	3.77123	0.02099	5.79116
C	23	-0.30211	1.99892	4.29063	0.01257	6.30211
N	24	-0.46012	1.99905	5.44697	0.01410	7.46012
C	25	-0.22883	1.99893	4.21816	0.01173	6.22883
H	26	0.25642	0.00000	0.74241	0.00117	0.74358
C	27	0.09945	1.99889	3.88068	0.02098	5.90055
H	28	0.25728	0.00000	0.74143	0.00128	0.74272
C	29	0.09781	1.99886	3.88669	0.01665	5.90219
Ni	30	0.53111	17.99125	9.46117	0.01647	27.46889
C	31	-0.07880	1.99876	4.06525	0.01479	6.07880
C	32	0.00344	1.99882	3.98375	0.01398	5.99656
C	33	0.00196	1.99882	3.98525	0.01397	5.99804
C	34	-0.23863	1.99882	4.22785	0.01196	6.23863
C	35	-0.23915	1.99882	4.22838	0.01195	6.23915

C	36	-0.01464	1.99887	4.00151	0.01426	6.01464
H	37	0.23926	0.00000	0.75885	0.00189	0.76074
H	38	0.23894	0.00000	0.75917	0.00189	0.76106
C	39	-0.07742	1.99875	4.06299	0.01568	6.07742
C	40	0.01709	1.99882	3.96947	0.01462	5.98291
C	41	0.00058	1.99882	3.98667	0.01393	5.99942
C	42	-0.23604	1.99881	4.22522	0.01200	6.23604
C	43	-0.24027	1.99882	4.22948	0.01197	6.24027
C	44	-0.01499	1.99887	4.00183	0.01428	6.01499
H	45	0.23767	0.00000	0.76043	0.00191	0.76233
H	46	0.23727	0.00000	0.76083	0.00190	0.76273
C	47	-0.70315	1.99923	4.69675	0.00717	6.70315
H	48	0.24957	0.00000	0.74861	0.00182	0.75043
H	49	0.24842	0.00000	0.74966	0.00193	0.75158
H	50	0.24480	0.00000	0.75375	0.00145	0.75520
C	51	-0.70424	1.99922	4.69787	0.00716	6.70424
H	52	0.26065	0.00000	0.73680	0.00255	0.73935
H	53	0.24537	0.00000	0.75288	0.00175	0.75463
H	54	0.24171	0.00000	0.75683	0.00146	0.75829
C	55	-0.69895	1.99923	4.69253	0.00719	6.69895
H	56	0.24812	0.00000	0.75019	0.00169	0.75188
H	57	0.24268	0.00000	0.75579	0.00153	0.75732
H	58	0.24651	0.00000	0.75188	0.00161	0.75349
C	59	-0.70419	1.99923	4.69782	0.00715	6.70419
H	60	0.25193	0.00000	0.74627	0.00181	0.74807
H	61	0.25138	0.00000	0.74680	0.00182	0.74862
H	62	0.24482	0.00000	0.75374	0.00144	0.75518
C	63	-0.70499	1.99923	4.69862	0.00714	6.70499
H	64	0.25269	0.00000	0.74550	0.00180	0.74731
H	65	0.25190	0.00000	0.74633	0.00178	0.74810
H	66	0.24535	0.00000	0.75321	0.00144	0.75465
C	67	-0.69961	1.99923	4.69315	0.00723	6.69961
H	68	0.25040	0.00000	0.74793	0.00167	0.74960
H	69	0.24459	0.00000	0.75386	0.00155	0.75541
H	70	0.24526	0.00000	0.75318	0.00156	0.75474
C	71	0.55452	1.99899	3.41023	0.03625	5.44548
C	72	-0.14288	1.99882	4.12848	0.01558	6.14288
C	73	-0.21138	1.99892	4.19985	0.01261	6.21138
C	74	-0.19220	1.99892	4.17907	0.01422	6.19220
C	75	-0.24267	1.99895	4.22959	0.01413	6.24267
H	76	0.25201	0.00000	0.74601	0.00198	0.74799
C	77	-0.24160	1.99895	4.22888	0.01377	6.24160
H	78	0.25741	0.00000	0.73991	0.00268	0.74259
C	79	-0.21796	1.99895	4.20539	0.01361	6.21796
H	80	0.24840	0.00000	0.74997	0.00162	0.75160
H	81	0.24860	0.00000	0.74978	0.00162	0.75140
H	82	0.24766	0.00000	0.75074	0.00160	0.75234
O	83	-0.57562	1.99974	6.55918	0.01670	8.57562
==========						
* Total *		-0.00000	113.94110	241.28390	0.77501	356.00000

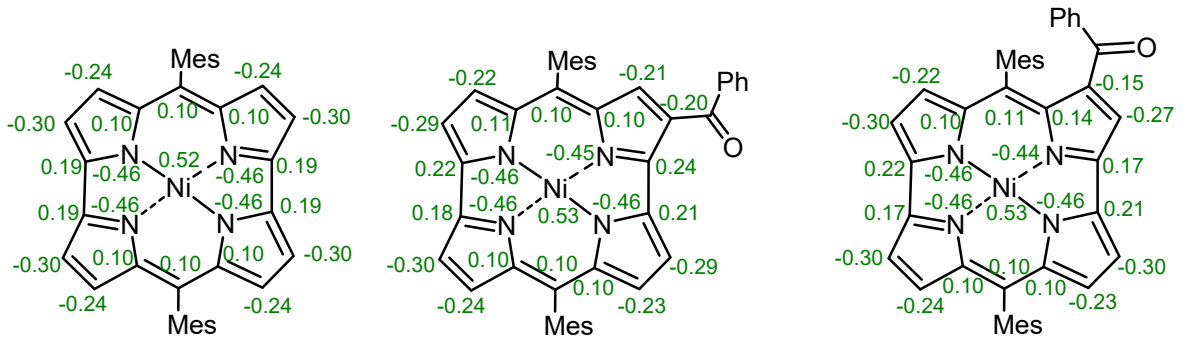

Figure S152. Comparison of the NPA charges distribution across macrocyclic ring atoms of **1b**, **3a**, and **4a**.

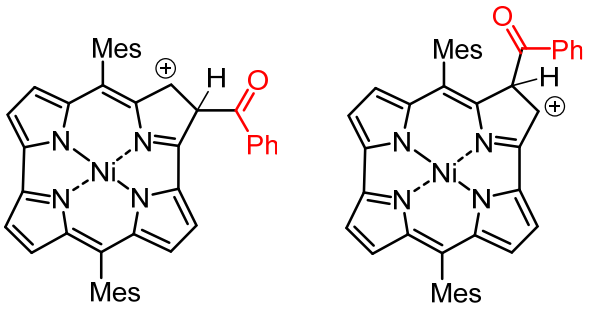

Figure S153. Comparison of the relative energies for DFT models of the benzoylation reaction intermediates [H**3a**]$^+$ and [H**4a**]$^+$.

References

1. Frisch, M. J.; Trucks, G. W.; Schlegel, H. B.; Scuseria, G. E.; Robb, M. A.; Cheeseman, J. R.; Scalmani, G.; Barone, V.; Mennucci, B.; Petersson, G. A.; Nakatsuji, H.; Caricato, M.; Li, X.; Hratchian, H. P.; Izmaylov, A. F.; Bloino, J.; Zheng, G.; Sonnenberg, J. L.; Hada, M.; Ehara, M.; Toyota, K.; Fukuda, R.; Hasegawa, J.; Ishida, M.; Nakajima, T.; Honda, Y.; Kitao, O.; Nakai, H.; Vreven, T.; Montgomery, Jr., J. A.; Peralta, J. E.; Ogliaro, F.; Bearpark, M.; Heyd, J. J.; Brothers, E.; Kudin, K. N.; Staroverov, V. N.; Kobayashi, R.; Normand, J.; Raghavachari, K.; Rendell, A.; Burant, J. C.; Iyengar, S. S.; Tomasi, J.; Cossi, M.; Rega, N.; Millam, J. M.; Klene, M.; Knox, J. E.; Cross, J. B.; Bakken, V.; Adamo, C.; Jaramillo, J.; Gomperts, R.; Stratmann, R. E.; Yazyev, O.; Austin, A. J.; Cammi, R.; Pomelli, C.; Ochterski, J. W.; Martin, R. L.; Morokuma, K.; Zakrzewski, V. G.; Voth, G. A.; Salvador, P.; Dannenberg, J. J.; Dapprich, S.; Daniels, A. D.; Farkas, Ö.; Foresman, J. B.; Ortiz, J. V.; Cioslowski, J.; Fox, D. J. Gaussian 09 Revision E.01.

2. A. D. Becke, *Phys.Rev.A*, **1988,** *38*, 3098.

3. A. D. Becke, *J.Chem.Phys.*, **1993,** *98*, 5648.

4. C. Lee, W. Yang, and R. G. Parr, *Phys.Rev.B*, **1988,** *37*, 785.

5. N. M. O'Boyle, A. L. Tenderholt, and K. M. Langner, *J.Comp.Chem.*, **2008,** *29*, 839.